

Spatial risk assessment of threats to yellow-eyed penguin/hoiho (Megadyptes antipodes)

New Zealand Aquatic Environment and Biodiversity Report No. 370.

J.O. Roberts, D.N. Webber

ISSN 1179-6480 (online) ISBN 978-1-991407-33-7 (online)

November 2025



Disclaimer

This document is published by Fisheries New Zealand, a business unit of the Ministry for Primary Industries (MPI). The information in this publication is not government policy. While every effort has been made to ensure the information is accurate, the Ministry for Primary Industries does not accept any responsibility or liability for error of fact, omission, interpretation, or opinion that may be present, nor for the consequence of any decisions based on this information. Any view or opinion expressed does not necessarily represent the view of Fisheries New Zealand or the Ministry for Primary Industries.

Requests for further copies should be directed to:

Fisheries Science Editor Fisheries New Zealand Ministry for Primary Industries PO Box 2526 Wellington 6140 NEW ZEALAND

Email: Fisheries-Science.Editor@mpi.govt.nz

Telephone: 0800 00 83 33

This publication is also available on the Ministry for Primary Industries websites at: http://www.mpi.govt.nz/news-and-resources/publications http://fs.fish.govt.nz go to Document library/Research reports

© Crown Copyright - Fisheries New Zealand

Please cite this report as:

Roberts, J.; Webber, D.N. (2025). Spatial risk assessment of threats to yellow-eyed penguin/hoiho (*Megadyptes antipodes*). New Zealand Aquatic Environment and Biodiversity Report No. 370. 162 p.

TABLE OF CONTENTS

EXE	CUTIV	E SUMMARY	. 1
1.	INTR	ODUCTION	. 2
	1.1	BACKGROUND	2
	1.2	ASSESSMENT AND MANAGEMENT OF THREATS	3
	1.3	RISK ASSESSMENT OBJECTIVES	4
2.	RISK	ASSESSMENT METHODOLOGY	. 4
	2.1	METHODS USED FOR EACH THREAT	4
	2.2	SELECTION OF THREATS	6
	2.3	SELECTION OF REGIONAL SUB-POPULATIONS	7
	2.4	RISK ASSESSMENT DEVELOPMENT PROCESS	8
3.	DEM	OGRAPHIC POPULATION ASSESSMENT	. 9
	3.1	METHODS	9
	3.1.1	MODEL INPUTS	9
	3.1.2	MODEL STATES, PARAMETERS, AND TRANSITIONS	10
	3.1.3	PRIORS AND CONSTRAINTS	13
	3.1.4	MODEL REGIONS AND MOVEMENT	14
	3.1.5	POPULATION PROJECTIONS	15
	3.2	RESULTS	15
	3.2.1	POPULATION MODEL INPUTS	15
	3.2.2	POPULATION MODEL OUTPUTS	16
	3.2.3	POPULATION PROJECTIONS	18
4.	SPAT	FIALLY EXPLICIT FISHERIES RISK ASSESSMENT (SEFRA)	21
	4.1	METHODS	21
	4.1.1	SEFRA INPUTS	21
	4.1.2	SEFRA MODEL	23
	4.1.3	MODEL PREDICTIONS	25
	4.1.3.	1 SIMULATED RANDOM VARIABLES	25
	4.1.3.	PREDICTING DEATHS AND RISK	26
	4.1.4	MODEL RUNS	27
	4.2	RESULTS	27
	4.3	SEFRA MODEL INPUTS	27
	4.4	SEFRA MODEL RESULTS	28
5.	RELA	ATIVE SPATIAL OVERLAP	34
	5.1	METHODS	34
	5.1.1	DERIVATION OF THREAT LAYERS	34
	5.1.2	GENERATION OF TERRESTRIAL PENGUIN LAYER	34
	5.1.3	CALCULATION OF RELATIVE OVERLAP	35
	5.2	RESULTS	35
6	COP	DELATIVE ASSESSMENT	20

	6.1	METHODS	8
	6.1.1	SURVIVORSHIP	8
	6.1.2	SEA SURFACE TEMPERATURE	8
	6.1.3	Assessing correlation	9
	6.2	RESULTS	9
7.	DISC	USSION4	1
	7.1	DEMOGRAPHIC DRIVERS OF POPULATION CHANGE	1
	7.2	KEY THREATS	1
	7.3	LIMITATIONS OF THIS ANALYSIS	4
	7.4	RECOMMENDATIONS FOR FUTURE RESEARCH	7
8.	ACKI	NOWLEDGEMENTS4	8
9.	REFE	ERENCES4	8
APPE	ENDIX	A. NECROPSY DATA SUMMARY5	3
		(B. SUPPLEMENTARY TABLES & FIGURES FROM DEMOGRAPHIC ULATON ASSESSMENT5	9
APPE	ENDIX	C. VALIDATION OF STAN POPULATION MODEL USING SEABIRD11	3
		D. SUPPLEMENTARY TABLES & FIGURES FROM THE SEFRA ESSMENT11	5
APPE	ENDIX	E. AT-SEA DENSITY OF YELLOW-EYED PENGUINS13	9
APPE	ENDIX	(F. THREAT MAPS14	4
APPE		G. SUPPLEMENTARY TABLES & FIGURES FOR SEA TEMPERATURE	0

PLAIN LANGUAGE SUMMARY

This research assessed the threats facing the northern population of yellow-eyed penguins/hoiho. The northern population includes the New Zealand South Island/Te Waipounamu and Stewart Island/Rakiura. Population models were developed for regional sub-populations from 1991 to 2023, to track changes in population size over time. The study found that hoiho numbers have declined across all areas, driven mainly by poor survival of juveniles and adults.

- Key threats include commercial set-net entanglements, which caused an estimated 17 deaths in 2022–23, mostly around Otago Peninsula, where risks have risen sharply since 2018–19.
- Malnutrition affects chicks and juveniles the most, particularly females, diseases have the greatest effect on chicks and juveniles, and predation primarily affects juveniles and adults.
- Warming sea temperatures across their range correlate with lower survival rates across all ages, suggesting climate change impacts on their main prey species.
- Otago Peninsula faces the highest overlap with human-related threats including direct interactions with humans and their dogs, recreational netting, oil spill risk, and other threats.

Projections suggested that the population could stabilise if either juvenile or adult deaths are halved, but eliminating chick deaths alone would not suffice.

This research provides information required for guiding conservation efforts to meet the goal of halting the decline.

EXECUTIVE SUMMARY

Roberts, J.¹; Webber, D.N.² (2025). Spatial risk assessment of threats to yellow-eyed penguin/hoiho (*Megadyptes antipodes*).

New Zealand Aquatic Environment and Biodiversity Report No. 370. 162 p.

This document describes a spatial multi-threat assessment for the northern population of yellow-eyed penguin/hoiho (*Megadyptes antipodes*).

Bespoke demographic population models were developed for regional sub-populations for the years 1991 (the 1990–91 breeding season, defined as the period from 1 August 1990 to 31 July 1991) to 2023, fitted to: mark capture-recapture observations, estimates of the annual number of breeding pairs, and the number of chicks hatching/fledgling. These models estimated the annual movement rate of immature birds between regional sub-populations which would otherwise have confounded the estimation of annual survivorship. The population models estimated declining population size in recent years in all regional sub-populations, with the least precipitous decline in the southern part of North Otago. Some common demographic patterns were estimated across most regional sub-populations, including worsening chick survival through time and a protracted period of poor juvenile survival. Generally, the estimated number of chick, juvenile, and adult deaths each year were approximately equal, although juvenile deaths were much more variable. Juvenile and adult survival rates were the major drivers of population change including the most recent period of decline. Projections indicated that population stability across the northern population could be achieved by approximately halving either juvenile or adult mortality rate, but could not be achieved with full alleviation of chick mortality rate alone.

Spatially explicit fisheries risk assessment (SEFRA) models were developed to estimate the number of annual deaths and population risk (R) of direct interactions with commercial fisheries. The reference model predicted a median of 16.6 deaths (95% credible interval = 9.6 – 27.7) from commercial fishing during the 2022–23 fishing season, with approximately half of deaths occurring around the Otago Peninsula and an increasing trend in this region. Estimated deaths in trawls were close to zero. Across the northern population and the assessed fisheries, the annual risk ratio was above one in the final three years of the assessment (2020–21 to 2022–23). This was largely driven by the increase in estimated fishing deaths at the Otago Peninsula, where the median risk ratio for females at Otago Peninsula exceeded a value of R = 1 in all assessed years since 2016–17 and was closer to R = 4 in the period 2020–21 to 2022–23.

The SEFRA model was extended to estimate annual deaths from coarse-level non-fisheries threats, including: malnutrition, diseases, predation, trauma, and other causes, based on proportional primary causes of death in the sample of necropsied birds. Based on this sample, malnutrition appears to have been a major issue for chicks and juveniles and is likely to be a greater issue for females. Disease also appears to be a major issue for chicks. The mix of threats affecting adults is likely to be more diverse, including predation by marine and terrestrial predators. The causes of malnutrition could not be determined from this analysis. However, negative correlations between survival rate and sea surface temperature for all life stages and for multiple regional sub-populations are consistent with oceanic warming negatively affecting the availability of key prey species, noting that longer time series of data and a better understanding of the underlying mechanistic drivers of prey availability are needed to confirm this relationship.

The relative intensity of other non-fisheries threats to regional sub-populations was assessed based on spatial overlap, including oil spill risk, recreational netting, direct interactions with dogs/humans, and others threats. This approach highlighted the Otago Peninsula population as experiencing relatively high threat intensity from multiple anthropogenic stressors.

_

¹ Anemone Consulting Ltd, New Zealand.

² Quantifish Ltd., New Zealand.

1. INTRODUCTION

1.1 Background

The yellow-eyed penguin/hoiho (*Megadyptes antipodes*) is endemic to New Zealand, with populations currently breeding on the South Island of New Zealand, Stewart Island/Rakiura, the Auckland Islands, and Campbell Island (Figure 1). Closely related but genetically distinct variants of the yellow-eyed penguin disappeared from the South Island (waitaha penguin; *Megadyptes antipodes waitaha*) and the Chatham Islands/Rēkohu/Wharekauri (*Megadyptes antipodes richdalei*) sometime after the arrival of humans to New Zealand. However, the Sub-Antarctic variant (*Megadyptes antipodes antipodes*) persisted on the Auckland Islands/Motu Maha and Campbell Island/Motu Ihupuku in the New Zealand Sub-Antarctic region and subsequently recolonised the southern South Island and Stewart Island/Rakiura over the past few hundred years (Boessenkool et al. 2009; Cole et al. 2019).

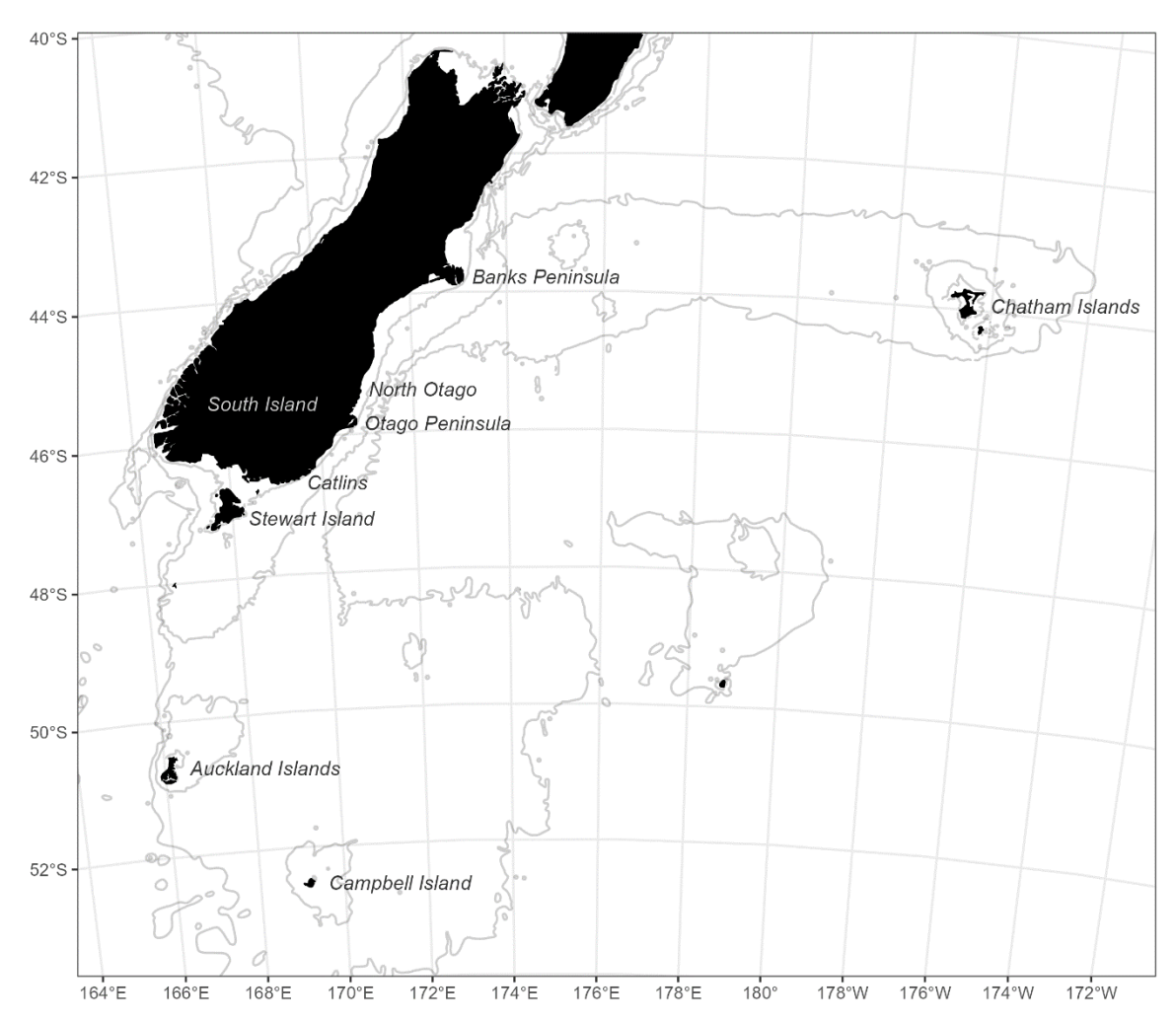


Figure 1: Map showing the locations of breeding populations of yellow-eyed penguin. Yellow-eyed penguin do not currently breed at the Chatham Islands, although a related variant existed there in the past. Grey lines represent the 50, 200, and 1000 m depth contours.

The species is commonly divided into two wider populations, based on location and information about dispersal: the northern population (including the South Island and Stewart Island); and the southern population (including the Auckland Islands and Campbell Island). Much more is known about the northern population, particularly on the South Island where there has been annual population monitoring, regular necropsying of carcasses, and intensive conservation management at some of the largest breeding colonies (reviewed by Webster 2018). By contrast, the southern population is likely to

be much larger in size (Moore 1992; Muller et al. 2020) but much less is known about population trends and threats.

Most of the South Island breeding colonies have been subjected to annual counts of active nests since the early 1980s. These data suggest periods of increasing (e.g., 1991³ to 1997, and 2006 to 2010) and decreasing (e.g., 1986 to 1991, 1997 to 2005, and 2009 to 2023) numbers of breeders through time (Figure 2). The recent period of decline has continued since 2009 and the most recent counts are consistent with breeder numbers being at their lowest point since at least 1981 (1991 was lower, although anomalously so relative to the years immediately before and after).

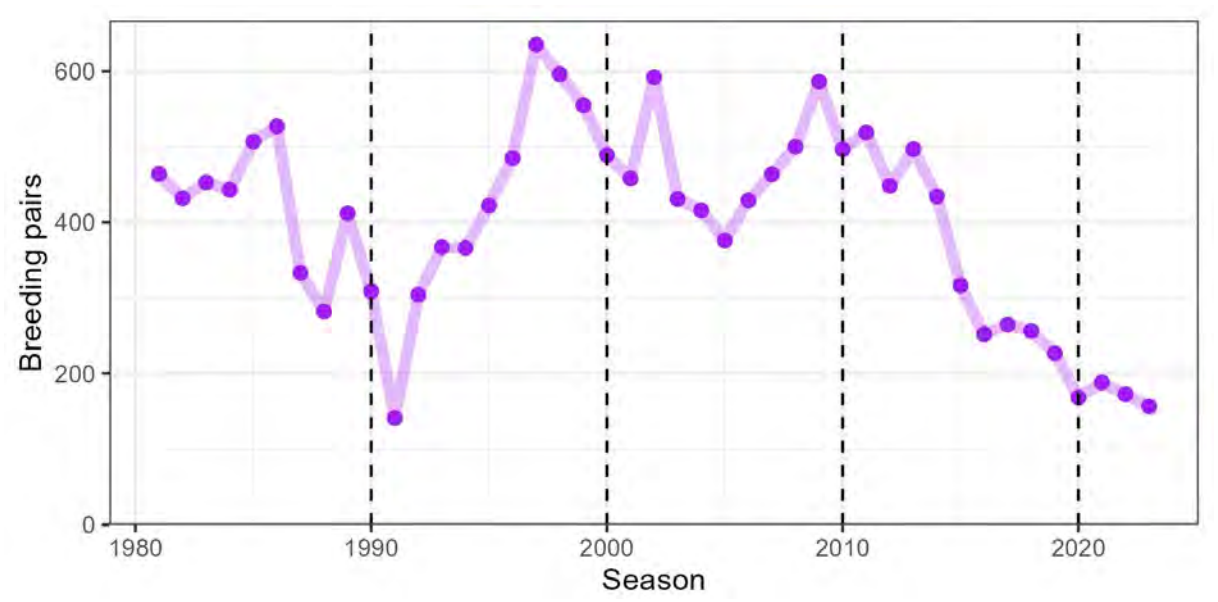


Figure 2: Estimated annual number of breeding pairs of yellow-eyed penguin on the South Island of New Zealand (DOC, unpublished data). This plot does not include Stewart Island for which nest counts are much more sporadic than for the South Island. Here model seasons are labelled using the end year of each breeding season, e.g., '1990' represents the 1989–90 season.

1.2 Assessment and management of threats

The current yellow-eyed penguin action plan/Te Mahere Rima Tau⁴ states a five-year goal to 'halt the decline of the northern population of hoiho'. Ideally the conservation response for achieving this goal would be guided by a good understanding of the major threats affecting population change. Recent implementations of the spatially explicit fisheries risk assessment (SEFRA) approach for New Zealand seabird species included the estimation of deaths and population risk posed by direct interactions with commercial fisheries (Edwards et al. 2023a; Richard et al. 2020). However, to date, there has been no quantitative multi-threat risk assessment for the species that would allow the robust determination of the key threats driving population changes experienced by the northern population. Despite this, the probable main threats are considered to be reasonably well-known, based on: the available necropsy information (e.g., Hocken 2005), field-based observations and anecdotal information (e.g., summarised by Webster 2018), previous assessments of commercial fishery interactions (e.g., Darby & Dawson 2000; Edwards et al. 2023a; Richard et al. 2020), and assessments relating demographic rates to climatic indices (Mattern et al. 2017). The threats to yellow-eyed penguin were also reviewed by Webster (2018) and include:

 diseases and parasites, some of which primarily affect chicks (e.g., diphtheric stomatitis (DS) or respiratory distress syndrome (RDS)) and other diseases also affecting later life stages (e.g., avian malaria);

-

³ the 1990–91 breeding season, defined as the period from 1 August to 31 July.

⁴ https://www.doc.govt.nz/globalassets/documents/conservation/native-animals/birds/sea-and-shore/te-mahere-rima-tau-2020.pdf

- factors affecting prey availability and malnutrition of yellow-eyed penguins at all life stages;
- direct and indirect interactions with commercial and recreational fishing;
- predation by marine and terrestrial predators;
- direct human disturbance (e.g., from tourism or researcher activities);
- fire and human-caused marine/terrestrial habitat degradation;
- demographic issues such as relating to skewed sex ratio and small population size, as well as other threats.

Notably, threats can have either a marine or a terrestrial origin, reflecting changes in the distribution and behaviours of yellow-eyed penguin throughout the annual breeding/moulting cycle. Recent conservation management has focused on the threats that can be most easily managed, including the rehabilitation of individuals suffering from diseases, parasites, or malnutrition, as well as measures to control predator numbers and improve terrestrial habitat at the main nesting sites (summarised by Webster 2018).

1.3 Risk assessment objectives

This document describes a spatial risk assessment of threats for the northern population of yelloweyed penguin, i.e., including South Island and Stewart Island regional sub-populations, but not the Sub-Antarctic populations. The specific Objectives of this research project were as follows:

- 1. Construct population models for yellow-eyed penguin at the appropriate colony/sub-population where possible within data availability constraints.
- 2. Map fishery and non-fishery threats to yellow-eyed penguins and estimate the overlap between penguin distributions and threats.
- 3. Apply the spatially-explicit fisheries risk assessment (SEFRA) method to estimate fisheries impact and risk to yellow-eyed penguins, using the new information from specific objectives 1 and 2 above, including at a regional sub-population level. This analysis should include estimation and partition of total mortalities attributable to different threats (with uncertainty) at a regional sub-population level.
- 4. In consultation with government scientists and managers, examine alternative spatial management scenarios through both modelling and participation in a multi-threat risk assessment workshop.

This document describes the spatial risk assessment methods, data inputs, and outputs under Objectives 1–3. With the aim of separating science and management considerations, the exploration of alternative spatial management scenarios (Objective 4) is not included in this report.

2. RISK ASSESSMENT METHODOLOGY

2.1 Methods used for each threat

The method used for assessing risk depended on the threat being assessed. For threats for which quantitative information about mortality rate **was available** (i.e., including commercial fisheries and some non-fisheries causes of death), the assessment used an extension of the SEFRA modelling approach to estimating annual deaths and population risk for some threats. This followed the basic approach of the spatial multi-threat risk assessment of Hector's dolphin (*Cephalorhynchus hectori hectori*) and Māui dolphin (*Cephalorhynchus hectori maui*) (Roberts et al. 2019), where commercial

fisheries were assessed by applying the standard SEFRA approach (i.e., based on fisheries observer captures and spatial overlap with the study species), and non-fisheries threats were assessed by partitioning out the remaining estimated annual deaths based on other sources of information (e.g., proportional causes of death in the necropsy data).

The SEFRA models used distributions of annual survival rate and population size that were estimated for each regional sub-population (see Section 2.3) using bespoke demographic population models. A schematic diagram of the key modelling processes is shown in Figure 3, highlighting the stage at which outputs were passed from the population models to the SEFRA models. For each regional sub-population, the assessment process was as follows:

- 1. Posteriors of key demographic rates and annual population size were estimated by the demographic population models, which were then used to generate priors of demographic rates and population size required by the SEFRA model.
- 2. The SEFRA model was applied to derive posteriors of the total annual number of deaths and population risk caused by direct interactions with commercial fisheries using standard SEFRA methods.
- 3. A SEFRA sub-model partitioned out the remaining total estimated annual number of deaths for each assessed non-fishing-related threat, using necropsy information to estimate the proportional causes of death.

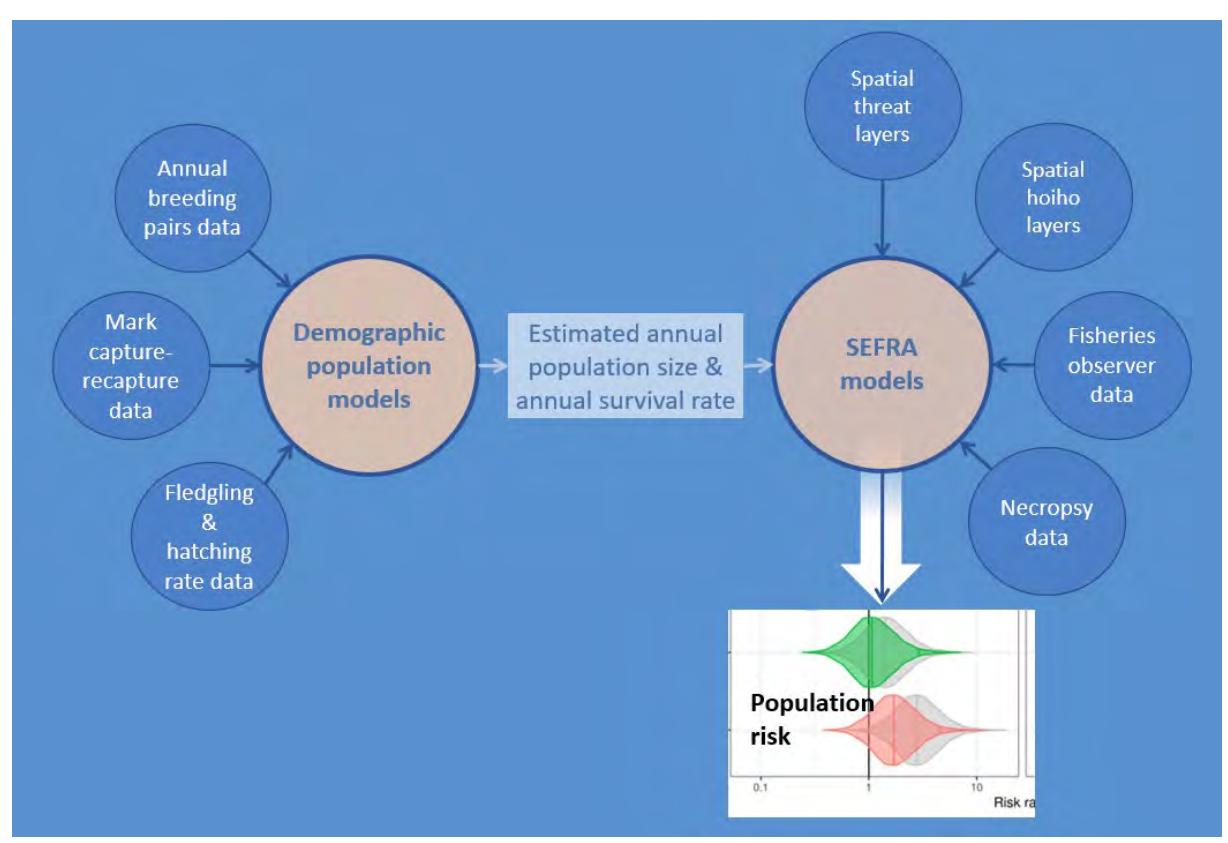


Figure 3: Schematic diagram of the risk assessment approach for threats for which we have mortality rate information, showing data inputs (blue circles), posteriors of the population model used to generate priors of the SEFRA model (white squares and thin arrows) and model outputs (white square and thick white arrow). Note that the demographic population models were also used to simulate future population size conditional on alternative assumed demographic rates.

Furthermore, the population models developed under item 1 were used to simulate future population trajectories under alterative assumptions of future demographic rates. The purpose being to identify target demographic rates of chicks, juvenile, and adults consistent with achieving population stability (i.e., the primary goal of the Hoiho Action Plan).

For threats for which quantitative information about mortality rate **was lacking**, although spatial threat intensity information **was available** (i.e., some non-fisheries threats and recreational netting) the assessment was based on relative spatial overlap only (following the approach of Roberts et al. 2019). For each regional sub-population, the relative overlap was calculated between yellow-eyed penguins and each marine/terrestrial threat. Because, for these threats, we lacked mortality rate information given the degree of overlap, the overlap units were not meaningful except in a comparative sense. Thus, while it was not possible to estimate annual deaths and risk using this method, it was possible to make comparison of the relative threat intensity experienced by the different regional sub-populations.

For threats for which we **lack** quantitative information about mortality rate or spatial threat intensity information **was not readily available** the assessment was based on qualitative discussion only. Thus, for these threats the assessment of risk was purely qualitative, although some comparison was still possible.

Additionally, following the basic approach of Mattern et al. (2017), a correlative approach was used for relating changes in sea surface temperature with estimated annual survivorship of yellow-eyed penguins for different life stages and regional sub-populations.

Initially, the risk assessment only used data from females to account for probable sex-specific differences in demographic rates, consistent with the significant male bias in birds observed at breeding colonies (Richdale 1957), and mortality rates from different threats (e.g., following the approach of Large et al. 2019). However, the assessment was subsequently extended to include males, given that males are captured in comparable numbers by commercial fisheries and that the required data inputs for males and females were generally of similar quality. This also facilitated the comparison of the demographic rates likely to be most responsible for the male bias in birds seen at the breeding colonies.

2.2 Selection of threats

The selection process for the list of potential threats to yellow-eyed penguin that would be addressed by this assessment was as follows:

- 1. Based on a review of the literature (e.g., Webster 2018), an initial list of threats that could be assessed was drafted and presented to the members of the AEWG (21 March 2023) and at a dedicated project workshop (hosted by Fisheries New Zealand 18 May 2023).
- 2. Finalise the list of threats to be addressed by the risk assessment based on reviewer recommendations.

Following this process, the threats/causes of death addressed by this risk assessment are listed in Table 1 along with the respective risk assessment methods used for each threat.

Table 1: Summary of threats considered by this risk assessment and methods used.

Threat Risk assessment method used

Commercial fishing – set net & trawl

Estimation of <u>spatially-explicit annual deaths and risk</u>

ratio using the standard SEFRA method

Malnutrition Estimation of <u>deaths only</u> using an extension of

Infectious diseases

SEFRA method. Note that specific aspects of some of these causes of death were also assessed based on relative spatial overlap or via qualitative discussion

Trauma (see below).

Predation by cats, stoats, New Zealand sea lions, or

sharks

Direct human/dog interactions

Road traffic

Fire

Recreational netting

Aquaculture

Oil pollution risk

Oceanic warming Correlative assessment, relative spatial overlap, and

qualitative review of the literature

Indirect effects of fishing on prey availability

Marine and terrestrial habitat degradation.

Pollution (pesticides & metals)

Scientific research

Qualitative discussion

Relative spatial overlap

2.3 Selection of regional sub-populations

For the purposes of this assessment, the northern population was divided into regional sub-populations (plotted in Figure 4), which were used in the development of demographic population models and for summarising outputs of the spatial risk assessment. These were based on the regionalisation used by other spatial assessments of yellow-eyed penguin (e.g., Mattern 2020), which specified outputs separately for (from north to south): North Otago, Otago Peninsula, Catlins, and Stewart Island / Rakiura. This assessment further divided the North Otago region into northern ('North Otago 1') and southern regions ('North Otago 2'), based on the differential population trajectories of hoiho in these areas and the movement of immature birds between them (see Section 3.2). A separate regional sub-population was also assumed for Banks Peninsula, noting the relative lack of demographic data available for this sub-population.

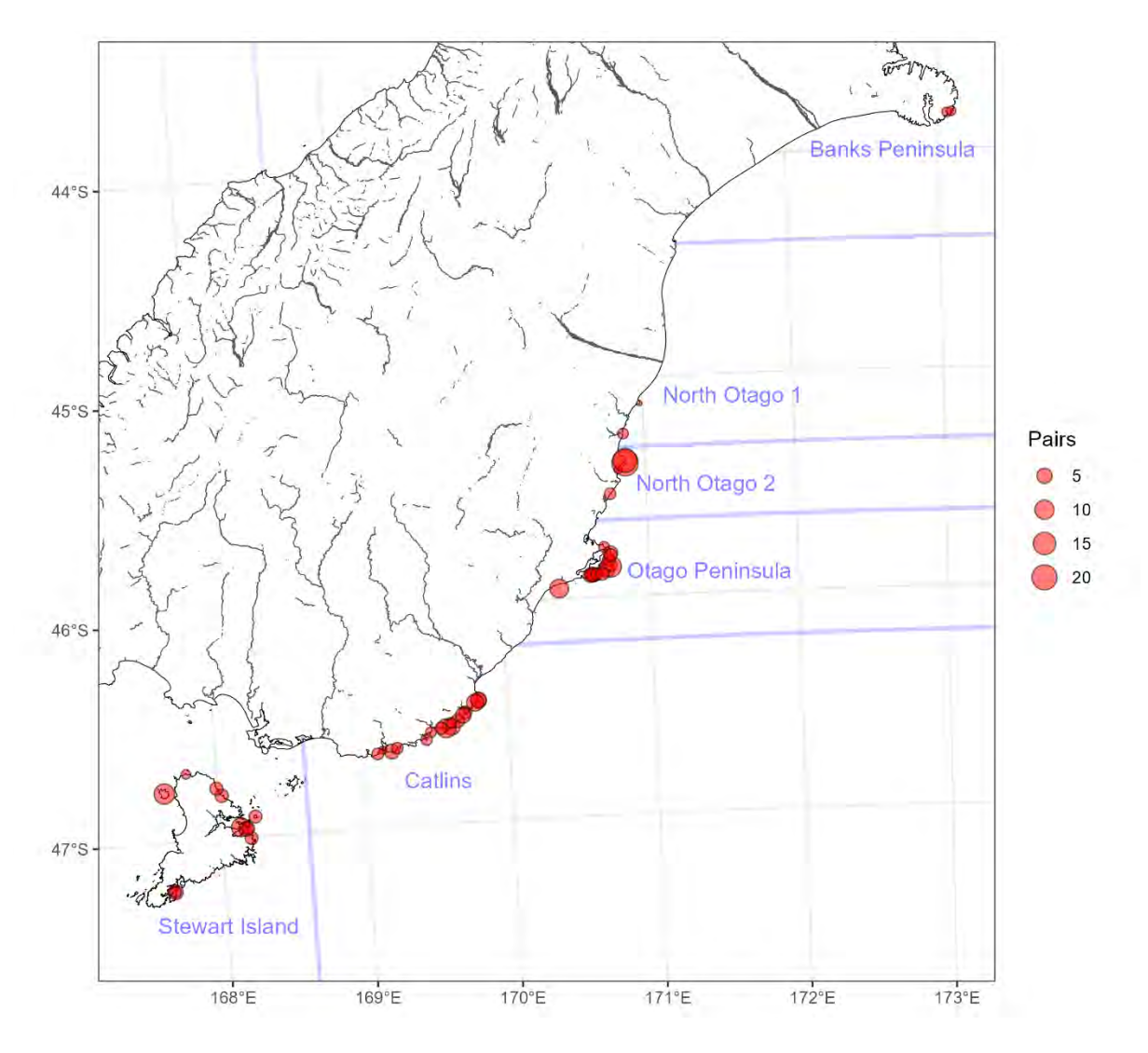


Figure 4: Locations of breeding colonies of the northern population of yellow-eyed penguin (DOC unpublished data), showing the number of breeding pairs and the bounds of regional subpopulation areas used by this assessment.

2.4 Risk assessment development process

The component inputs that were updated by this risk assessment were developed separately and evaluated prior to applying the respective risk assessment methods. This was to minimise the potential for bias to affect decision-making and to ensure the independent review of each set of inputs based on its own merits. Model estimates of annual deaths and risk ratios or relative spatial overlap plots/statistics were not produced until the development of all model inputs was well-advanced.

All inputs were reviewed on multiple occasions by members of Fisheries New Zealand's Aquatic Environment Working Group (AEWG) and by the members of the Hoiho Technical Group (HTG); and by the attendees of a dedicated workshop for this assessment (hosted by Fisheries New Zealand, 18 May 2023). The assessment methods were revised in accordance with many of the reviewer suggestions.

3. DEMOGRAPHIC POPULATION ASSESSMENT

This section describes a demographic population assessment for five of the six defined regional sub-populations of yellow-eyed penguin comprising the northern population (i.e., excluding the small and relatively data-poor Banks Peninsula population). In addition to estimating population change through time and identifying the demographic drivers of population change, the analysis in this section provided year-varying posteriors of annual survivorship and population size by age that were used by the SEFRA models (see Section 4) and by population projections, described in this section.

3.1 Methods

3.1.1 Model inputs

The demographic population models were fitted to several different types of data that were informative of population size and demographic rates, including:

- 1. observations of the annual number of breeding pairs (active nests) across regional subpopulations;
- 2. individual mark capture-recapture histories of known-age (banded as chicks) and unknown-age birds (banded as subsequent ages); and
- 3. observations of the number of chicks hatching and fledging from individual nests that was summarised into annual totals across regional sub-populations.

For all these sources, a subset of records was made including breeding seasons from 1990–91 (the first year with nest counts that can be resolved at the regional level) to 2020–21 (the final year of data in the extract of yellow-eyed penguin database (YEPDB) (Hickcox et al. 2023). Models were fitted separately to demographic mark-capture recapture histories of females and males, although these models used the same breeding pairs and hatching/fledging data, which were not gender-specific.

Breeding pairs

The estimated annual numbers of breeding pairs for each sub-population were derived from an extract of the Microsoft Excel workbook 'YEP breeding pairs on the mainland - DOCDM-28226', which was provided by DOC on 23 December 2022 (DOC, unpublished data). These data comprise annual minimum counts of active nests based on searches at known breeding locations from Banks Peninsula in the north to Stewart Island in the south. This workbook 'interpolated' the number of active nests in the years these were not counted at the respective breeding locations. The methods used to derive these estimates varied through time and by location. However, based on explorations of these data (presented to an AEWG meeting on 13 February 2023 and 21 March 2023), it was concluded that inaccuracies in these estimates would have a minor effect on the accuracy of estimates at the regional sub-population level. As such, these interpolations were combined with actual counts when compiling observations of the total number of breeding pairs by regional sub-population.

The Stewart Island counts are an exception to this, where it was considered that there was a considerable potential for even the more comprehensive counts to miss a substantial portion of the active nests. However, no attempt was made by the current assessment to account for any potential undercounting of nests at Stewart Island.

For breeding sites at the Banks Peninsula, an update to the number of active nests was provided by DOC (unpublished data), including historical counts from 1988–89 to 2022–23 that were not included in the main Excel workbook provided by DOC. The updated nest counts for Banks Peninsula were displayed in this report (see later), although were not used by this assessment, due to other data limitations for this region.

Mark capture-recapture histories

The mark capture-recapture data and nest-based data were both derived from records in the YEPDB, of which an extract of the full database was provided by DOC on 4 November 2022. This version of YEPDB was groomed and updated by Hickcox et al. (2023) and included records up to the end of the 2020–21 field season (where field seasons were defined by the current assessment to start 1 August, i.e., just prior to the start of breeding).

The mark-recapture histories of birds, by sex, were prepared primarily using records in the 'Marking' and 'Resightings' tables of YEPDB, using the 'BirdID' field to link observations in the two tables. The sex of each bird was based on information in the 'Sex' table, using the following hierarchy of data fields: 'SexVerified' (considered the most reliable information), 'SexDF', and then 'Sex' (least reliable).

A subset of birds was made including birds that were first marked with a flipper band, a microchip, or both mark types. The annual states of birds in subsequent years were determined based on observed breeding history, where an individual that was observed was considered immature until the season in which it was first recorded as breeding. Thereafter, these individuals were determined to be breeders or non-breeders depending on information in the 'AnnualStage' field of the 'Resightings' table. Birds that were recorded as being breeders and non-breeders in the same season were assumed to be breeders in that year.

The region used by a bird each season was determined by linking the resightings data to the 'Location' table of YEPDB. Where a bird was recorded as occurring in more than one region in a year, the region of the most recent preceding resighting year was used.

Based on initial data summaries, some temporal gaps in the resighting data were apparent. It was found that supplementing the resighting histories using individual breeding histories in the 'Nesting' table of YEPDB effectively filled most of these gaps.

Hatching and fledging rate data

Annual hatching and fledging rate frequencies, in terms of the number of monitored nests producing 0, 1, or 2 hatchlings/fledglings, were prepared using the information in the 'Nesting' table (i.e., the values given in 'NHatched' and 'NFledged' fields). The frequencies of hatchlings and fledglings were summed across all breeding locations for each respective regional sub-population.

3.1.2 Model states, parameters, and transitions

A bespoke demographic model for hoiho was coded in the Stan programming language (Stan Development Team 2023). The model tracked the number of female or male birds within a set of model states (k) by season (t; from 1991 to 2023), denoted $x_{k,t}$ (Table 2). The model states included immature birds aged 0 to 4 years old (codes 'I0', 'I1', 'I2', 'I3', and 'I4'). All birds were assumed to be mature by age 5. Once mature, a bird was either classified as a breeder ('B') or a non-breeder ('NB') and the model no longer kept track of a bird's age, which was only used to estimate maturation rate (see below). An overview of the model states and possible transitions for a single region is shown in Figure 5. The model also kept track of the number of dead birds ('D') in the model population, so that the rows of the transition matrix always summed to one. A summary of the estimated model parameters is given in Table 3.

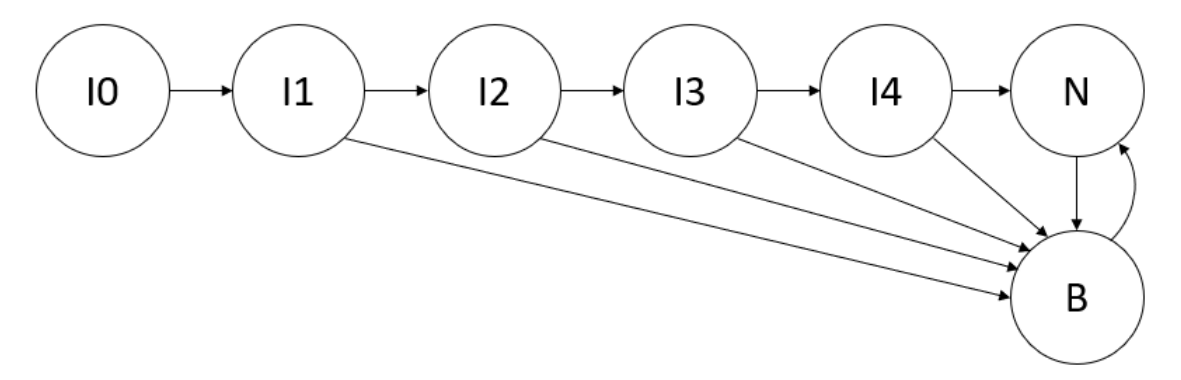


Figure 5: Schematic diagram of the model states for demographic population models and possible transitions between them. This only shows the transitions with a single region, so excludes the states for multiple regions and transitions between regions. The codes used for each model state are defined in Table 2.

Table 2: Model states and observable states.

Age	Maturity	Model	states	Observation states				
		Code	Notation	Description	Code	Notation	Description	
0	Immature	I0	$x_{\mathrm{I0},t}$	Fledglings	10	$y_{10,t}$	Fledglings	
1	Immature	I1	$x_{\mathrm{I1}.t}$	Immature age 1	I1	$y_{11.t}$	Immature age 1	
2	Immature	I2	$x_{12,t}$	Immature age 2	I2	$y_{12,t}$	Immature age 2	
3	Immature	I3	$x_{\mathrm{I3},t}$	Immature age 3	I3	$y_{13,t}$	Immature age 3	
4	Immature	I4	$x_{\mathrm{I4},t}$	Immature age 4	I4	$y_{14,t}$	Immature age 4	
2+	Mature	В	$x_{\mathrm{B},t}$	Breeder	В	$y_{\mathrm{B},t}$	Breeder	
1+	Mature	NB	$x_{\mathrm{NB}.t}$	Non breeder	NB	$y_{\mathrm{NB},t}$	Non breeder	
_	_	D	$x_{\mathrm{D}t}$	Dead	NS	$y_{NS,t}$	Not seen	

Table 3: Estimated model parameters.

Notation	Description
<i>N</i> ⁰	Initial number of birds
ω_k	Proportion of the initial number of birds within each state
ϕ_t^{0}	Probability of survivorship for chicks (I0)
ϕ_t^{1+}	Probability of survivorship for all other states (I1, I2, I3, I4, B, N)
$oldsymbol{\eta}_t = \{\eta_t^{\mathrm{I1}}, \eta_t^{\mathrm{I2}}, \eta_t^{\mathrm{I3}}\}$	Probability of an immature (I1, I2, or I3) becoming a breeder
γ_t	Probability of a non-breeder (I4 or N) becoming a breeder
$egin{array}{c} {\gamma}_t \ {\delta}_t \end{array}$	Probability of a breeder (B) remaining a breeder
$\boldsymbol{\psi}_{t} = \{\psi_{t}^{0}, \psi_{t}^{1}, \psi_{t}^{2}\}$	Proportion of breeders hatching 0, 1, or 2 chicks
$arphi_t$	Proportion of hatchlings surviving to become fledglings
$r_{a,t}^{ m NB} \ r_{a,t}^{ m B}$	Probability that a non-breeder (I0, I1, I2, I3, I4, N) is observed
$r_{a,t}^{\mathrm{B}}$	Probability that a breeder (B) is observed
$\kappa_{a o b}$	Probability of moving from region a to region b .

The number of female or male birds in each state in 1990–91(the first model year) was:

Equation 1:
$$x_{k,1} = N^0 \omega_k$$

where N^0 was the total number of birds in 1990–91, and ω_k was the proportion of birds in each of the model states (Table 2). The number of chicks hatched could either be 0, 1, or 2 individuals and the total number of female or male chicks hatched (N_t^{hatch}) at each time step was defined as:

Equation 2:
$$N_t^{\text{hatch}} = 0.5(\psi_t^1 x_{B,t} + 2\psi_t^2 x_{B,t})$$

where the 0.5 was used because each breeding female is assumed to produce a chick with a 50% probability of being female (Richdale 1957). The likelihood for the number of hatchlings was:

Equation 3:
$$N_t^{\text{hatch}} \sim \text{multinomial}(\psi_t)$$

The total number of female or male chicks fledged at each time step was also defined as the number recruiting to the model as:

Equation 4:
$$N_t^{\rm fledge} = x_{{\rm I}0,t} = N_t^{\rm hatch} \varphi_t$$

$$\varphi_t = \frac{N_t^{\rm fledge}}{N_t^{\rm hatch}}$$

where φ_t was the proportion of hatchlings that survive to become fledglings each time step. The likelihood for the number of hatchlings and fledglings were:

Equation 5:
$$N_t^{\text{fledge}} \sim \text{binomial}(N_t^{\text{hatch}}, \varphi_t)$$

The number of chick deaths each year was defined as:

Equation 6:
$$N_t^{\text{hatch}} - N_t^{\text{fledge}} = N_t^{\text{hatch}} (1 - \varphi_t)$$

The likelihood for the number of breeding pairs was:

Equation 7:
$$N_t^{\rm B} \sim \mathcal{N}(x_{{\rm B},t}, \sqrt{x_{{\rm B},t}})$$

The transition between model states due to ageing, maturation, or death was defined as a deterministic process using transition probabilities:

Equation 8:
$$N(x_{k,t}) = \sum_{j} N(x_{j,t-1}) \cdot p(x_{k,t-1})$$
$$\sum_{k} N(x_{k,t}) = \sum_{k} N(x_{k,t-1})$$

where $p(x_{k,t-1})$ is the probability of transitioning from state j to state k during time step t. The transition probabilities, not including movement, are defined in Table 4. For example:

$$p(x_{\mathrm{I}1,t}|x_{\mathrm{I}0,\mathrm{t}-1}) = \phi_t^0$$

defines the probability of transitioning from state I0 to I1 and is defined as the probability of survivorship for chicks (ϕ_t^0). The chicks that do not survive are placed in the dead state D using the probability:

$$p(x_{D,t}|x_{I0,t-1}) = 1 - \phi_t^0$$

hence, the transition probabilities for state I0 sum to one (i.e., all rows of Table 4 sum to one).

Table 4: Transition probabilities from time t-1 to time t. Note that this table does not include movement probabilities.

	t							
t-1	<u>I0</u>	I1	I2	I3	I4	В	N	D
10	_	ϕ_t^0	_	_	_	_	_	$1 - \phi_t^{0}$
I1	_	_	$\phi_t^{1+}(1-\eta_t^{11})$	_	_	$\phi_t^{1+}\eta_t^{\text{I}1}$		$1 - \phi_t^{1+}$
I2	_	_	_	$\phi_t^{1+}(1-\eta_t^{12})$	_	$\phi_t^{1+}\eta_t^{12}$	_	$1 - \phi_t^{1+}$
I3	_	_	_	_	$\phi_t^{1+}(1-\eta_t^{13})$		_	$1 - \phi_t^{1+}$
I4	_	_	_	_	_	$\phi_t^{1+}\gamma_t$	$\phi_t^{1+}(1-\gamma_t)$	$1 - \phi_t^{1+}$
В	_	_	_	_	_		$\phi_t^{1+}(1-\delta_t)$	
N	_	_	_	_	_	$\phi_t^{1+}\gamma_t$		
D	_	_	_	_	_	_	_	1

The mark recapture data were used to inform the transition probabilities (Table 4) between model states (Table 2) and were linked using observation or resight probabilities (Table 5). For example, $y_{B,t}$ identifies a tagged individual that was observed at time t as a breeder (state B) and was observed with probability:

$$p(y_{B,t}|y_{B,t}) = r^{B}$$

where $r^{\rm B}$ is the probability of observing a breeder. Likewise, the probability of not seeing a breeder, conditional on it being alive, was:

$$p(y_{\mathrm{NS},t}|y_{\mathrm{B},t}) = 1 - r^{\mathrm{B}}$$

Table 5: Resight probabilities between model states and observed states.

							Obser	ved state
Model state	I0	I1	I2	I3	I4	В	N	NS
I0	$r^{ m NB}$	_	_	_	_	_	_	$1-r^{\rm NB}$
I1	_	$r^{ m NB}$	_	_	_	_	_	$1-r^{\rm NB}$
I2	_	_	$r^{ m NB}$	_	_	_	_	$1-r^{\rm NB}$
I3	_	_	_	$r^{ m NB}$	_	_	_	$1-r^{\rm NB}$
I4	_	_	_	_	$r^{ m NB}$	_	_	$1-r^{\rm NB}$
В	_	_	_	_	_	$r^{ m B}$	_	$1 - r^{B}$
N	_	_	_	_	_	_	$r^{ m NB}$	$1-r^{\rm NB}$
D	_	_	_	_	_	_	_	1

3.1.3 Priors and constraints

The proportion of breeders hatching zero (ψ_t^0) , one (ψ_t^1) , or two (ψ_t^2) chicks was defined to sum to one each season:

$$\begin{split} \boldsymbol{\psi}_t &= \{\psi_t^0, \psi_t^1, \psi_t^2\}\\ \psi_t^0 + \psi_t^1 + \psi_t^2 &= 1 \, \forall t \end{split}$$

The probability of an immature bird (I1, I2, or I3) becoming a breeder was constrained to be higher for older immature classes:

$$\eta_t^{\text{I}1} \le \eta_t^{\text{I}2} \le \eta_t^{\text{I}3} \quad \forall t$$

Uninformative priors were defined for most model parameters:

$$N^{0} \sim \mathcal{N} \left(100, 1000^{2}\right)$$

 $\omega_{k} \sim \text{Dirichlet}(1, ..., 1)$
 $\gamma_{t} \sim \text{Beta}(1, 1)$
 $\delta_{t} \sim \text{Beta}(1, 1)$
 $\kappa \sim \text{Beta}(1, 2)$
 $r^{\text{NB}} \sim \text{Beta}(1, 1)$
 $r^{\text{B}} \sim \text{Beta}(1, 1)$

A prior was placed on the number of individuals in the I0 state during the first year:

Equation 9:
$$x_{\text{I}0,1} \sim \mathcal{N}\left(\mu_{\text{I}0}, \sqrt{\mu_{\text{I}0}}^2\right) \\ \mu_{\text{I}0} = 0.5 \left(\psi_t^1 x_{\text{B},t} + 2\psi_t^2 x_{\text{B},t}\right)$$

The proportion of breeders hatching 0, 1, or 2 chicks (ψ_t), probability of survivorship each time step (ϕ_t^0 and ϕ_t^{1+}), and the proportion of a hatchlings surviving to become a fledgling (φ_t) were treated as random effects and set up as:

$$\psi_{t} \sim \operatorname{Beta}(\alpha_{\psi}, \beta_{\psi})$$

$$\alpha_{\psi} \sim \operatorname{Student}(3, 0, 2.5^{2})$$

$$\beta_{\psi} \sim \operatorname{Student}(3, 0, 2.5^{2})$$

$$\phi_{t}^{0} \sim \operatorname{Beta}(\alpha_{\phi^{0}}, \beta_{\phi^{0}})$$

$$\alpha_{\phi^{0}} \sim \operatorname{Student}(3, 0, 2.5^{2})$$

$$\beta_{\phi^{0}} \sim \operatorname{Student}(3, 0, 2.5^{2})$$

$$\phi_{t}^{1+} \sim \operatorname{Beta}(\alpha_{\phi^{1+}}, \beta_{\phi^{1+}})$$

$$\alpha_{\phi^{1+}} \sim \operatorname{Student}(3, 0, 2.5^{2})$$

$$\beta_{\phi^{1+}} \sim \operatorname{Student}(3, 0, 2.5^{2})$$

$$\varphi_{t} \sim \operatorname{Beta}(\alpha_{\varphi}, \beta_{\varphi})$$

$$\alpha_{\varphi} \sim \operatorname{Student}(3, 0, 2.5^{2})$$

$$\beta_{\varphi} \sim \operatorname{Student}(3, 0, 2.5^{2})$$

$$\beta_{\varphi} \sim \operatorname{Student}(3, 0, 2.5^{2})$$

Alternatively, an AR(1) process was trialled, although was not retained in any of the final model runs because the parameters tended to wander off in either the first year, the last year, or both the first and last year.

3.1.4 Model regions and movement

Using multi-region models allowed the estimation of movement rates of immature birds, and also facilitated the sharing of population parameters across different model regions. Using the model described above, two separate model runs were done using the observations from different combinations of regional populations:

- North Otago 1 and North Otago 2 (the **northern model**); and
- Otago Peninsula, Catlins, and Stewart Island (the southern model).

These models were repeated for females and males. Models included the seven live model states for each of the regional populations, as well as the state for dead birds applied across all regions, giving a total of 15 model/observation states for the northern population and 22 for the southern model.

The relocation of immature birds between regional sub-populations was represented using movement parameters. The annual proportion of birds moving between regions was defined as $\kappa_{a\to b}$ which is the probability of moving from one region a to another region b. Based on the outputs of initial model exploration, a non-trivial proportion of females moved between North Otago 1 and North Otago 2, and from the Catlins to Otago Peninsula (Figure B.7). Accordingly, movement was permitted between each of these two regional pairings, but not between Stewart Island and the other southern model regions. This was because no birds marked at Otago Peninsula or the Catlins were subsequently observed at Stewart Island and, while one bird marked at Stewart Island was seen at Otago Peninsula (and a few more at North Otago 2), none were observed breeding anywhere else (Figure B.7). Note that not permitting movement between Stewart Island and the other regions of the southern model required the removal from the mark capture-recapture data of the solitary female that relocated from Stewart Island to the Otago Peninsula.

3.1.5 Population projections

Sex and sub-population level demographic rates used for doing model projections were derived from the demographic model. The projected probability of hatching 0, 1, or 2 chicks was the mean by area and sex from 2016–2020, estimates were replaced from 2021 (Figure B.67). The projected chick survival was based on the mean and standard deviation (SD) from 2016–2020 (Figure B.68). Projected juvenile survival was based on the mean and SD from 2013–2017 for North Otago 1 and North Otago 2 and 2015–2019 for Otago Peninsula, Catlins, and Stewart Island (Figure B.69). Projected adult survival was based on the mean and SD from 2018–2022 (Figure B.69). The annual probability of breeding was set to be the same as the time invariant annual probability of breeding in the demographic model. A 22-year projection was done from 2024 to 2045. Demographic scenarios that projected alternative levels of lower chick, juvenile, or adult mortality rates were also done. These mortality rates were reduced by 0% (no alleviation) to 100% (full alleviation), in 10% increments.

3.2 Results

3.2.1 Population model inputs

Summary plots of the data inputs to the population models are shown in Appendix B. At a subregional level, interpolated numbers of breeding pairs appeared to be reasonable given the data in adjacent years for which there were counts (Figure B.1 to Figure B.5). The interpolated number of breeding pairs by regional sub-population is shown in Figure B.6. For North Otago 1, North Otago 2, and Otago Peninsula, the annual totals based only on counted nests (open circles in Figure B.6) was similar in most years to the interpolated value across all breeding locations (closed circles), indicating that few nests were left uncounted in most years. For Stewart Island, most nests were not counted in the typical year, with much higher total counts in the years with the more comprehensive surveys (1999–00, 2008–09, 2020–21). Thus, for Stewart Island, it was decided only to use estimates from these three years of most comprehensive counting. Note that the earlier estimate for Stewart Island in 1992–93 was not used, since this was largely based on extrapolation and was deemed by members of HTG to be much less reliable than the later more comprehensive counts.

For both sexes, chicks were marked in most years in North Otago 1 (Figure B.8), North Otago 2 (Figure B.9), and Otago Peninsula (Figure B.10). However, there were some temporal gaps in the marking effort at the Catlins (Figure B.11) and Stewart Island (Figure B.12), and an apparent low subsequent resighting rate of birds marked at Stewart Island (Figure B.12).

There was reasonably good sampling coverage with respect to year and region in the observations of the number of chicks hatching (Figure B.13) and fledging (Figure B.14).

3.2.2 Population model outputs

This subsection describes the outputs of the northern and southern demographic population model runs for females and males (i.e., a total of four model runs). Key outputs are shown in the main text and other associated tables and figures are shown in Appendix B, which are shown for the female northern model (Table B.4 and Figure B.15 to Figure B.27), the male northern model (Table B.5 and Figure B.28 to Figure B.40), the female southern model (Table B.6 and Figure B.41 to Figure B.53), and finally the male southern model (Table B.7 and Figure B.54 to Figure B.66).

There was no evidence of non-convergence for any of these model runs (Table B.4 to Table B.7, Figure B.15, Figure B.28, Figure B.41, and Figure B.54). The posteriors for the **northern model** were summarised for females (Figure B.16 and Table B.4) and males (Figure B.29 and Table B.5). The posteriors for the **southern model** were also summarised for females (Table B.6 and Figure B.42), and for males (Table B.7 and Figure B.55).

Good model fits were achieved for all regional sub-populations to: annual breeding pairs data (Figure B.17, Figure B.30, Figure B.43, and Figure B.56); annual number of chicks hatching observations (Figure B.18, Figure B.31, Figure B.44, Figure B.57); annual number of chicks fledging observations for females (Figure B.19 and Figure B.45) and for males (Figure B.32 and Figure B.58), and the mark capture-recapture data for females (Figure B.20 and Figure B.46) and for males (Figure B.33 and Figure B.59).

Posterior distributions of selected model parameters for the **northern model** are shown in Figure B.21 to Figure B.27 (females) and in Figure B.34 to Figure B.40 (males). These outputs are consistent with:

- a major decrease in sighting probability of all breeding stages since 1998–99,
- around 10% of immature birds moving from North Otago 1 to North Otago 2 each year,
- fluctuation in chick survival rate through time,
- protracted periods of high and low juvenile survival through time,
- annual survival probability of adults ranging from 0.85 to 0.90, with occasional years of lower rates,
- generally better adult survival rates for males than females (comparing Figure B.26 and Figure B.39), and
- most individuals breeding for the first time by age 4.

The analogous plots of posteriors are shown for the **southern model** in Figure B.47 to Figure B.53 (females) and Figure B.60 to Figure B.66 (males). These outputs are consistent with:

- a smaller decrease in sighting probability since 1998–99 (compared with the northern model outputs).
- around 10% of immature birds moving from the Catlins to Otago Peninsula each year,
- fluctuation in chick survival rate through time and greater chick survival rate at the Catlins relative to the other regional sub-populations,
- periods of high and low juvenile survival through time that generally agree with the patterns form the northern model (i.e., lower survival rate in 2006–07 to 2014–15),
- annual survival probability of adults ranging from 0.75 to 0.95, with generally lower survival rate of adults at Otago Peninsula and Stewart Island than at the Catlins, and
- generally better juvenile survival rate for males than females (comparing Figure B.51 and Figure B.64).

The estimated annual number of females across all regions has declined markedly over the past decade for chicks, fledglings, non-breeders, and breeders alike (Figure 6). The estimated annual number of female breeders by regional sub-population are consistent with a decline in the most recent years for all regional sub-populations apart from North Otago 2, which was estimated to have been stable across the final five model years. (Figure 7).

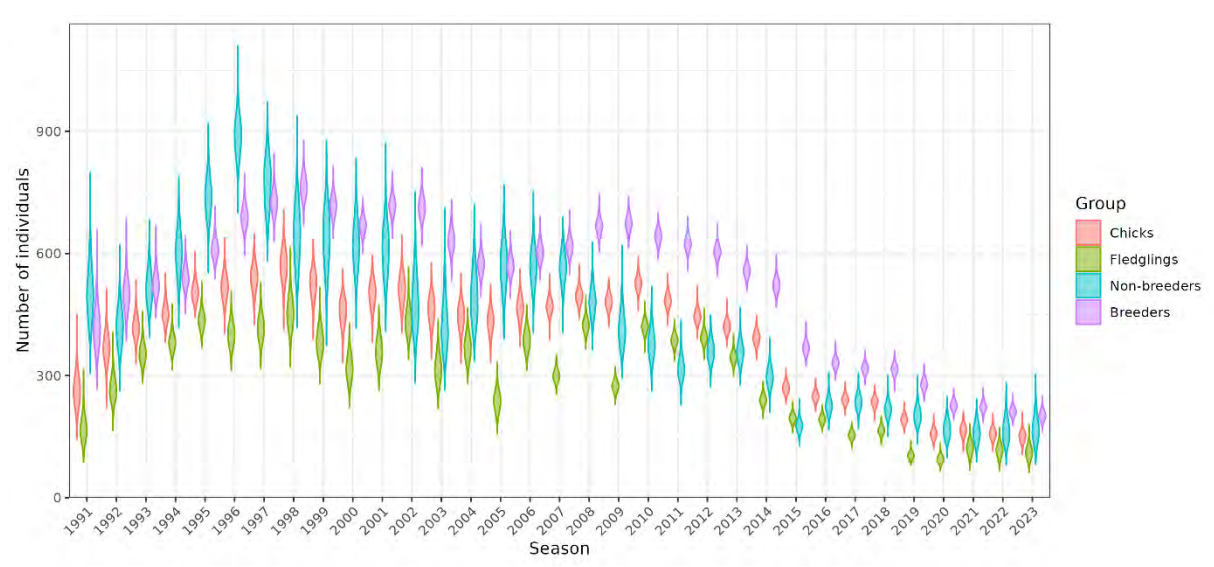


Figure 6: Posterior distributions of the number of <u>females</u> by fishing year and age-stage group, across all regional sub-populations.

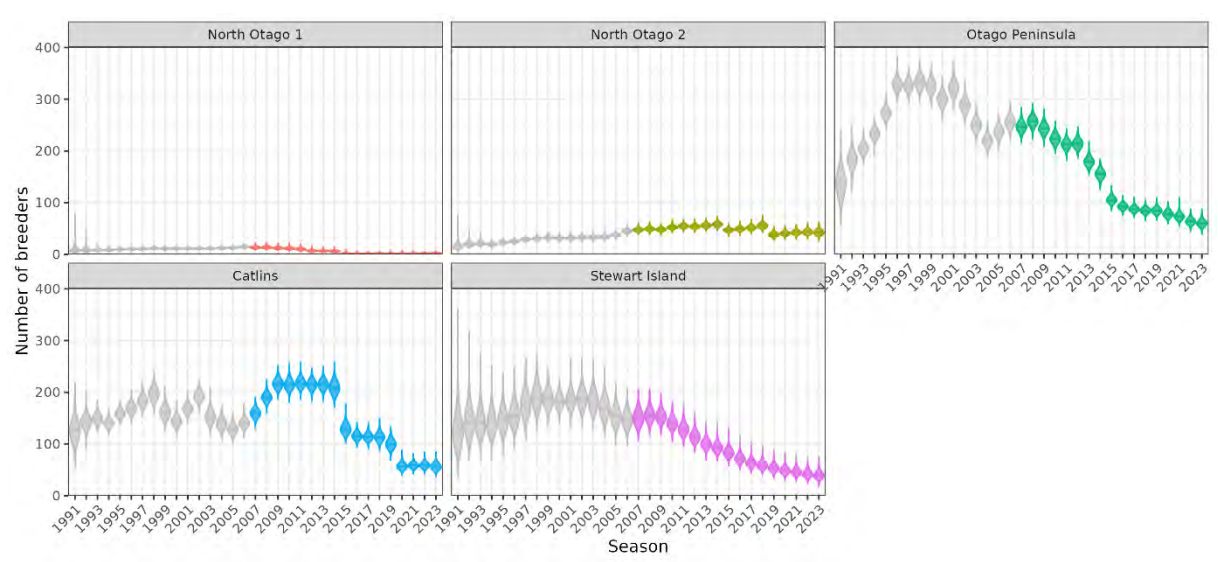


Figure 7: Posterior distributions of the number of the of <u>female</u> breeders by season and region from the demographic population models (grey violins), and posterior distributions from the SEFRA model (coloured violins).

The total estimated number of annual female deaths for chicks, juveniles, and adults has also declined markedly over the past five years or so as the population has declined (Figure 8). The number of birds dying in each of these age groups is approximately equal in the average year. However, the number of juvenile deaths fluctuates much more than that of adults, which generally tracks changes in breeder numbers over time (comparing with Figure 6). Estimated chick mortalities alternated between years of high and low survival rate between 2000–01 and 2009–10 (Figure 8). However, there appear to be regional differences in the mortality rate of females at different ages (Figure 9, e.g., relatively low chick mortality rate at the Catlins compared with the same comparison at Otago Peninsula).

The posteriors of population size by age group and regional sub-population were used as inputs for the SEFRA models described in the next section, along with posteriors of annual survival for different age groups.

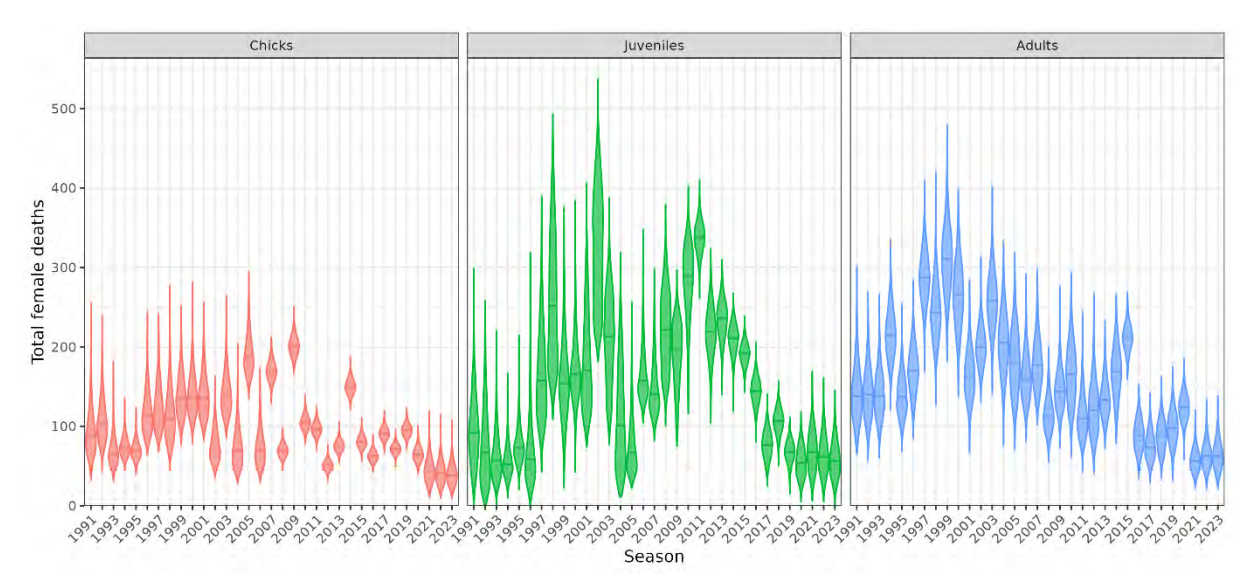


Figure 8: Posterior distributions of the number of female deaths by season and age group, across all regional sub-populations.

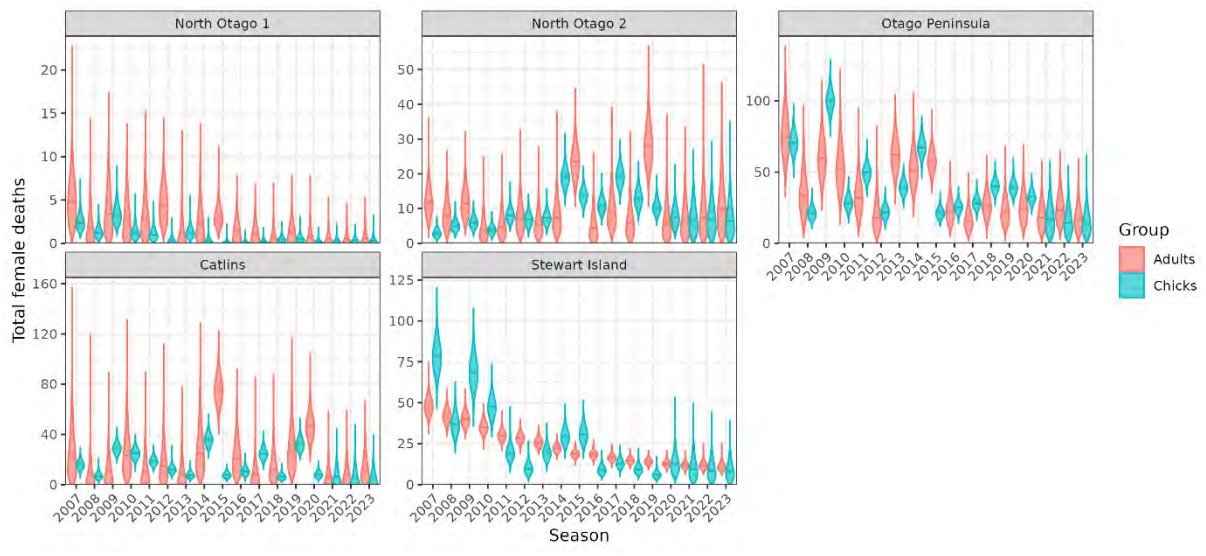


Figure 9: Posterior distributions of the number of female deaths by season and regional sub-population, comparing chicks and adults.

3.2.3 Population projections

With the continuation of recent demographic rates, the total population size for all sub-populations was predicted to decline in the future for both females and males (Figure B.70). The decline by the year 2045 was predicted to be greatest for the southern model sub-populations (Otago Peninsula, Catlins, and Rakiura), which were collectively predicted to number fewer than 70 birds (females and males, CI 44.2 - 114) by the year 2045. By comparison, the North Otago sub-populations were predicted to decline much less, although the overall population size of these is relatively small compared with the other sub-populations comprising the northern population.

The effect of alleviating chick mortality was comparatively meagre, with even 100% alleviation of chick mortality still resulting in population decline of <u>mature</u> birds in the northern population (Figure 10). When assuming a 50% alleviation of either juvenile (Figure 11) or adult (Figure 12) mortality rate, the <u>mature</u> population trend was predicted to stabilise, with increasing population trends predicted at even higher rates of alleviation.

The same predictions were also shown broken down by sub-population (Figure B.71, Figure B.72, Figure B.73), which indicated that future population stability may be achieved using less extreme reductions in mortality rate for the North Otago populations, whereas greater reductions in mortality rate would be required to stop population decline for the other sub-populations. For example, population stability at North Otago might be achieved by alleviating chick mortality rate only, compared with a minor effect of chick mortality alleviation at the northern population level (comparing Figure 10 with Figure B.71). In another example, near full alleviation of juvenile mortality would be required to stabilise the Catlins population (Figure B.72).

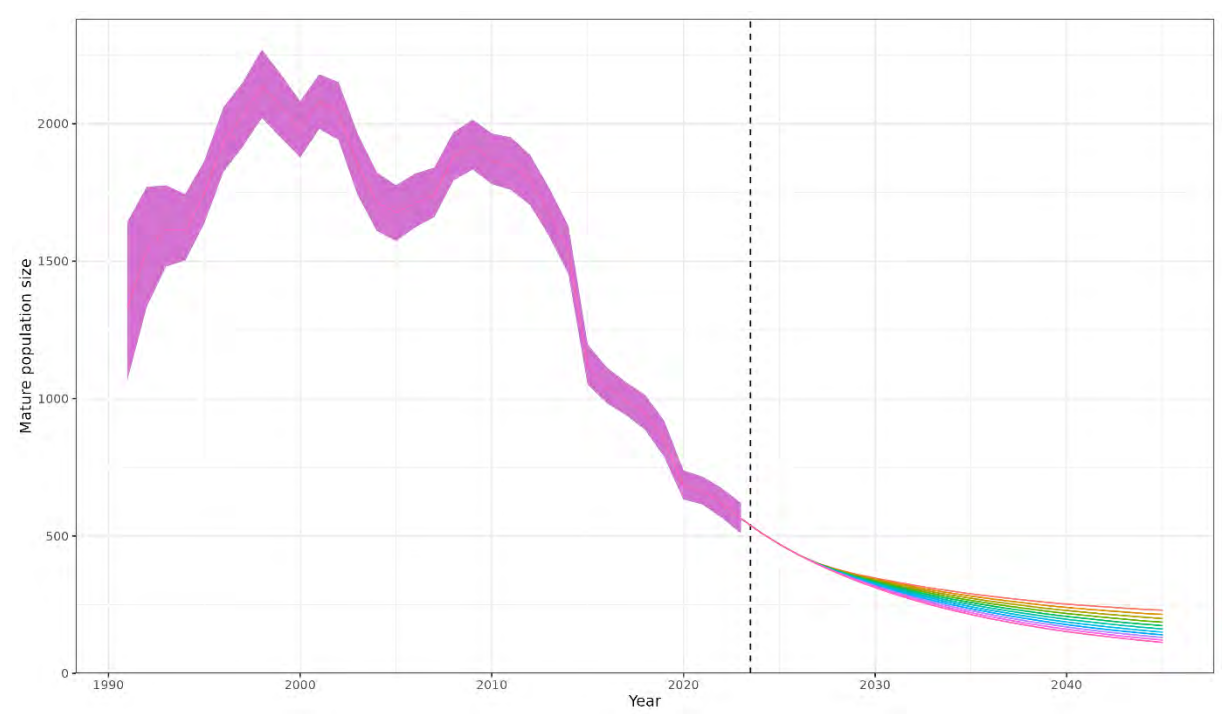


Figure 10: Predicted mature population size across the northern population assuming alternative future levels of chick mortality rate, ranging from 0% alleviation of recent rates (the bottom projection line) up to 100% alleviation (the top projection line) in 10% increments. The shaded period up to 2025 represents the 95% credible interval of the combined predictions of the male and female models.

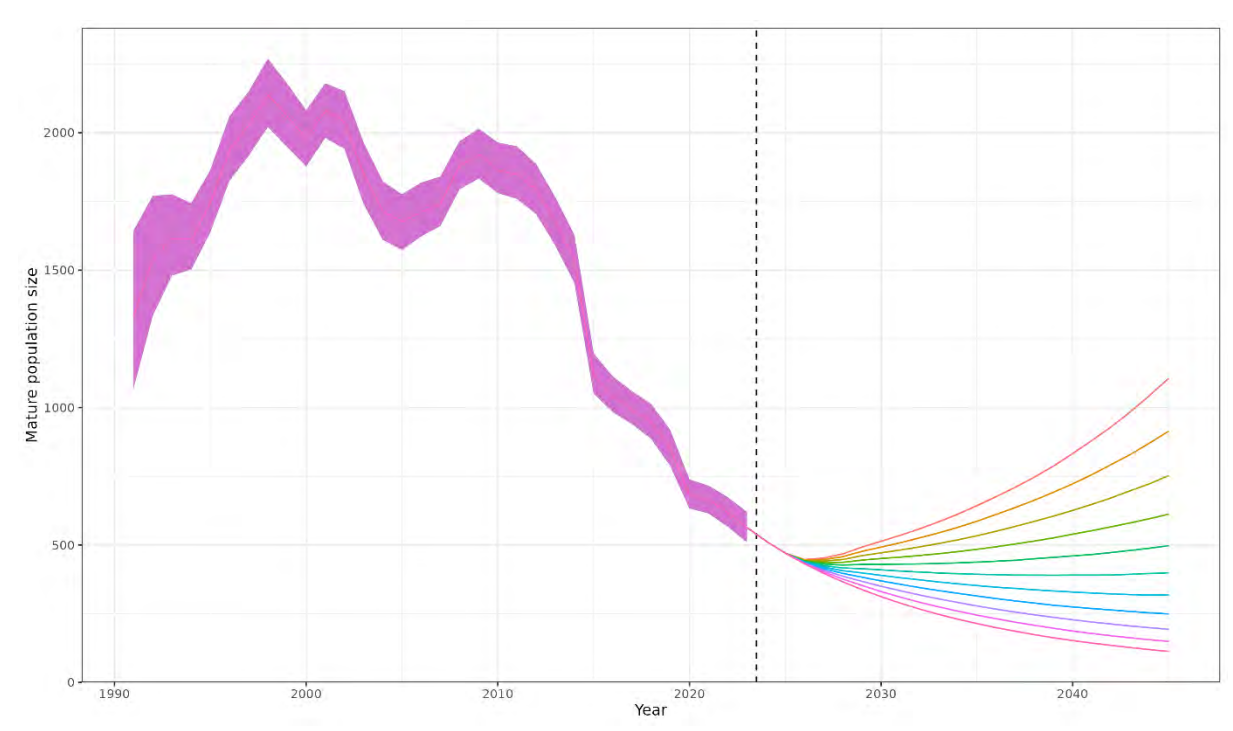


Figure 11: Predicted mature population size across the northern population assuming alternative future levels of <u>juvenile mortality</u> rate, ranging from 0% alleviation of recent rates (the bottom projection line) up to 100% alleviation (the top projection line) in 10% increments. The shaded period up to 2025 represents the 95% credible interval of the combined predictions of the male and female models.

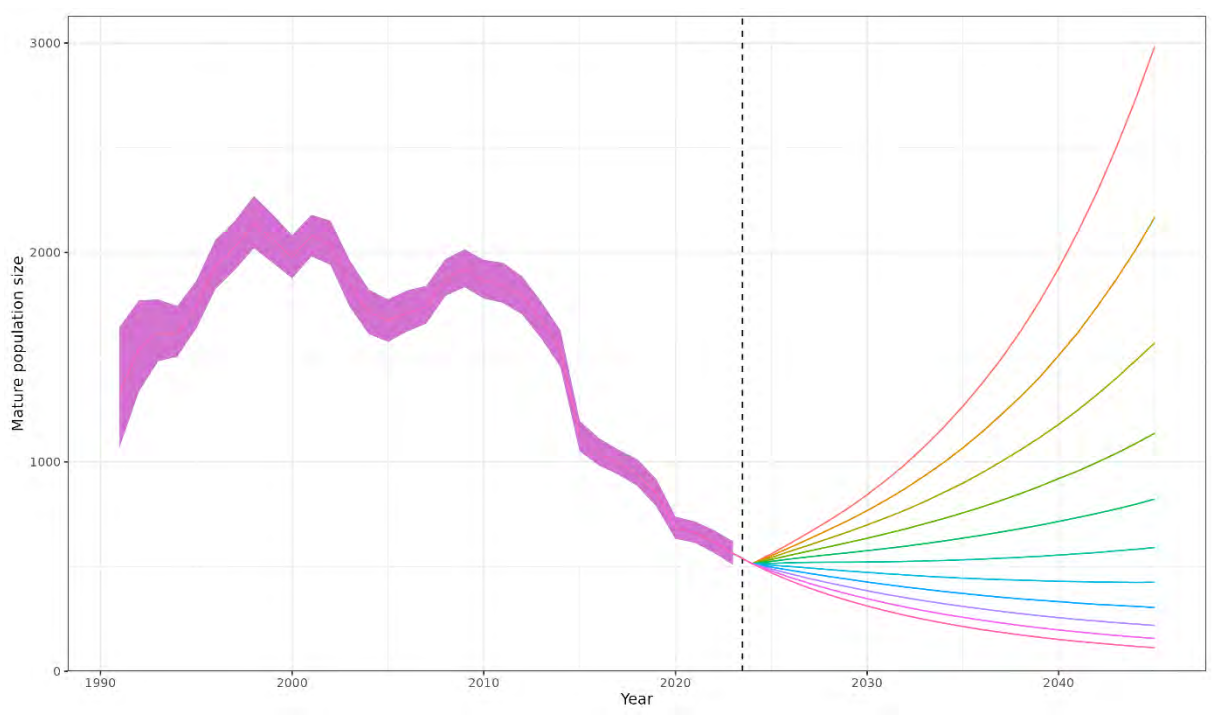


Figure 12: Predicted mature population size across the northern population assuming alternative future levels of <u>adult mortality</u> rate, ranging from 0% alleviation of recent rates (the bottom projection line) up to 100% alleviation (the top projection line) in 10% increments. The shaded period up to 2025 represents the 95% credible interval of the combined predictions of the male and female models.

4. SPATIALLY EXPLICIT FISHERIES RISK ASSESSMENT (SEFRA)

This section describes a SEFRA model (Sharp 2018) which estimated annual deaths and risk relating to direct interactions with commercial fisheries and from other major causes of death in the necropsy records (Appendix A).

4.1 Methods

The spatial risk model for yellow-eyed penguins was based on the SEFRA method, in which risk (*R*) is expressed as the ratio between a threat-specific estimate of deaths in the numerator and a 'Population Sustainability Threshold' (PST) in the denominator. The PST was inspired by the Potential Biological Removal (PBR) approach used for identifying anthropogenic mortality thresholds for wild marine megafauna populations (Wade 1998). As with the PBR approach, the SEFRA method estimates annual threat-specific mortalities and relates these to a mortality threshold (PST instead of PBR)—the maximum number of annual deaths that a population unit can sustain without impacting on a population recovery objective. The estimation of annual deaths (*D*) by SEFRA models is spatially-explicit—i.e., it accounts for spatial overlap when estimating threat-specific threats from information on capture rate.

4.1.1 SEFRA inputs

The various information sources used in the SEFRA calculation of annual deaths and risk ratio are shown in Figure 13. This calculation requires information with respect to:

- The spatial abundance of the study species;
- Spatially-resolved mortality rate information (e.g., commercial fisheries observer records) pertaining to a threat; and
- Total spatial intensity of a threat (e.g., all commercial set net fishing effort records, including observed and unobserved), so that mortality rate information from above can be used to predict the total number of deaths relating to a threat given spatial overlap.

The derivation of PST requires information with respect to:

- Intrinsic population growth rate (r^{\max}) ;
- A specified population reference outcome to inform the choice of the calibration coefficient
 (φ). The reference outcome is expressed in terms of recovery to and/or stabilisation of the impacted population at a defined proportion of the unimpacted population state, at equilibrium;
 and
- Estimates of annual population size (note that this is also used for estimating *D*).

All of these inputs were estimated/updated by the risk assessment for yellow-eyed penguin, with the exception of the intrinsic population growth rate (r^{\max}), for which the posterior from a recent study estimating this for yellow-eyed penguin was used (Edwards et al. 2023a); and the calibration coefficient (ϕ), for which Fisheries New Zealand specified a value of 0.2, consistent with population recovery to at least 90% the unimpacted population state under a default assumption of linear density dependence (Darryl MacKenzie unpublished data).

Spatial abundance of yellow-eyed penguin

The assumed relative spatial abundance for juveniles and adults was predicted for the northern population only using the models produced by Roberts et al. (2022) for fledglings (juveniles) and adults, respectively (Figure E.1 to Figure E.5). Thus, these layers differ from those produced for the species by Roberts et al. (2022), particularly for juveniles, which were observed and predicted to range up to hundreds of kilometres from the point of fledging.

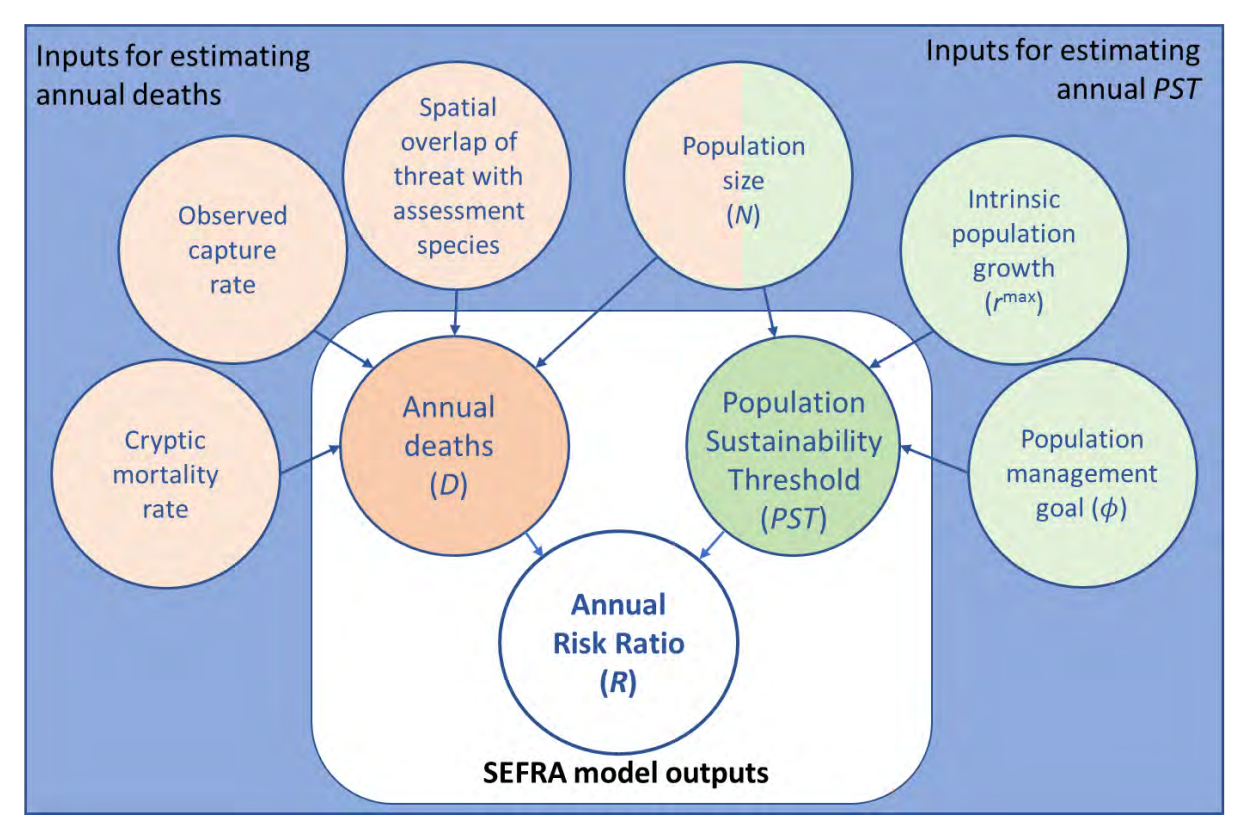


Figure 13: Conceptual diagram of spatially-explicit risk model approach and data inputs. Note that the population size is used in both the derivation of annual deaths and the Population Sustainability Threshold (PST).

Necropsy data

Necropsy data were used by an extension of the SEFRA model to estimate annual deaths not relating to direct interactions with commercial fishing. A summary of the mortality data in the 'Death' table of YEPDB is provided by the tables and plots in Appendix A. Three types of mortality data are recorded here: formal necropsy, informal necropsy, and mortality records with no necropsy (Table A.1). Only the formal necropsy data were used for fitting SEFRA models, using data: from 2008–09 to 2015–16 (the period for which HTG advised that all freshly dead carcasses that were encountered were necropsied). Using these data, and excluding deaths attributed to entanglement in commercial set-nets (which are instead addressed using the SEFRA model) as well as those for which a primary cause of death could not be determined, the data were summarised by the total number of deaths within each of the main coarse-level causes of death (see later). These data were then used for fitting the SEFRA models.

Fishery inputs

Version 9 of the Protected Species Captures (PSC) database ('PSCv9') was provided by Fisheries New Zealand in January 2025, which included the following records up to and including the 2022–23 fishing year:

- commercial fishing effort data per fishing event;
- fisheries observer data per fishing event; and
- fisheries observer-recorded protected species captures, per capture event.

The carcasses of yellow-eyed penguins captured on observed fishing events were subject to necropsy, providing confirmation of individual sex and age stage (i.e., juvenile or adult plumage), which were

used to update the observer-reported data. These necropsy data were provided by Biz Bell (Wildlife Management Limited) for use by this project. Note that these records are distinct from the other necropsy records described under the previous heading.

4.1.2 SEFRA model

The SEFRA method was used to estimate commercial fishery-related deaths for yellow-eyed penguins. The fishery data, along with spatio-temporal species distribution maps and priors for all model parameters, inform the SEFRA model. All variables used to describe the model are shown in Table 6.

Table 6: Variable symbols, support, and descriptions. Estimated parameters are estimated within the model while random variables are simulated from a prior outside the model (i.e., within the generated quantities block of the Stan code).

Symbol	Support	Description
Indices i g z	$i = \{1,2, \dots\}$ $g = \{1,2\}$ $z = \{1,2,3,4,5,6\}$	A fishing event (e.g., a net is set or a trawl tow begins) that occurs at a time and location Commercial fishery group – set net (SN) or trawl Demographic group – juvenile, North Otago 1, North Otago 2, Otago Peninsula, Catlins, Stewart Island
k	$k = \{1,2,3,4,5\}$	Necropsy type – malnutrition, disease, predation, trauma, other
<u>Data</u>		
$C'_{z,g,i}$	≥ 0	Number of observed dead captures
Covariates		
a_{gi}^{\prime},a_{gi}	≥ 0	Observed fishing intensity and fishing intensity (km of net for set net and number of tows for trawl)
$p_{z,i}$	∈ [0,1)	Relative density of hoiho at the location and time of each fishing event
O'_{zqi} , O_{zqi}	≥ 0	Observed overlap and overlap
Estimated parame	eters	
q_g	<u>≥</u> 0	Catchability
$N_{z,i}$	> 0	Population size for each demographic group
$ ho_{z,k}$	∈ (0,1)	Proportion of non-fishery deaths for each necropsy type
Simulated randon		
$p_g^{ m obs}$	∈ (0,1)	Probability that an event is observable
r^{\max}	> 0	Intrinsic population growth rate for each sub-species
$S_{z,t}$	∈ (0,1)	Annual survival rate
Fixed parameters		
$\overline{\phi}$	∈ (0,1)	Calibration coefficient
Derived quantities	<u>s</u>	
$C_{z,g,i}$	≥ 0	Total number of dead captures
$D_{z,g}$	≥ 0	Deaths
PST_z	≥ 0	Population sustainability threshold
$R_{z,g}$	≥ 0	Risk ratio
k_{g}^{3}	≥ 0	Cryptic mortality

This implementation of the SEFRA method included two commercial fishery groups (g) considered to pose a risk to hoiho—set netting (SN) and trawling (including bottom and midwater trawls, based on the recommendations of Beentjes & Bian 2022). Fishing events were either observed (an observer was on-board the fishing vessel at the time) or unobserved. Yellow-eyed penguin captures recorded by fisheries observers on the observed portion of the fishing effort were used to estimate model parameters by fitting a relationship between this effort and observed captures. Observed captures may be recorded as being alive or dead, but all observed yellow-eyed penguin captures were recorded as being dead, so all captures were assumed to be dead, negating the requirement for live-release survival parameters. The combination of observed and unobserved effort, along with the estimated parameters, was used to predict the total number of commercial fishery related captures, deaths, and risk.

Fishing effort per fishing event (i) has an associated fishing intensity (a_{gi}) , measured in kilometres of net length for set net and number of trawl events for trawl. Observed fishing events are denoted using the prime symbol as a'_{gi} where:

$$a'_{gi} \subset a_{gi}$$

meaning that observed effort is a subset of all fishing effort. Note that for a small number of 1-km grid cells, the aggregated fishing intensity for observed fishing events exceeded that of the total (observed and unobserved) fishing intensity. The reasons for this discrepancy in the input data were not identified or accounted for by this assessment.

This implementation of the SEFRA method modelled the number of captures of two demographic groups (juveniles and adults). Observed overlap was calculated for each demographic group (z) and commercial fisheries group (g), for each fishing event (i):

Equation 10:
$$O'_{z,g,i} = a'_{g,i}p_{z,i}$$

Six demographic sub-groups (d) were defined, consistent with the regional sub-population units used by the demographic population assessment, i.e.: juveniles across New Zealand, and adults (here defined as individuals with adult plumage, i.e., after the second moult) for each of the five assessed regional sub-populations (North Otago 1, North Otago 2, Otago Peninsula, Catlins, and Stewart Island). The number of juveniles available to be caught by fishing gear was determined by the probability that they will be moulting:

Equation 11:
$$N_{z,i} = N_{t \in i}^{\text{juv}} \left(1 - P_{m \in i}^{\text{moult}} \right)$$

where the prior for N_t^{juv} was derived from the posterior distribution in the demographic models and the probability that they will be moulting is defined in Table 7. The number of adults available to be caught by fishing gear was determined by the probability that they will be attending the nest or the probability that they are moulting:

Equation 12:
$$N_{z,i} = N_{d \in i, t \in i}^{\text{B}} \left(1 - P_{m \in i}^{\text{nest}} \right) \left(1 - P_{m \in i}^{\text{moult}} \right) + N_{d \in i, t \in i}^{\text{NB}} \left(1 - P_{m \in i}^{\text{moult}} \right)$$

where the prior for $N_{d,t}^{\rm B}$ and $N_{d,t}^{\rm NB}$ were derived from the posterior distribution in the demographic models.

Table 7: Assumed proportion of yellow-eyed penguins that would be moulting or attending a nest in any given season. Values based on table 152 of Edwards et al. (2023b).

Month	Probability that any individual is moulting $(P_{m,t}^{\text{moult}})$	Probability that a breeder is attending a nest $(P_{m,t}^{nest})$
January	0.00	0.00
February	0.00	0.00
March	0.40	0.00
April	0.40	0.00
May	0.00	0.00
June	0.00	0.00
July	0.00	0.00
August	0.00	0.00
September	0.00	0.25
October	0.00	0.50
November	0.00	0.50
December	0.00	0.25

Fisheries observer data (protected species captures on observed fishing events) by fishing event (i) were used to estimate model parameters. Fishing events were observed during each fishing year (t) from 2006–07 to 2022–23 (the terminal year of the PSCv9 extract). Four catchability parameters ($q_{z,g}$) were estimated – one for each commercial fisheries group (set-nets and trawls) and age stage group (juveniles and adults) pairing. Uninformative but non-uniform catchability priors were specified in log-space to help with Markov chain Monte Carlo (MCMC) mixing:

$$\log(q_{z,q}) \sim \text{normal}(0, 10^2)$$

The expected number of observed captures was:

$$\lambda'_{z,q,i} = O'_{z,q,i} N_{z,i} q_{z,q}$$

A Poisson distribution was assumed for the observable captures:

Equation 13:
$$C'_{z,q,i} \sim \text{Poisson}(\lambda'_{z,q,i})$$

noting that the Poisson distribution assumes the same mean and variance. Bayesian inference was done using *Stan* making use of its Hamiltonian Monte Carlo (HMC) algorithm (Stan Development Team, 2023).

4.1.3 Model predictions

4.1.3.1 Simulated random variables

Three variables were simulated (i.e., in the generated quantities block of the Stan model) rather than estimated as parameters within the model. These variables included the probability that an event was observable (given that an observer was on watch) for each fisheries group (p_g^{obs}) , the intrinsic population growth rate (r^{max}) , and survival $(S_{s,t})$.

Throughout this document reference is made to cryptic mortality rate which was defined as:

Equation 14:
$$k_g = \frac{1}{p_g^{\text{obs}}}$$

For trawls, the prior for the probability that an event was observable was a Beta distribution that was consistent with the prior developed for seabird species in trawl nets by Edwards et al. (2023a) (see table 4 of that publication), i.e., resulting in a mean cryptic mortality rate (*k*) with a mean of 1.30 and 95% CI of 1.10–1.70. The parameters of the Beta prior were found iteratively so that the same mean and 95% CI were achieved. Thus, for captures in trawl gear, the following informed prior was assumed:

$$p_{g=Trawl}^{\text{obs}} \sim \text{Beta}(13.86152, 4.022151)$$

For commercial set-nets, the prior for the probability that an event was observable was determined based on a review of the information relating to the direct interactions of seabird and teleost species with commercial set-net gear. The recent SEFRA assessment of Hector's and Māui dolphins by Roberts et al. (2019) developed a prior for this species, which was deemed unsuitable for yellow-eyed penguins, since: these dolphins are much larger than yellow-eyed penguins and were assumed to be more prone to dropping out on hauling of the gear between the water's surface and being landed; and the dolphin prior did not include sub-surface loss of dead individuals. No relevant studies or examples were found for the pre-catch losses of any proxy seabird species. However, several studies estimating

the pre-catch losses of Pacific salmon species (Oncorhynchus sp.) from oceanic commercial set-nets (there called 'gill-nets') were done in the 1960s, that were summarised or reviewed by French & Dunn (1973) and Ricker (1976). Overall, the review by Ricker (1976) concluded that around 25% of final year salmon captured in coastal gill-nets were lost prior to landing (and not less than 50% for smaller fish), including sub-surface losses and drop-outs. Accordingly, the following informed prior was assumed for set-net captures, which was consistent with an average cryptic mortality rate (k) of 1.25 and an upper 95% CI of 1.50:

$$p_{q=SN}^{\text{obs}} \sim \text{Beta}(10.28773, 3.429245)$$

The intrinsic population growth rate (r^{max}) for yellow-eyed penguins was based on the posterior of λ^{max} estimated for this species by Edwards et al. (2023a) (see table 14 of that publication), using the approach of Dillingham et al. (2016), which had a mean of 1.15 and 95% CI of 1.11–1.20. The parameters of the lognormal prior were found iteratively so that the same mean and 95% CI were achieved. Thus, the prior for this input is simulated from:

$$r^{\text{max}} \sim \text{lognormal}(\log(1.15), 0.02002823^2)$$

Both these priors are plotted in Figure D.13.

Beta priors were derived for adult survival (survival of individuals equal to or greater than one year old represented by 1+). These priors are illustrated in Figure D.10.

4.1.3.2 Predicting deaths and risk

Model predictions were done using both observed and unobserved fishing events $(a_{g,t,i})$ by demographic group (z), fishery group (g), and fishing event (i):

$$O_{z,g,t} = \sum_{i \in t} a_{g,t,i} p_{z,i}$$

The number of deaths was calculated as:

$$D_{z,g,t} \sim \text{Poisson}(O_{z,g,t}N_{z,t}q_{z,g}k_g)$$

A mortality constraint, as described in Sharp (2018), was not imposed but was monitored:

$$\sum_{g} D_{z,g,t} < \left(1 - S_{z,t}\right) N_{z,t}$$

The population sustainability threshold (PST) was calculated for each subpopulation unit as:

$$PST_{z,t} = \frac{1}{2}\phi r^{\max} N_{z,t}$$

where ϕ is a calibration coefficient set to the value of $\phi = 0.2$ specified by Fisheries New Zealand. The risk ratio $(R_{z,t})$ is:

$$R_{z,t} = \frac{D_{z,t}}{PST_{z,t}}$$

where a risk ratio > 1 is consistent with annual deaths exceeding the PST for a sub-species or subpopulation unit.

4.1.4 Model runs

A total of five SEFRA model runs were completed:

- The **reference** run: was fit to observed captures of individuals that were confirmed to be male or female, excluding two individuals of unknown sex and one individual of unknown age stage (Table D.1); used the cryptic mortality priors (see previous sub-section); and fit to necropsy observations from 2008–09 to 2015–16 (Table A.3), the period in which all freshly-dead carcasses that were encountered were sent for necropsy (according to the advice provided by HTG 5 July 2023);
- The **unk_fem** run was as the reference run, except that all observed captures for which the sex was not determined were assumed to be females and, if age group was also not determined, then these were assumed to be adults. This run was done for females only;
- The **no_cryptic** run was as the base run, except that it was assumed there was no cryptic mortality relating to direct fishery interactions. This run was done for males and females.

4.2 Results

4.3 SEFRA model inputs

Summary plots of inputs for the SEFRA model runs are shown in Appendix D.

Inputs from population models

There was almost perfect agreement between the posteriors from the population models and the posteriors from the SEFRA models, for both annual population size and annual survivorship (Figure D.5 to Figure D.10). The only difference being juvenile survival, which, for each sex, was averaged across the posteriors from the northern and southern population models (Figure D.9).

Other biological inputs

The predicted at-sea spatial abundance of the northern population of yellow-eyed penguins is shown in Appendix E. The assumed layer for adults is shown in Figure E.1. For juveniles (e.g., Figure E.2 to Figure E.5), the prediction for the northern population domain was very different to that estimated at the species level by Roberts et al. (2022), since the northern population excludes a large number of southern population individuals that were predicted by Roberts et al. (2022) to forage around Stewart Island and to the south of Fiordland.

The assumed distribution of r^{max} is plotted in Figure D.13. This was centred around 0.14 and had a distribution that was consistent with the outputs of Edwards et al. (2023b).

Fishery inputs

The spatial distribution of total fishing effort for commercial set-net and trawls within the relevant area of New Zealand are shown in Figure D.1. The spatial distribution of observer coverage is shown in Figure D.2. Observer coverage has improved for all sub-population areas since around 2015–16 (Figure D.3). Since 2006–07, a total of 24 captures were observed, all in the set-net fishery, of which 11 were females, 10 were males, and 3 were of unknown sex (Table D.1). Of the 24 observed captures 18 were confirmed to be adults, 4 were confirmed to be juveniles, and the remaining 2 were of unknown age stage. The observed captures of adults are plotted spatially in Figure D.4, including individuals of unknown sex (used in the unk_fem model run), and compared with the empirical spatial

overlap between observed set-net events and the assumed distribution of adult yellow-eyed penguins. Other than the three observed captures of adult males to the north, there is reasonable agreement between empirical overlap and observed captures.

Necropsy data

Around 75% of formal necropsies of bird carcasses found onshore resulted in a primary cause of death. The main coarse-level causes of death in this sample were (in descending order of prevalence across all ages and regions): malnutrition, diseases, predation (by marine and terrestrial predators), and trauma (which is likely to include some predation events), which together comprised around 95% of the deaths for which a primary cause was determined (Table A.2). Non-necropsied records are much less likely to have a primary cause of death, although they do reveal some other threats for yellow-eyed penguin (e.g., fire) (Table A.1).

The necropsy observations fitted to by the SEFRA model are shown in Table A.3 and are plotted in Figure 14. Notably, more females were determined to have died from malnutrition than males at all ages, based on the raw data, and this is particularly so for chicks and juveniles. The data were also plotted in Figure A.1 as proportions across each sex, age group, and region, although this time including unknown causes of death. This plot indicates that the proportional causes of death are similar across regions for both chicks and adults. For juveniles, the prevalence of malnutrition cases in the sample appeared to be greater further south, although the sample size of juvenile necropsies was smaller here relative to that of other ages (Figure A.2).

A plot of formal necropsy samples over time indicates that the necropsy rate of carcasses has varied since the early 1990s (Figure A.3), although the coarse level proportional causes of death do not appear to have changed much over the same time period (Figure A.4).

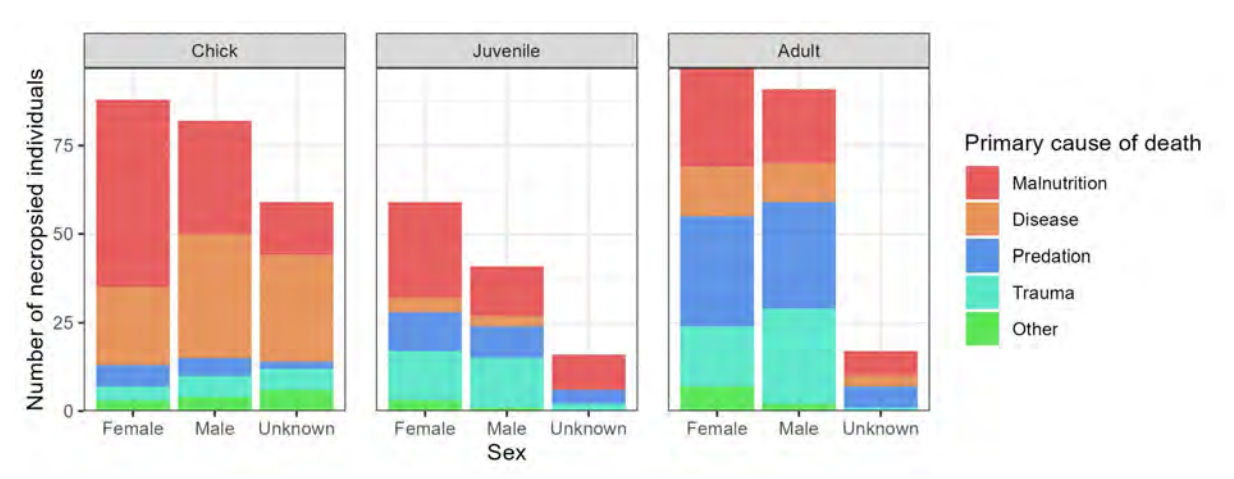


Figure 14: Summary of formal necropsy data, showing the number of carcasses by age, sex and coarse-level primary cause of death. This figures excluded carcasses for which the cause of death could not be determined or known fishery bycatch cases.

4.4 SEFRA model results

No lack of convergence was detected for the **reference** model run, based on good mixing of the traces for all estimated model parameters (Figure D.11). The posteriors for the same model are summarised in Table D.2 and shown in Figure D.13 for a selection of parameters.

The **reference** model fit to observed captures of females is plotted with respect to age group and region (Figure D.15) as well as by fishing year (Figure D.16, Figure D.17). Except for North Otago 1, the fits were reasonably good, given the small total number of female (11) and male (10) captures across all observed events.

The **reference** model prediction of annual deaths across the commercial set-net and trawl fisheries was around 12 female deaths annually from 2006–07 to 2012–13 (around 24 annually across both sexes), reducing thereafter to approximately 5 female deaths per annum, before increasing slightly in the most recent assessment years (Table 8, Figure D.18). On average, approximately half of the estimated annual deaths occurred around the Otago Peninsula, with nearly all of these caused by the commercial set-net fishery and almost zero deaths predicted for the trawl fisheries annually (Figure 15).

Female PST for the northern population of yellow-eyed penguins declined steadily over time (Figure D.19). This decline was driven by the estimated decrease in female population size over this time. The median estimated annual risk ratio using the **reference** model across the commercial set-net and trawl fisheries and across the northern population exceeded a value of 1 from 2020–21 to 2022–23 (Figure D.20), mostly caused by increases in female risk ratio in Otago Peninsula (Figure 16).

Assuming that all observed captures of unknown sex were adult females (**unk_fem** run) resulted in a small increase in annual risk ratio of females in all regions (Figure D.21). Assuming no cryptic mortality (**no_cryptic**) resulted in a small decrease in annual risk ratio estimates, although the median risk ratio in the final four years still exceeded a value of 1 around the Otago Peninsula (Figure D.22), as with the **reference** model run.

Extending the SEFRA model to fit to necropsy data suggested that malnutrition was the primary cause of female deaths (Figure 17) and was a lesser but still important factor for males (Figure 18). Based on this analysis, there were more than 100 juvenile female deaths from malnutrition in most years between 2007 and 2015 (Figure 17) and malnutrition may also have killed more than 100 juvenile males in some years during this period (Figure 18). Malnutrition was also estimated to be the main cause of death for chicks, killing around 100 of both sexes annually, with around 100 females estimated to have been killed in each of two years (2007 and 2009). Predation was estimated to kill around 100 juvenile females and 100 adult females annually, considerably more than the estimated number of female chick mortalities from predation (Figure 17, Figure 18).

Table 8: Summary (median and 95% credible interval) of the number of deaths for females and males and female risk ratio in the reference model run.

									Deaths		R	isk ratio
Year			Females			Males		Co	ombined			Females
	2.5%	50%	97.5%	2.5%	50%	97.5%	2.5%	50%	97.5%	2.5%	50%	97.5%
2007	5.5	11.4	22.3	4.6	10.0	20.0	13.0	22.1	36.2	0.264	0.553	1.078
2008	5.5	12.2	28.1	4.9	11.0	26.8	13.3	24.2	45.4	0.247	0.555	1.281
2009	5.2	11.3	23.2	4.5	10.1	21.9	12.9	21.9	37.7	0.275	0.589	1.199
2010	5.5	12.2	26.8	4.9	11.1	26.0	13.6	24.0	44.1	0.273	0.604	1.340
2011	5.4	11.9	25.4	4.9	10.9	24.4	13.5	23.5	41.9	0.292	0.640	1.369
2012	5.1	11.3	24.8	4.7	10.5	24.2	12.7	22.5	41.3	0.270	0.595	1.307
2013	3.6	8.1	19.5	3.2	7.8	19.5	9.0	16.6	32.2	0.199	0.461	1.104
2014	3.3	7.2	16.1	2.9	6.7	15.8	8.2	14.4	26.7	0.221	0.486	1.089
2015	2.7	5.9	12.3	2.6	6.0	13.1	7.0	12.2	21.4	0.258	0.572	1.192
2016	2.0	4.6	10.7	1.9	4.5	10.7	5.2	9.4	17.6	0.191	0.437	1.017
2017	2.6	5.8	12.0	2.4	5.4	11.9	6.6	11.5	20.1	0.263	0.582	1.204
2018	2.9	6.1	12.4	2.5	5.6	11.9	7.1	12.0	20.3	0.292	0.625	1.254
2019	2.5	5.3	10.5	2.3	5.1	10.3	6.2	10.6	17.6	0.299	0.646	1.269
2020	3.1	6.7	13.3	2.8	6.1	12.5	7.7	13.2	21.5	0.460	0.977	1.916
2021	3.7	7.9	15.5	3.2	7.1	14.2	9.0	15.4	25.1	0.528	1.122	2.192
2022	4.3	9.3	18.2	3.8	8.3	17.0	10.3	18.0	29.9	0.634	1.353	2.615
2023	3.9	8.5	16.9	3.5	7.7	15.8	9.6	16.6	27.7	0.591	1.260	2.470

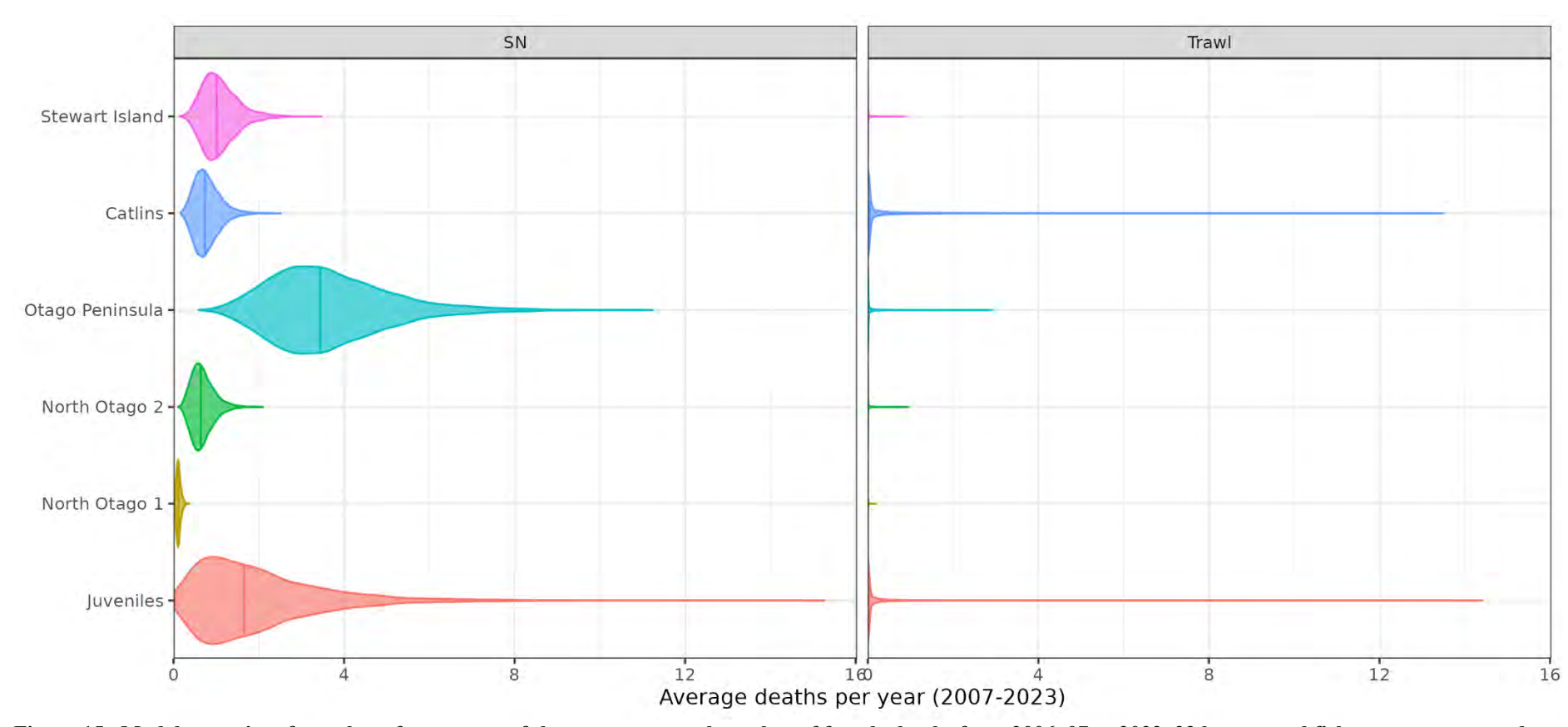


Figure 15: Model posteriors from the reference run of the average annual number of female deaths from 2006–07 to 2022–23 by assessed fishery, age group and regional sub-population (adults only).

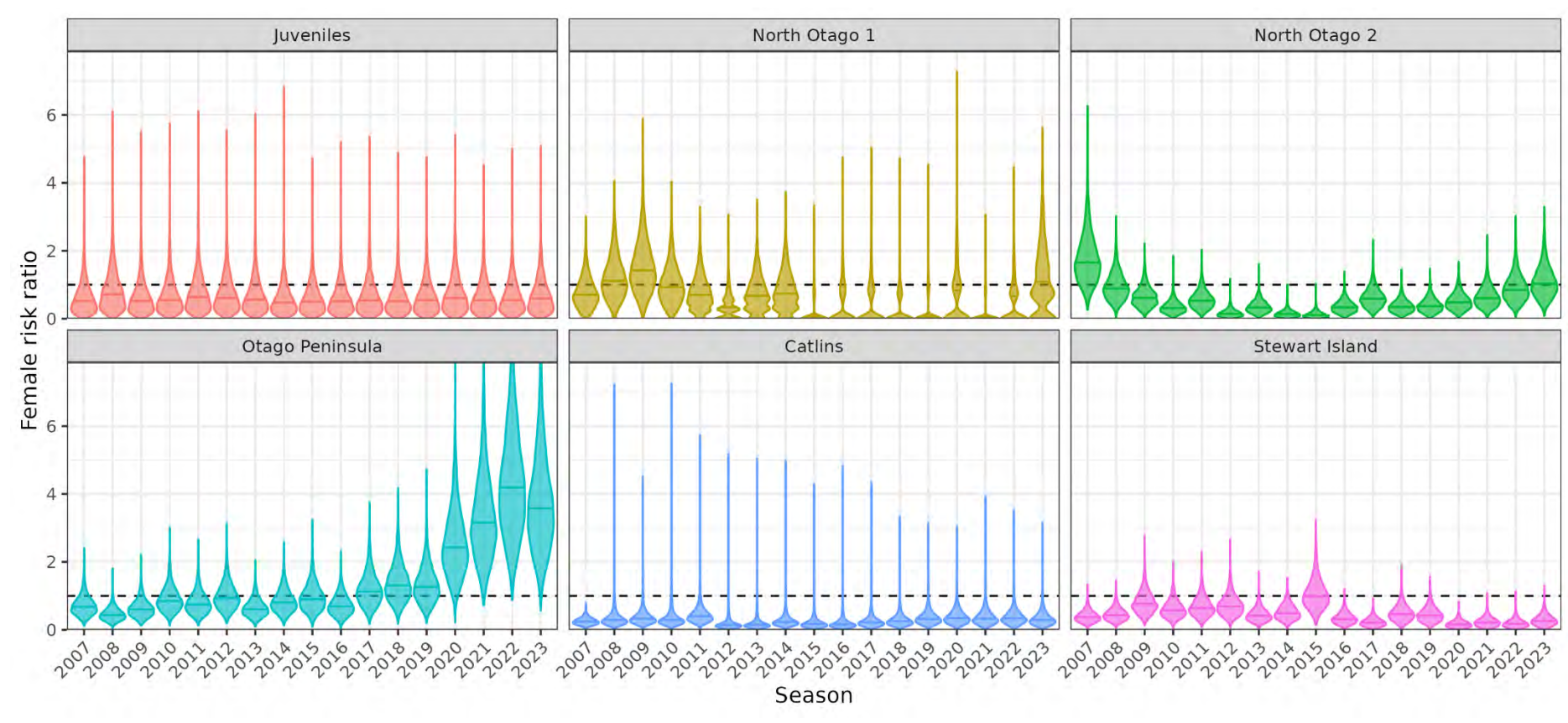


Figure 16: Model posteriors from the reference run of risk ratio for commercial set-nets by fishing year, age group, and regional sub-population (female adults only), when assuming $\phi = 0.2$. The dashed line represents a risk ratio equal to 1, above which the management goal would not be achieved at equilibrium.

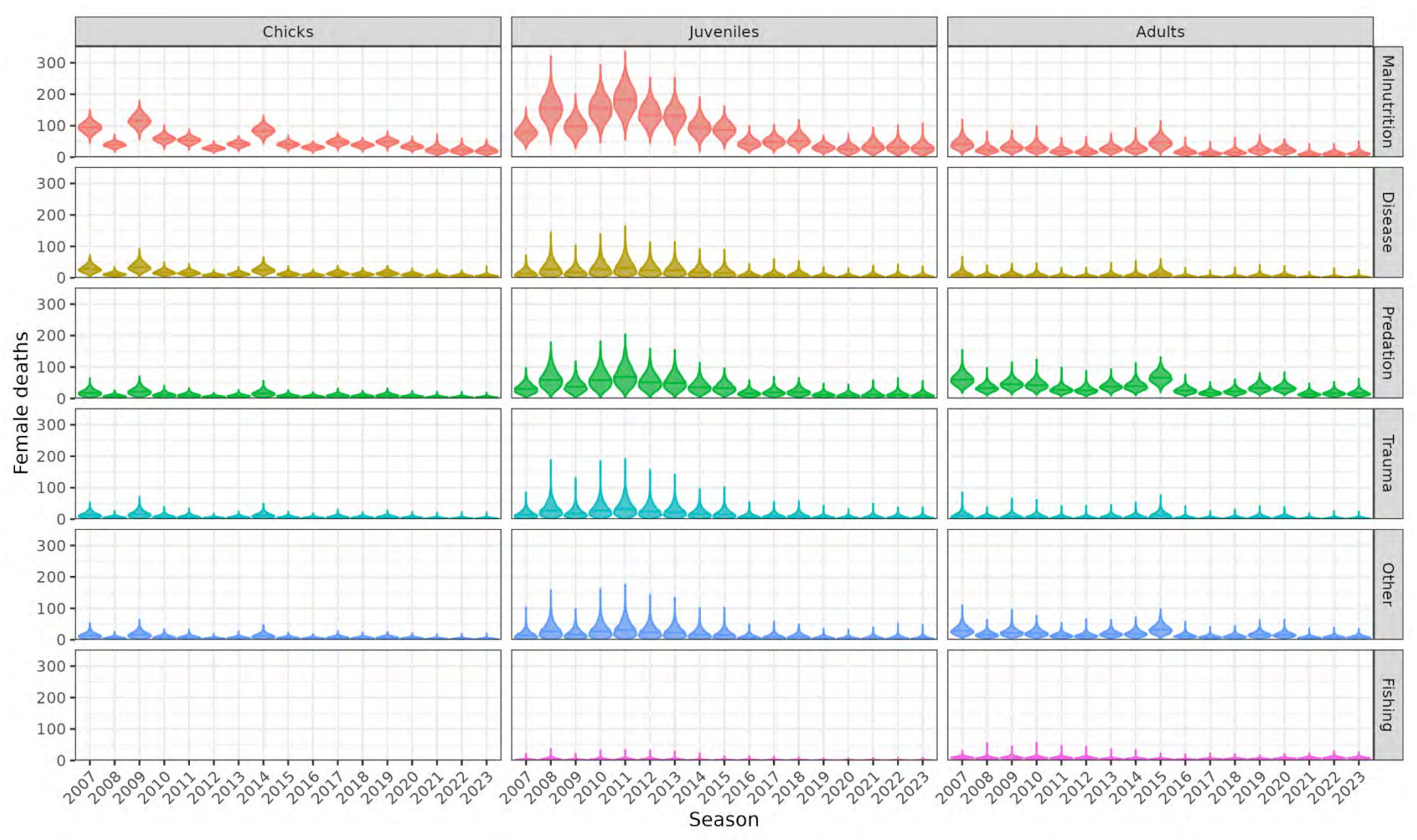


Figure 17: Model posteriors from the reference run of the number of female deaths by age group and coarse-level cause of death for the reference model run.

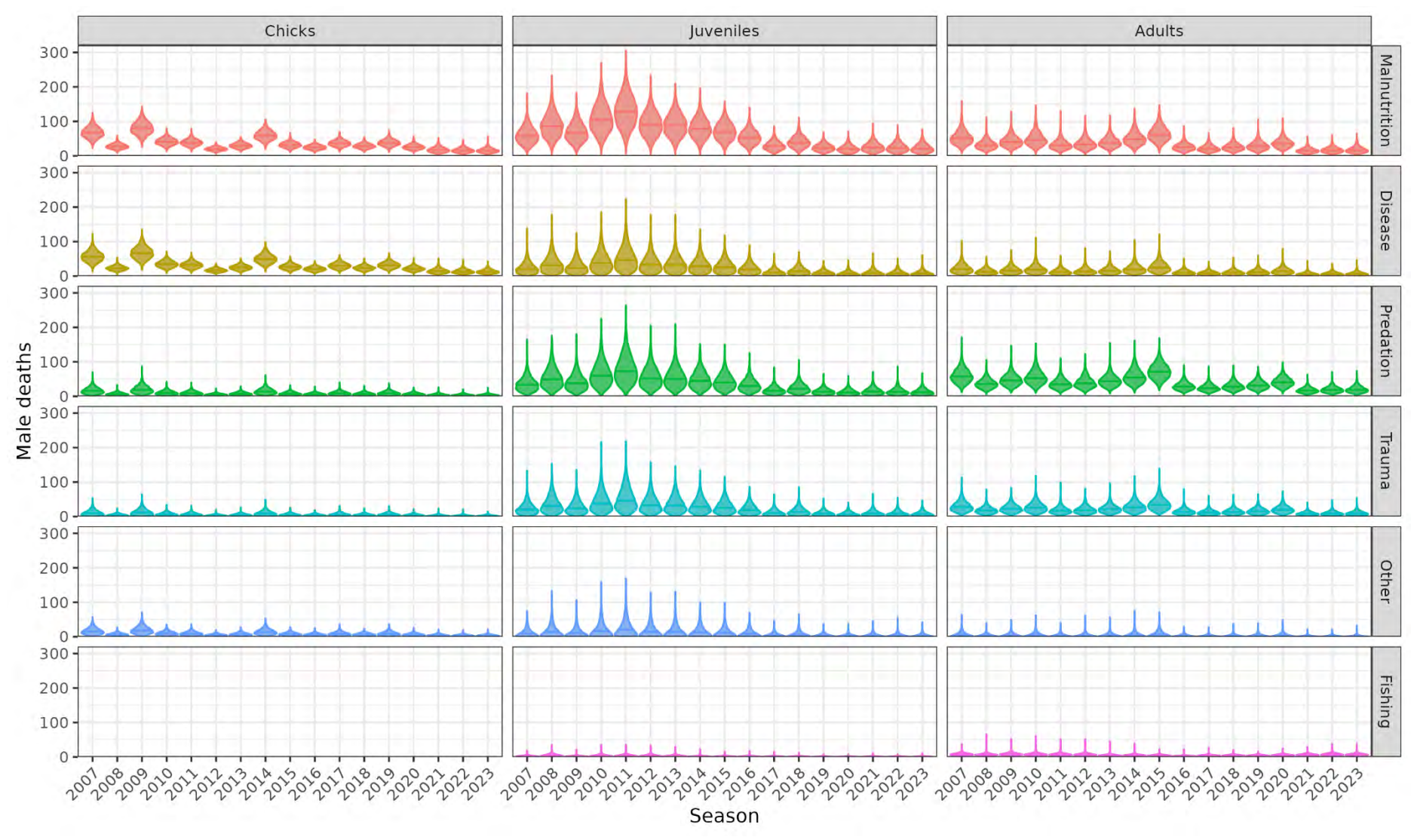


Figure 18: Model posteriors from the reference run of the number of <u>male</u> deaths by age group and coarse-level cause of death for the reference model run.

5. RELATIVE SPATIAL OVERLAP

5.1 Methods

5.1.1 Derivation of threat layers

Rasterised layers of relative threat intensity were produced for all threats that could be spatially resolved. The data sources for each threat layer are shown in Table F.1 of Appendix F. The resulting threat layers are shown in Figure F.1 to Figure F.15.

Some of these layers were produced by other research and were not modified for this project (i.e., recreational netting, aquaculture, oil pollution risk, shark predation, direct interaction with humans/dogs, predation by stray cats, predation by stoats, fire, and road traffic accidents). For the remaining threats for which spatial intensity layers were produced (i.e., commercial fishing effort, slope in sea surface temperature, and predation by New Zealand sea lions) custom layers were produced by this assessment.

For **commercial fishing effort**, spatially-gridded layers of total effort were produced for commercial set-net and trawls using data from version 9 of the PSC database (the same extract as was used by the SEFRA analysis described in Section 4). Vessel-reported effort (in terms of kilometres of set-net or number of trawl events) was summed for each grid cell across the final three fishing years for which there were data in the PSC database extract (i.e., 2020–21 to 2022–23). Note that the resulting layers were produced for this analysis only and were not used by the SEFRA model, which used the reported point location information for all fishing events.

For the **slope in SST**, data for the period January 1990 to December 2022 were extracted from the ERA5 monthly averaged data (Hersbach et al. 2023) for the spatial domain around the South Island and Stewart Island. The slope in SST through time was then calculated using the *sens.slope* function in the *trend R* package (Pohlert 2023).

For the **predation threat from New Zealand sea lions**, a terrestrial layer was produced based on the assumption that most predation events of yellow-eyed penguins by the species will be on land. This was derived from land-based public sightings of New Zealand sea lions extracted from iNaturalist Community (2023), which were then related to New Zealand human population density by census mesh block (Davis 2014). Only 'research grade' sightings were used, resulting in a dataset of 1188 sightings made from 1981 to 2023. These were then converted to rasterised counts using a 32-km grid cell resolution. The summed counts were then divided by the human population density for the corresponding grid cells.

5.1.2 Generation of terrestrial penguin layer

The terrestrial layer for yellow-eyed penguins used by this analysis was derived from two sources: abundance information from a database of the nests by breeding location and year (DOC unpublished data), and their latitude-longitude locations obtained from YEPDB (Hickcox et al. 2023). For each breeding location, the mean of the estimated number of active nests was calculated for the latest 5 years of data (2018–19 to 2022–23). These were then converted to rasterised counts per 1-km grid cell. This resolution was chosen based on field-based observations, which indicate that individual yellow-eyed penguins rarely venture further than 1 km across land from their respective nest location (Seddon & Davis 1989).

The at-sea predictions for the northern population of adults (Figure E.1) were used for comparing with marine threats.

5.1.3 Calculation of relative overlap

Terrestrial and marine threats (Table F.1) were compared with terrestrial and marine spatial abundance layers produced for yellow-eyed penguins, respectively. The calculation of relative overlap between yellow-eyed penguins and terrestrial/marine threats followed the approach of Roberts et al. (2019). Briefly, this was calculated as follows:

- 1. rescale each threat raster layer to sum to 1; then
- 2. for each regional sub-population, rescale bird density layers to sum to 1; then
- 3. for each region, multiply the outputs of steps 1 and 2, and them sum the values for each layer, yielding the relative overlap statistic for each threat/region combination.

For the purposes of visualising outputs, the resulting overlap statistics by region were rescaled so that the maximum value calculated across all regions was equal to 1 and, therefore, overlap was reported relative to the maximum. For most threats there should be an approximate linear relationship between relative overlap and the threat level experienced in each region (confirmed for the toxoplasmosis threat by Roberts et al. 2019). However, this may not be the case for overlap with the slope in SST, since this threat layer will proxy for changes in different aspects of penguin habitat, including prey and the physical habitat, which are likely to have non-linear responses to changes in sea temperature through time.

5.2 Results

The resulting values of relative overlap for the assessed marine threats are shown for each region-threat combination in Figure 19. All spatial overlap with fish cage and non-cage based aquaculture was with the Stewart Island regional sub-population. The calculated overlap with recreational netting and oil spill risk was greatest for the Otago Peninsula regional sub-population. Shark predation risk was calculated as greatest for the North Otago populations.

The analogous output is shown for terrestrial threats in Figure 20. The Otago Peninsula population stands out as having relatively high overlap with stray cats, human and dogs, stoats, and moderate relative overlap with roads and fire risk.

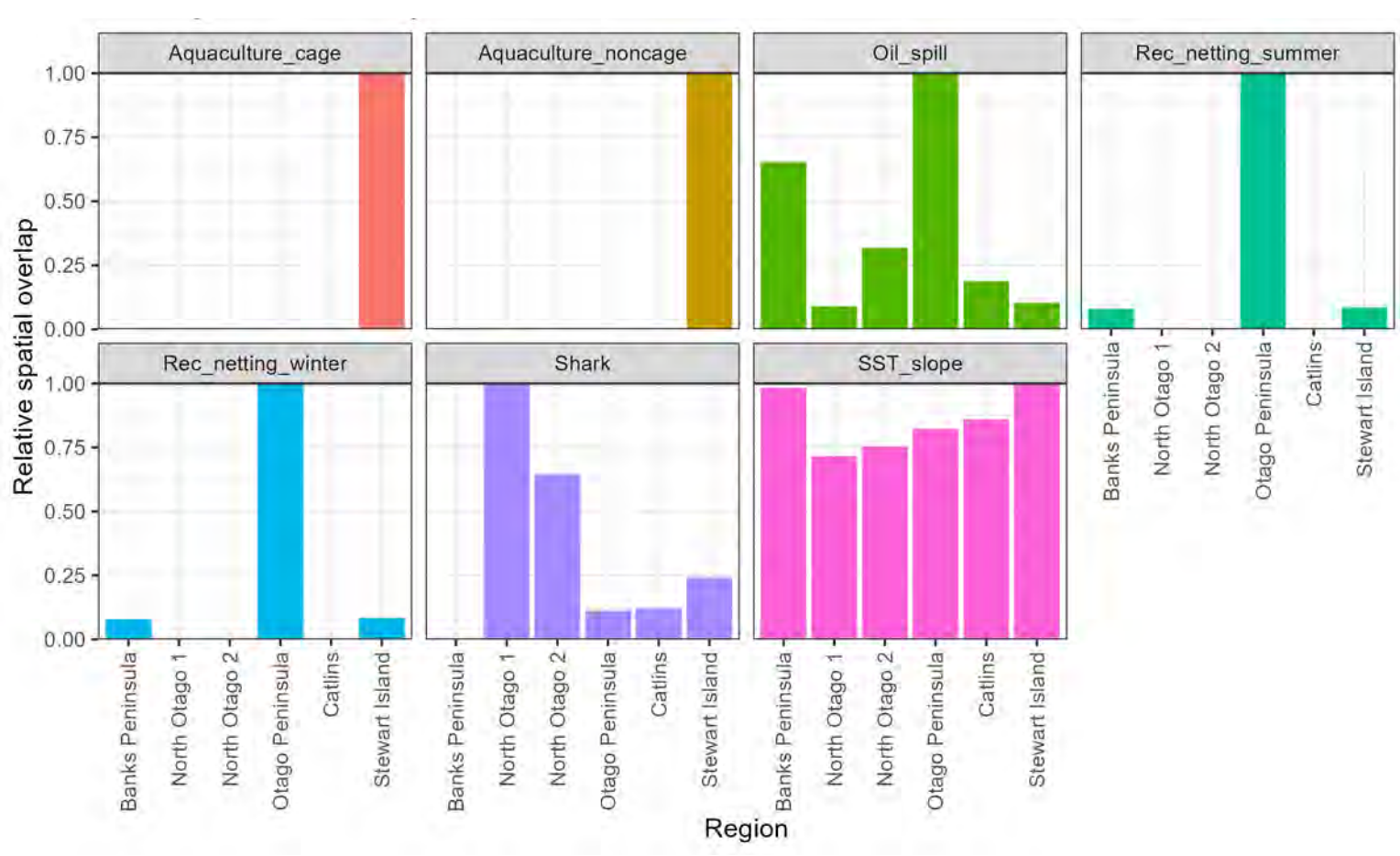


Figure 19: Relative spatial overlap of marine threats with regional sub-populations of yellow-eyed penguin.

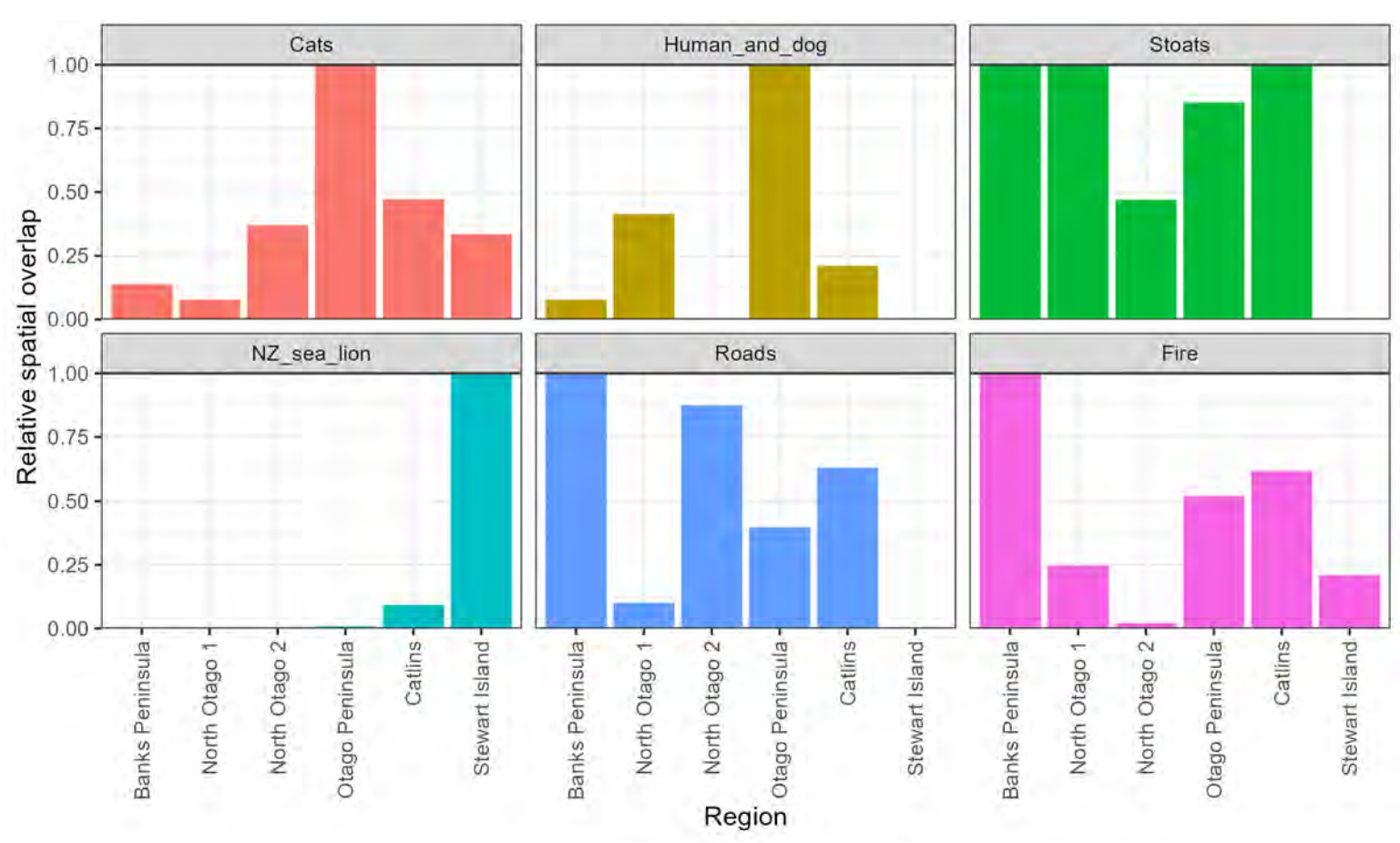


Figure 20: Relative spatial overlap of terrestrial threats with regional sub-populations of yellow-eyed penguin.

6. CORRELATIVE ASSESSMENT

This section describes an analysis of the degree of correlation between sea surface temperature (SST) and the estimated annual survivorship of different life stages of yellow-eyed penguin (outputs of Section 3. This was inspired by the analysis of Mattern et al. (2017), which concluded that, of an array of assessed environmental variables, SST was the best covariate of the survival probability of both juvenile and adult yellow-eyed penguins at Boulder Beach, Otago Peninsula. For the purposes of the current analysis, only female demographic rates were used, although these are comparable to male rates (e.g., see Figure B.69), so this will approximate to the degree of correlation with male rates also.

6.1 Methods

6.1.1 Survivorship

The demographic population assessment in Section 3 provided the posteriors of annual survival probability of female chicks (defined as the period between hatching and fledging), juveniles (from fledging to the next season), and adults (all later ages) used in this correlative analysis. For chicks and adults, the annual posteriors for the respective regional sub-population were used by the correlative analysis with SST. The at-sea foraging distributions of juveniles fledged in different regions are known to overlap with each other (Young et al. 2022), and this is reflected in the similar patterns in annual survival estimated for juveniles in different regions (comparing Figure B.25 and Figure B.51). Hence the combined posteriors across all regions that was used by the SEFRA model (Figure D.9) was used for this analysis also.

Due to data sparsity, adult survival at Stewart Island was assumed to be constant with respect to year and, so, this demographic group was not included in this analysis. In addition, the time series of survival posteriors used for this analysis was shortened for chicks and juveniles, omitting years that were not well-informed by the data (i.e., 2021–2022 for chick survival for all regions and 1996 – 2006 at Stewart Island, as well as 2018–2022 for juvenile survival). The time series of survival estimates used for each group is shown in Table 9.

6.1.2 Sea surface temperature

The SST data for 1959–2022 were extracted from the ERA5 monthly averaged data (Hersbach et al. 2023) for the spatial domain around the South Island and Stewart Island. The mean values for each season were used for this analysis.

The SST layers were then weighted using the predicted at-sea foraging densities of the different regional populations. The approach was different for adults (for which we had a constant spatial abundance layer with respect to month; Figure E.1) and for juveniles (for which we have monthly layers; Figure E.2 to Figure E.5). For **adults (and their dependent chicks)**, this was achieved by: using the regional boundaries to clip the predicted adult at-sea raster for each respective regional population, which were then rescaled to sum to 1; then these at-sea rasters were multiplied by the SST raster for each season (calculated as the arithmetic mean average across all rasters within each respective twelve-month season starting 1 August), the cell values of which were then summed yielding the weighted SST value for each respective season.

For **juveniles**: the at-sea foraging prediction for each month was rescaled to sum to 1; this was then multiplied by the respective SST raster for each month (for each season); the weighted SST value for each season was calculated by summing the resulting rasters; and the mean was then calculated across all months within each season (i.e., across all months within each season, starting 1 August).

6.1.3 Assessing correlation

The degree of correlation was assessed between paired values of SST and female survival probability by season. This was achieved using the Pearson product moment correlation coefficient (r), and the associated 95% confidence interval was calculated using the *cor.test* function in the stats R package (R Core Team 2023). No lag time was assumed (e.g., to account for a potential lag effect of changing temperatures on prey availability), given that Mattern et al. (2017) found that no lag period did as well or better than using lag times.

6.2 Results

The resulting SST indices had a similar pattern through time for all demographic groups, with the warmest temperatures in the northernmost regions (Banks Peninsula and then North Otago 1) (Figure 21). The SST indices for juveniles were colder than for adult birds, which is consistent with juveniles foraging in slightly cooler offshore waters (comparing Figure 22 with Figure E.2 to Figure E.5). There was a general increasing trend in SST for all groups, particularly since around 2000, with periods of high SST (e.g., 1999 – 2002) and low SST (e.g., 1992 – 1998) relative to the long-term trend. The period prior to 1991 was not used by the correlative assessment, although is presented here for context.

Plots of the generated SST and survival times series are shown in Figure G.1, Figure G.3, and Figure G.5. Scatterplots of the same data are shown in Figure G.2, Figure G.4, and Figure G.6. Sea surface temperature was found to be negatively correlated with the estimated survival of all the assessed groups, consistent with a negative effect of increasing SST on female survivorship at all life stages. However, the degree of correlation was stronger for some groups, e.g., juveniles (r(25) = -0.44; 95% confidence interval (ci) = -0.70 - -0.07) and adults at Otago Peninsula (r(30) = -0.40; 95% ci = -0.66 - -0.06), than for others, e.g., chicks at the Catlins (r(28) = -0.03; 95% ci = -0.38 - 0.34) or adults also at the Catlins (r(30) = -0.09; 95% ci = -0.43 - -0.27).

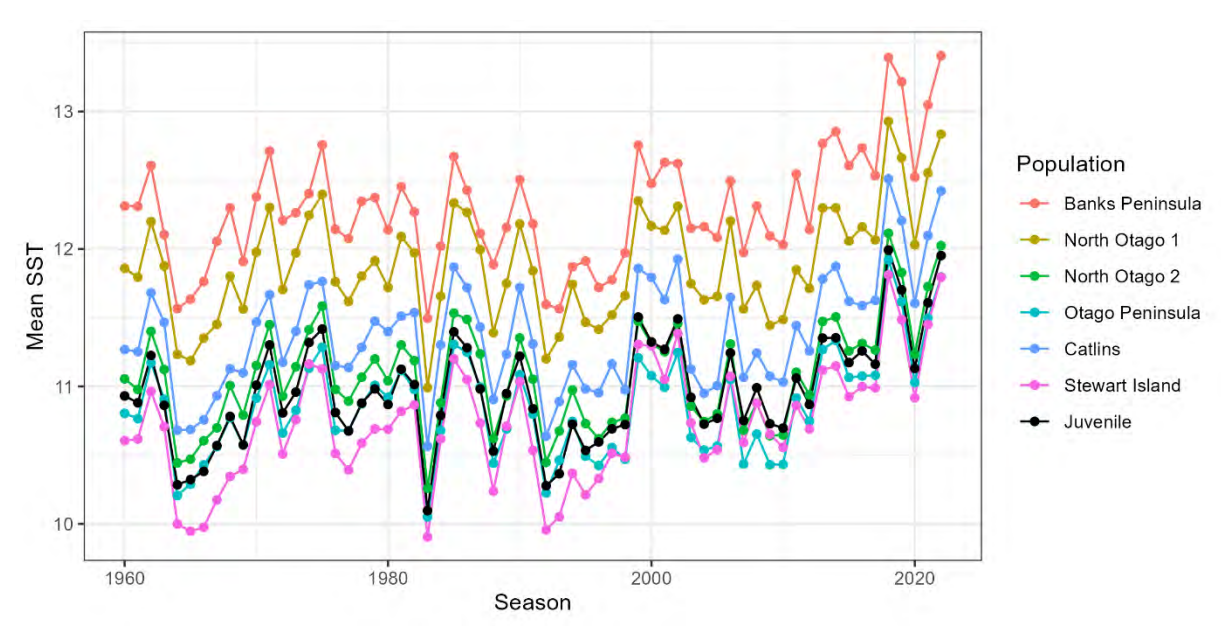


Figure 21: Mean sea surface temperature by season for chicks and adults (by regional sub-population) and for juveniles (across the northern population).

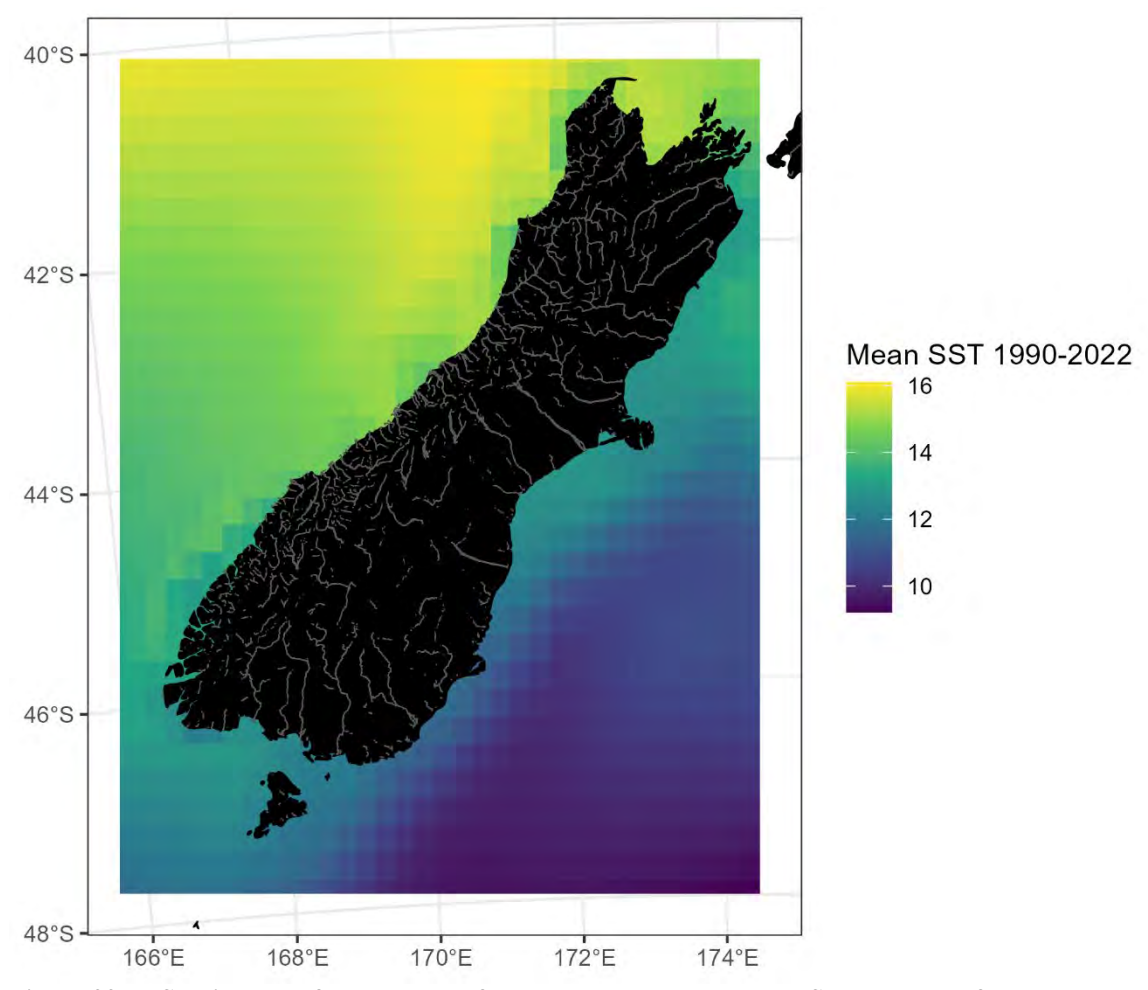


Figure 22: Spatial plot of mean sea surface temperature around the South Island of New Zealand (mean °C from 1990 to 2022).

Table 9: Correlation between sea surface temperature and estimated female survival of different age groups and regional sub-populations. Values indicative of a negative correlation are coloured red.

Age group	Regional sub-population	Years compared	Degrees of freedom	Pearson's correlation coefficient (95% confidence interval)
Chick	North Otago 1	1991 - 2020	28	-0.39 (-0.66 – -0.04)
	North Otago 2	1991 - 2020	28	-0.43 (-0.68 – -0.08)
	Otago Peninsula	1991 - 2020	28	-0.43 (-0.68 – -0.08)
	Catlins	1991 - 2020	28	-0.03 (-0.38 – 0.34)
	Stewart Island	$1991 - 1995, \\ 2007 - 2020$	17	-0.08 (-0.53 – 0.37)
Juvenile	All	1991 – 2017	25	-0.44 (-0.70 – -0.07)
Adult	North Otago 1	1991 - 2022	30	-0.26 (-0.56 – 0.09)
	North Otago 2	1991 - 2022	30	-0.27 (-0.57 – 0.08)
	Otago Peninsula	1991 - 2022	30	-0.40 (-0.66 – -0.06)
	Catlins	1991 - 2022	30	-0.09 (-0.43 – 0.27)

7. DISCUSSION

7.1 Demographic drivers of population change

The demographic population models described in Section 3 fitted well to the various data types, including the annual number of breeding pairs and, so, were considered a reasonably good representation of the five assessed regional sub-populations. The models did not allow for time-varying breeding rates including maturation as well as the probability of breeding, which were less well-informed by the data than annual survivorship, although are likely to be responsive to changes in resources through time. There were clear differences in annual chick survival rates among colonies, which might explain some of the colony-specific differences in population trajectory. For example, the estimated chick survival rate at the Catlins and in North Otago 2 was generally better than at North Otago 1, Otago Peninsula or Stewart Island (e.g., Figure D.8), but appears to have worsened in multiple regions since around 2013. The number of hatchlings per nest was relatively low at Stewart Island and appears to have had a downwards trend since around 2010 (e.g., Figure B.44). There was less regional variation in the annual survival rate of adults (e.g., Figure D.10), with evidence for poor years across multiple regions (e.g., 2015).

When presented as annual deaths by age group across all regions, juvenile deaths have fluctuated more than deaths of chicks or adults over time (Figure 8). Juveniles had the strongest long-term changes in estimated survival, with the same period of consistently low annual rates (2007 to 2015) estimated across multiple regions (Figure B.25 and Figure B.51) and which immediately preceded the drop in breeder numbers estimated across all regions around this time (Figure 6). The high net movement rate of immature birds from North Otago 1 to North Otago 2, as well as from the Catlins to Otago Peninsula, is also likely to have influenced regional differences in population trajectory.

In summary, while it is not possible to draw any conclusions about potential changes in breeding rate through time, there were occasional years of poor adult survival, periods of poor juvenile survival, and evidence of worsening chick survival in recent years. Juvenile survival appears to be a major driver of population trajectory, based on the population simulation analysis (e.g., Figure 11). Notably, given repeated observations of a highly male-biased adult sex ratio (ASR) of yellow-eyed penguins (e.g., Richdale 1957; also reviewed by Webster 2018), multiple studies, including one of Magellanic penguin (Spheniscus magellanicus) (Gownaris & Boersma 2019) and meta-analyses across multiple seabird taxa (e.g., Eberhart-Phillips et al. 2018) have determined that sex-biased juvenile survival rate is a major driver of biased ASR. An earlier review of this topic by Breitwisch (1989) concluded that "smaller body size may act synergistically with inexperience and with farther natal dispersal in juvenile females to produce higher mortality rates than in juvenile males", which was also concluded by the Gownaris & Boersma (2019) study of Magellanic penguins. Based on the population projections, adult survival is likely to be of comparable influence to juvenile survival on the trajectory of the northern population (comparing Figure 11 and Figure 12). Taken together, the combined sexspecific differences in juvenile and adult survival rate explain the male bias in numbers of each of the assessed sub-populations, as predicted by the population models of the current study (Figure B.70).

7.2 Key threats

The SEFRA model was extended to estimate annual deaths by age group, year, and proximal cause of death, based on the necropsy proportions. This made the strong assumption of equal detection probability of different causes of death, which is unlikely to be true. Even so, these estimates were largely insensitive to the time series of necropsy observations used (based on a prior analysis not shown here), which may partly relate to the coarse grouping used (e.g., 'disease' comprises multiple different diseases that will affect different life stages differentially). Based on this analysis, malnutrition, diseases, and predation were major drivers of population change over the period of this assessment (Figure 17, Figure 18), although commercial fishery deaths are likely to have comprised an increasing proportion of total deaths across the northern population (Figure 17, Figure 18) and would

be a major driver of population change at Otago Peninsula, based on the outputs of this assessment (Figure 16).

According to the outputs of the risk model, **malnutrition** caused a substantial number of annual deaths at all life stages (chicks, juveniles, and adults), and appears to be a particularly major issue for females, given the apparent female bias in deaths from malnutrition at all life stages (Figure 14) and the results of the SEFRA model (comparing Figure 17 and Figure 18). The SEFRA model estimates of annual female juvenile deaths between 2007 and 2015 were particularly high, exceeding 100 females in most years during that period (Figure 17). As noted above, juvenile and female penguins appear to be more prone to starvation than adults and males, respectively, due to the negative effects of smaller body size on foraging efficiency and the range of available prey species (Gownaris & Boersma 2019).

A previous analysis concluded that the annual survival rate of juvenile and adult yellow-eyed penguins at Boulder Beach, Otago Peninsula is negatively correlated with SST (e.g., Mattern et al. 2017), which was supported by the correlative analysis of the current study based on female demographic rates, described in Section 6. Additionally, the current analysis identified potential negative correlations between SST and the estimated survivorship of chicks at North Otago (1 and 2) and Otago Peninsula. This could be consistent with the availability of key prey species in these regions being reduced during or immediately after periods of warmer sea temperature. The most comprehensive dietary analysis of yellow-eyed penguins was by van Heezik (1990), who found that red cod (Psuedophychis bachus), opalfish (Hemerocoetes spp.), and sprat (Sprattus spp.) were the main prey species in terms of dietary mass. However, dietary studies since then have indicated a lesser importance of red cod and sprat (e.g., Young et al. 2020; also reviewed by Mattern & Ellenberg 2018). Taylor & Marriot (2004) determined that the peak in sprat spawning occurs during periods of cool water temperatures around New Zealand (9.0–10.5°C), which could plausibly be affected by long-term changes in sea temperature. Also, Beentjes & Renwick (2001) identified a potential negative relationship between SST and fishery catch rate of red cod around the South Island of New Zealand. This was supported by an updated analysis based on fishery catch rate data of red cod from 1990 to 2023, although not along the South Coast of the South Island where there was no relationship between SST and red cod catch rate (J. Roberts, unpublished research).

There was no evidence for any correlation between SST and the survivorship of either *chicks* or *adults* at the Catlins or Stewart Island (Table 9). Thus, despite recent warming in these regions also (Figure 21), the outputs of the correlative assessment are not consistent with a negative effect of warming on prey availability in these regions specifically, which would be consistent with the lack of an obvious temperature effect on red cod catch rate in this region (J. Roberts, unpublished research). However, note that the survival of *juveniles* does appear to be negatively correlated with SST (Table 9), such that the Catlins and Stewart Island sub-populations may still be negatively affected by oceanic warming via impacts on their juveniles as they disperse along the East Coast of the South Island (Figure E.2 to Figure E.5).

The potential indirect effects of commercial fishing on prey availability were reviewed by Mattern & Ellenberg (2018) and more recently by Beentjes & Bian (2022). Mattern & Ellenberg (2018) highlighted a change in the volume of commercial catch of red cod through time and speculated that fishing pressure may have contributed to a decline in the size of the red cod stock. Beentjes & Bian (2022) concluded that 'analyses of commercial catch data, research trawl data, and observer data do not show any trends of declining abundance or changes in the size composition for prey species considered to be important to hoiho diet' – although with the caveats that smaller bodied prey such as sprat would have low vulnerability to trawl gear, and that biomass estimates of red cod from research trawl surveys typically have a high coefficient of variation, such that long-term changes in biomass through time might not be detected using data from research trawls. An analysis of fishery catch rate data from commercial trawls (J. Roberts unpublished data) identified strong inter-annual patterns in red cod catch rate through time, although with differences between different regions of New Zealand. The temporal pattern in red cod CPUE was less variable along the east coast of the South Island than along the west and north coasts, although with low catch rate periods shared across all these regions,

including all assessed fishing years since 2020. In these regions there was a negative relationship between red cod CPUE and SST, as noted previous by Beentjes & Renwick (2001), suggesting that red cod catch rates in these regions are largely responsive to changes in climate, although potential relationships with fishery extractions were not explored. The trend in red cod catch rate along the South Coast of the South Island was different to all other assessed regions, with relatively better catch rates since around 2011 (J. Roberts unpublished data).

Based on the SEFRA model outputs, **diseases** are likely to cause a significant number of deaths at all life stages, although perhaps constitute a lesser threat than malnutrition when assuming an equal detection probability for these causes of death (Figure 17, Figure 18). The SEFRA model used a single group for all diseases, although at least three diseases could have a significant effect on yellow-eyed penguins, each affecting different life stages:

- diphtheric stomatitis (DS) is currently the most prevalent disease affecting yellow-eyed penguins and is a bacterial infection primarily affecting older chicks, but that can be successfully treated in around 90% of case using antibiotics;
- respiratory distress syndrome (RDS; or 'red-lung') primarily affecting young chicks, was first identified in 2019, is currently the main disease-based cause of death for yellow-eyed penguins with a ~90% mortality rate in recent years, and appears to be associated with gyrovirus (*Anelloviridae*) infection (Wierenga et al. 2023); and
- avian malaria is a protozoan disease that is spread by insect vectors including mosquitos (*Culicidae*) and black flies (*Simuliidae*), and is a sporadic and seasonal cause of death of adults and chicks that is not easily treated and appears to have had increasing prevalence in yellow-eyed penguin populations through time (reviewed by Webster 2018).

Based on the necropsies, a greater proportion of chicks appear to die from diseases than do juveniles or adults (Figure 14). However, because more juveniles and adults die in the average year (Figure 8), annual disease mortalities at each of these older life stages are comparable to those of chicks (Figure 17, Figure 18). Despite the annual mortality rate of chicks being lower at Catlins than for the other regions (Figure D.8), the proportional causes of death for chicks do not appear to be very different by region, including for disease (Figure A.1). Hence, it does not appear as though regional differences in chick survival were driven by either diseases or malnutrition alone, although it is possible that chick mortalities from diseases and malnutrition covary, e.g., in the situation where malnutrition exacerbates susceptibility to diseases.

Based on the necropsy proportions (Figure 14) and the outputs of the SEFRA model (Figure 17, Figure 18), **predation** may be a greater issue for juveniles and adults than for chicks. A likely explanation for this difference is that chicks are not yet susceptible to marine predators (e.g., barracouta (*Thyrsites atun*) and sharks) and that predator control measures (summarised by Webster 2018) have been successful in diminishing terrestrial predators (e.g., mustelids and feral cats) during the 2009–2022 period of the necropsy data used by this assessment. New Zealand sea lion populations are likely to be more heterogenous in space than other terrestrial predators and comprising fewer individuals, such that the effects on yellow-eyed penguins will be highly localised (Lalas et al. 2007). Note that, while the spatial overlap with sea lions was estimated to be relatively low at the Otago Peninsula (Figure 20), this is likely to be an artefact of the way the respective threat layer (Figure F.13) was calculated (i.e., the number of public sightings divided by the resident human population density) and the relative predation threat by this species is likely to be higher in reality, and growing with the rapid recovery of this species on the mainland, as well as at Stewart Island (Roberts & Edwards 2023).

By comparison, the estimated number of annual deaths across the northern population resulting from **direct interactions with commercial fisheries** was smaller (Figure 17, Figure 18). However, estimated commercial fishery deaths were relatively high in the final years of the assessment, exceeding the northern population PST in all years from 2020–21 to 2022–23 (Table 8). This was

largely driven by an increase in estimated fishing deaths at the Otago Peninsula, where the median risk ratio for females at Otago Peninsula exceeded a value of R=1 in all assessed years of the SEFRA model since 2016–17 and was closer to R=4 in the period 2020–21 to 2022–23 (Figure 16). For reference, anthropogenic mortalities consistent with a risk ratio of R=1 or R=4 would be consistent with population stabilisation at around 90% or 60% of unimpacted status at equilibrium, respectively, in the absence of other stressors and with multiple other assumptions, e.g., in the shape of density dependence.

The SEFRA model estimates of annual deaths and risk were relatively insensitive to the assumption of cryptic mortality rate in commercial set-nets (Figure D.22) e.g., estimated risk remained above 1 in recent years for the Otago Peninsula region even when cryptic mortality was removed.. No pre-existing studies were found of cryptic mortality rate of penguins in set-net gear, so the priors were based on experimental studies of salmon species (e.g., Ricker 1976), though it is not known how representative this is likely to be for yellow-eyed penguins. Including estimated cryptic mortalities is necessary to counter the assumption that all captures are observable, which evidence from studies on other protected species would not support (Baker et al. 2021).

Some sporadic and largely unexplained mortality events have been attributed to marine biotoxins, e.g., around 150 birds that died at Otago Peninsula and North Otago in 1989–90 (Gill & Darby 1993; Efford et al. 1996), and 67 birds that died around the Otago Peninsula in 2012–13 (Gartrell et al. 2017). Although no threat intensity layer was produced for marine biotoxins, harmful algal blooms are predicted to become more likely when the water column is more strongly stratified, e.g., as driven by projected warming (summarised by Ministry for the Environment and Stats New Zealand 2020). Sporadic bush fires have also been responsible for killing large numbers of birds in some years, e.g., at least 60 birds killed in the Catlins in 1995 (Sutherland 1999). This assessment identified some regional sub-populations that might be more prone to bush fires, including the small Banks Peninsula sub-population (Figure 20).

Relating this back to the population model, when assuming a 50 % alleviation of either juvenile (Figure 11) or adult (Figure 12) mortality rate, the mature population trend was predicted to stabilise, with increasing population trends predicted at even higher rates of alleviation. The model estimated ~40 female ~40 male chick deaths in 2023, ~60 juvenile male as well as female deaths, and ~55 female and ~65 male deaths. Therefore, to stop the decline (achieve stability), the number of annual deaths to be prevented (in addition to existing efforts) is ~30 female juveniles (or ~60 of both sexes) or ~27 female adults (or ~60 of both sexes). Therefore, even the full alleviation of commercial fishery deaths, would not be sufficient to achieve population stability, given the median estimate of ~15 deaths annually in the most recent assessment years (Table 8). Even so, based on this assessment, commercial fishery deaths are still likely to be a significant contributing factor for the population decline in the Otago Peninsula region, where they could account for a 10–40 % reduction in population size below unimpacted levels at equilibrium, with a number of assumptions (Figure 16).

This assessment did not produce any spatially resolved layers representative of physical habitat degradation. Nor was there any useful information in the necropsy records about the importance of physical habitat degradation relative to other causes of death. However, it is highly likely that habitat changes, including changes in land use and increased coastal sedimentation, have impacted on the northern population through time (reviewed by Webster 2018).

7.3 Limitations of this analysis

For commercial fisheries, the estimation of annual deaths and risk was limited by the small number of observed captures across all years of observer data extract (24 captures in total). Given the small number of observed captures, stochasticity can affect the observed number of captures and the resulting risk model predictions of annual deaths and risk. Notably, the sample size of catch rate information of yellow-eyed penguin will have increased substantially with the full rollout during the 2023–24 fishing year of onboard camera-based monitoring of commercial fishing events, including

protected species captures monitoring⁵. Thus, updating the risk model with additional years of data could affect SEFRA model estimates of annual deaths and risk ratio.

Yellow-eyed penguins prefer to forage at-sea during daylight hours. However, a general lack of information about the time of day at both the start and end of unobserved fishing events precluded an assessment of the diel period of fishing on historical annual deaths (i.e., prior to the implementation of electronic reporting). This could be explored by future assessments once sufficient years of fishing data with comprehensive date-time information have been collected.

Generally, the observed captures of adult yellow-eyed penguins were located within the spatial domain of the calculated overlap between observed fishing events and the assumed adult foraging distribution layer (Figure D.4). However, a number of captures were observed off the northern part of North Otago, where there was almost no overlap. Furthermore, several captures were observed in Foveaux Strait where the calculated overlap was minimal. The sample size of observed captures (24 individuals in the PSCv9 sample) is still quite small, such that a mismatch could still result from sampling error. However, it is also possible that the assumed spatial distribution layers, which were derived based on the available at-sea distribution data (i.e., pings from birds at the surface), were not fully representative of the spatial distribution of yellow-eyed penguins foraging near the seafloor, i.e., where they are more likely to interact with commercial set-nets. Where this is the case, the results of this SEFRA model assessment should be treated with some caution. For example, if the degree of spatial overlap with the North Otago sub-population turned out to be higher than was estimated by the current study, then the risk of commercial fishing here would also be higher here (and lower elsewhere) than was estimated by the SEFRA model. An alternative explanation for the observed captures in the North Otago 1 area would be that these were immature or non-breeding mature birds, which were assumed by the current SEFRA models to have the same at-sea distribution as breeding adults (Figure E.1). Therefore, one solution might be to trial using the juvenile/fledgling at-sea distribution (Figure E.2, Figure E.5), which is less concentrated than the assumed adult distribution, for immature and even non-breeding mature birds in the SEFRA model.

Despite these limitations, commercial fishing is still likely to have the best information about mortality rate of any of the probable threats to yellow-eyed penguins. The necropsy data were informative of the mortality rate of other proximate causes of death, including malnutrition, disease, predation, and trauma. However, there are likely to be inherent biases in these data affecting their representativeness of wider population-level causes of death, since many of these causes of death are the ones being targeted by active management and, so, may be overly represented in the necropsy records (based on advice received from the Hoiho Technical Group, 3 April 2023). Furthermore, each of these threats will ultimately be caused by an unknown mixture of natural and anthropogenic threats, e.g., malnutrition could plausibly be driven by natural fluctuations in marine prey, as well as longer term changes driven by multiple human stressors. This uncertainty led to the decision to not estimate population risk from these causes of death, leaving only commercial fisheries to be assessed in this way.

Thus, for most other threats we lacked any mortality rate information that could be applied at a population level. For some of these it was possible to estimate or use threat intensity layers, some of which used proxy information, to estimate relative spatial overlap. For these threats, the quality of assessment would largely depend on the quality of the respective threat intensity layers, which is likely to be not so good for some threats (e.g., the predation threat from terrestrial predators), compared with others (e.g., aquaculture). There was no quantitative assessment for some of the more diffuse threats, such as the indirect effects of fishing on prey species and habitat, increasing sedimentation of coastal waters, pollutants, and changes in land use through time (reviewed by Webster 2018), although some of these could plausibly have affected major changes in population size and trajectory.

_

⁵ https://www.mpi.govt.nz/fishing-aquaculture/commercial-fishing/fisheries-change-programme/on-board-cameras-for-commercial-fishing-vessels/#Tf

The risk assessment developed plausible population models for each of the five assessed regions, estimated annual deaths for some threats, population risk from commercial fisheries, as well as the population effects of reducing mortality rates, but did not assess the *population effects of specific threats*, which could be achieved using population projections. This was not included in the objectives for this project specified by Fisheries New Zealand, although the population models described in Section 3 could be used for this purpose.

For the purposes of guiding the management response, it also would be helpful to know the population benefits of management. Some threats are being actively managed, e.g., the rehabilitation of birds with disease or malnutrition, and the control of introduced terrestrial predators, although the risk assessment did not estimate the effects of management on demographic rates, population risk, or population trajectory. Lalas et al. (2023) concluded that the recovery in breeder numbers at Moeraki (the main breeding colonies in North Otago 2; see the plots of Barracouta Bay (Okahau Point) and Katiki Point of Figure B.2) was primarily driven by the rehabilitation of juveniles and adults that were encountered locally with apparent life-threatening injuries.

Also, there was no assessment of the effects of scientific monitoring, e.g., flipper banding has been estimated to have a major effect on the survival rate of some penguin populations, e.g., around a 6% reduction in the annual survival rate of an Australian population of little blue penguins (*Eudyptula minor*) in the first year after marking and around a 4% reduction per annum thereafter (Dann et al. 2014). For yellow-eyed penguins, flipper banding was replaced at most locations by marking with transponders after around 2010. Stein (2012) assessed the effects on the apparent survival of birds that were single versus double flipper banded and estimated a potentially substantial negative effect for one marking year (2001), but not in another (1992), although apparently could not assess the effects of a single flipper band (compared with none) given the available data. Hence, flipper banding may have had a significant effect on survival rate prior to this change, although this assessment appears to be hampered by the available sample of yellow-eyed penguins that were marked with both flipper bands and transponders (in addition to individuals marked with transponders only).

During the development of the demographic population models described in Section 3, a decision was made to account for movement rather than potential mark loss, since the former was considered to have a greater confounding effect on the estimation of annual survival rate for some regions (Maunder et al. 2007). The rate of annual mark loss is likely to vary considerably depending on the mark type used, e.g., comparing flipper bands and transponders and methods used to attach them to penguins, as well as the penguin species and their respective physiologies and behaviours (summarised by Whitney 2014). With respect to mark type, it is likely that band loss rate is likely to be low, if not negligible, compared with the loss rate of transponders, which was as high as 5% in the first year for a population of little blue penguin in Australia (Dann et al. 2014). However, the estimation of band loss rate for yellow-eyed penguins appears to be hampered by the small sample of individuals that were double marked (a total of 434 birds across both sexes across the extract of YEPDB, of which 372 were marked at Boulder Beach, Otago Peninsula), and a lack of information in YEPDB on the number of bands seen during resighting events.

This assessment also did not assess the effects of marine pollutants, although it should be noted that the historical usage of organochlorine pesticides and polychlorinated biphenyls (PCBs; banned in New Zealand in 2004) have been relatively low around New Zealand (Buckland et al. 1998). The use of DDT has been restricted in New Zealand since the 1970s, but it does have a long half-life and can persist in the environment for long periods. Little is known about the effects of these pollutants on yellow-eyed penguins specifically (reviewed by Webster 2018).

There was a general sparsity of demographic, population, and necropsy information from the Stewart Island sub-population. This population arguably had the most adverse population trajectory (based on individual breeding locations, since island-wide counts are infrequent) and most adverse hatching/fledgling rates of any of the assessed regions. Likewise, apart from the nest counts, data for the small Banks Peninsula sub-population were too sparse to inform a plausible population model.

7.4 Potential research

The following suggestions are made with respect to potential research on the **inputs of population models and risk assessments** for yellow-eyed penguins:

- Continued collection of information that can be used to identify the diel period of individual fishing events, given daytime foraging preference of yellow-eyed penguins.
- With the objective of improving SEFRA model estimates of spatial overlap with commercial set-nets:
 - an increase in the sample of juvenile and adult foraging studies of yellow-eyed penguin that includes paired geolocation and time-depth recorder monitoring would facilitate the generation of representative spatial distribution layers of yellow-eyed penguin foraging near the seafloor; and
 - o the SEFRA model could trial assuming that a portion (e.g., immature/non-breeders) of the observed captures of adults are actually juveniles (this would assume the juvenile/fledgling distribution layer instead of using the adult distribution layer as was done in the current assessment).
- Consideration of collecting information that would help with the estimation of mortality rate caused by marking with flipper bands, which continues at some locations including Boulder Beach, Otago Peninsula. This would require the double-marking of a portion of the population, which may also be helpful for the estimation of transponder loss rate.
- More frequent and comprehensive monitoring of the Stewart Island and Banks Peninsula subpopulations would facilitate the identification of demographic drivers of change there and the threat-specific causes of population change.
- The estimation of mortality rate from non-fisheries causes of death benefits from periods of relatively non-selective sampling of carcasses for necropsy, such that threat-specific biases in relative detection probability can be minimised.
- The consideration of experimental research that can be used to inform the development of cryptic mortality rate priors for yellow-eyed penguins and other species in commercial setnets

The following suggestions are made with respect to **risk assessment approaches** for yellow-eyed penguins:

- The population models developed by this project could be modified to distinguish birds that have been subject to rehabilitation, so that the effects of rehabilitation on demographic rates and population trajectory can be estimated.
- The population models could also be modified to assess the population effects of alleviating specific threats or in response to the application of management measures.
- With the modifications proposed under the previous point, the tentative negative relationships between SST and survival rate could be used to predict the effects of future climate scenarios on the regional sub-populations of yellow-eyed penguin.
- Compare the effects of daytime versus nighttime fishing events on risk model estimates of annual deaths.

8. ACKNOWLEDGEMENTS

We thank the Hoiho Technical Group, the members of the Fisheries New Zealand's Aquatic Environment Working Group, members of the Yellow-eyed Penguin Trust, and attendees of the project workshop, who provided many useful comments and suggestions to help improve this assessment.

We also thank the numerous field scientists and volunteers who collected the demographic and population size data used by this assessment, as well as the wildlife pathologists who contributed to the necropsy data used.

The Department of Conservation for maintaining the YEPDB since the late 1980s, and Proteus for grooming and updating the database under Fisheries New Zealand contract PSB2020-05.

NIWA for their characterisation of commercial fishing activity overlapping with hoiho under Fisheries New Zealand contract PSB2020-06.

This research was supervised by William Gibson from Fisheries New Zealand under project PRO2022-01, which was awarded to Quantifish Limited.

9. REFERENCES

- Aguilar, G.D.; Farnworth, M.J.; Winder, L. (2015). Mapping the stray domestic cat (*Felis catus*) population in New Zealand: Species distribution modelling with a climate change scenario and implications for protected areas. *Applied Geography*, 63: 146–154.
- Baker, G.B.; Candy, S.; Parker, G. (2021). Improving estimates of cryptic mortality for use in seabird risk assessments: loss of seabirds from longline hooks. *New Zealand Aquatic Environment and Biodiversity Report No. 268.* 7 p.
- Beentjes, M.P.; Bian, R. (2022). Characterisation of commercial fishing activity overlapping with South Island hoiho (*Megadyptes antipodes*) distribution. *New Zealand Aquatic Environment and Biodiversity Report No. 297.* 92 p.
- Beentjes, M.P.; Renwick, J.A. (2001). The relationship between red cod, *Pseudophycis bachus*, recruitment and environmental variables in New Zealand. *Environmental Biology of Fishes*, 61: 315–328.
- Boessenkool, S.; Austin, J.J.; Worthy, T.H.; Scofield, P.; Cooper, A.; Seddon, P.J.; Waters, J.M. (2009). Relict or colonizer? Extinction and range expansion of penguins in southern New Zealand. *Proceedings Royal Society B, 276*: 815–821.
- Breitwisch, R. (1989). Mortality Patterns, Sex Ratios, and Parental Investment in Monogamous Birds. In: Power, D.M. (eds) Current Ornithology. *Current Ornithology, vol 6*. Springer, Boston, MA. pp 1–50.
- Buckland, S.J.; Ellis, H.K.; Salter, R.T. (1998). Organochlorines in New Zealand: Ambient concentrations of selected organochlorines in soils. Ministry for the Environment, Wellington. 176 p.
- Cole, T.L.; Ksepka, D.T.; Mitchell, K.J.; Tennyson, A.J.D.; Thomas, D.B.; Pan, H.; Zhang, G.; Rawlence, N.J.; Wood, J.R.; Bover, P.; Bouzat, J.L.; Cooper, A.; Fiddaman, S.R.; Hart, T.; Miller, G.; Ryan, P.G.; Shepherd, L.D.; Wilmshurst, J.M.; Waters, J.M. (2019). Mitogenomes uncover extinct penguin taxa and reveal island formation as a key driver of speciation. *Molecular Biology and Evolution*, 36: 784–797.

- Dann, P.; Sidhu, L.A.; Jessop, R.; Renwick, L.; Healy, M.; Dettmann, B.; Baker, B.; Catchpole, E.A. (2014). Effects of flipper bands and injected transponders on the survival of adult little penguins *Eudyptula minor*. *Ibis*, 156: 73–83.
- Darby, J.T.; Dawson, S.M. (2000). Bycatch of yellow-eyed penguins (*Megadyptes antipodes*) in gillnets in New Zealand waters 1979-1997. *Biological Conservation*, *93*: 327–332.
- Davis, S. (2014). *New Zealand population density by meshblock*. Shapefile based on data collected by Stats NZ. URL: https://koordinates.com/layer/7322-new-zealand-population-density-by-meshblock/.
- Department of Conservation (2014). *Distribution of Stoat in New Zealand (2014)*. URL https://docdeptconservation.opendata.arcgis.com/datasets/bedcacbb2a00464e966dd576548ce34b_0/about.
- Dillingham, P.W.; Moore, J.E.; Fletcher, D.; Cortes, E.; Curtis, K.A.; James, K.C.; Lewison, R.L. (2016). Improved estimation of intrinsic growth *rmax* for long-lived species: integrating matrix models and allometry. *Ecological Applications* 26: 322–333.
- Eberhart-Phillips, L.J.; Küpper, C.; Carmona-Isunza, M.C.; et al. (2018). Demographic causes of adult sex ratio variation and their consequences for parental cooperation. *Nature Communications: 9*: 1651.
- Edwards, C.T.T.; Peatman, T.; Goad D.; Webber, D.N. (2023a). Update to the risk assessment for New Zealand seabirds. *New Zealand Aquatic Environment and Biodiversity Report No. 314*. 66 p. URL: https://www.mpi.govt.nz/dmsdocument/57181/direct
- Edwards, C.T.T.; Peatman, T.; Goad D.; Webber, D.N. (2023b). Review of biological inputs for the New Zealand Seabird Risk Assessment. New Zealand Aquatic Environment and Biodiversity Report No. 312. 193 p. URL: https://fs.fish.govt.nz/Doc/25400/AEBR-312-Review-Of-Biological-Inputs-For-New-Zealand-Seabird-Risk-Assessment-4357-2023.pdf.ashx
- Efford, M.; Spencer, N.; Darcy, J. (1996). Population studies of yellow-eyed penguins 1993–94 progress report. Department of Conservation, Wellington. 30 p. URL: https://www.researchgate.net/publication/247207877_Population_studies_of_yellow-eyed_penguins
- Francis, R.I.C.C.; Sagar, P.M. (2012). Modelling the effect of fishing on southern Buller's albatross using a 60-year dataset. *New Zeala/nd Journal of Zoology 39*: 3–17.
- French, R.R.; Dunn, J.R. (1973). Loss of salmon from high-seas gillnetting with reference to the Japanese salmon mothership fishery. *Fishery Bulletin*, 71: 845–875. URL: https://spo.nmfs.noaa.gov/sites/default/files/pdf-content/1973/713/french.pdf
- Gartrell, B.; Agnew, D.; Alley, M.; Carpenter, T.; Ha, H.J.; Howe, L.; Hunter, S.; McInnes, K.; Munday, R.; Roe, W.; Young, M. (2017). Investigation of a mortality cluster in wild adult yellow-eyed penguins (*Megadyptes antipodes*) at Otago Peninsula, New Zealand. *Avian Pathology*, 46: 278–288.
- Gill, J.M. Darby, J.T. (1993). Deaths in yellow-eyed penguins (*Megadyptes antipodes*) on the Otago Peninsula during the summer of 1990, *New Zealand Veterinary Journal*, 41: 39–42.
- Gownaris, N.J.; Boersma, P.D. (2019). Sex-biased survival contributes to population decline in a long-lived seabird, the Magellanic Penguin. *Ecological Applications* 29: e01826.
- Hersbach, H.; Bell, B.; Berrisford, P.; Biavati, G.; Horányi, A.; Muñoz Sabater, J.; Nicolas, J.; Peubey, C.; Radu, R.; Rozum, I.; Schepers, D.; Simmons, A.; Soci, C.; Dee, D.; Thépaut, J-N. (2023). *ERA5 monthly averaged data on single levels from 1940 to present*. Copernicus Climate Change Service (C3S) Climate Data Store (CDS). (Accessed on 10-12-2022)
- Hickcox, R.P.; Young, M.J.; MacKenzie, D.I. (2023). Grooming and preparation of the Yellow-eyed Penguin Database. *New Zealand Aquatic Environment and Biodiversity Report No.* 307. 136 p.

- Hocken, G. (2005). Necropsy findings in yellow-eyed penguins (*Megadyptes antipodes*) from Otago, New Zealand. *New Zealand Journal of Zoology*, 32: 1–8.
- iNaturalist Community (2023). Observations of New Zealand sea lion (*Phocarctos hookeri*) observed from Jan 1981 to March 2023. Exported from https://www.inaturalist.org on 8 March 2023.
- Lalas, C.; Goldsworthy, R.; Ratz, H. (2023). Assessing the effectiveness of rehabilitation for management of an endangered seabird, the Yellow-eyed Penguin. *Emu Austral Ornithology* 123(4): 1–10. DOI: 10.1080/01584197.2023.2241880
- Lalas, C.; Ratz, H.; McEwan, K.; McConkey, S.D. (2007). Predation by New Zealand sea lions (*Phocarctos hookeri*) as a threat to the viability of yellow-eyed penguins (*Megadyptes antipodes*) at Otago Peninsula, New Zealand. *Biological Conservation*, 135: 235–246.
- Land Information New Zealand (2011). *NZ road centrelines*. URL: https://data.linz.govt.nz/layer/50329-nz-road-centrelines-topo-150k/.
- Large, K.; Roberts, J.; Francis, M.; Webber, D.N. (2019). Spatial assessment of fisheries risk for New Zealand sea lions at the Auckland Islands. *New Zealand Aquatic Environment and Biodiversity Report No. 224*. 85 p.
- Mattern, T. (2020). Modelling marine habitat utilisation by yellow-eyed penguins along their mainland distribution: baseline information. *New Zealand Aquatic Environment and Biodiversity Report* 243. 29 p.
- Mattern, T.; Ellenberg, U. (2018). Yellow-eyed penguin diet and indirect effects affecting prey composition. Report prepared by Eudyptes EcoConsulting for the Conservation Services Programme, Department of Conservation, Wellington. 39 p. URL: https://www.doc.govt.nz/our-work/conservation-services-programme/csp-reports/2017-18/yellow-eyed-penguin-diet-and-indirect-effects-affecting-prey-composition/
- Mattern, T.; Meyer, S.; Ellenberg, U.; Houston, D.M.; Darby, J.T. Young, M.; van Heezik, Y.; Seddon, P.J. (2017). Quantifying climate change impacts emphasises the importance of managing regional threats in the endangered yellow-eyed penguin. *PeerJ*, 5:e3272.
- Maunder, M.N.; Houston, D.M.; Dunn, A.; Seddon, P.J.; Kendrick T.H. (2007). Assessment to risk of yellow-eyed penguins *Megadyptes antipodes* from fisheries incidental mortality in New Zealand fisheries and definition of information requirements for managing fisheries related risk. Unpublished Report held by Fisheries New Zealand. 23 p.
- Ministry for the Environment and Stats NZ. 2020: New Zealand's Environmental Reporting Series: Our freshwater 2020. Wellington, New Zealand. 94 p.
- Moore, P.J. (1992). Yellow-eyed penguin population estimates on Campbell and Auckland Islands 1987-90. *Notornis*, *39*: 1–15.
- Muller, C.G.; Chilvers, B.L.; French, R.K.; Hiscock, J.A.; Battley, P.F. (2020). Population estimate for yellow-eyed penguins (*Megadyptes antipodes*) in the subantarctic Auckland Islands, New Zealand. *Notornis*, 67: 299–319.
- Navigatus Consulting (2015). Marine Oil Spill Risk Assessment 2015 (MOSRA 15). Report prepared by Navigatus Consulting for Maritime New Zealand. 397 p. URL https://www.maritimenz.govt.nz/public/environment/documents/MOSRA-report-2015.pdf
- Pohlert, T. (2023). Trend: Non-Parametric Trend Tests and Change-Point Detection. R package version 1.1.5, URL https://CRAN.R-project.org/package=trend
- R Core Team (2023). R: A language and environment for statistical computing. R Foundation for Statistical Computing, Vienna, Austria. ISBN 3-900051-07-0, URL http://www.R-project.org/.
- Richard, Y.; Abraham, E.; Berkenbusch, K. (2020). Assessment of the risk of commercial fisheries to New Zealand seabirds, 2006–07 to 2016–17. New Zealand Aquatic Environment and Biodiversity Report 237. 57 p.

- Richdale, L.E. (1957). A population study of penguins. Oxford University Press. 195 p.
- Ricker, W.E. (1976). Review of the rate of growth and mortality of Pacific salmon in salt water, and noncatch mortality caused by fishing. *Journal of the Fisheries Research Board of Canada*, 33: 1483–1524.
- Roberts, J.; Edwards, C.T.T. (2023). Population size estimate of New Zealand sea lion (*Phocarctos hookeri*) for 2022. New Zealand Aquatic Environment and Biodiversity Report No. 320. 33 p.
- Roberts, J.O.; Webber, D.N.; Goad, D.W.; Arnould, J.P.Y.; Bell, E.A.; Crowe, P.; Deppe, L.; Elliott, G.P.; Landers T.J.; Freeman, A.N.D.; Mattern, T.; Moore, P.J.; Nicholls, D.G.; Parker, G.P.; Rexer-Huber, K.; Taylor, G.A.; Thompson, D.R.; Walker, K.J.; Waugh, S.M.; Young, M.J. (2022). Spatial distribution modelling of at-risk seabirds in New Zealand commercial fisheries. *New Zealand Aquatic Environment and Biodiversity Report No. 298.* 167 p.
- Roberts, J.O.; Webber, D.N.; Roe, W.T.; Edwards, C.T.T.; Doonan, I.J. (2019). Spatial risk assessment of threats to Hector's/Māui dolphins (*Cephalorhynchus hectori*). New Zealand Aquatic Environment and Biodiversity Report No. 214. 168 p.
- Seddon, P.J.; Davis, L.S. (1989). Nest-site selection by yellow-eyed penguins. Condor, 91: 653-659.
- Sharp, B.R. (2018). Spatially-explicit fisheries risk assessment (SEFRA): a framework for quantifiying and managing incidental commercial fisheries impacts on non-target species. In: Aquatic Environment and Biodiversity Annual Review 2017. Ministry for Primary Industries. pp. 20–56. URL https://www.mpi.govt.nz/dmsdocument/34854-aquatic-environment-and-biodiversity-annual-review-aebar-2018-a-summary-of-environmental-interactions-between-the-seafood-sector-and-the-aquatic-environment
- Stan Development Team (2023). Stan Modeling Language Users Guide and Reference Manual, version 2.32. URL: https://mc-stan.org
- Stein, A. (2012). Lifetime reproductive success in yellow-eyed penguins: influence of life-history parameters and investigator disturbance. MSc thesis, University of Otago. 67 p.
- Sutherland, F. (1999). After the fire. Forest and Bird magazine, 294: 18-19.
- Taylor, P.R., Marriot, P.M. (2004) A summary of information on spawning of the small inshore pelagic species, anchovy (*Engraulis australis*), garfish (*Hyporhamphus ihi*), pilchard (*Sardinops sagax*), and sprat (*Sprattus antipodum* and *S. muelleri*), with a series of stock boundaries proposed for future testing. Unpublished Final Research Report produced for MFish Project PEL2002/01 and held by Fisheries New Zealand. 33 p.
- van Heezik, Y. (1990) Seasonal, geographical, and age-related variations in the diet of the yellow-eyed penguin (*Megadyptes antipodes*). *New Zealand Journal of Zoology*, 17: 201–212.
- Wade, P. (1998). Calculating limits to the allowable human-caused mortality of cetaceans and pinnipeds. *Marine Mammal Science*, *14*: 1–37.
- Webster, T. (2018). The pathway ahead for hoiho Te ara whakamua; Impacts on hoiho: literature review and recommendations. 89 p. URL: https://www.yellow-eyedpenguin.org.nz/app/uploads/2018/06/YEPT_The-pathway-ahead-for-hoiho-February-2018.pdf.
- Whitney, M. (2014). Are transponders a reliable primary mark for yellow-eyed penguins? Report in fulfilment of post-graduate diploma, University of Otago. 33 p.
- Wierenga, J.R.; Morgan, K.J.; Hunter, S.; Taylor, H.S.; Argilla, L.S.; Webster, T.; Dubrulle, J.; Jorge, F.; Bostina, M.; Burga, L.; Holmes, E.C.; McInnes, K.; Geoghegan, J.L. (2023). A novel gyrovirus is abundant in yellow-eyed penguin (*Megadyptes antipodes*) chicks with a fatal respiratory disease. *Virology*, *579*: 75–83.

- Young, M.J.; Dutoit, L.; Robertson, F.; van Heezik, Y.; Seddon, P.J.; Robertson, B.C. (2020). Species in the faeces: DNA metabarcoding as a method to determine the diet of the endangered, yellow-eyed penguin. *Wildlife Research*, 47: 509–522.
- Young, M.J.; Seddon, P.J.; Pütz, K.; Agnew, P.; Mattern, T.; Hickcox, R.P.; Robertson, B.C.; van Heezik, Y. (2022) Conservation implications for post-fledging dispersal of yellow-eyed penguins/hoiho. *Marine Ecology Progress Series* 695: 173–188.

Appendix A. NECROPSY DATA SUMMARY

Table A.1: Summary of the total number of yellow-eyed penguins for which mortality information was available in the necropsy records, by attributed primary cause of death and type of assessment. This table does not include a small number of records in YEPDB of: Sub-Antarctic recoveries (out of scope of assessment); approximately 20 records prior to 1990; and records of hoiho recorded as found offshore (nearly all of these found in set net gear, and which were addressed by the SEFRA model).

Primary cause of death	No necropsy	Formal necropsy	Informal necropsy	All
Unknown	553	154	8	715
Malnutrition	83	211	0	294
Disease	4	120	0	124
Trauma – unknown cause	14	96	1	111
Predation – unknown cause	14	42	0	56
Unexplained mortality	29	23	0	52
Predation – dog	22	25	0	47
Fire	25	0	0	25
Predation – shark	5	18	0	23
Natural	5	13	0	18
Drowned - set net	8	8	0	16
Predation – pinniped	4	8	0	12
Predation – mustelid	1	8	1	10
Accidental	2	3	0	5
Other medical	0	5	0	5
Drowned – unknown cause	0	3	1	4
Assumed	3	0	0	3
Human - intentional	2	0	0	2
Other	2	0	0	2
Drowned - trawl net	1	0	0	1
Poisoned	0	1	0	1
Research	0	1	0	1
Total	777	739	11	1 527

Table A.2: Summary of the total number of yellow-eyed penguins for which formal a formal necropsy was done, by attributed primary cause of death and examiner.

							Primary caus	se of death
Examiner	Malnutrition	Disease	Predation	Trauma	Drowned – set net	Other	Unknown	Total
Wildbase Massey University	154	110	61	57	4	18	103	507
Department of Conservation	36	10	34	34	2	5	18	139
Otago Museum	15	0	6	3	2	1	40	67
Unknown	6	0	0	1	0	2	15	24
Oamaru Veterinary Services	0	0	0	1	0	0	0	1
Wildlife Hospital Dunedin	0	0	0	0	0	0	1	1
All	211	120	101	96	8	26	177	739

Table A.3: Summary of the causes of death of female and male yellow-eyed penguins from the formal necropsy records, as used by the SEFRA model. This table excludes carcasses (15 females and 13 males from the short time series) for which the primary cause of death could not be determined and, so, were not included in these models.

					-	Number of birds
Sex	Malnutrition	Disease	Predation	Trauma	Other	Total
3.6.1	21	10	1.1	_	2	7.1
Male	21	12	11	5	2	51
Female	34	7	15	4	7	67

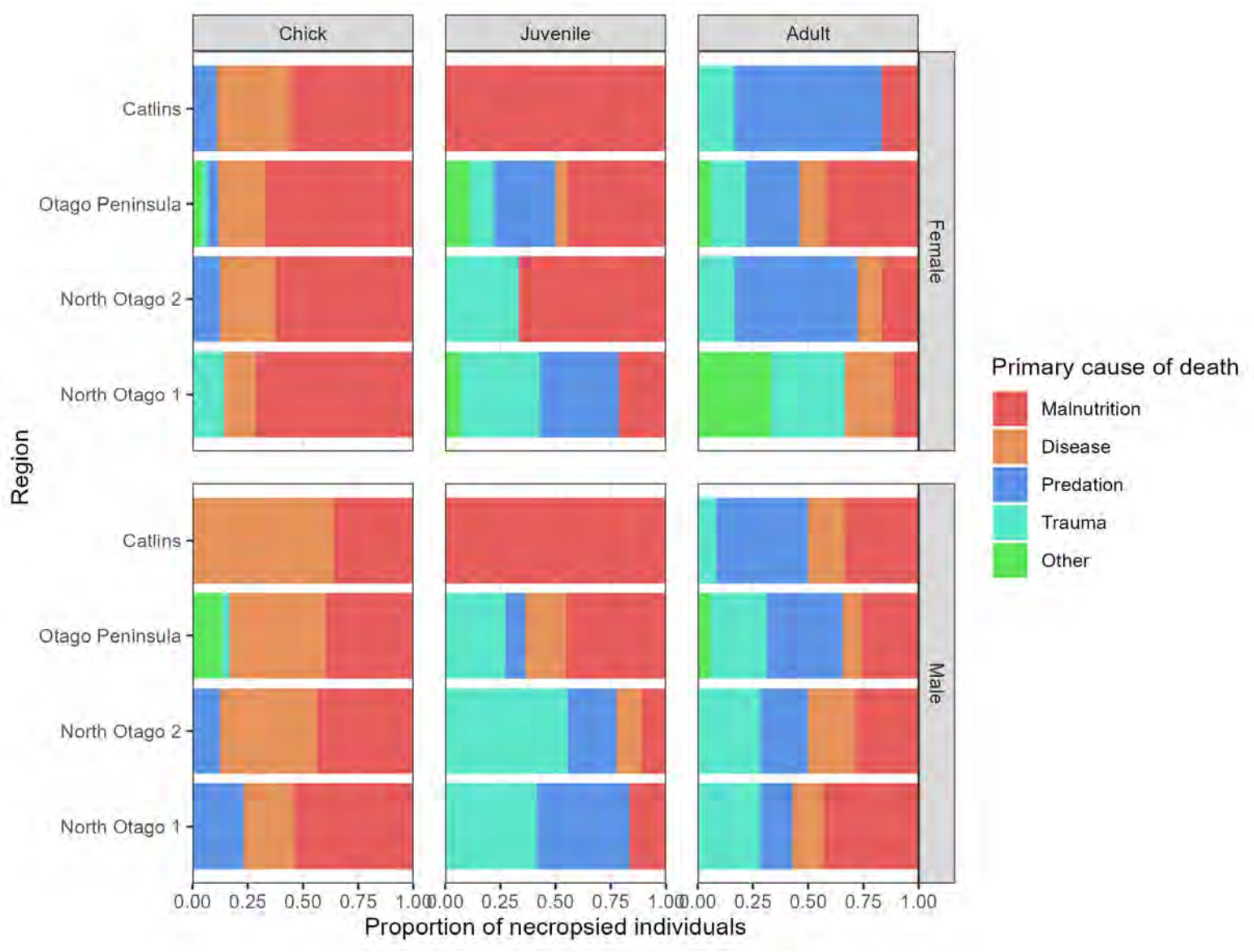


Figure A.1: Proportional primary causes of death from formal necropsy records, by regional sub-population, sex, and age.

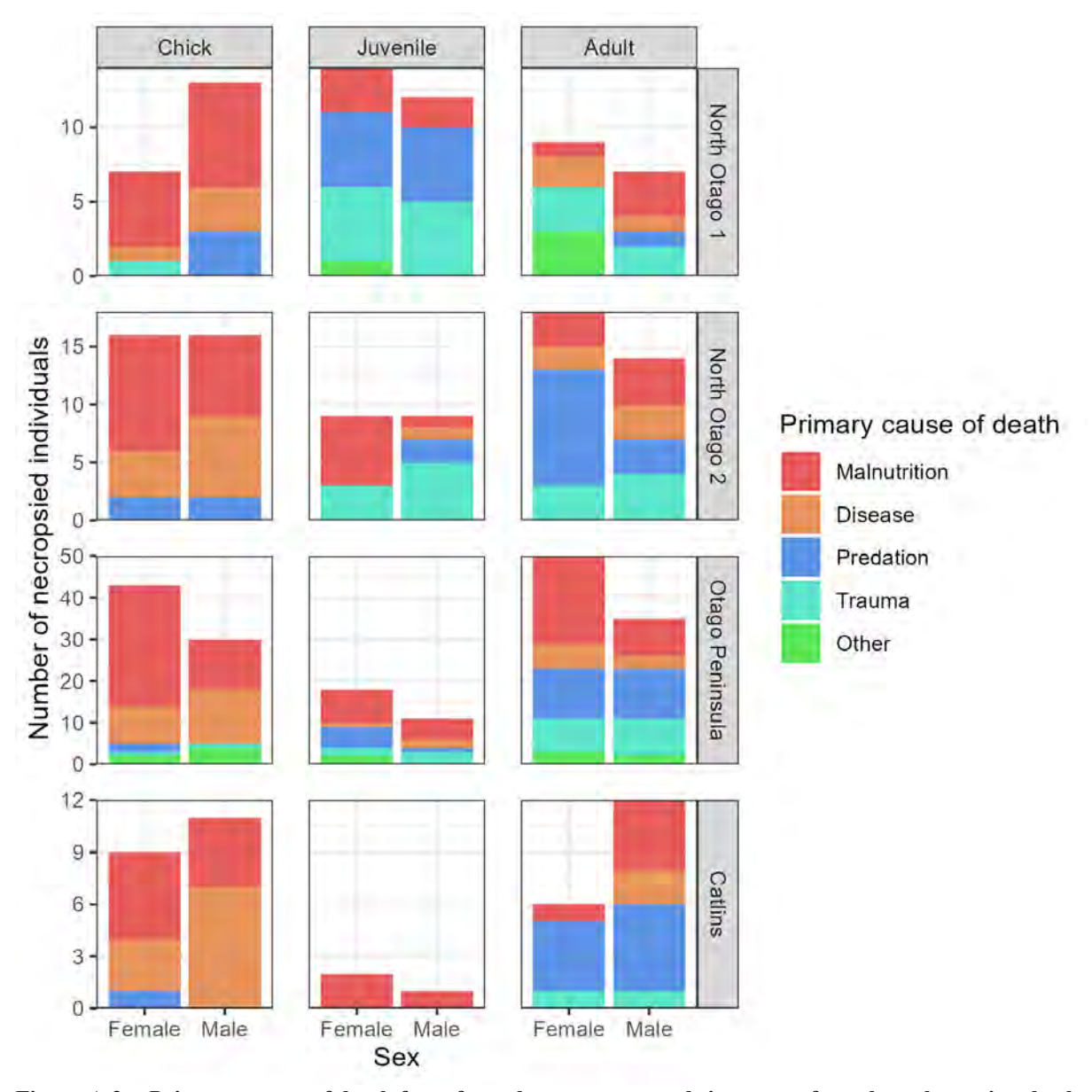


Figure A.2: Primary causes of death from formal necropsy records in terms of numbers, by regional sub-population, sex, and age.

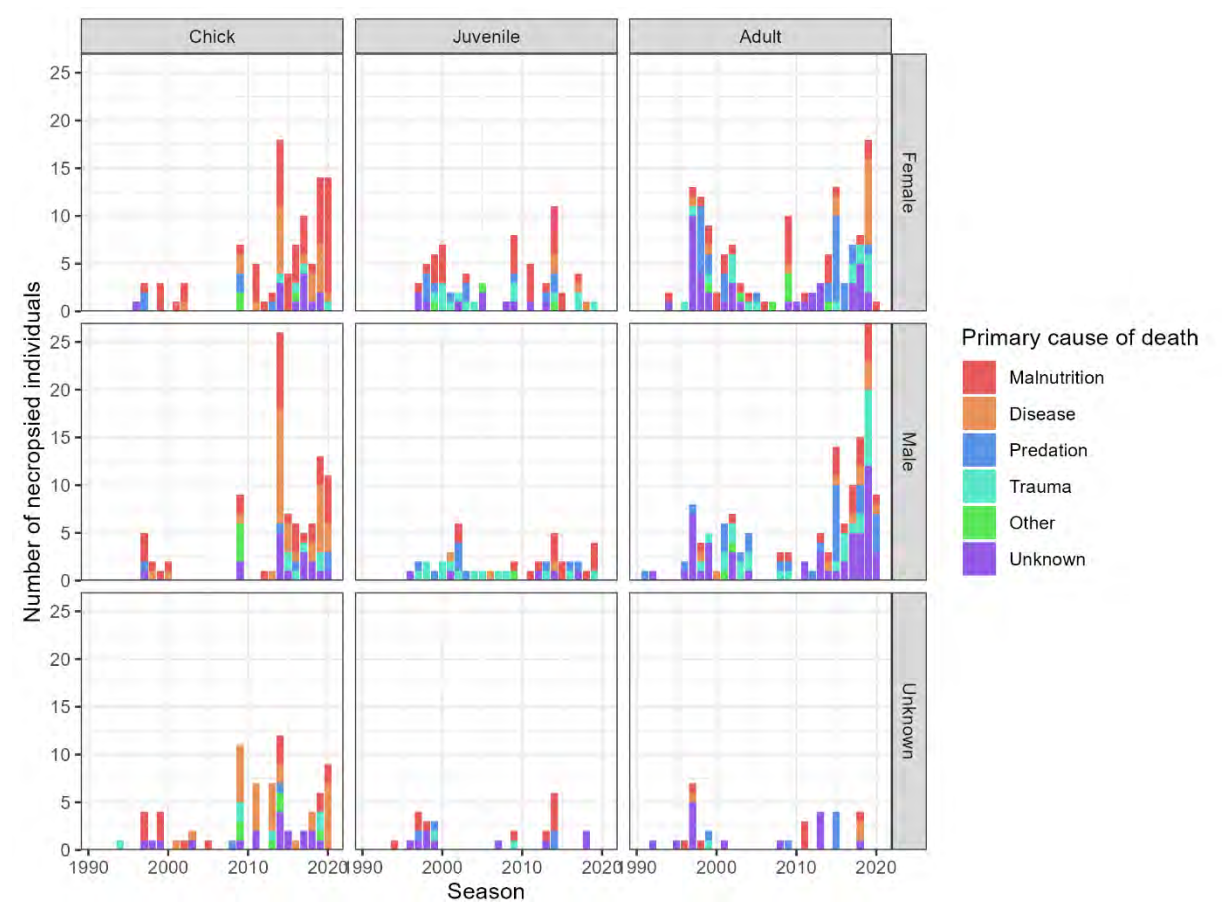


Figure A.3: Primary causes of death from formal necropsy records in terms of numbers, by season, sex, and age.

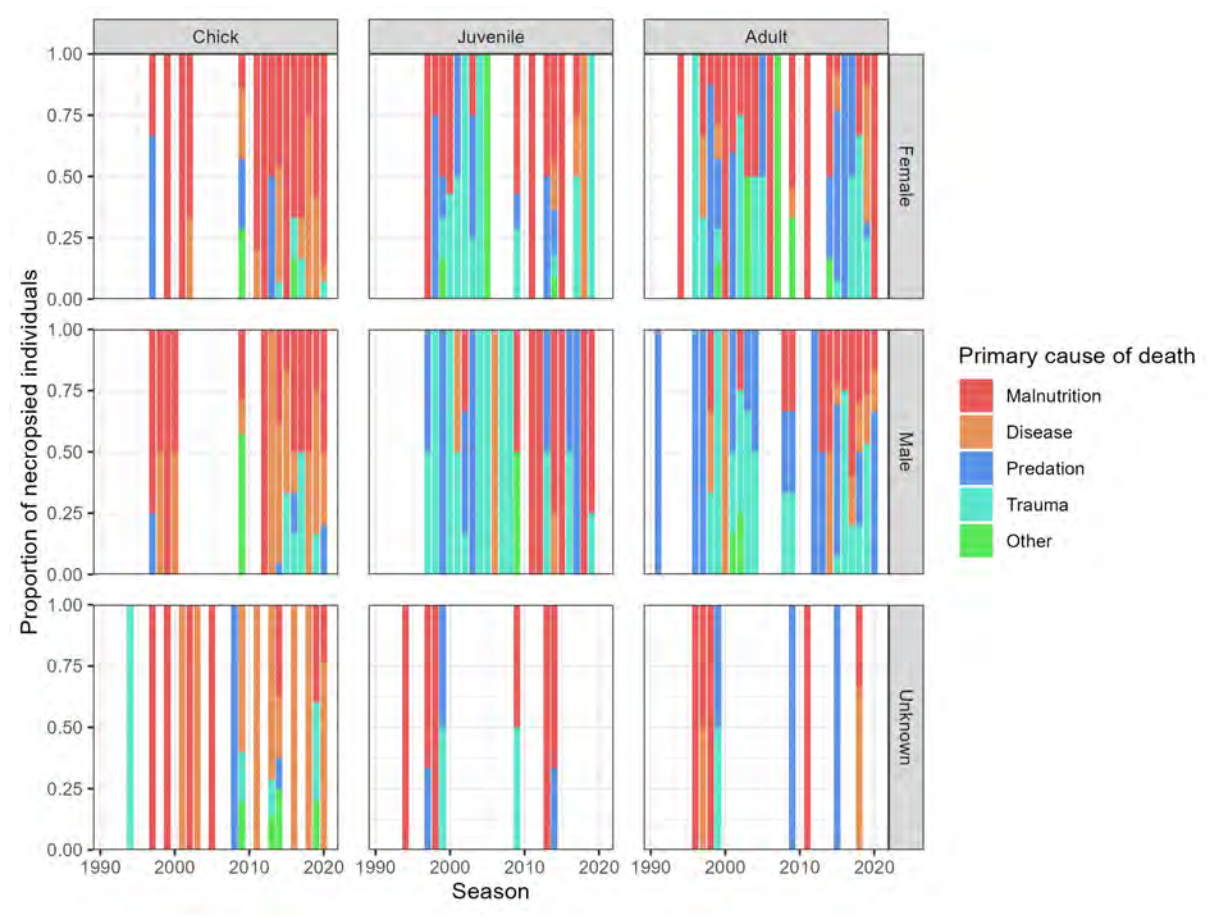


Figure A.4: Proportional primary causes of death from formal necropsy records, by season, sex, and age.

This plot excludes records for which the cause of death could not be determined.

Appendix B. SUPPLEMENTARY TABLES & FIGURES FROM DEMOGRAPHIC POPULATON ASSESSMENT

Annual breeding pairs

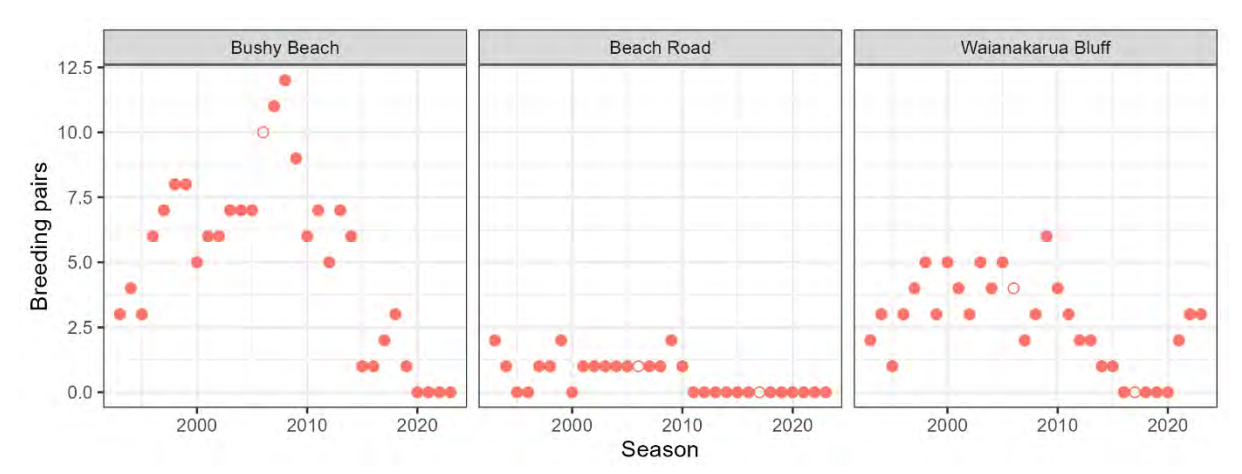


Figure B.1: Estimated number of breeding pairs at North Otago 1 by season and breeding colony. Closed circles are minimum counts and open circles are interpolations (for seasons where a count was not done).

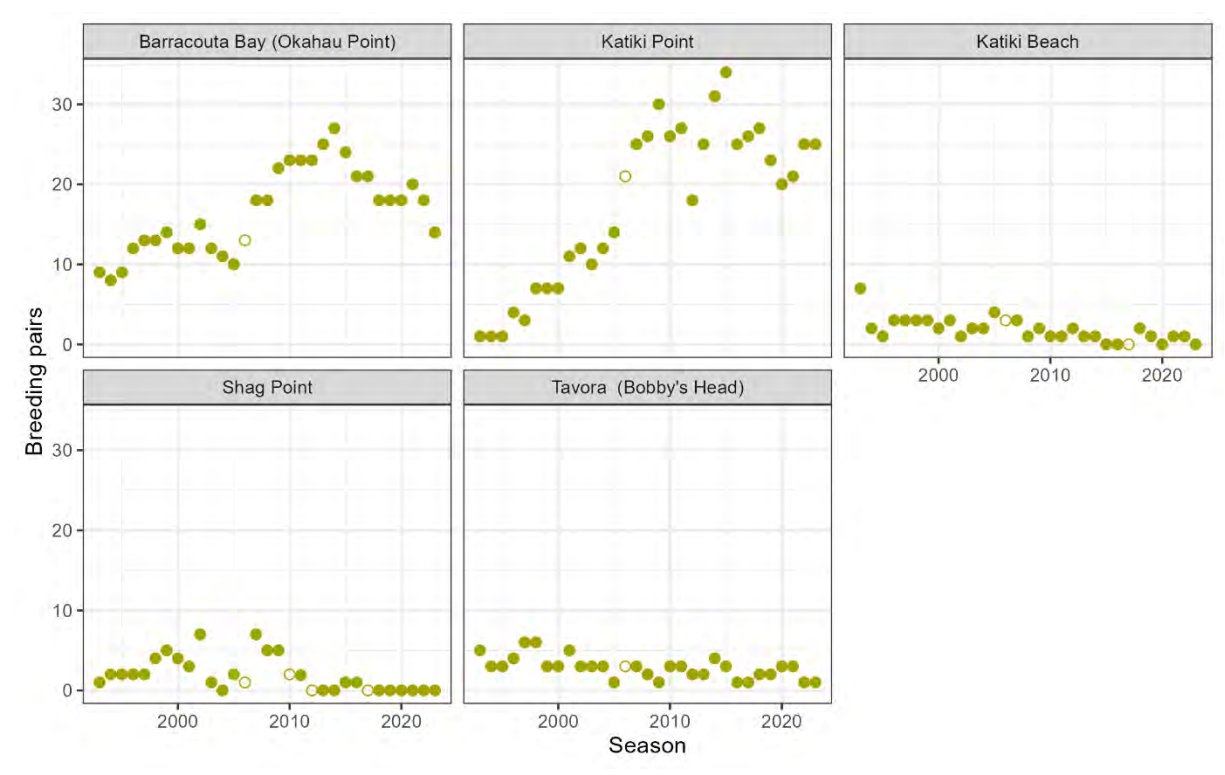


Figure B.2: Estimated number of breeding pairs at North Otago 2 by season and breeding colony. Closed circles are minimum counts and open circles are interpolations (for seasons where a count was not done).

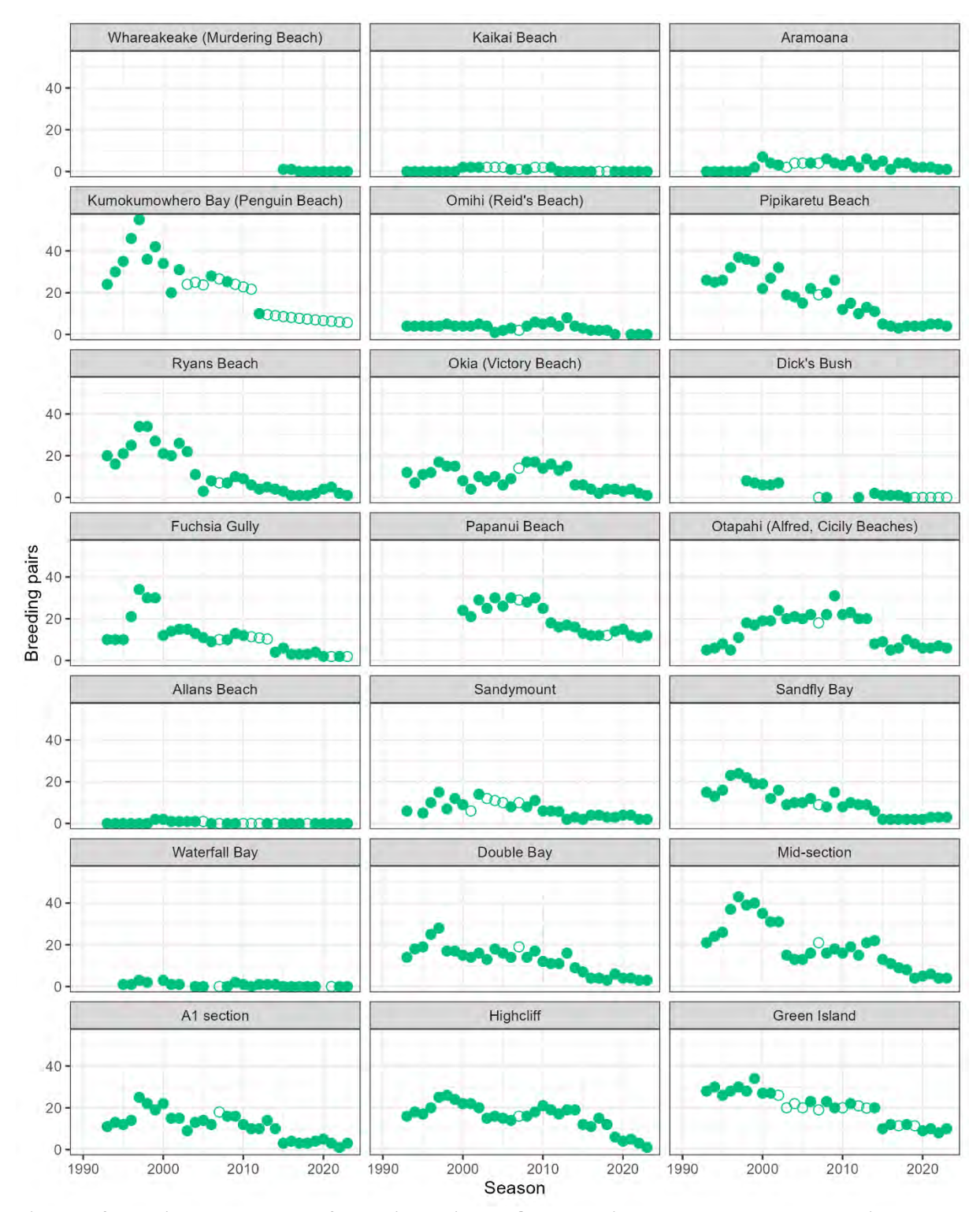


Figure B.3: Estimated number of breeding pairs at Otago Peninsula by season and breeding colony. Closed circles are minimum counts and open circles are interpolations (for seasons where a count was not done).

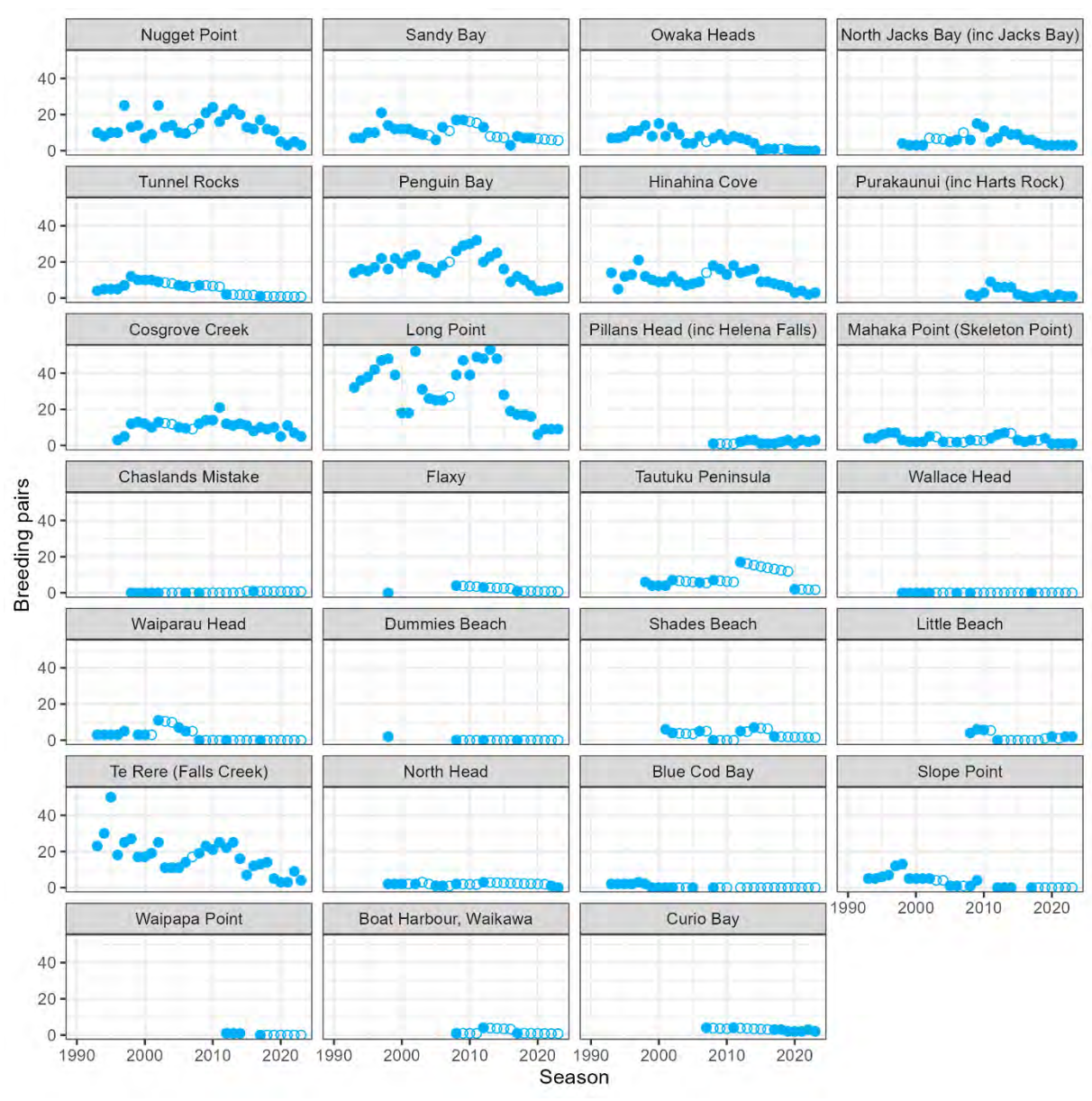


Figure B.4: Estimated number of breeding pairs at the <u>Catlins</u> by season and breeding colony. Closed circles are minimum counts and open circles are interpolations (for seasons where a count was not done).

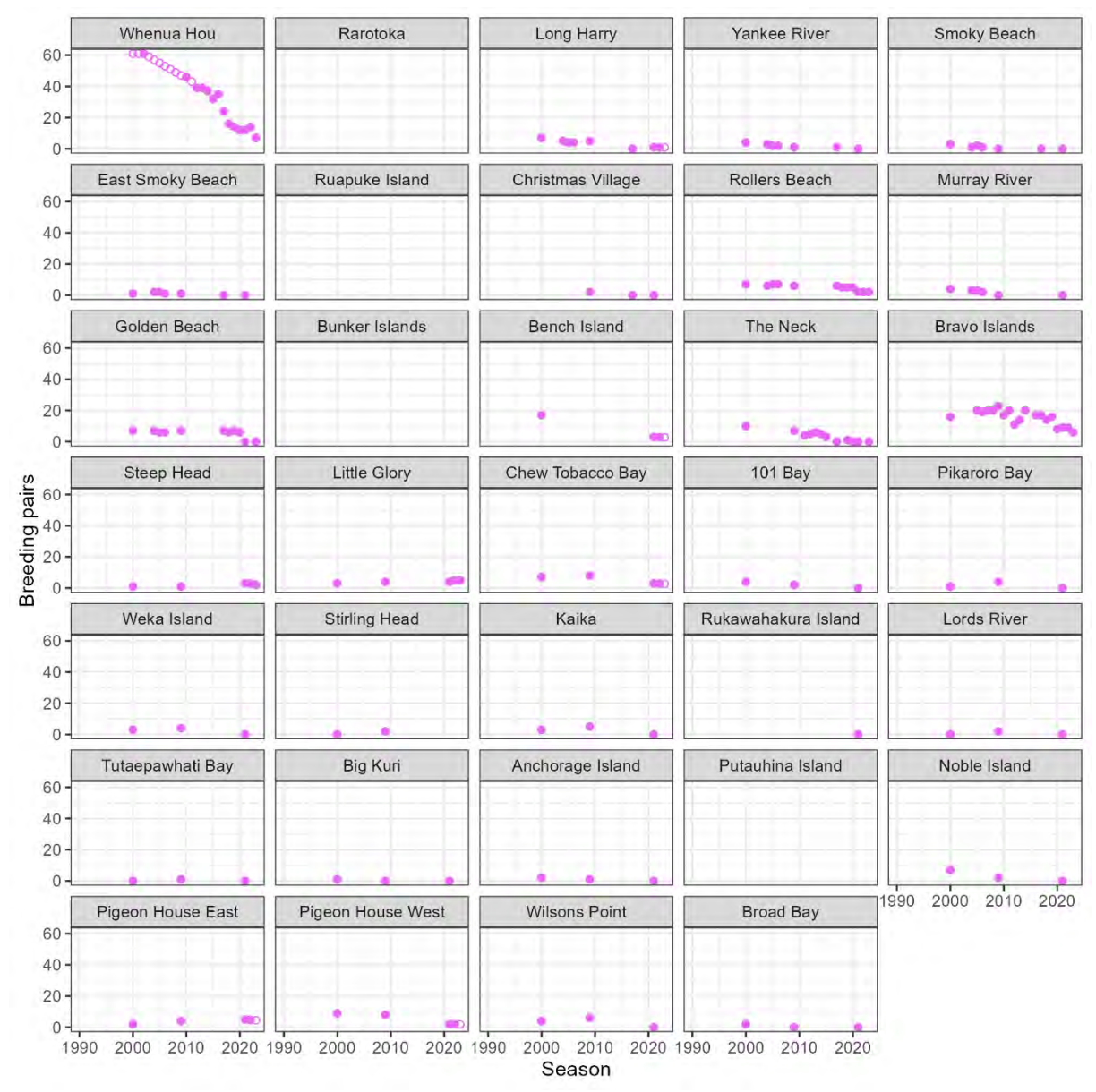


Figure B.5: Estimated number of breeding pairs at <u>Stewart Island</u> by season and breeding colony. Closed circles are minimum counts and open circles are interpolations (for seasons where a count was not done).

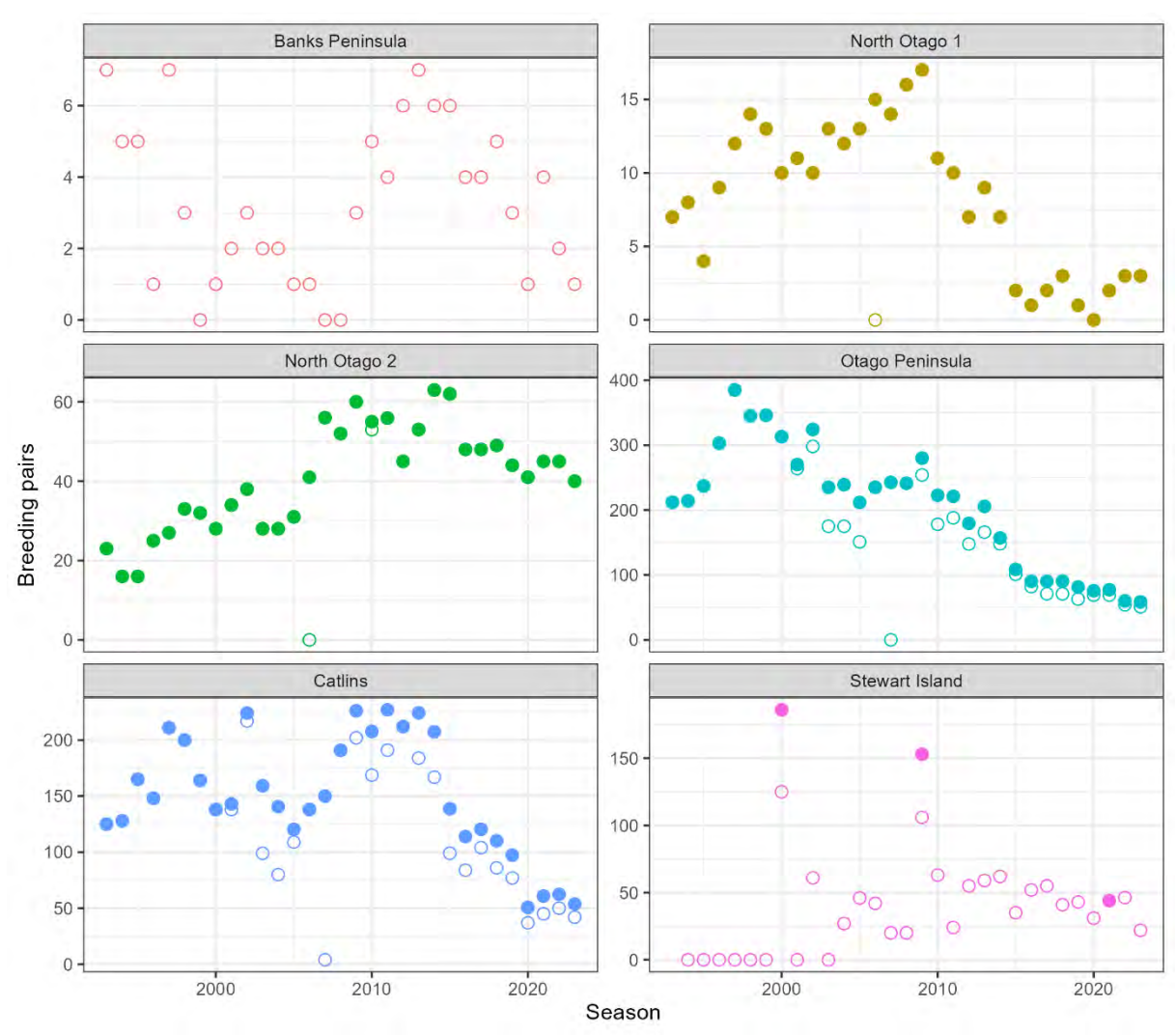


Figure B.6: Estimated number of breeding pairs by season and regional sub-population. Closed circles are the values used by population models (i.e., including interpolations in some years where counts were not done at all breeding colonies); open circles are minimum counts across all colonies for each respective sub-population. Note that the Banks Peninsula data were not used by the population assessment, though are included here for completeness.

Mark capture-recapture data

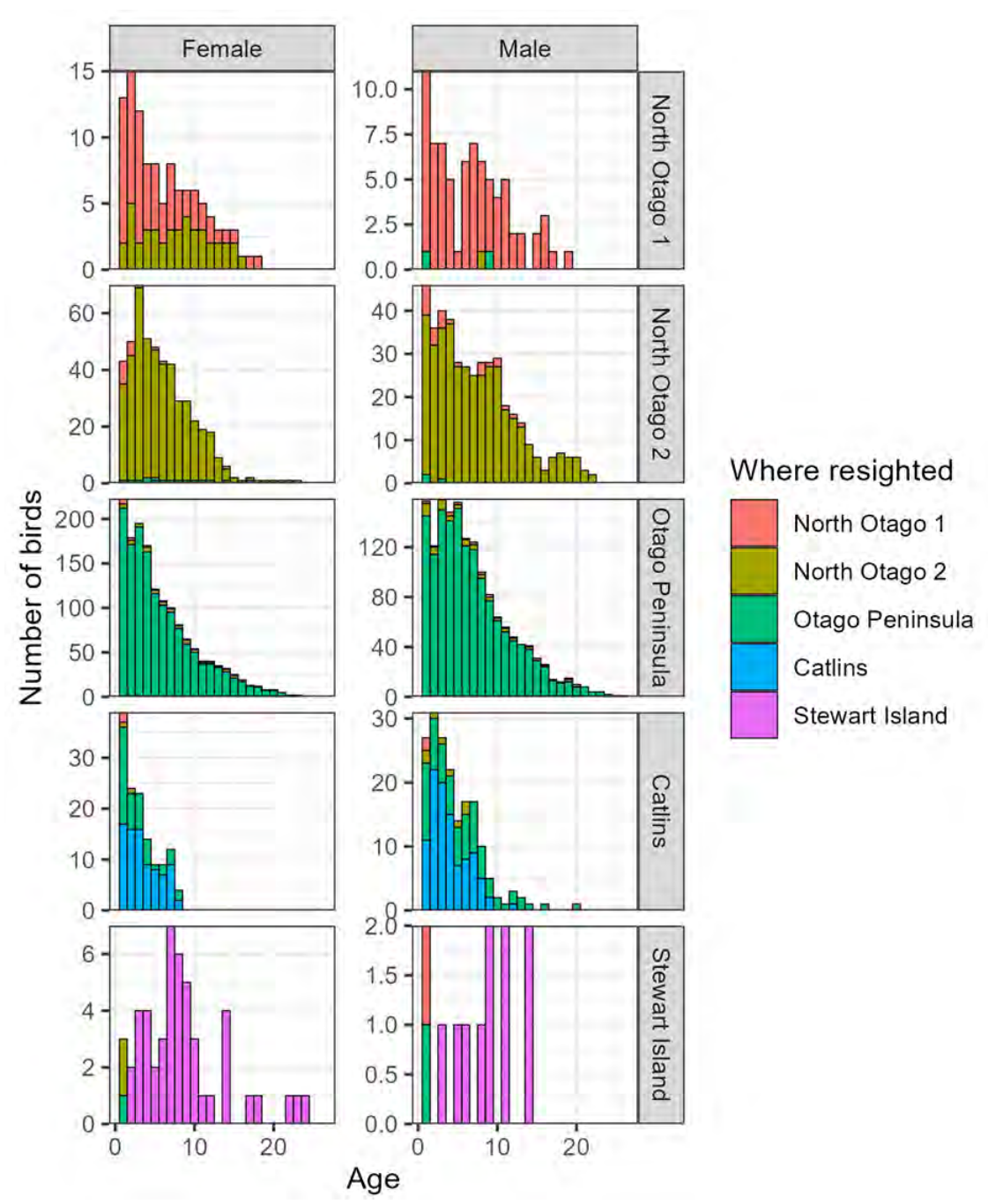


Figure B.7: Region in which female and male yellow-eyed penguins were seen by age and region of marking as chicks.

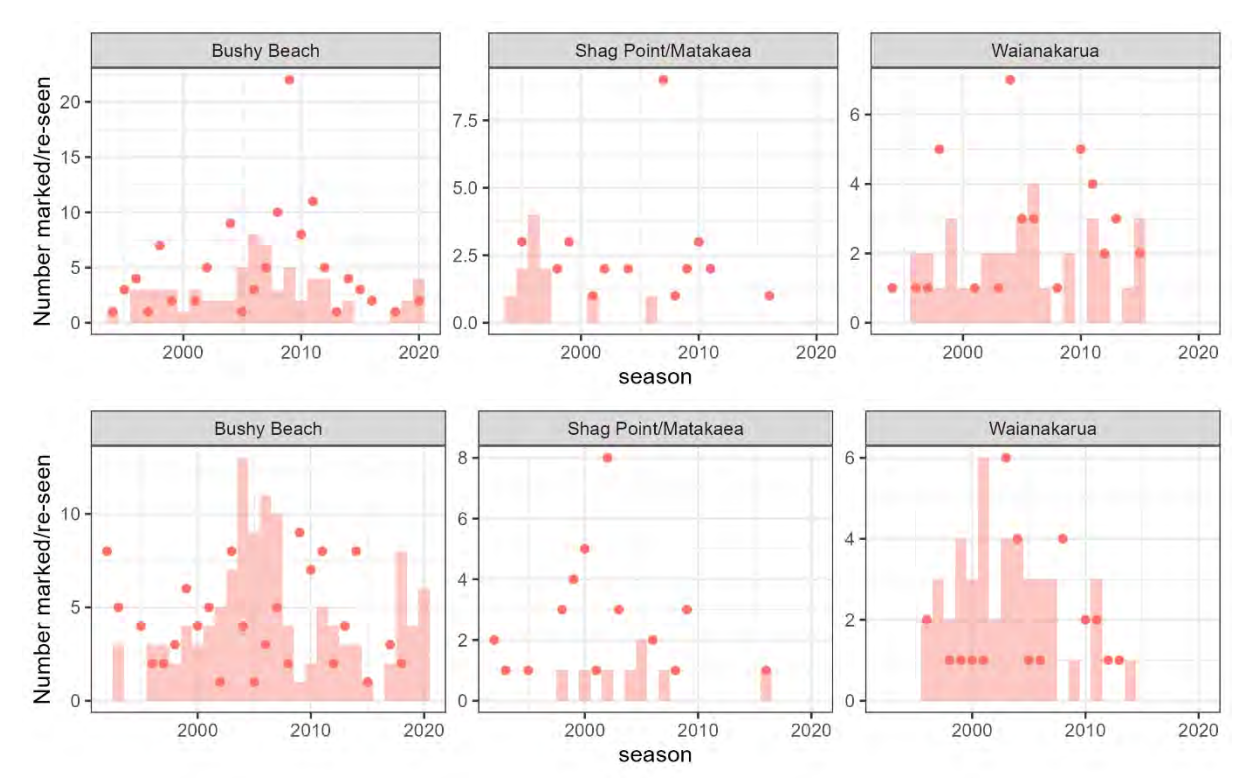


Figure B.8: Annual number of females (top row of plots) and males (bottom row of plots) marked (circles) and reseen (bars) by breeding colony at North Otago 1. Only colonies for which at least 25 birds were marked across all years were included in these plots.

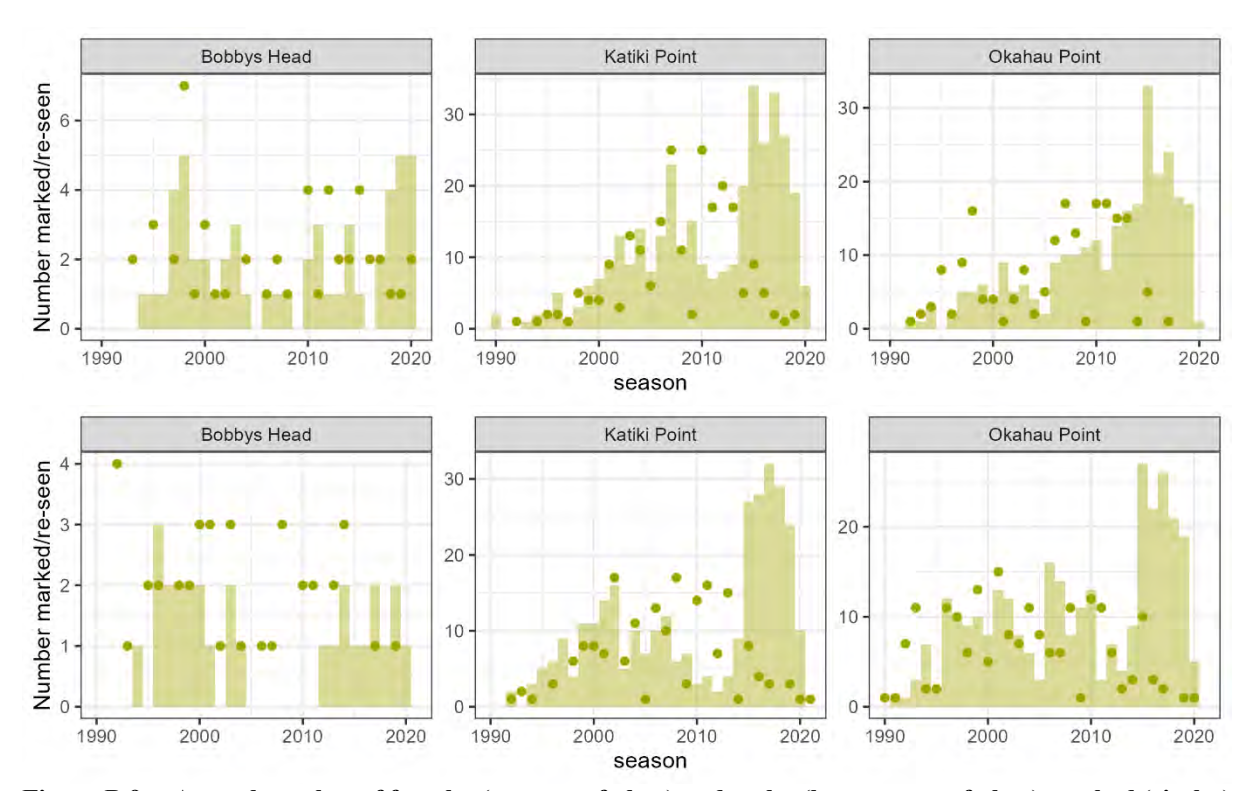


Figure B.9: Annual number of females (top row of plots) and males (bottom row of plots) marked (circles) and reseen (bars) by breeding colony at North Otago 2. Only colonies for which at least 25 birds were marked across all years were included in this plot.

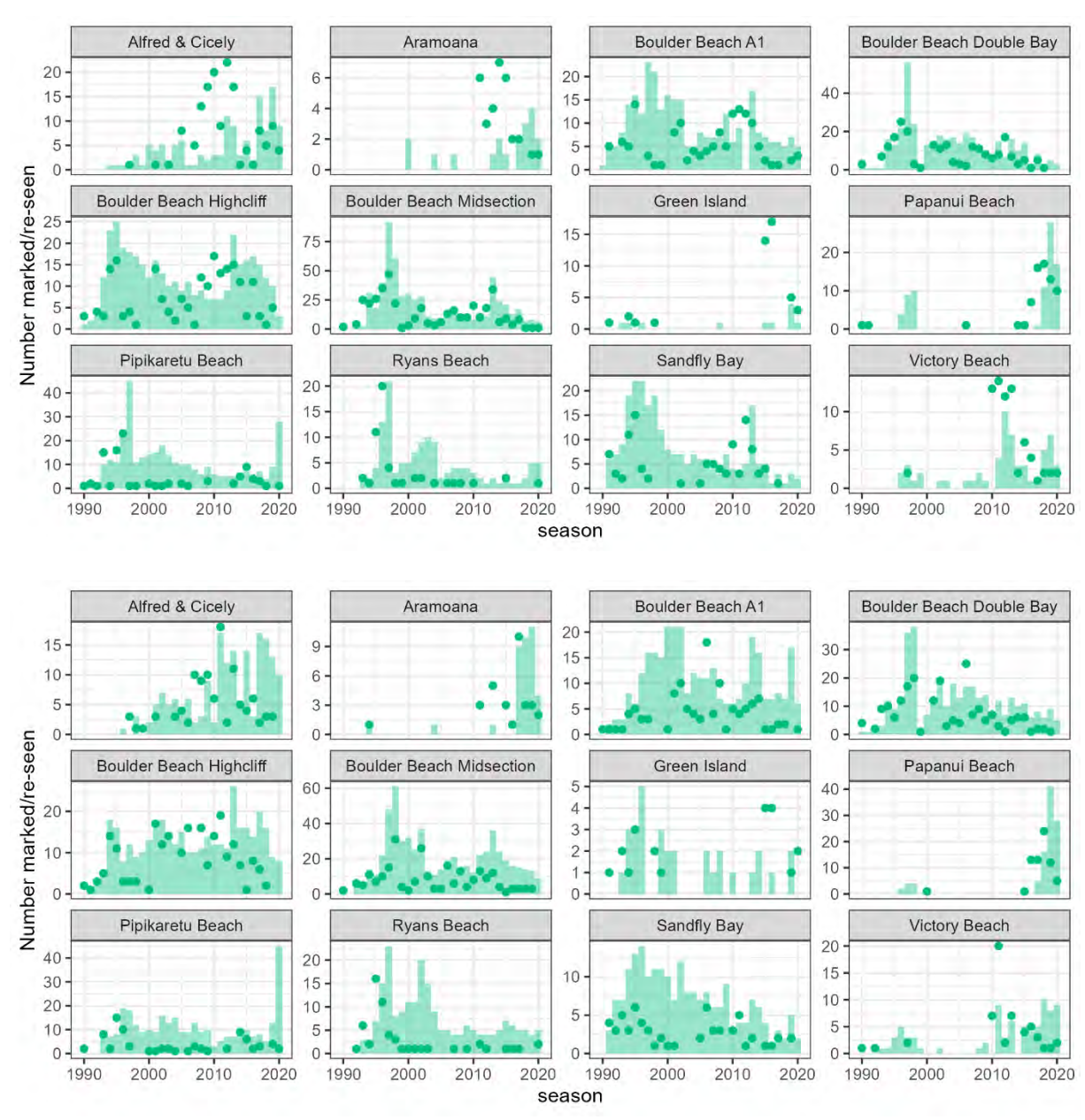


Figure B.10: Annual number of females (top group of plots) and males (bottom group of plots) marked (circles) and reseen (bars) by breeding colony at Otago Peninsula. Only colonies for which at least 25 birds were marked across all years were included in this plot.

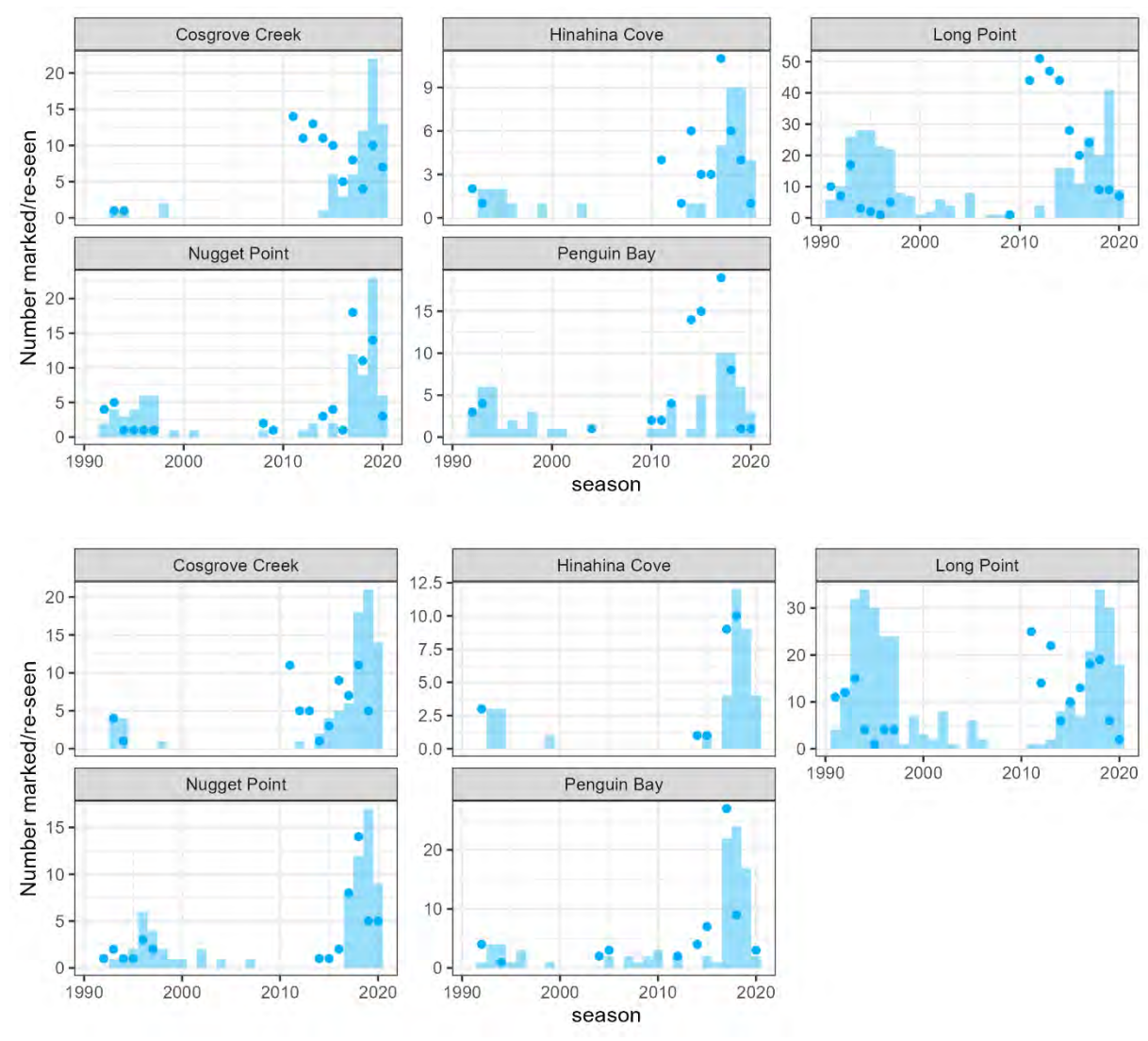


Figure B.11: Annual number of females (top group of plots) and males (bottom group of plots) marked (circles) and reseen (bars) by breeding colony at the <u>Catlins</u>. Only colonies for which at least 25 birds were marked across all years were included in this plot.

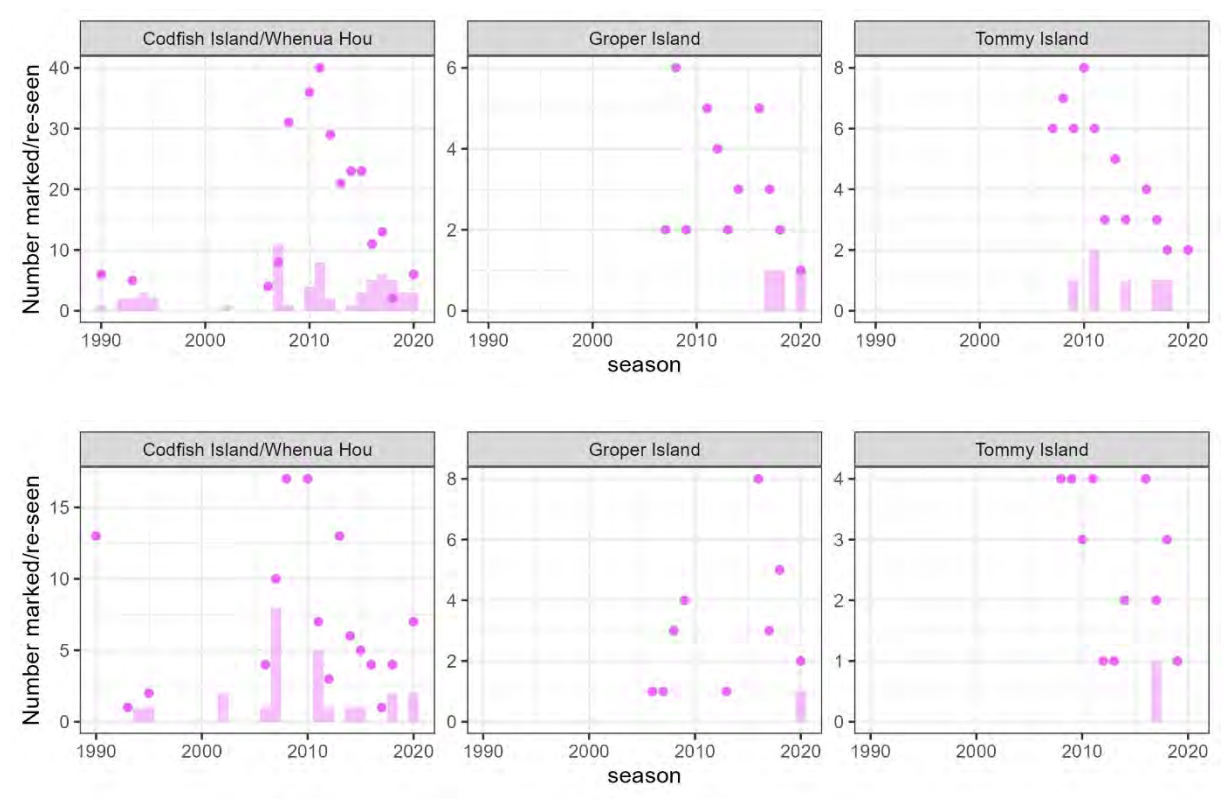


Figure B.12: Annual number of females (top row of plots) and males (bottom row of plots) marked (circles) and reseen (bars) by breeding colony at <u>Stewart Island</u>. Only colonies for which at least 25 birds were marked across all years were included in this plot.

Nest data

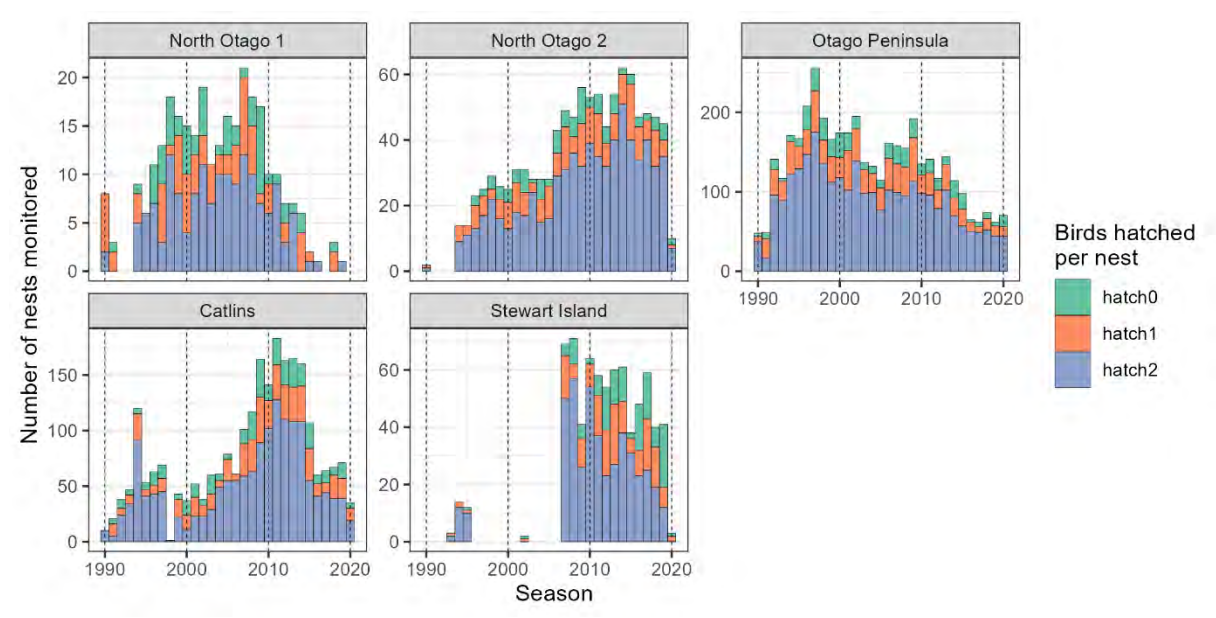


Figure B.13: The number of <u>eggs hatched</u> across all monitored nests, by season and regional sub-population.

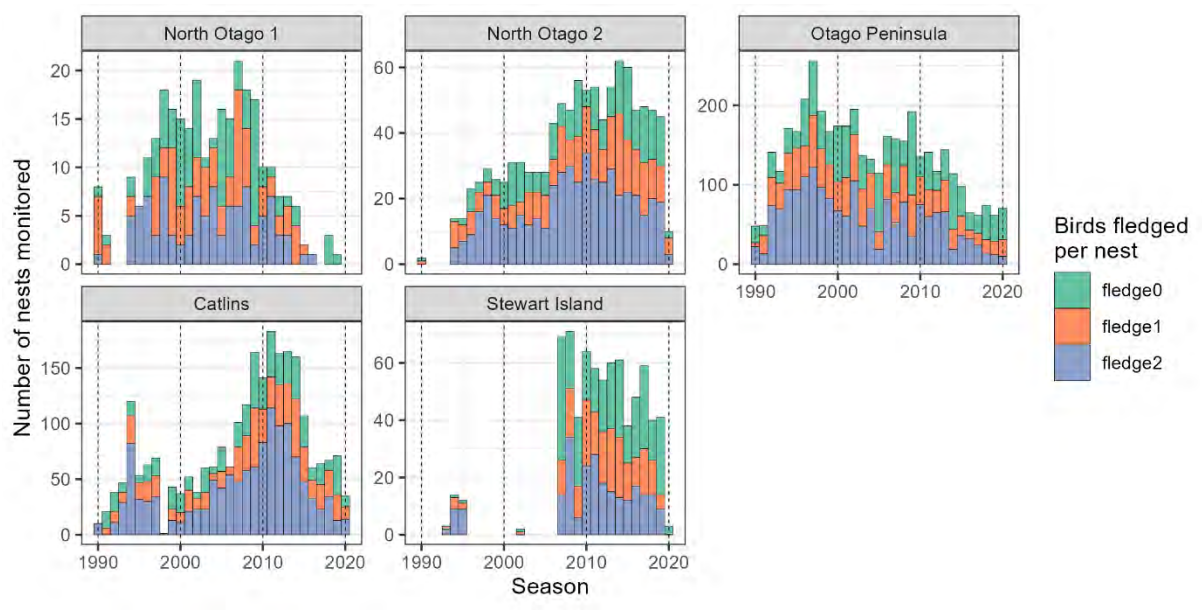


Figure B.14: The number of <u>chicks fledged</u> across all monitored nests, by season and regional sub-population.

Northern model run (North Otago 1 and North Otago 2)

Table B.4: Summary of posteriors of estimated model parameters for the <u>female</u> northern model (regional sub-populations were North Otago 1 and North Otago 2) including the effective sample size (effective N, should be greater than 400) and the Rhat statistic (should be less than 1.05).

Label	Parameter	Mean	2.5%	Median	97.5%	Effective N	Rhat
N init	N^0	97.695	53.310	89.790	187.418	2 712	1.000
alpha_surv1[1]	$lpha_{m{\phi}^0}$	1.579	0.713	1.487	2.972	1 016	1.000
beta surv1[1]	$eta_{m{\phi}^0}^{'}$	1.956	0.823	1.822	3.875	1 060	1.000
alpha surv2[1]	$\alpha_{\phi^{1+}}$	2.831	1.104	2.618	5.717	762	1.008
alpha surv2[2]	$\alpha_{\phi^{1+}}$	9.824	3.641	8.974	21.429	857	1.008
beta surv2[1]	$eta_{\phi^{1+}}^{r}$	0.671	0.258	0.616	1.383	514	1.010
beta surv2[2]	$\beta_{\phi^{1+}}$	1.365	0.545	1.243	2.887	730	1.009
alpha hatch[1]	$lpha_{\psi}$	2.347	0.971	2.125	4.958	918	1.003
alpha_hatch[2]	$lpha_{\psi}^{^{arphi}}$	3.449	1.400	3.126	7.482	1 046	1.003
alpha hatch[3]	$lpha_{\psi}^{\tau}$	1.991	0.867	1.817	3.983	1 181	1.005
alpha hatch[4]	$lpha_{\psi}^{\tau}$	5.601	2.427	5.113	11.748	1 568	1.002
beta hatch[1]	$oldsymbol{eta_{\psi}}^{ au}$	9.158	3.610	8.101	20.199	1 012	1.003
beta_hatch[2]	$oldsymbol{eta_{\psi}}$	28.658	10.406	25.680	64.729	1 169	1.002
beta_hatch[3]	$eta_{\psi}^{'}$	5.858	2.486	5.369	12.075	1 288	1.004
beta_hatch[4]	$eta_{\psi}^{'}$	21.087	8.584	19.130	44.712	1 585	1.002
alpha_fledge[1]	$lpha_{m{arphi}}$	4.223	1.696	3.913	8.780	1 244	1.004
alpha_fledge[2]	$lpha_{m{arphi}}$	7.780	3.902	7.439	13.569	2 821	1.000
beta_fledge[1]	$eta_{m{arphi}}$	1.276	0.514	1.189	2.557	1 025	1.005
beta_fledge[2]	$eta_{m{arphi}}$	2.094	1.121	2.008	3.523	2 664	1.000
<pre>p_immature_breeding_raw[1]</pre>	$\eta_t^{\mathrm{I1}} \ \eta_t^{\mathrm{I2}} \ \eta_t^{\mathrm{I3}}$	-0.772	-1.151	-0.764	-0.428	3 708	1.000
p_immature_breeding_raw[2]	$\eta_t^{ ext{I2}}$	-0.441	-0.799	-0.451	-0.020	4 000	1.000
<pre>p_immature_breeding_raw[3]</pre>	$\eta_t^{{ m I}3}$	-0.218	-0.646	-0.237	0.330	4 745	1.000
p_non_breeder_breeding[1]	γ_{t}	0.371	0.283	0.370	0.469	6 696	1.000
p_breeder_breeding[1]	$\delta_t \ r_{a,t}^{ m NB}$	0.849	0.795	0.851	0.896	3 888	0.999
p_non_breeder_seen[1]	$r_{a,t}^{\text{NB}}$	0.471	0.300	0.468	0.643	6 955	1.000
p_non_breeder_seen[2]	$r_{a,t}^{\text{ND}}$	0.197	0.161	0.196	0.239	4 236	1.000
p_breeder_seen[1]	$r_{a,t}^{\mathrm{B}}$	0.748	0.459	0.756	0.980	5 340	1.000
p_breeder_seen[2]	$r_{a,t}^{\mathrm{B}}$	0.526	0.374	0.522	0.704	5 770	1.000
p_breeder_seen[3]	$r_{a,t}^{\mathrm{B}}$	0.911	0.712	0.932	0.998	7 088	1.000
p_breeder_seen[4]	$r_{a,t}^{\mathrm{B}}$	0.825	0.749	0.826	0.896	3 612	1.001
p_move[1]	κ	0.134	0.070	0.132	0.216	4 596	1.001
p_move[2]	κ	0.031	0.016	0.030	0.052	6 398	1.000

Table B.5: Summary of posteriors of estimated model parameters for the <u>male</u> northern model (regional sub-populations were North Otago 1 and North Otago 2) including the effective sample size (effective N, should be greater than 400) and the Rhat statistic (should be less than 1.05).

Label	Parameter	Mean	2.5%	Median	97.5%	Effective N	Rhat
N init	N^{0}	125.016	75.961	118.052	223.992	2 251	1.000
alpha surv1[1]	$lpha_{m{\phi}^0}$	1.143	0.552	1.082	2.066	1 104	1.009
beta_surv1[1]	$eta_{m{\phi}^0}$	1.440	0.596	1.361	2.761	942	1.009
alpha surv2[1]	$\alpha_{\phi^{1+}}$	4.779	1.682	4.373	10.262	558	1.011
alpha_surv2[2]	$lpha_{\phi^{1+}}$	8.609	3.183	7.550	20.009	736	1.004
beta surv2[1]	$eta_{\phi^{1+}}^{'}$	1.068	0.365	0.989	2.192	440	1.015
beta surv2[2]	$eta_{\phi^{1+}}$	0.839	0.316	0.752	1.885	557	1.004
alpha_hatch[1]	$\overset{'}{lpha}_{\psi}$	2.349	0.991	2.120	5.035	905	1.005
alpha_hatch[2]	$lpha_{\psi}^{'}$	3.519	1.412	3.212	7.807	960	1.000
alpha_hatch[3]	$lpha_{\psi}^{'}$	2.047	0.886	1.870	4.205	922	1.003
alpha_hatch[4]	$lpha_{m{\psi}}$	5.561	2.376	5.138	11.474	1 216	1.001
beta_hatch[1]	eta_{ψ}^{\cdot}	9.074	3.593	8.212	20.039	1 029	1.005
beta_hatch[2]	$eta_{\psi}^{'}$	29.989	10.667	27.321	68.308	1 021	1.000
beta_hatch[3]	eta_{ψ}^{\cdot}	6.009	2.506	5.440	12.743	1 077	1.003
beta_hatch[4]	eta_{ψ}	21.045	8.448	19.271	45.231	1 271	1.000
alpha_fledge[1]	$lpha_{m{arphi}}$	4.367	1.792	4.051	8.792	1 102	1.002
alpha_fledge[2]	$lpha_{arphi}$	7.717	3.989	7.372	13.054	2 241	1.002
beta_fledge[1]	$eta_{m{arphi}}$	1.331	0.564	1.228	2.650	1 019	1.001
beta_fledge[2]	$eta_{m{arphi}}$	2.047	1.107	1.971	3.404	2 000	1.002
<pre>p_immature_breeding_raw[1]</pre>	$\eta_t^{ m I_1} \ \eta_t^{ m I_2}$	-1.649	-2.223	-1.636	-1.150	3 387	1.001
<pre>p_immature_breeding_raw[2]</pre>	η_t^{I2}	-1.040	-1.508	-1.042	-0.576	3 363	1.000
<pre>p_immature_breeding_raw[3]</pre>	$\eta_t^{{ m I}3}$	-0.774	-1.269	-0.788	-0.220	3 474	1.001
p_non_breeder_breeding[1]	γ_t	0.291	0.238	0.290	0.350	5 422	1.000
p_breeder_breeding[1]	$\delta_t \ r_{a,t}^{ m NB} \ r_{a,t}^{ m NB}$	0.774	0.716	0.775	0.830	3 094	1.002
p_non_breeder_seen[1]	$r_{a,t}^{\text{NB}}$	0.312	0.227	0.311	0.406	5 284	1.000
p_non_breeder_seen[2]	$r_{a,t}^{\text{NB}}$	0.224	0.187	0.223	0.266	3 518	1.000
p_breeder_seen[1]	$r_{a,t}^{ m B}$	0.848	0.595	0.869	0.993	6 773	0.999
p_breeder_seen[2]	$r_{a,t}^{\mathrm{B}}$	0.552	0.433	0.548	0.689	4 286	1.001
p_breeder_seen[3]	$r_{a,t}^{\mathrm{B}}$	0.812	0.642	0.816	0.961	4 261	1.000
p_breeder_seen[4]	$r_{a,t}^{\mathrm{B}}$	0.808	0.696	0.809	0.919	3 366	1.001
p_move[1]	K	0.075	0.022	0.071	0.150	5 017	1.000
p_move[2]	κ	0.042	0.025	0.041	0.064	5 021	1.001

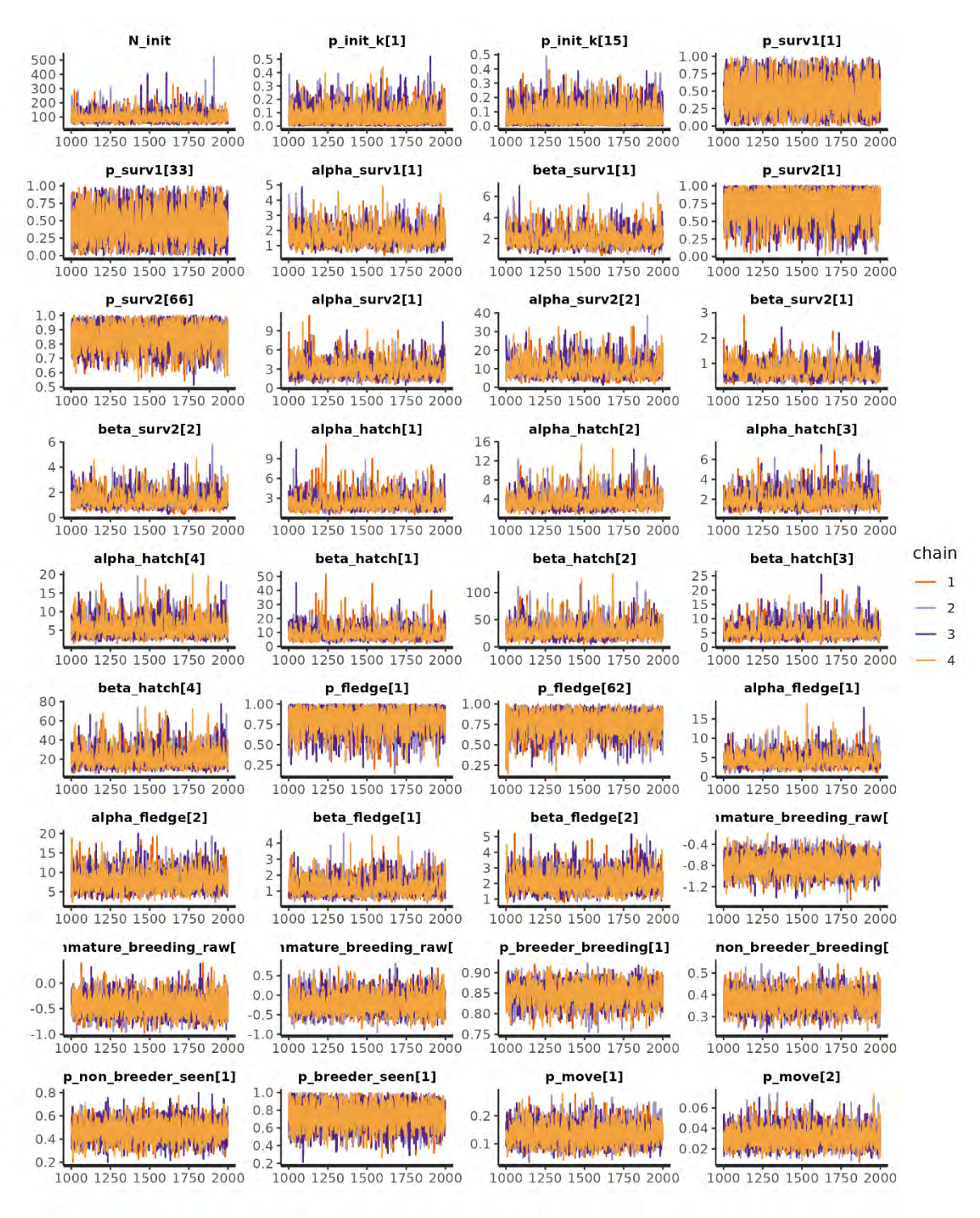


Figure B.15: MCMC trace plots for a subset of estimated parameters from the <u>female northern model</u> run (North Otago 1 and North Otago 2).

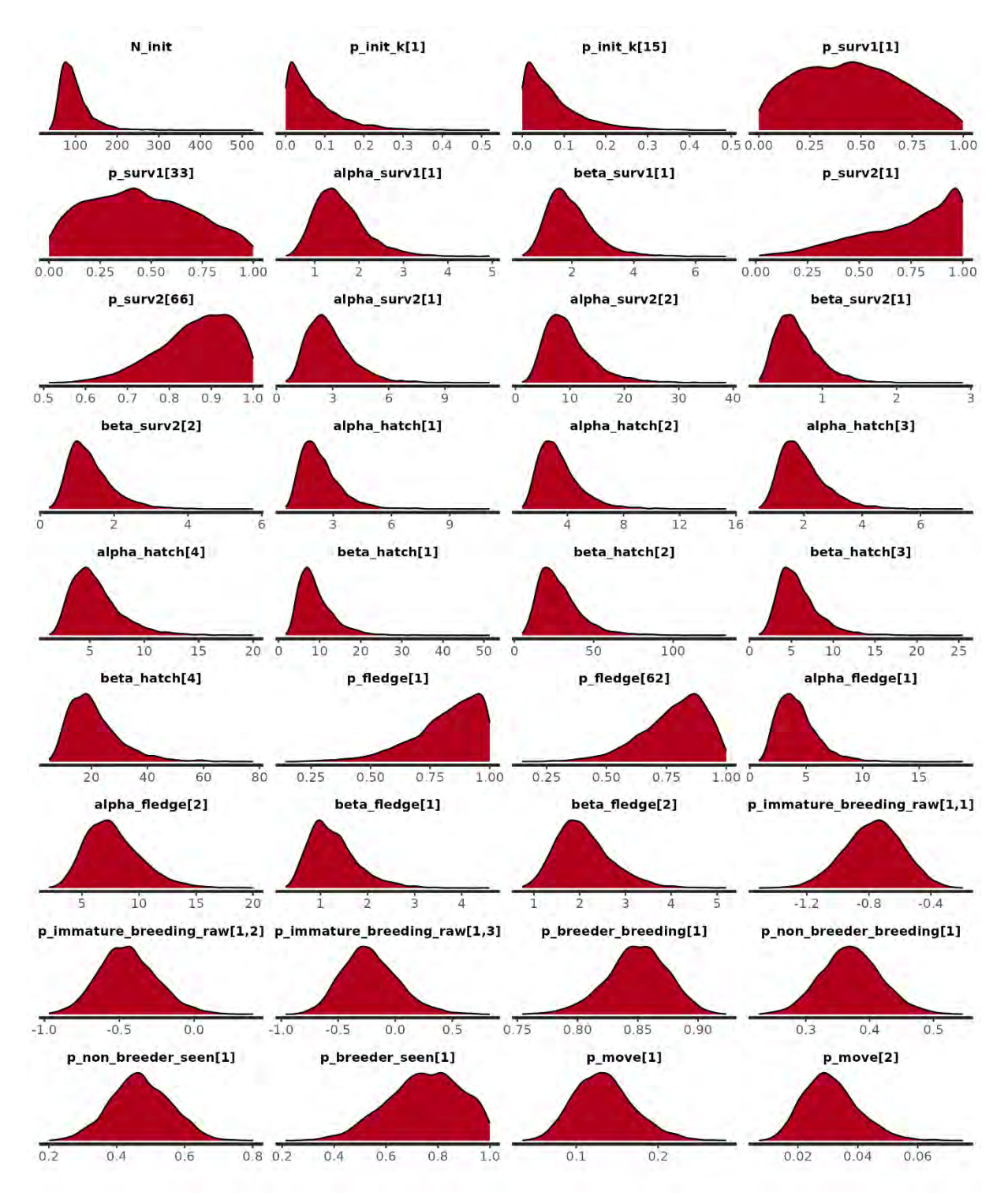


Figure B.16: Posterior distribution for a subset of parameters from the <u>female northern model</u> run (North Otago 1 and North Otago 2).

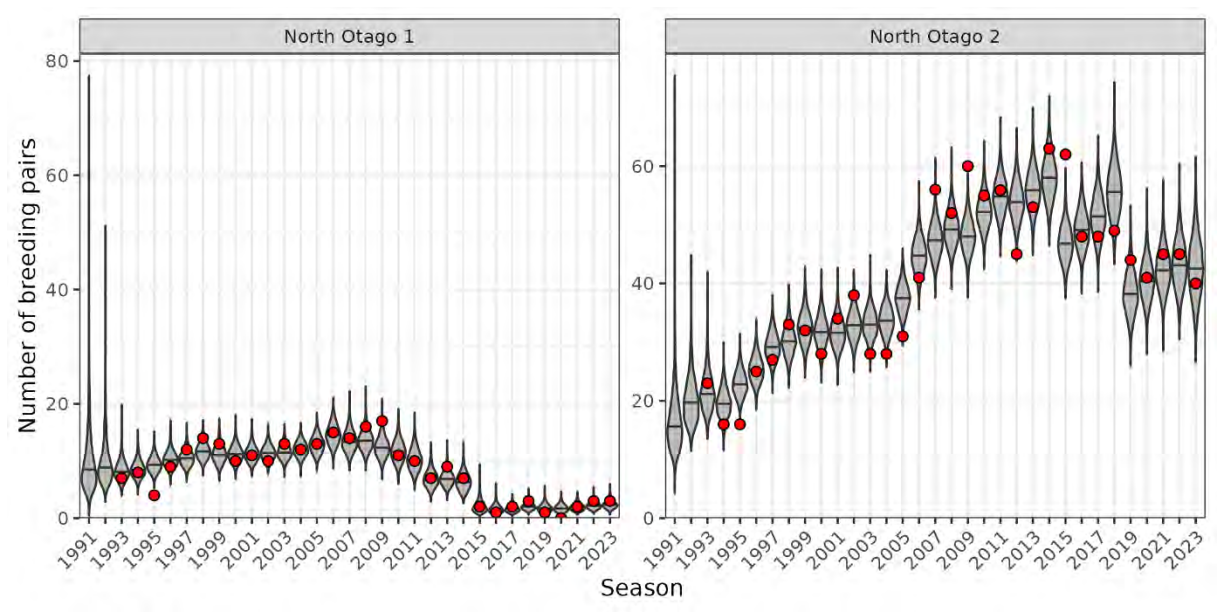


Figure B.17: Posterior distribution of the number of breeding pairs by season from the <u>female northern</u> <u>model</u> run (North Otago 1 and North Otago 2), compared with the 'observed' estimate of breeding pairs for each regional sub-population (red points).

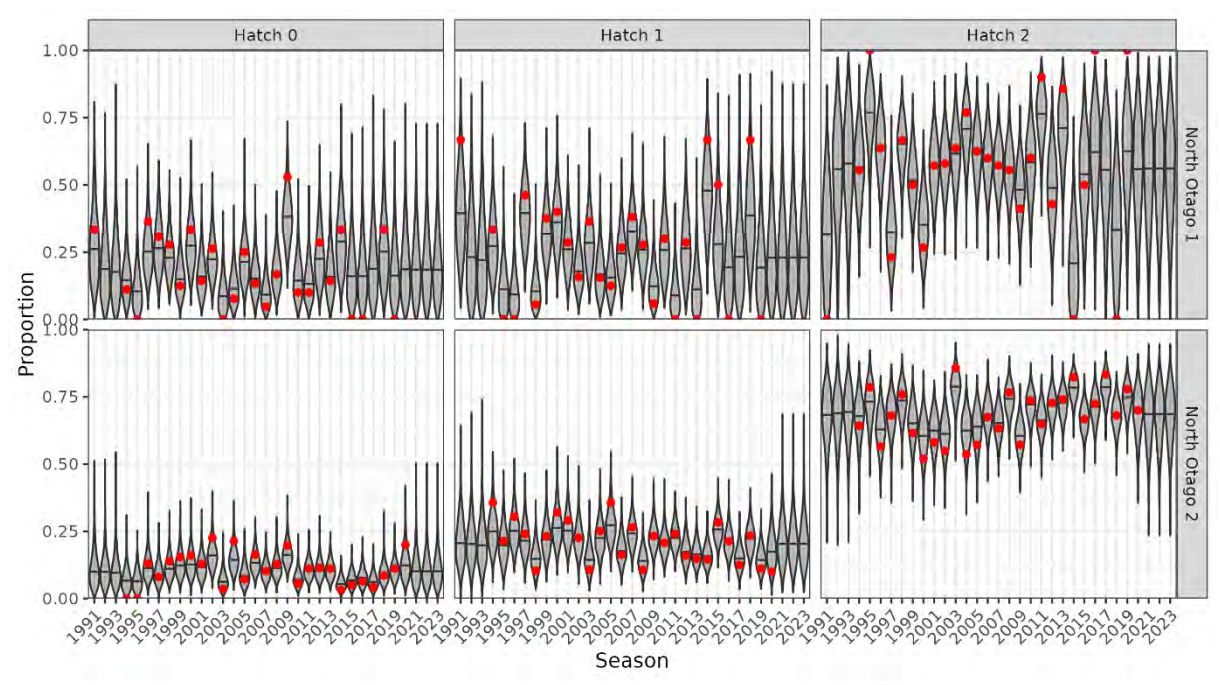


Figure B.18: Posterior distribution of the proportion of nesting events producing zero, one, or two hatchlings by season from the <u>female northern model</u> run (North Otago 1 and North Otago 2), compared with the 'observed' proportions for each regional sub-population (red points).

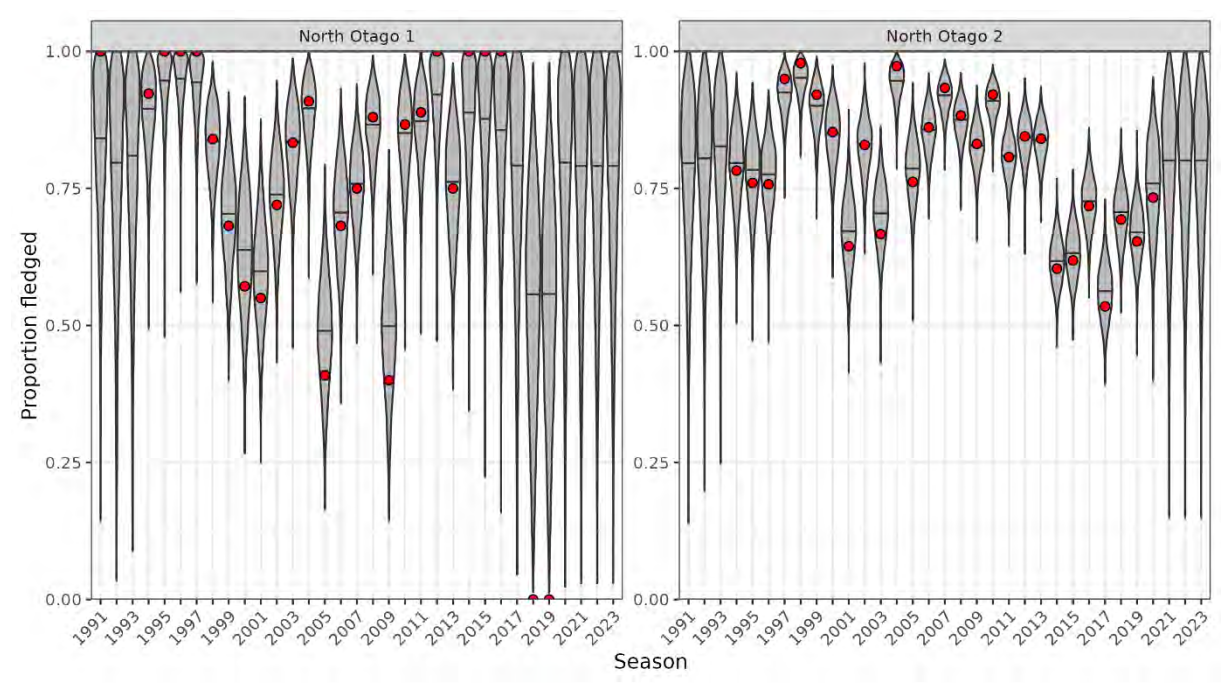


Figure B.19: Posterior distribution of the proportion of hatchlings that fledged by season from the <u>female</u> <u>northern model</u> run (North Otago 1 and North Otago 2) (horizontal lines represent the median values), compared with the 'observed' proportions for each regional sub-population (red points).

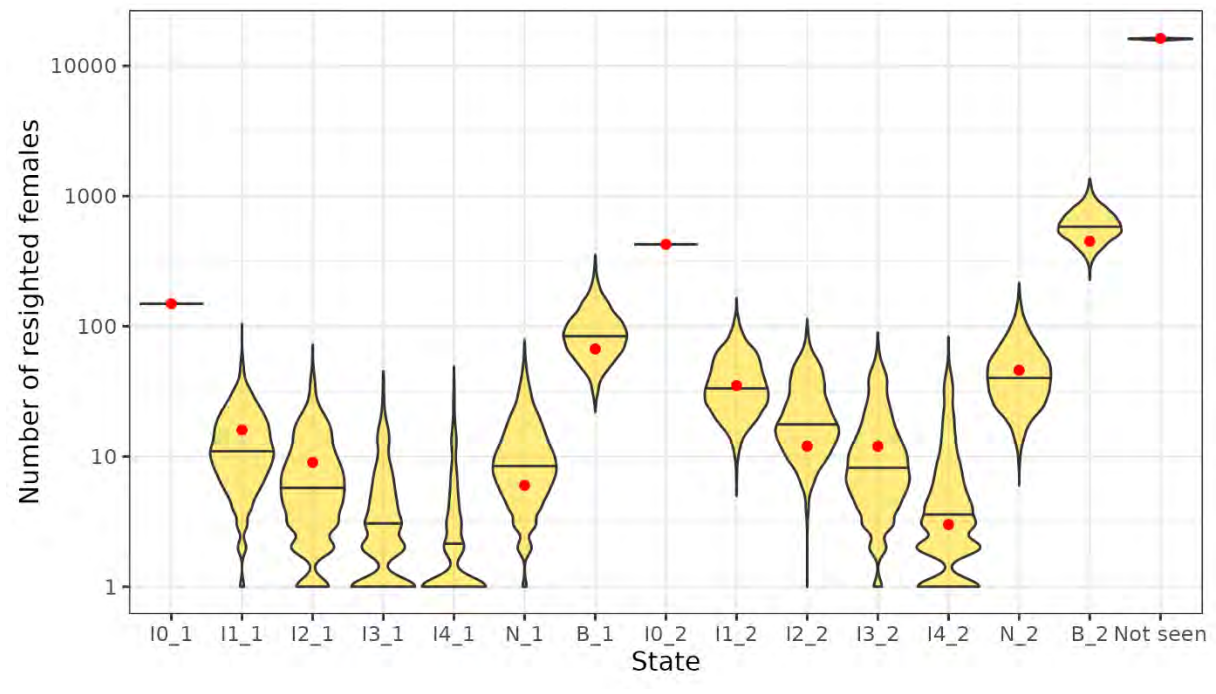


Figure B.20: Posterior distribution of the observed number of resighted birds by model state from the <u>female northern model</u> run (North Otago 1 and North Otago 2) (horizontal lines represent the median values), compared with the 'observed' numbers for each regional sub-population (red points). Model states with suffix '-1' and '-2' apply to North Otago 1 and North Otago 2, respectively.

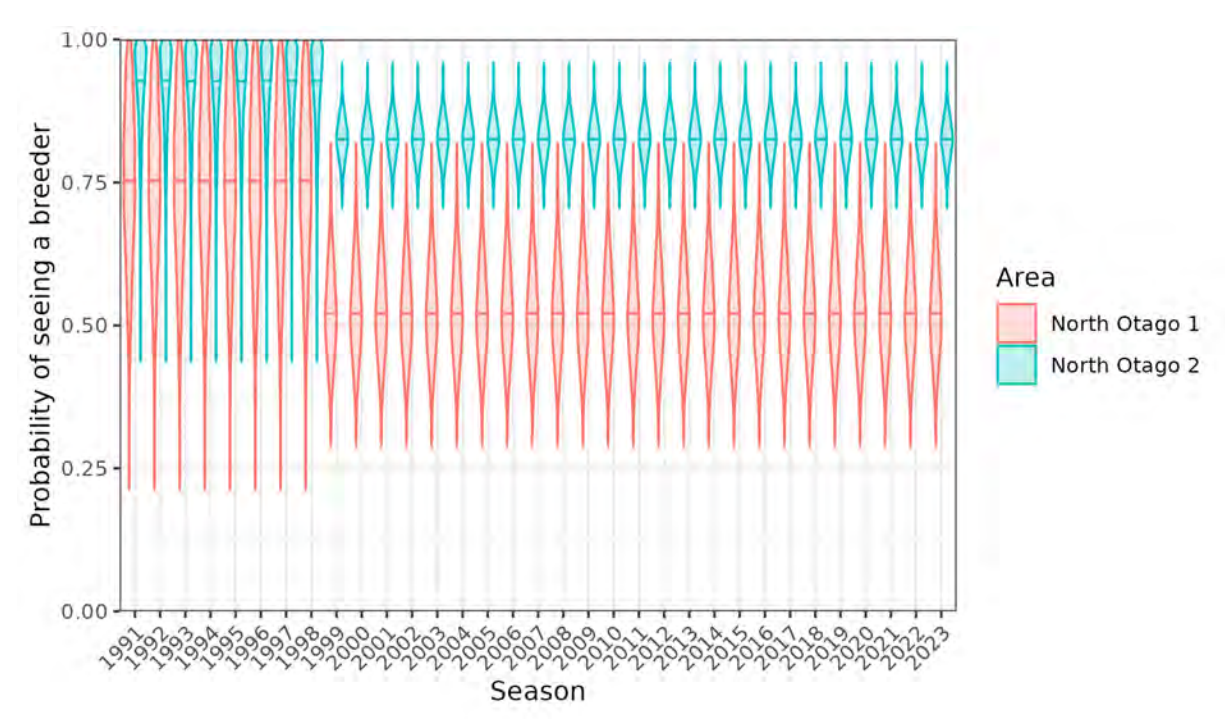


Figure B.21: Posterior distributions of the probability of a breeder being seen by season and regional sub-population, for the <u>female northern model</u> run (North Otago 1 and North Otago 2).

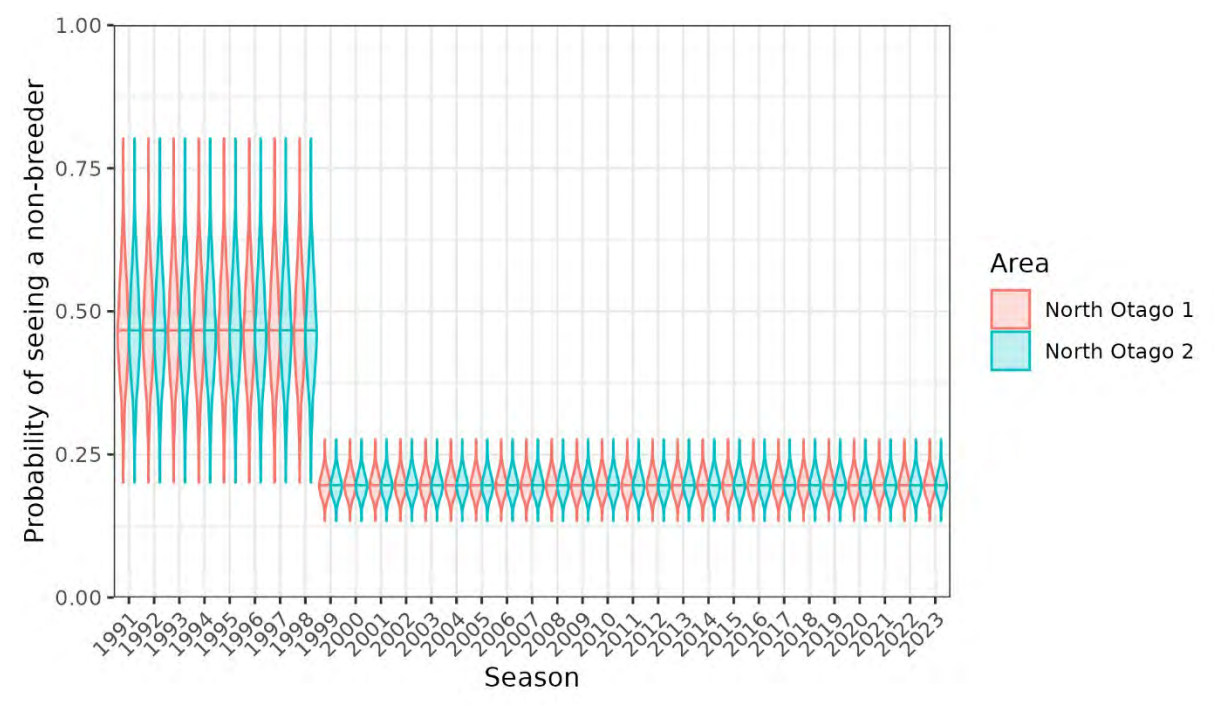


Figure B.22: Posterior distributions of the probability of a non-breeder being seen by season and regional sub-population, for the <u>female northern model</u> run (North Otago 1 and North Otago 2). Note that these were assumed to be the same across both model regions.

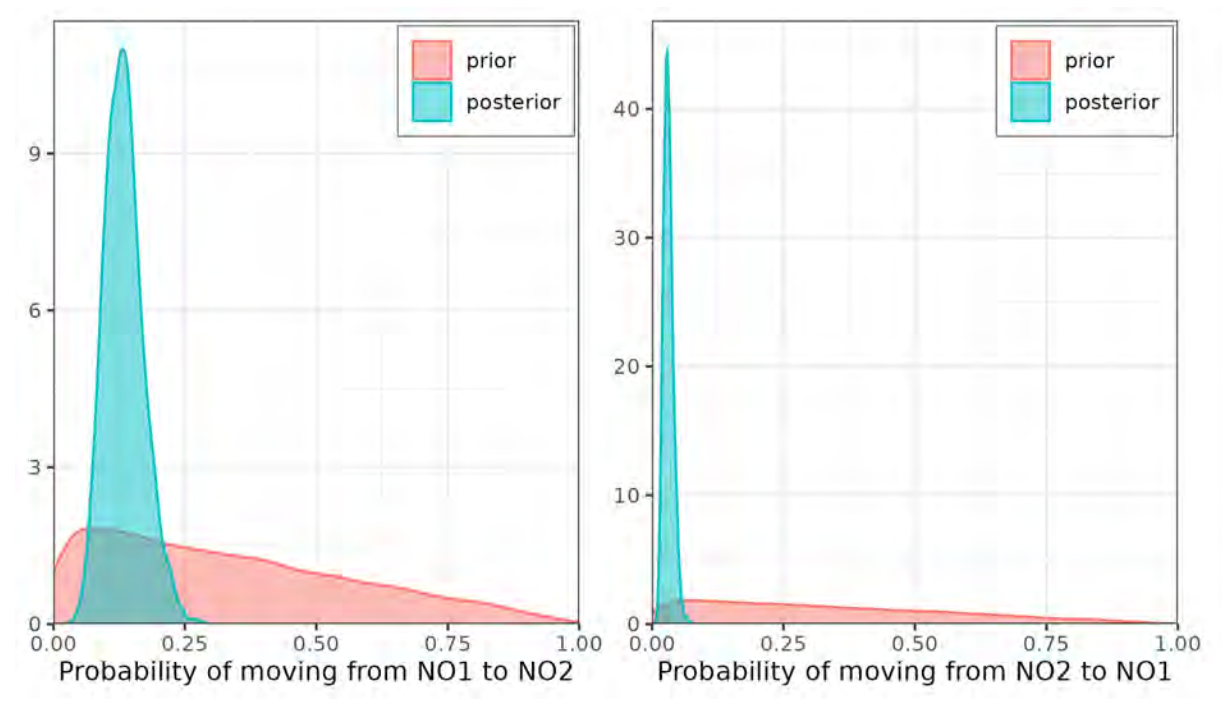


Figure B.23: Prior and posterior distributions (pink and blue polygons, respectively) of the annual probabilites of immature birds moving between regions of the <u>female northern model</u> run (North Otago 1 and North Otago 2). 'NO1' = North Otago 1 and 'NO2' = North Otago 2.

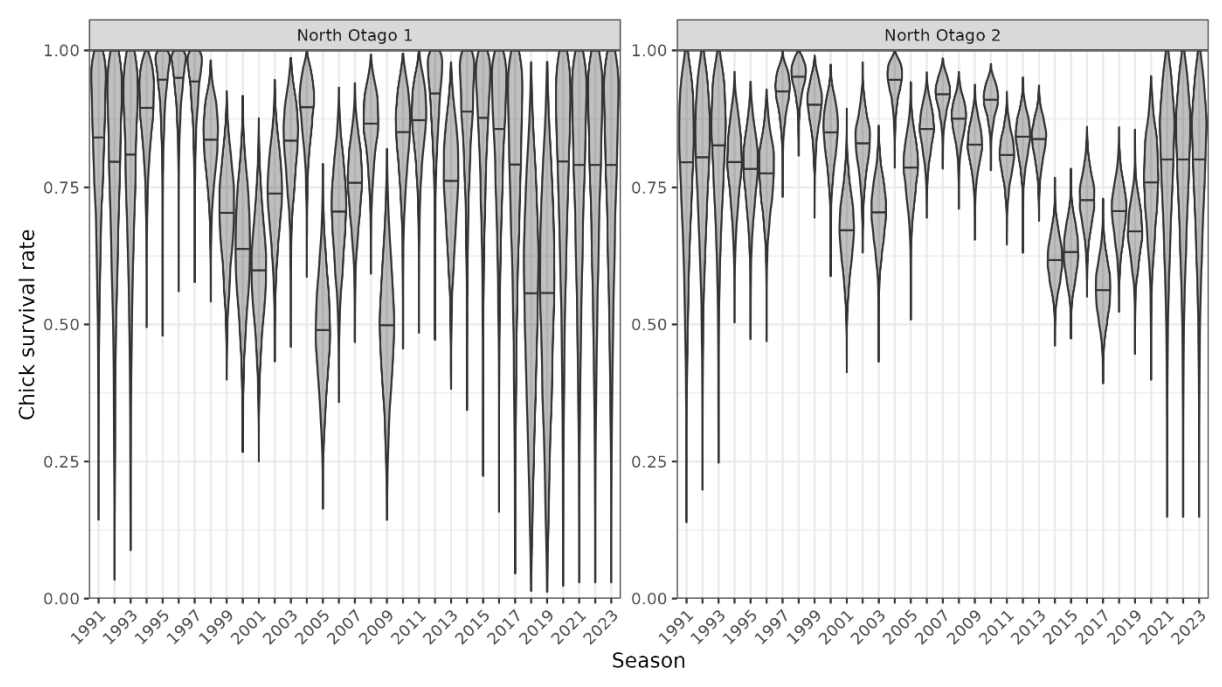


Figure B.24: Posterior distributions of the probability of chick survival (from hatching to fledgling) by season and regional sub-population, for the <u>female northern model</u> run (North Otago 1 and North Otago 2).

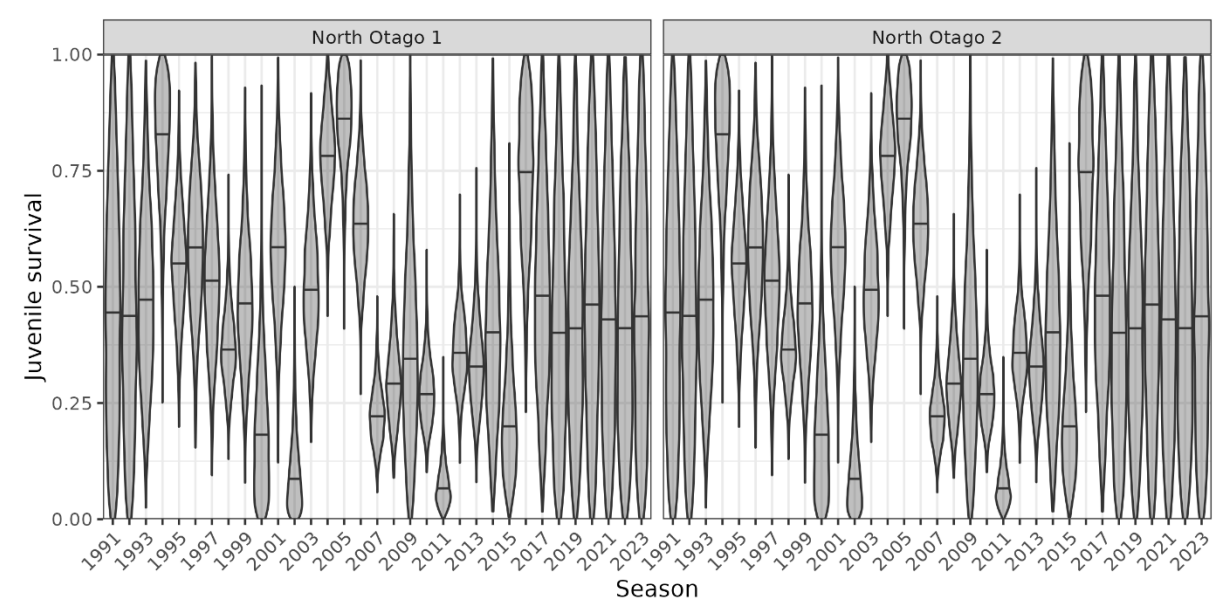


Figure B.25: Posterior distributions of the probability of juvenile survival (from fledgling to the following year) by season and regional sub-population, for the <u>female northern model</u> run (North Otago 1 and North Otago 2). Note that these were assumed to be the same across both regions.

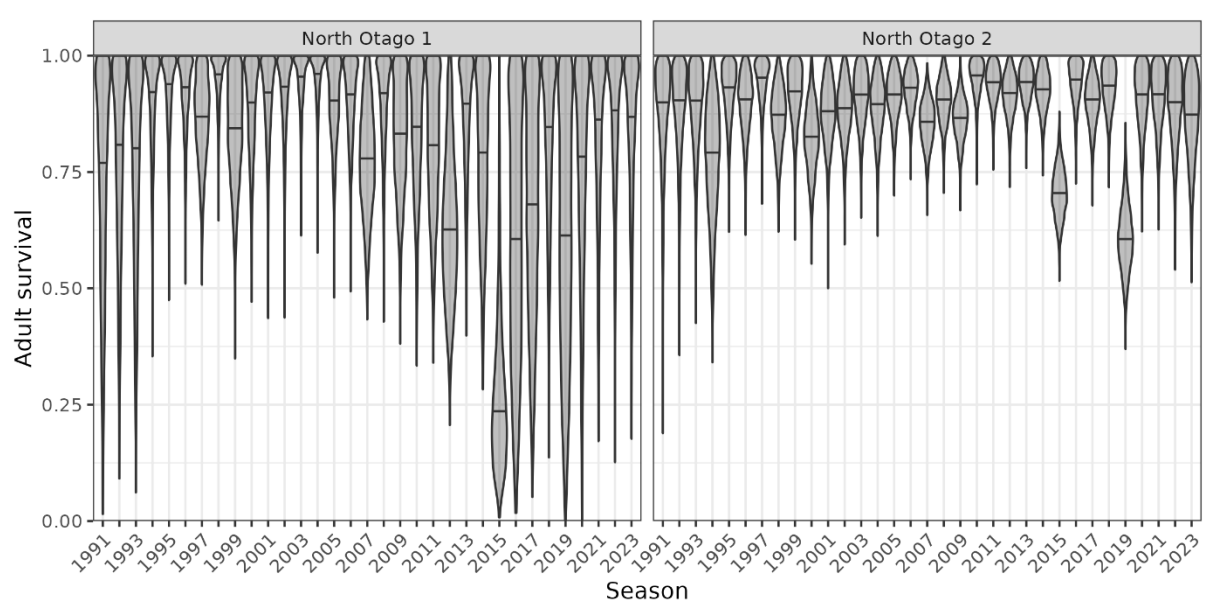


Figure B.26: Posterior distributions of the probability of adult survival by season and regional sub-population, for the <u>female northern model</u> run (North Otago 1 and North Otago 2).

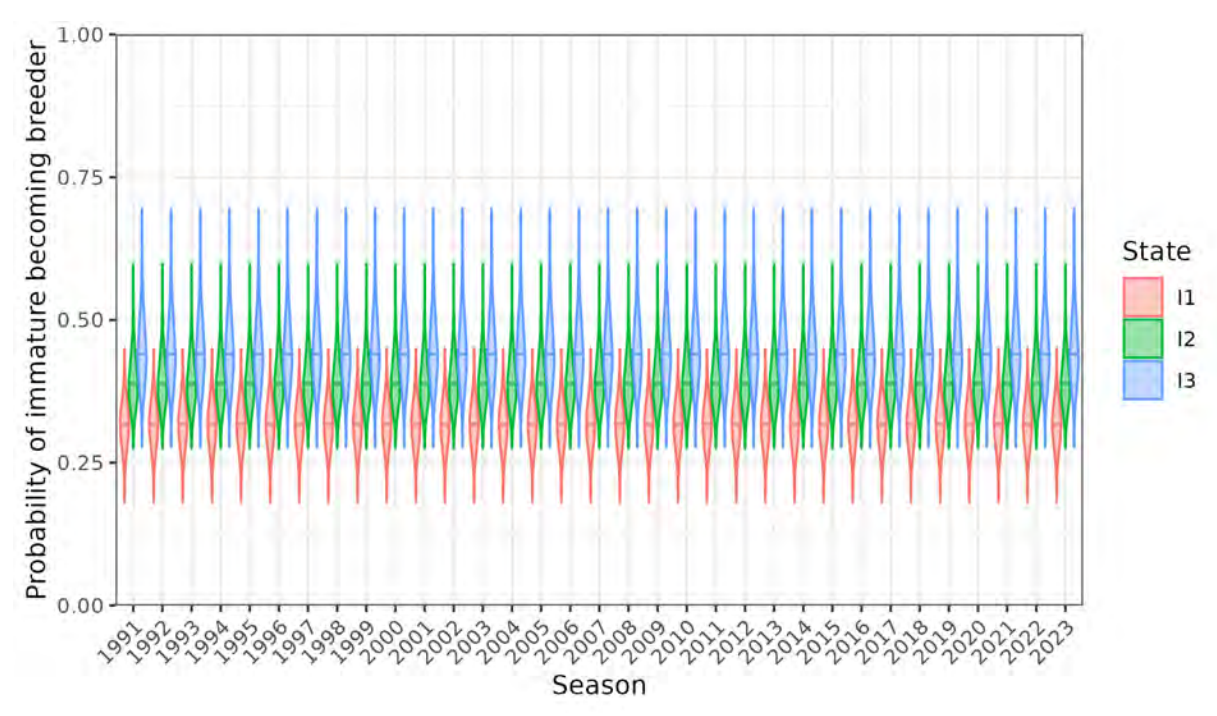


Figure B.27: Posterior distributions of the annual probabilites of immature birds at ages 1 (I1), 2 (I2), and 3 (I3) becoming breeders at the following ages, for the <u>female northern model</u> run (North Otago 1 and North Otago 2).

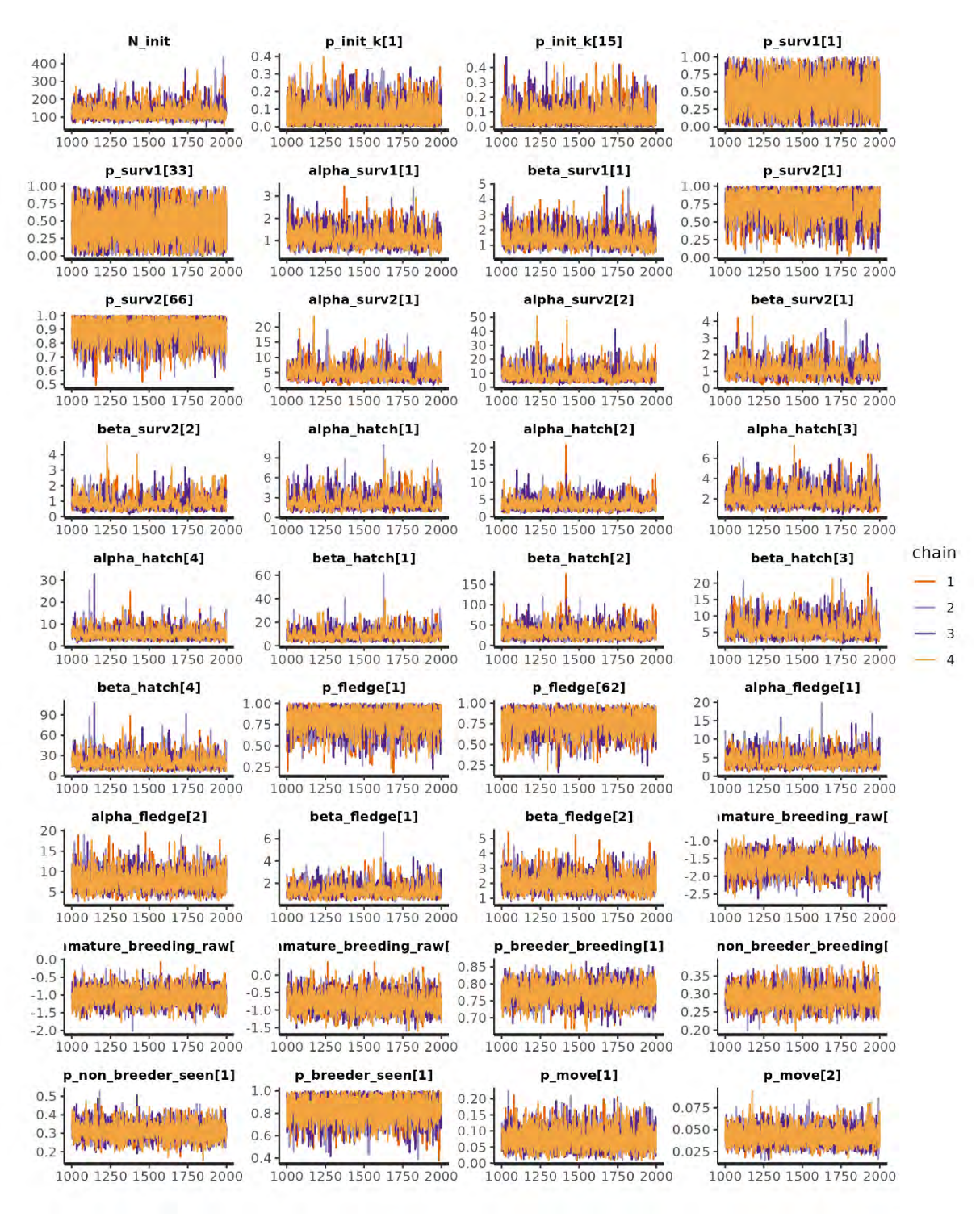


Figure B.28: MCMC trace plots for a subset of estimated parameters from the <u>male northern model</u> run (North Otago 1 and North Otago 2).

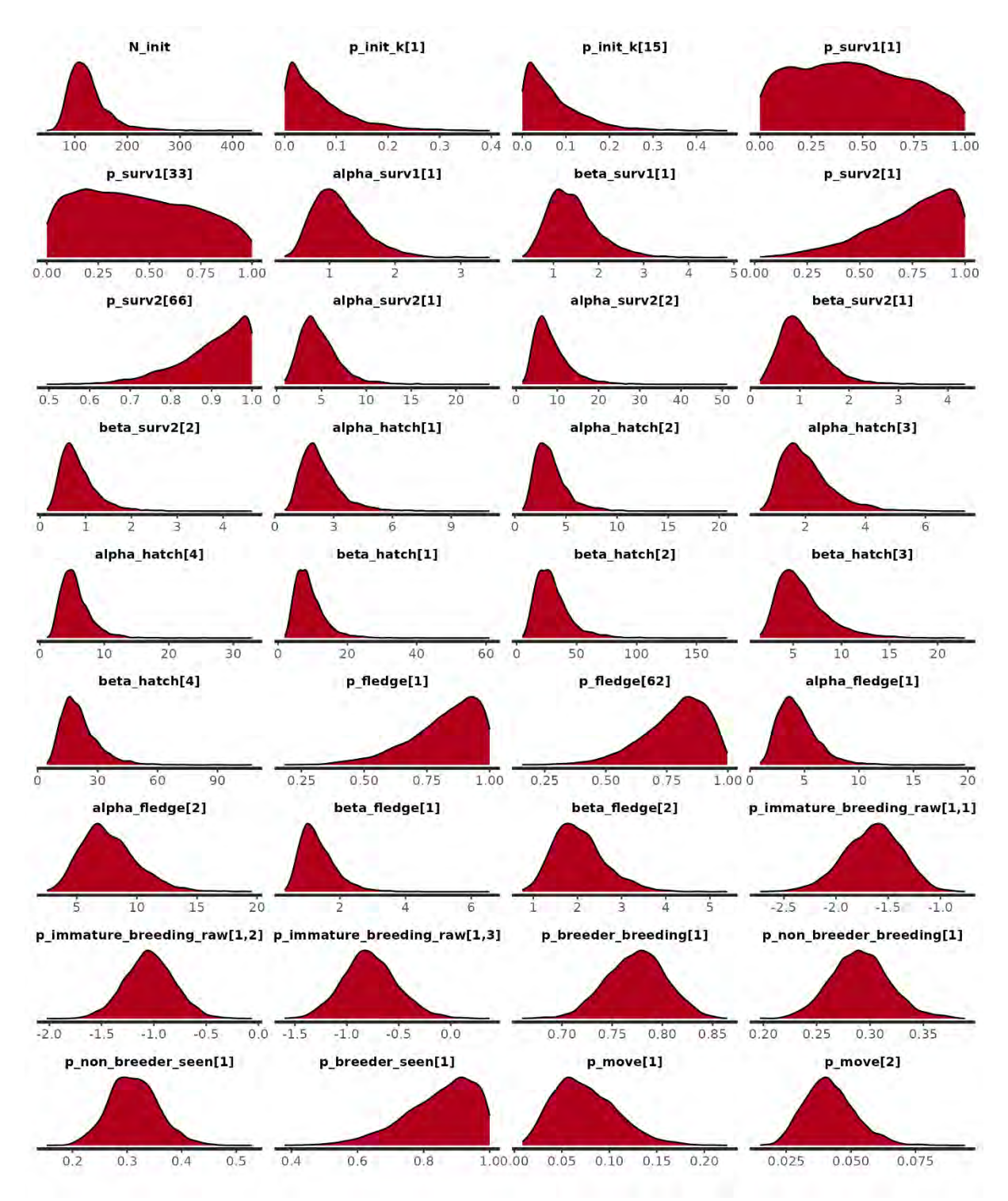


Figure B.29: Posterior distribution for a subset of parameters from the <u>male northern model</u> run (North Otago 1 and North Otago 2).

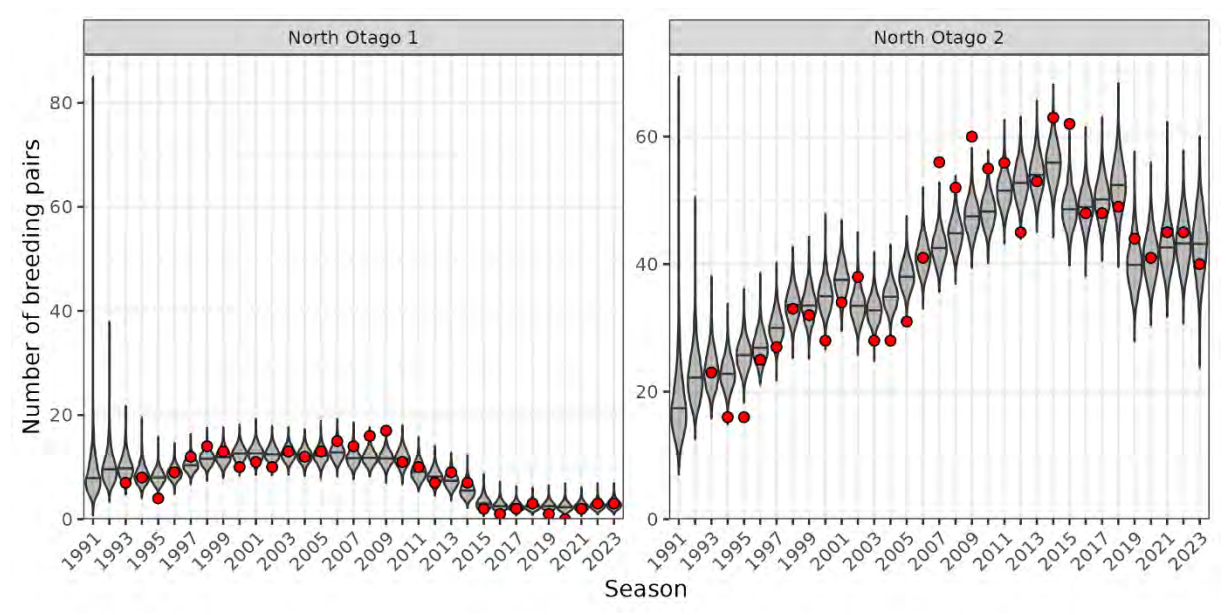


Figure B.30: Posterior distribution of the number of breeding pairs by season from the <u>male northern model</u> run (North Otago 1 and North Otago 2), compared with the 'observed' estimate of breeding pairs for each regional sub-population (red points).

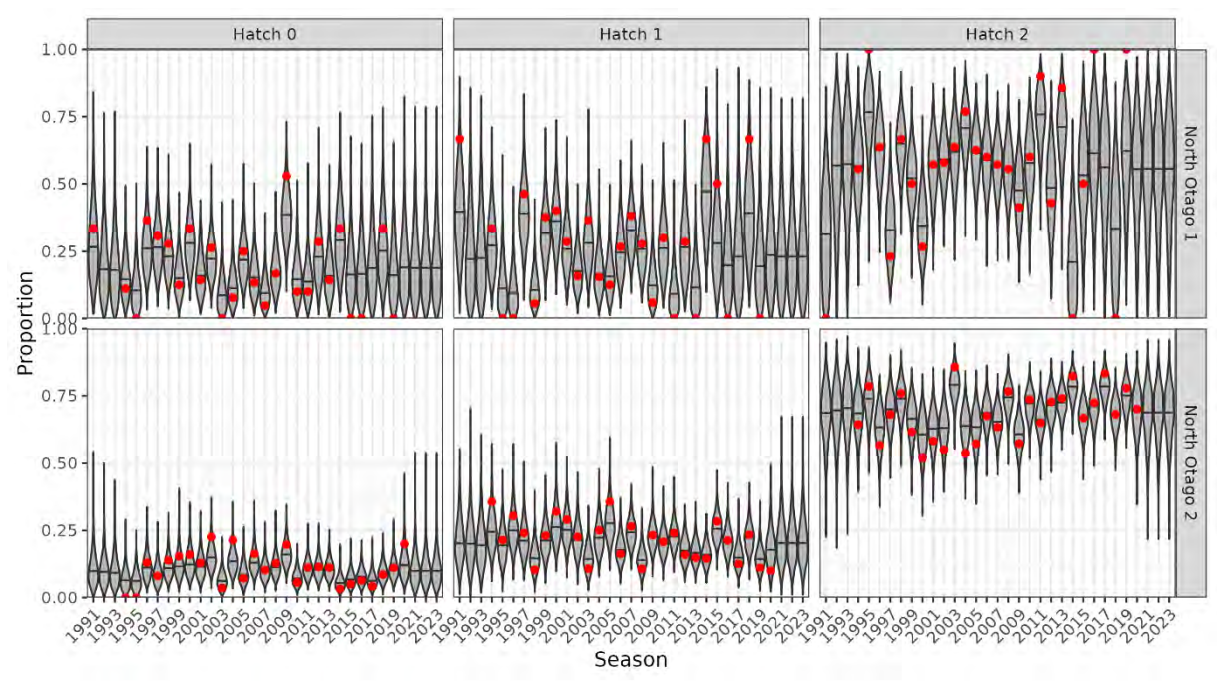


Figure B.31: Posterior distribution of the proportion of nesting events producing zero, one, or two hatchlings by season from the <u>male northern model</u> run (North Otago 1 and North Otago 2), compared with the 'observed' proportions for each regional sub-population (red points).

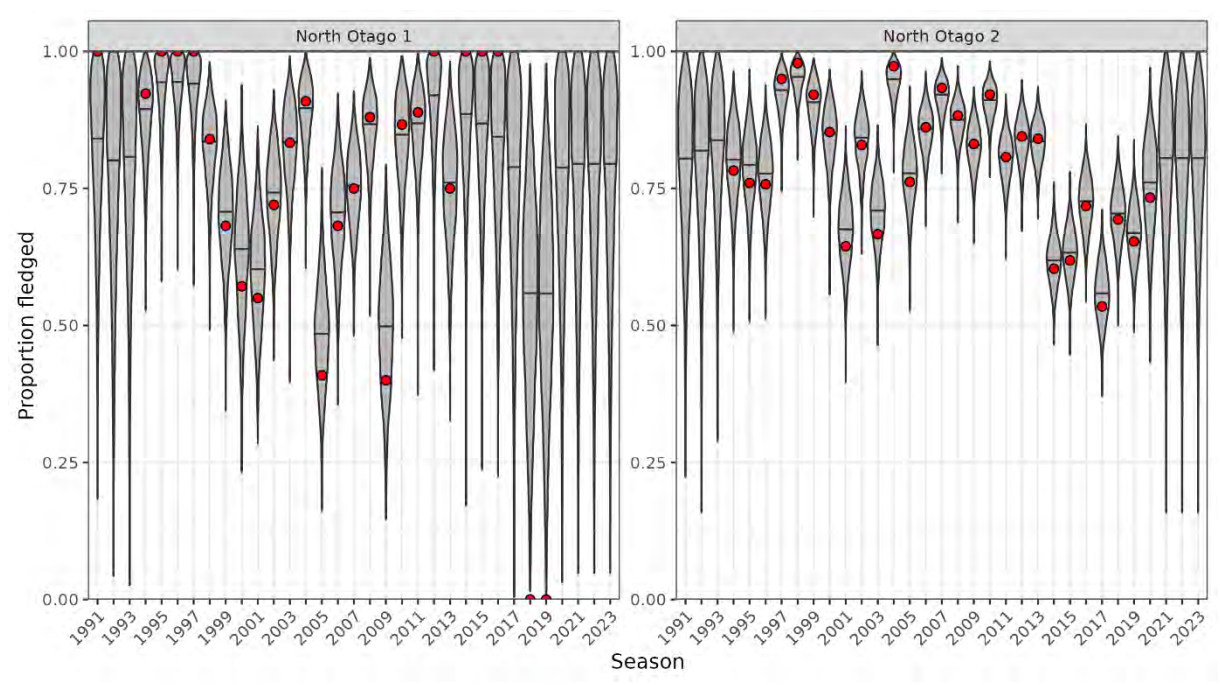


Figure B.32: Posterior distribution of the proportion of hatchlings that fledged by season from the <u>male</u> <u>northern model</u> run (North Otago 1 and North Otago 2) (horizontal lines represent the median values), compared with the 'observed' proportions for each regional sub-population (red points).

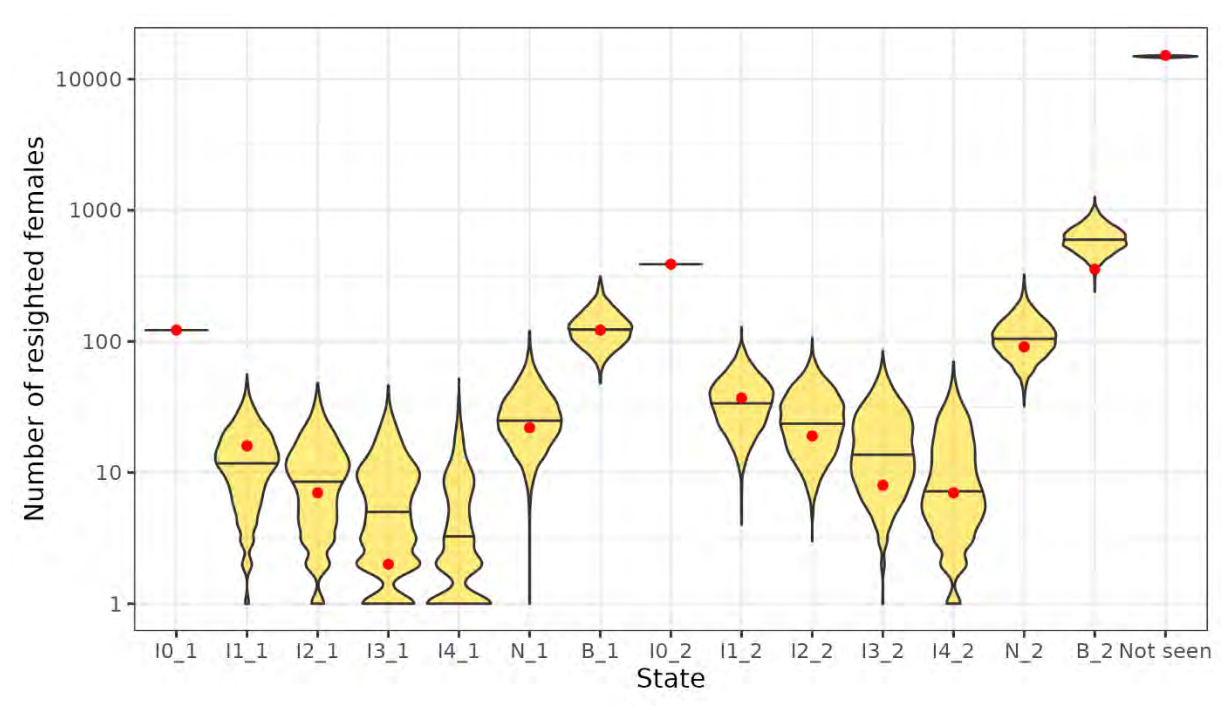


Figure B.33: Posterior distribution of the observed number of resighted birds by model state from the <u>male</u> <u>northern model</u> run (North Otago 1 and North Otago 2) (horizontal lines represent the median values), compared with the 'observed' numbers for each regional sub-population (red points). Model states with suffix '-1' and '-2' apply to North Otago 1 and North Otago 2, respectively.

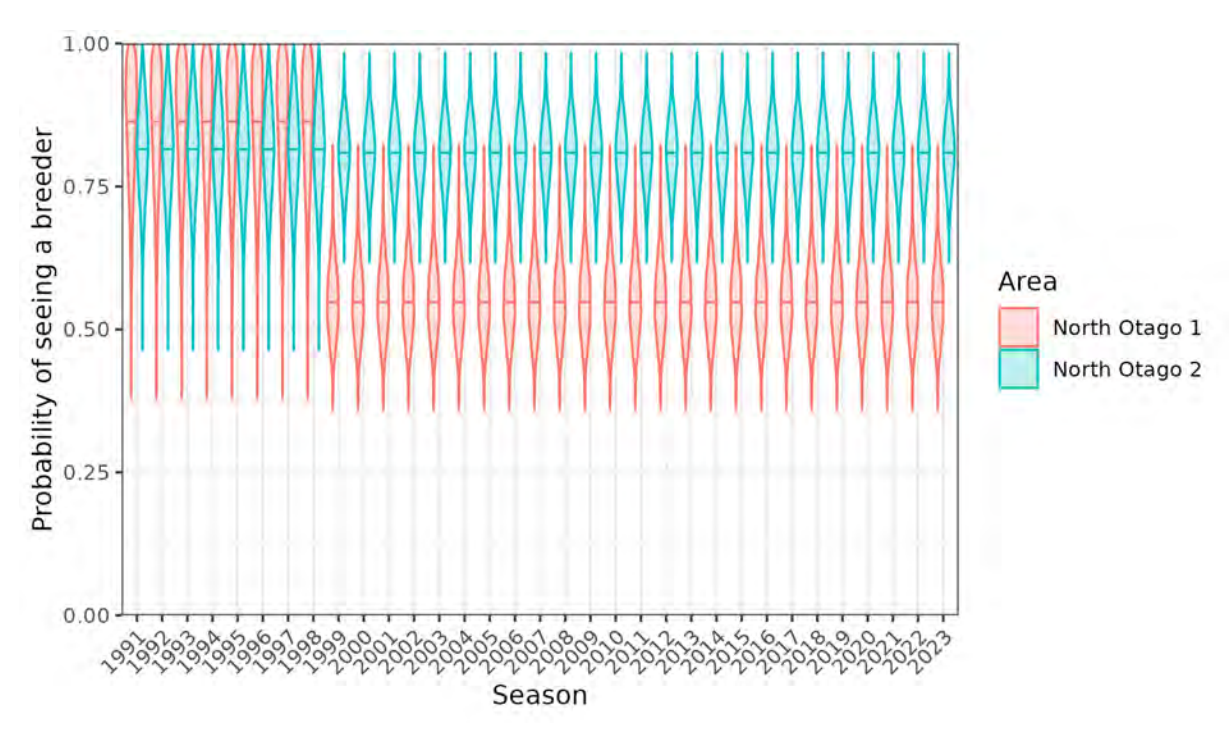


Figure B.34: Posterior distributions of the probability of a breeder being seen by season and regional sub-population, for the <u>male northern model</u> run (North Otago 1 and North Otago 2).

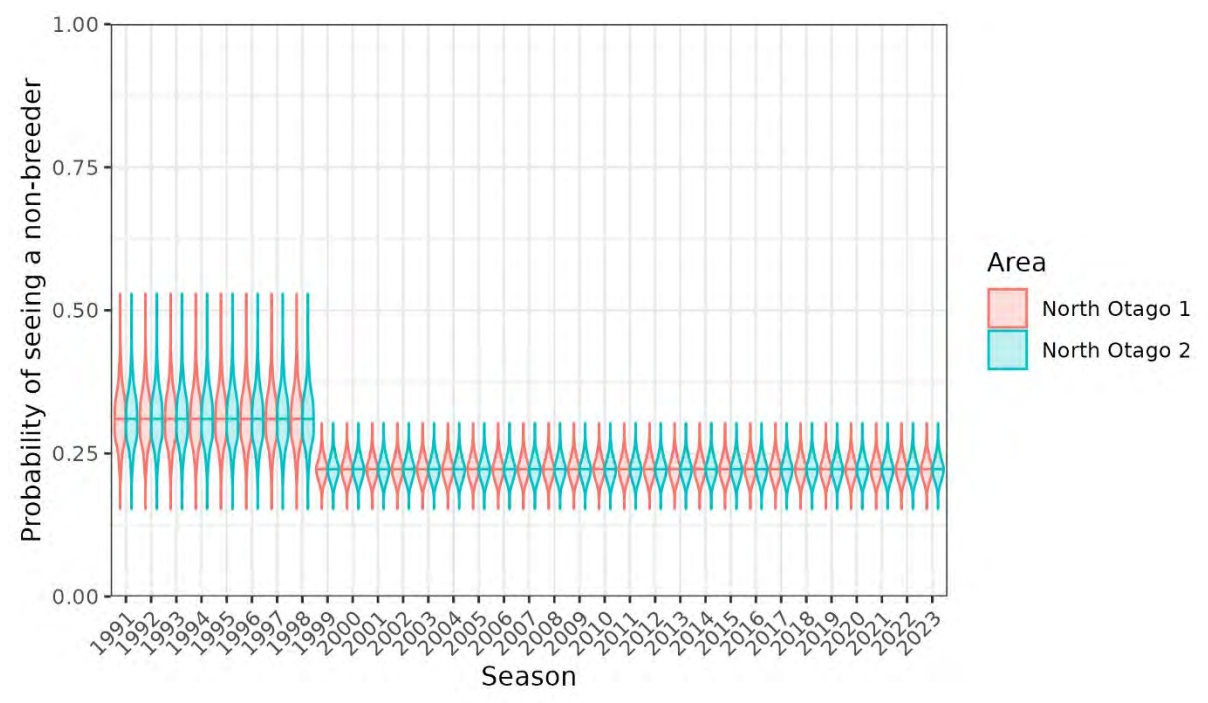


Figure B.35: Posterior distributions of the probability of a non-breeder being seen by season and regional sub-population, for the <u>male northern model</u> run (North Otago 1 and North Otago 2). Note that these were assumed to be the same across both model regions.

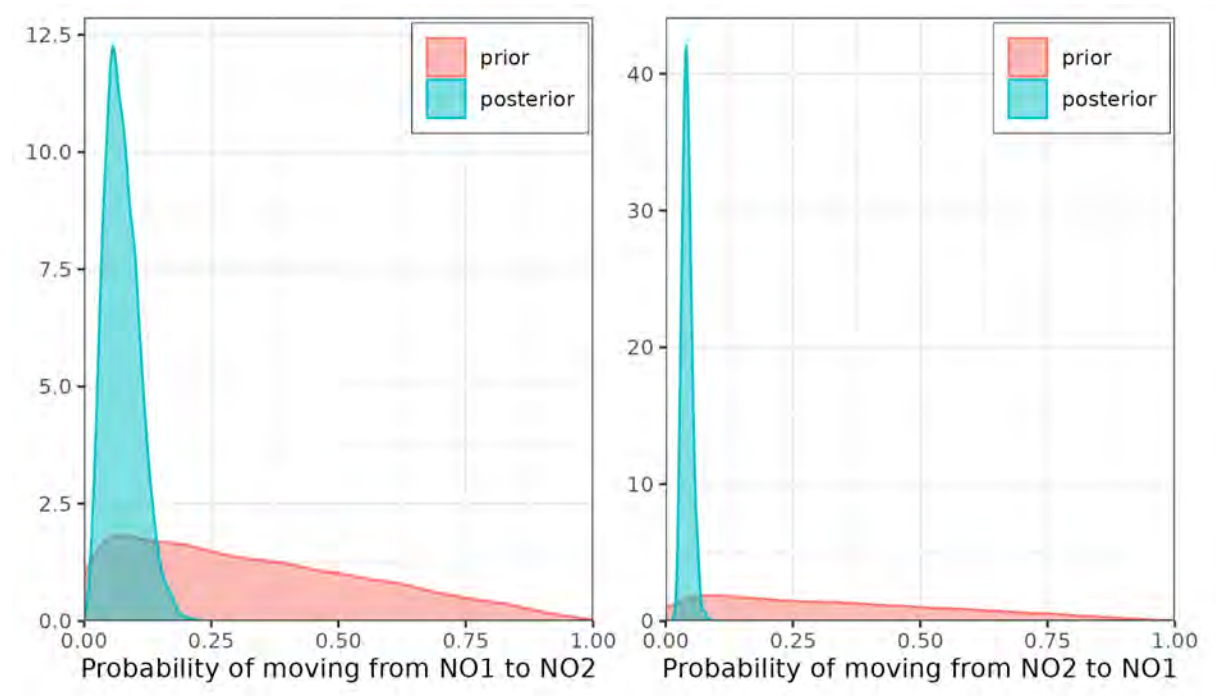


Figure B.36: Prior and posterior distributions (pink and blue polygons, respectively) of the annual probabilites of immature birds moving between regions of the <u>male northern model</u> run (North Otago 1 and North Otago 2). 'NO1' = North Otago 1 and 'NO2' = North Otago 2.

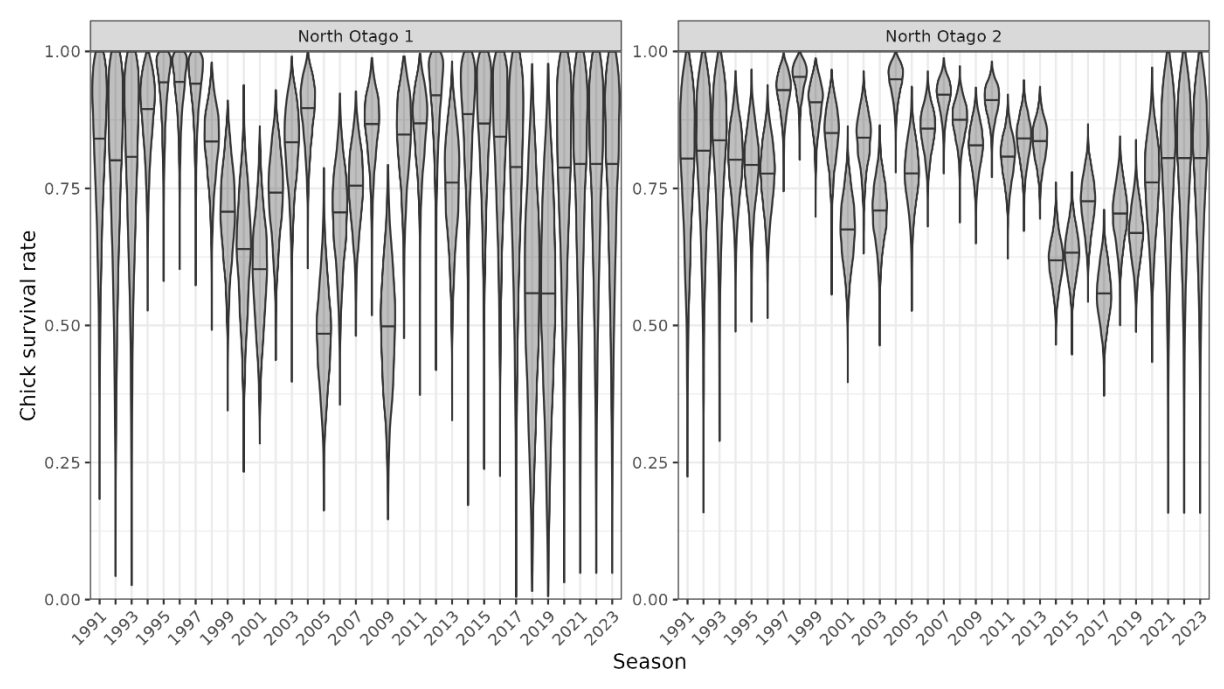


Figure B.37: Posterior distributions of the probability of chick survival (from hatching to fledgling) by season and regional sub-population, for the <u>male northern model</u> run (North Otago 1 and North Otago 2).

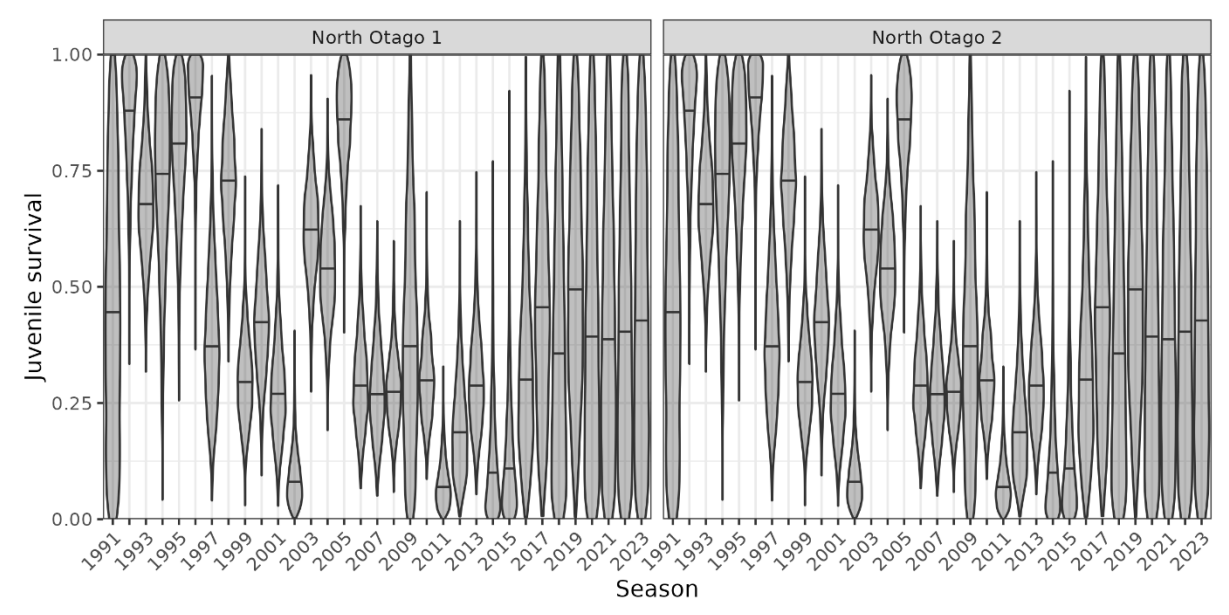


Figure B.38: Posterior distributions of the probability of juvenile survival (from fledgling to the following year) by season and regional sub-population, for the <u>male northern model</u> run (North Otago 1 and North Otago 2). Note that these were assumed to be the same across both regions.

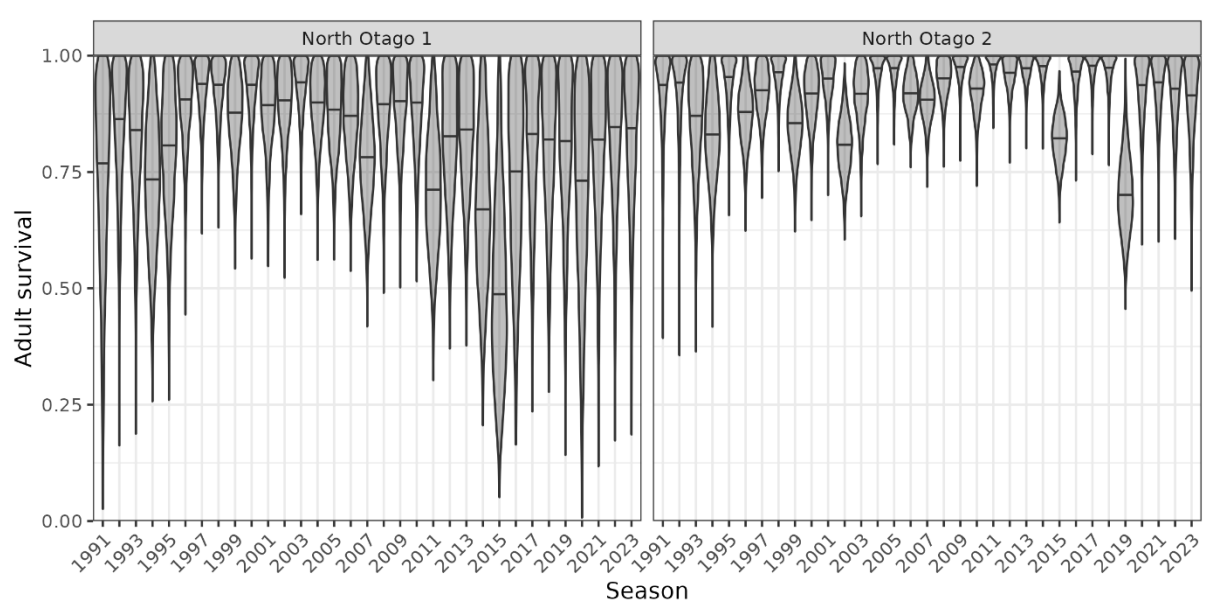


Figure B.39: Posterior distributions of the probability of adult survival by season and regional sub-population, for the <u>male northern model</u> run (North Otago 1 and North Otago 2).

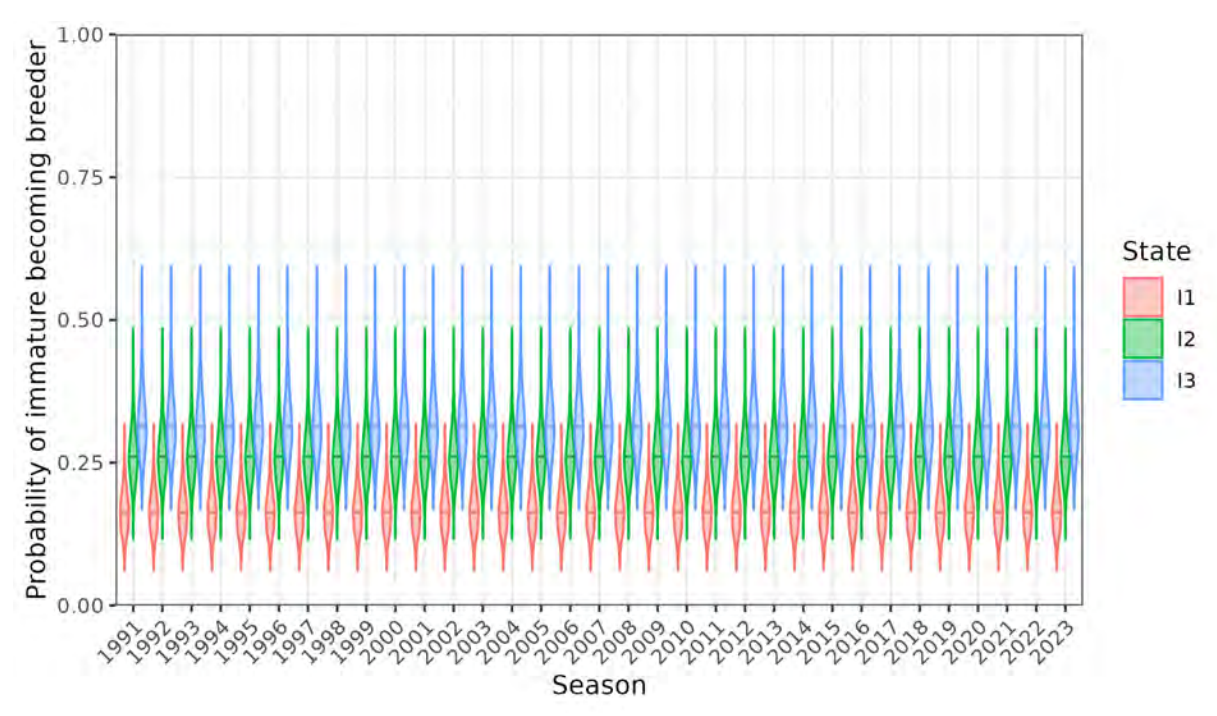


Figure B.40: Posterior distributions of the annual probabilites of immature birds at ages 1 (I1), 2 (I2), and 3 (I3) becoming breeders at the following ages, for the <u>male northern model</u> run (North Otago 1 and North Otago 2).

Southern model run (Otago Peninsula, Catlins, and Stewart Island)

Table B.6: Summary of posteriors of estimated model parameters for the <u>female southern model</u> (regional sub-populations were Otago Peninsula, the Catlins, and Stewart Island).

N_init N° 1070.230 851.576 1053.072 1389.647 4 035 1.001 alpha surv1[2] α_{ϕ}^{a} 0.847 0.463 0.815 1.392 2 155 1.001 beta surv1[2] β_{ϕ}^{a} 0.580 0.274 0.553 1.039 1.085 1.001 beta surv1[2] β_{ϕ}^{a} 1.609 0.801 1.540 2.771 2.385 1.001 alpha surv2[1] α_{ϕ}^{a+} 12.389 5.746 11.794 22.993 2.250 1.003 alpha surv2[3] α_{ϕ}^{a+} 4.780 0.620 3.821 14.352 5.94 1.000 beta surv2[3] β_{ϕ}^{a+} 2.403 1.158 2.2276 4.428 1.970 1.002 beta surv2[3] β_{ϕ}^{a+} 1.665 0.218 1.460 4.392 6.593 0.999 beta surv2[3] β_{ϕ}^{a+} 1.665 0.218 1.406 4.392 6.593 0.999 beta surv2[3] β_{ϕ}^{a+}	Label	Parameter	Mean	2.5%	Median	97.5%	Effective N	Rhat
$ \begin{array}{c ccccccccccccccccccccccccccccccccccc$	N init	N^{0}	1070.230	851.576	1053.072	1389.647	4 035	1.001
$\begin{array}{c ccccccccccccccccccccccccccccccccccc$	_	α_{ϕ^0}	0.847					
$\begin{array}{c ccccccccccccccccccccccccccccccccccc$		•						
$\begin{array}{c ccccccccccccccccccccccccccccccccccc$								
$\begin{array}{c ccccccccccccccccccccccccccccccccccc$	=	•						
$\begin{array}{c ccccccccccccccccccccccccccccccccccc$								
$\begin{array}{c ccccccccccccccccccccccccccccccccccc$		•						
$\begin{array}{c ccccccccccccccccccccccccccccccccccc$		•						
$\begin{array}{c ccccccccccccccccccccccccccccccccccc$		•						
$\begin{array}{c ccccccccccccccccccccccccccccccccccc$		•						
$\begin{array}{c ccccccccccccccccccccccccccccccccccc$		•						
$\begin{array}{c ccccccccccccccccccccccccccccccccccc$		•						
$\begin{array}{c ccccccccccccccccccccccccccccccccccc$		•						
$\begin{array}{c ccccccccccccccccccccccccccccccccccc$		•						
$\begin{array}{c ccccccccccccccccccccccccccccccccccc$		•						
$\begin{array}{c ccccccccccccccccccccccccccccccccccc$		•						
$\begin{array}{c ccccccccccccccccccccccccccccccccccc$		$lpha_{\psi}$						
$\begin{array}{c ccccccccccccccccccccccccccccccccccc$		•						
$\begin{array}{c ccccccccccccccccccccccccccccccccccc$		•						
$\begin{array}{c ccccccccccccccccccccccccccccccccccc$								
$\begin{array}{c ccccccccccccccccccccccccccccccccccc$	beta_hatch[3]	eta_{ψ}	6.351	2.653		12.824	2 062	
$\begin{array}{c ccccccccccccccccccccccccccccccccccc$	beta_hatch[4]		34.049	14.298	31.260	68.399	2 718	1.001
$\begin{array}{c ccccccccccccccccccccccccccccccccccc$	beta_hatch[5]	$eta_{m{\psi}}$	17.239	7.815	15.908	33.876	2 516	1.000
$\begin{array}{c} \text{alpha} \text{ fledge}[2] & \alpha_{\varphi} & 5.180 & 2.610 & 4.939 & 8.922 & 4.448 & 1.000 \\ \text{alpha} \text{ fledge}[3] & \alpha_{\varphi} & 4.559 & 2.011 & 4.303 & 8.717 & 1.338 & 1.001 \\ \text{beta} \text{ fledge}[1] & \beta_{\varphi} & 2.266 & 1.361 & 2.225 & 3.433 & 5.517 & 1.000 \\ \text{beta} \text{ fledge}[2] & \beta_{\varphi} & 1.054 & 0.597 & 1.023 & 1.698 & 4.011 & 1.000 \\ \text{beta} \text{ fledge}[3] & \beta_{\varphi} & 2.328 & 1.050 & 2.206 & 4.375 & 1.349 & 1.001 \\ \text{p_immature_breeding_raw}[1] & \eta_t^{11} & -1.576 & -1.849 & -1.575 & -1.310 & 6.162 & 1.000 \\ \text{p_immature_breeding_raw}[2] & \eta_t^{12} & 0.228 & -0.039 & 0.229 & 0.509 & 4.645 & 1.000 \\ \text{p_immature_breeding_raw}[3] & \eta_t^{13} & 0.472 & 0.132 & 0.453 & 0.889 & 4.613 & 1.000 \\ \text{p_non_breeder_breeding} & \gamma_t & 0.446 & 0.390 & 0.446 & 0.503 & 8.007 & 1.000 \\ \text{p_non_breeder_breeding} & \delta_t & 0.824 & 0.793 & 0.825 & 0.853 & 4.302 & 1.000 \\ \text{p_non_breeder_seen}[1] & \tau_{a,t}^{NB} & 0.499 & 0.450 & 0.499 & 0.548 & 6.765 & 1.000 \\ \text{p_non_breeder_seen}[2] & \tau_{a,t}^{NB} & 0.293 & 0.257 & 0.293 & 0.331 & 6.835 & 1.000 \\ \text{p_non_breeder_seen}[4] & \tau_{a,t}^{NB} & 0.420 & 0.329 & 0.419 & 0.520 & 7.371 & 0.999 \\ \text{p_non_breeder_seen}[5] & \tau_{a,t}^{NB} & 0.966 & 0.923 & 0.968 & 0.997 & 3.617 & 1.000 \\ \text{p_breeder_seen}[2] & \tau_{a,t}^{B} & 0.866 & 0.822 & 0.866 & 0.909 & 5.021 & 1.000 \\ \text{p_breeder_seen}[3] & \tau_{a,t}^{B} & 0.866 & 0.822 & 0.866 & 0.909 & 5.021 & 1.000 \\ \text{p_breeder_seen}[3] & \tau_{a,t}^{B} & 0.866 & 0.822 & 0.866 & 0.909 & 5.021 & 1.000 \\ \text{p_breeder_seen}[3] & \tau_{a,t}^{B} & 0.350 & 0.247 & 0.325 & 0.414 & 9.512 & 0.999 \\ \text{p_breeder_seen}[4] & \tau_{a,t}^{B} & 0.326 & 0.247 & 0.325 & 0.414 & 9.512 & 0.999 \\ \text{p_breeder_seen}[5] & \tau_{a,t}^{B} & 0.326 & 0.247 & 0.325 & 0.414 & 9.512 & 0.999 \\ \text{p_breeder_seen}[5] & \tau_{a,t}^{B} & 0.326 & 0.247 & 0.325 & 0.414 & 9.512 & 0.999 \\ \text{p_breeder_seen}[5] & \tau_{a,t}^{B} & 0.326 & 0.247 & 0.325 & 0.414 & 9.512 & 0.999 \\ \text{p_breeder_seen}[5] & \tau_{a,t}^{B} & 0.326 & 0.247 & 0.325 & 0.414 & 9.512 & 0.999 \\ \text{p_breeder_seen}[5] & \tau_{a,t}^{B} & 0.326 & 0.247 & 0.325 & 0.414 & 9$	beta_hatch[6]	$eta_{m{\psi}}$	10.627	4.141	9.773	22.656	1 301	1.002
$\begin{array}{c ccccccccccccccccccccccccccccccccccc$	alpha_fledge[1]	$lpha_{arphi}$	4.974	2.839	4.855	7.756	5 453	1.000
$\begin{array}{c ccccccccccccccccccccccccccccccccccc$	alpha_fledge[2]	$lpha_{arphi}$	5.180	2.610	4.939	8.922	4 448	1.000
$\begin{array}{c ccccccccccccccccccccccccccccccccccc$	alpha_fledge[3]	$lpha_{arphi}$	4.559	2.011	4.303	8.717	1 338	1.001
$\begin{array}{c ccccccccccccccccccccccccccccccccccc$	beta_fledge[1]	eta_{arphi}	2.266	1.361	2.225	3.433	5 517	1.000
$\begin{array}{c ccccccccccccccccccccccccccccccccccc$	beta_fledge[2]	$oldsymbol{eta}_{oldsymbol{arphi}}$	1.054	0.597	1.023	1.698	4 011	1.000
$\begin{array}{c ccccccccccccccccccccccccccccccccccc$	beta_fledge[3]		2.328	1.050	2.206	4.375	1 349	1.001
$\begin{array}{c ccccccccccccccccccccccccccccccccccc$	<pre>p_immature_breeding_raw[1]</pre>	$\eta_t^{ m I1}$	-1.576	-1.849	-1.575	-1.310	6 162	1.000
$\begin{array}{c ccccccccccccccccccccccccccccccccccc$	p_immature_breeding_raw[2]	η_t^{12}	0.228	-0.039	0.229	0.509	4 645	1.000
$\begin{array}{cccccccccccccccccccccccccccccccccccc$	<pre>p_immature_breeding_raw[3]</pre>	$\eta_t^{{ m I}3}$	0.472		0.453		4 613	1.000
$\begin{array}{cccccccccccccccccccccccccccccccccccc$		γ_t						
$\begin{array}{cccccccccccccccccccccccccccccccccccc$		δ_t						
$\begin{array}{cccccccccccccccccccccccccccccccccccc$		$r_{a,t}^{\text{NB}}$						
$\begin{array}{cccccccccccccccccccccccccccccccccccc$		$r_{a.t}^{\text{NB}}$						
$\begin{array}{cccccccccccccccccccccccccccccccccccc$		$r_{a,t}^{\text{NB}}$						
$\begin{array}{llllllllllllllllllllllllllllllllllll$		$r_{a,t}^{\mathrm{NB}}$						
$\begin{array}{cccccccccccccccccccccccccccccccccccc$		$r_{a,t}^{\mathrm{NB}}$						
$\begin{array}{cccccccccccccccccccccccccccccccccccc$	p_breeder_seen[1]	$r_{a,t}^{ m B}$					3 617	
$\begin{array}{cccccccccccccccccccccccccccccccccccc$		$r_{a,t}^{ m B}$						
p_breeder_seen[5] $r_{a,t}^B$ 0.237 0.172 0.235 0.315 6 726 1.000 p_move[1] κ 0.003 0.000 0.002 0.007 8 001 0.999		$r_{a,t}^{\mathrm{B}}$						
p_move[1] κ 0.003 0.000 0.002 0.007 8 001 0.999		$r_{a,t}^{ m B}$						
p_move[1] κ 0.003 0.000 0.002 0.007 8 001 0.999		$r_{a,t}^{\mathrm{B}}$						
p_move[2] κ 0.132 0.097 0.131 0.170 5 197 0.999								
	p_move[2]	К	0.132	0.097	0.131	0.170	5 197	0.999

Table B.7: Summary of posteriors of estimated model parameters for the <u>male southern model</u> (regional sub-populations were Otago Peninsula, the Catlins, and Stewart Island).

Label	Parameter	Mean	2.5%	Median	97.5%	Effective N	Rhat
N_init	N^0	1490.452	1193.66 7	1470.218	1880.125	2 355	1.002
alpha_surv1[1]	$lpha_{m{\phi}^0}$	0.836	0.443	0.805	1.432	1 374	1.005
alpha_surv1[2]	$lpha_{m{\phi}^0}$	1.015	0.425	0.947	2.013	751	1.007
beta_surv1[1]	$oldsymbol{eta_{oldsymbol{\phi}^0}}$	1.348	0.650	1.291	2.400	1 361	1.006
beta_surv1[2]	$eta_{oldsymbol{\phi}^0}$	0.778	0.278	0.703	1.724	626	1.008
alpha_surv2[1]	$\alpha_{\phi^{1+}}$	18.052	8.448	16.934	33.344	1 307	1.000
alpha surv2[2]	$lpha_{\phi^{1+}}$	4.844	2.272	4.568	8.953	1 021	1.006
alpha_surv2[3]	$\alpha_{\phi^{1+}}$	4.647	0.609	3.772	14.244	4 354	1.000
beta_surv2[1]	$eta_{\phi^{1+}}$	3.119	1.512	2.933	5.695	1 254	1.000
beta_surv2[2]	$eta_{\phi^{1+}}$	0.741	0.343	0.695	1.395	629	1.008
beta_surv2[3]	$eta_{\phi^{1+}}$	1.642	0.236	1.429	4.260	4 689	1.000
alpha_hatch[1]	$lpha_{m{\psi}}$	4.518	2.200	4.274	8.286	2 564	1.000
alpha_hatch[2]	$lpha_{m{\psi}}$	3.173	1.552	2.988	5.824	2 393	1.000
alpha_hatch[3]	$lpha_{\psi}$	1.561	0.712	1.455	2.931	1 245	1.001
alpha_hatch[4]	$lpha_{m{\psi}}$	9.329	4.229	8.547	18.976	1 970	1.002
alpha_hatch[5]	$lpha_{m{\psi}}$	5.007	2.439	4.666	9.443	1 929	1.000
alpha_hatch[6]	$lpha_{m{\psi}}$	3.225	1.382	2.985	6.417	1 337	1.000
beta_hatch[1]	$eta_{\psi}^{^{arphi}}$	33.690	15.412	31.895	64.330	2 594	1.000
beta_hatch[2]	$eta_{\psi}^{\;$	17.011	7.693	15.884	32.224	2 378	1.000
beta_hatch[3]	eta_{ψ}^{arphi}	6.586	2.857	6.106	13.040	1 530	1.001
beta_hatch[4]	eta_{ψ}^{arphi}	34.525	15.248	31.525	71.365	2 046	1.002
beta_hatch[5]	eta_{ψ}	17.123	7.859	15.892	33.074	2 039	1.000
beta_hatch[6]	eta_{ψ}	10.704	4.227	9.733	22.577	1 355	1.000
alpha_fledge[1]	$\alpha_{m{\varphi}}$	5.027	2.934	4.908	7.895	3 588	1.000
alpha_fledge[2]	$lpha_{m{arphi}}$	5.188	2.645	4.994	8.868	2 324	1.002
alpha_fledge[3]	$lpha_{m{arphi}}^{ au}$	4.671	2.142	4.458	8.687	1 508	1.000
beta_fledge[1]	$oldsymbol{eta}_{oldsymbol{arphi}}^{^{ au}}$	2.297	1.398	2.252	3.451	3 554	1.000
beta_fledge[2]	$oldsymbol{eta}_{oldsymbol{arphi}}$	1.058	0.603	1.025	1.688	1 985	1.003
beta_fledge[3]	$oldsymbol{eta}_{oldsymbol{arphi}}$	2.260	1.046	2.149	4.173	1 440	1.001
p_immature_breeding_raw[1]	$\eta_t^{{ m I}1}$	-2.302	-2.716	-2.301	-1.928	4 280	1.000
p_immature_breeding_raw[2]	$\eta_t^{ ext{I2}}$	-0.546	-0.799	-0.544	-0.305	4 362	0.999
p_immature_breeding_raw[3]	$\eta_t^{{ m I}3}$	-0.294	-0.588	-0.306	0.054	4 398	
p_non_breeder_breeding	γ_t	0.355	0.316	0.354	0.393	6 117	0.999
p_breeder_breeding	δ_t	0.756	0.723	0.757	0.787	3 059	0.999
p_non_breeder_seen[1]	$r_{a,t}^{ m NB}$	0.417	0.362	0.416	0.474	5 443	1.000
p_non_breeder_seen[2]	$r_{a,t}^{ m NB}$	0.342	0.311 0.154	0.342	0.374	4 151	1.000
p_non_breeder_seen[3]	$r_{a,t}^{ m NB}$	0.227		0.225	0.315	6 003	1.000
p_non_breeder_seen[4]	$r_{a,t}^{ m NB}$	0.395	0.321 0.002	0.393	0.479	5 182 6 497	1.000 1.000
p_non_breeder_seen[5]	$r_{a,t}^{ m NB}$	0.012	0.002	0.011 0.979	0.031 0.999	3 982	1.000
<pre>p_breeder_seen[1] p breeder seen[2]</pre>	$r_{a,t}^{\mathrm{B}}$	0.975 0.845	0.928	0.979	0.999	3 982	0.999
p_breeder_seen[2] p_breeder_seen[3]	$r_{a,t}^{ m B} \ r_{a,t}^{ m B}$	0.843	0.801	0.843	0.890	3 492	0.999
p_breeder_seen[3] p_breeder_seen[4]	$r_{a,t}^{\mathrm{B}}$	0.874	0.783	0.873	0.330	5 492 5 470	0.999
p_breeder_seen[5]	$r_{a,t}^{\mathrm{B}}$	0.200	0.199	0.239	0.330	5 934	1.000
p_move[1]	'a,t K	0.120	0.073	0.123	0.194	5 950	1.000
p_move[2]	κ	0.063	0.042	0.063	0.089	4 792	1.000
1		2.500	- · · · -		2.307	. , , =	

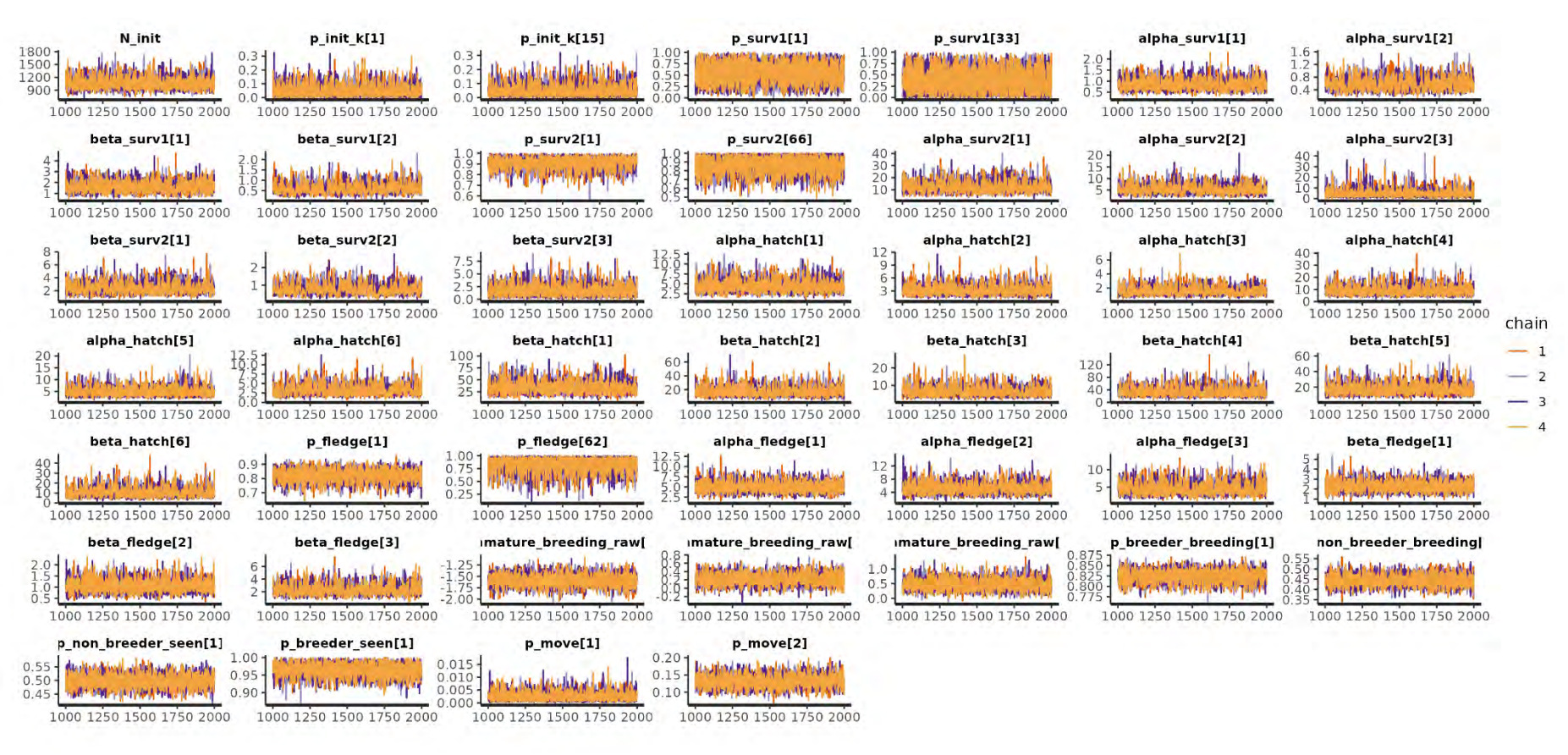


Figure B.41: MCMC trace plots for a subset of estimated parameters from the female southern model run (Otago Peninsula, Catlins, and Stewart Island).

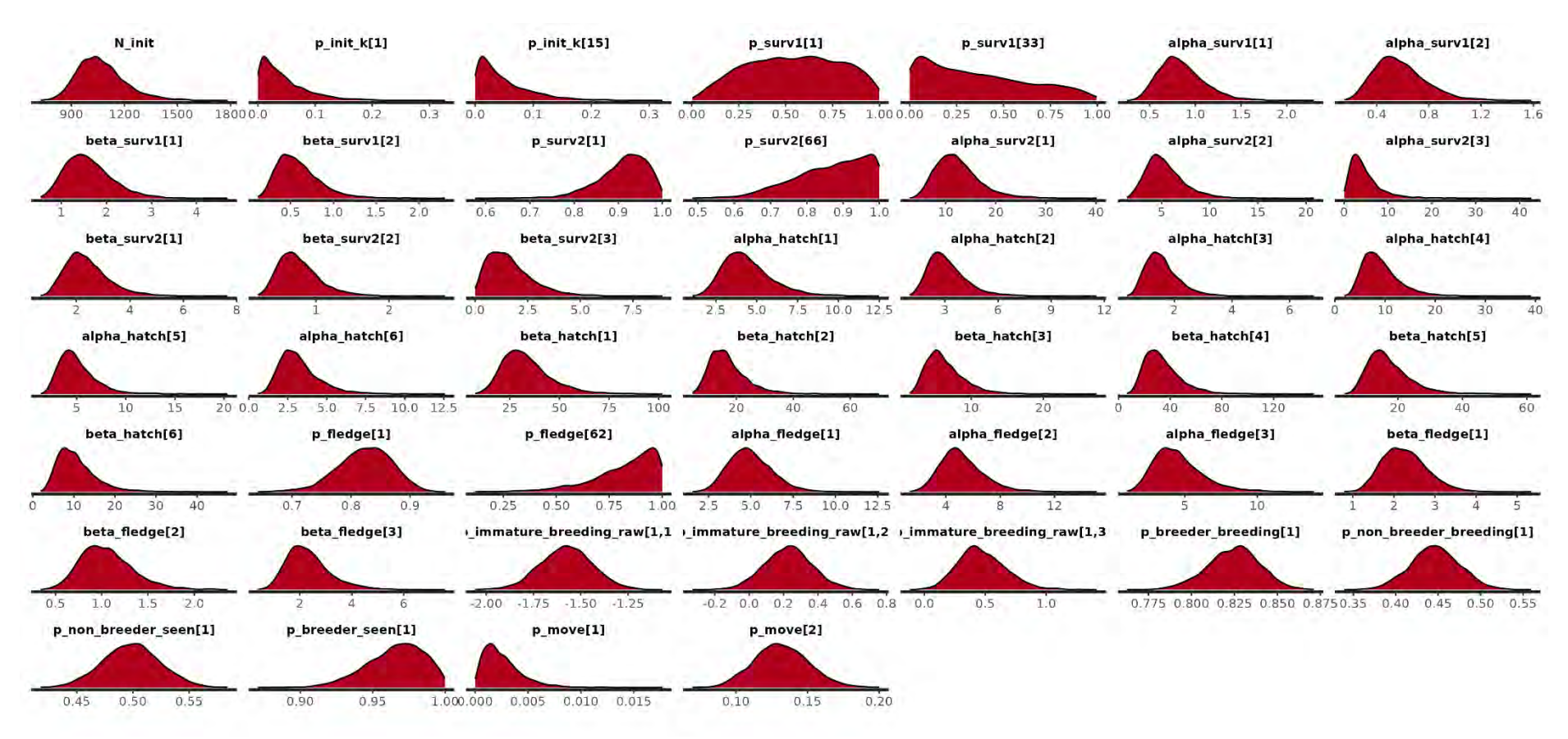


Figure B.42: Posterior distribution for a subset of parameters from the female southern model run (Otago Peninsula, Catlins, and Stewart Island).

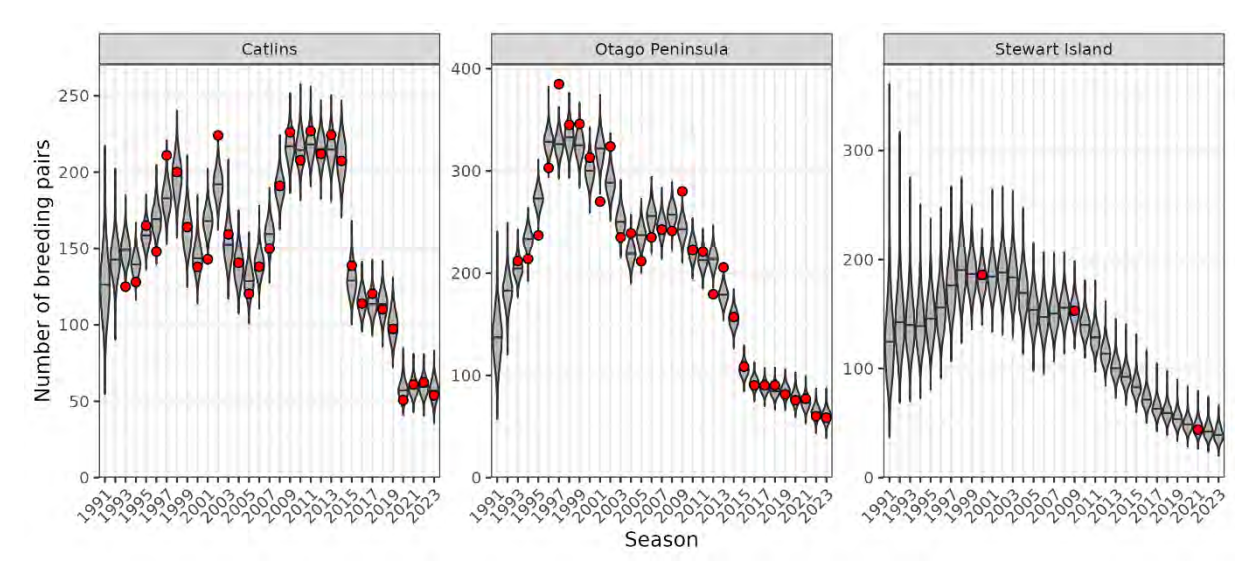


Figure B.43: Posterior distribution of the number of breeding pairs by season from the <u>female southern</u> <u>model</u> run (Otago Peninsula, Catlins, and Stewart Island, compared with the 'observed' estimate of breeding pairs for each regional sub-population (red points).

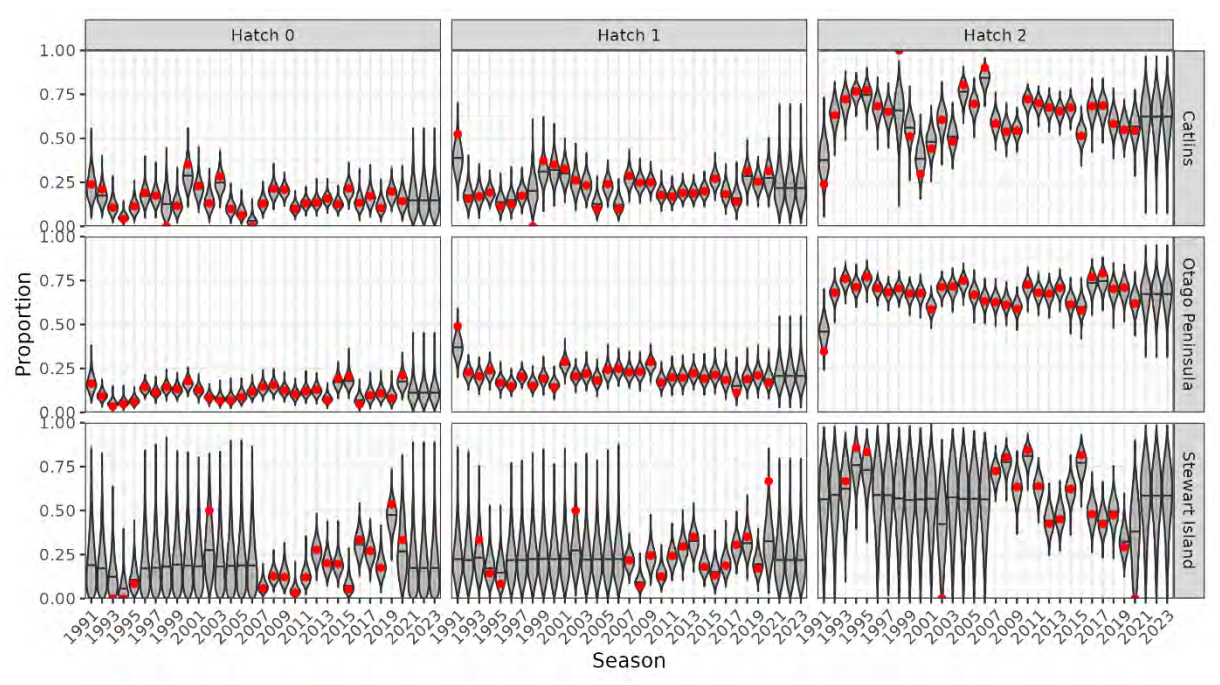


Figure B.44: Posterior distribution of the proportion of nests producing zero, one, two hatchlings by season from the <u>female southern model</u> run (Otago Peninsula, Catlins, and Stewart Island), compared with the 'observed' proportions for each regional sub-population (red points).

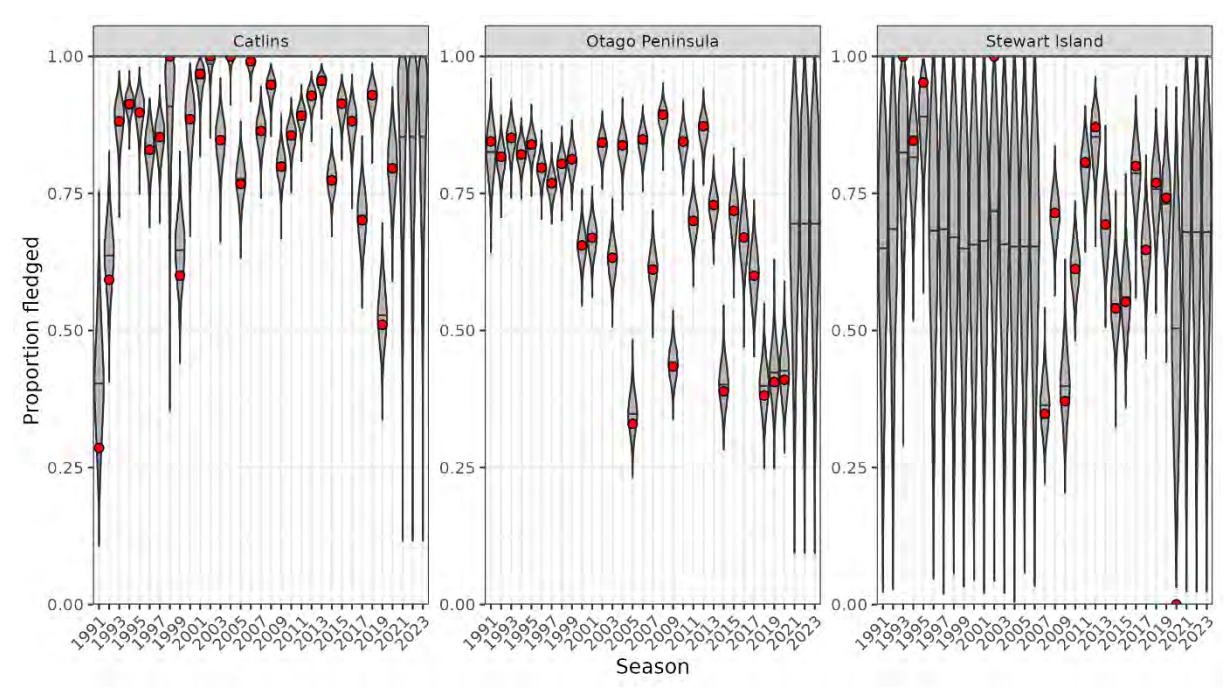


Figure B.45: Posterior distribution of the proportion of hatchlings that fledged by season from the <u>female</u> <u>southern model</u> run (Otago Peninsula, Catlins, and Stewart Island) (violin plots, horizontal lines represent the median values), compared with the 'observed' proportions for each regional sub-population (red points).

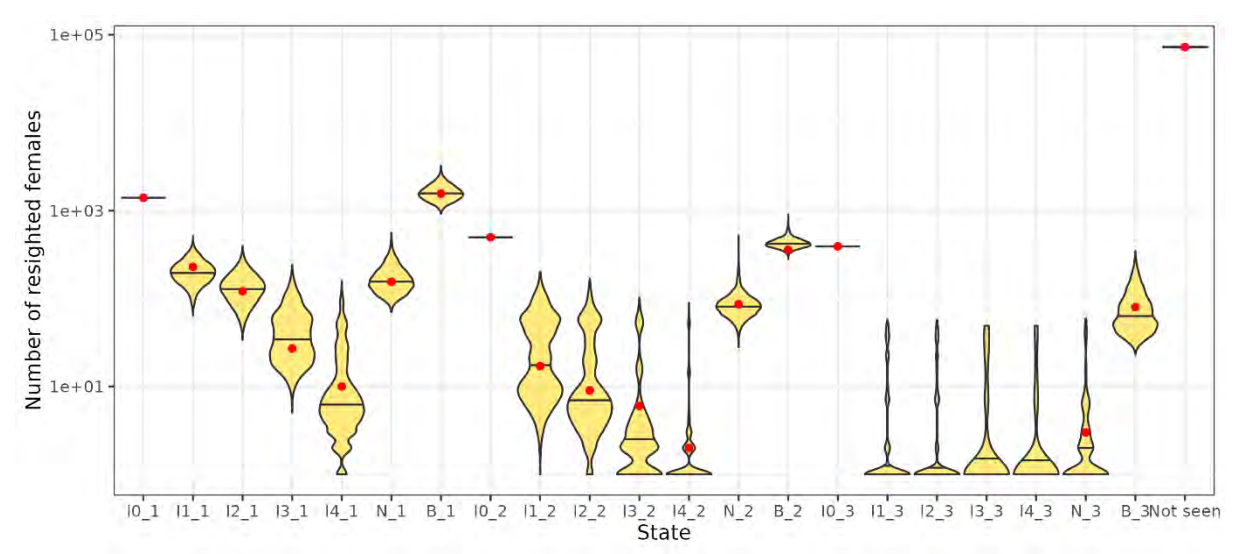


Figure B.46: Posterior distribution of the observed number of resighted birds by model state from the <u>female southern model</u> run (Otago Peninsula, Catlins, and Stewart Island) (violin plots, horizontal lines represent the median values), compared with the 'observed' numbers for each regional sub-population (red circles). Model states with suffix '-1', '-2', and '-3' apply to Otago Peninsula, Catlins, and Stewart Island, respectively.

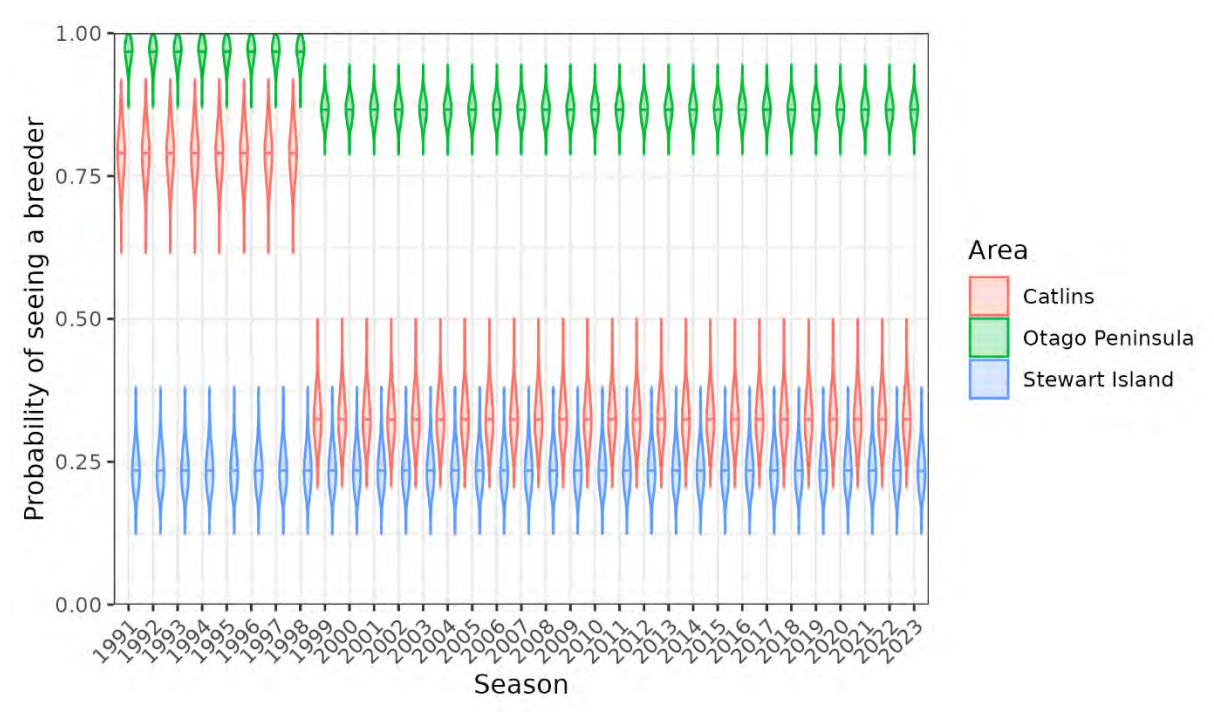


Figure B.47: Posterior distributions of the probability of a breeder being seen by season and regional subpopulation, for the <u>female southern model</u> run (Otago Peninsula, Catlins, and Stewart Island).

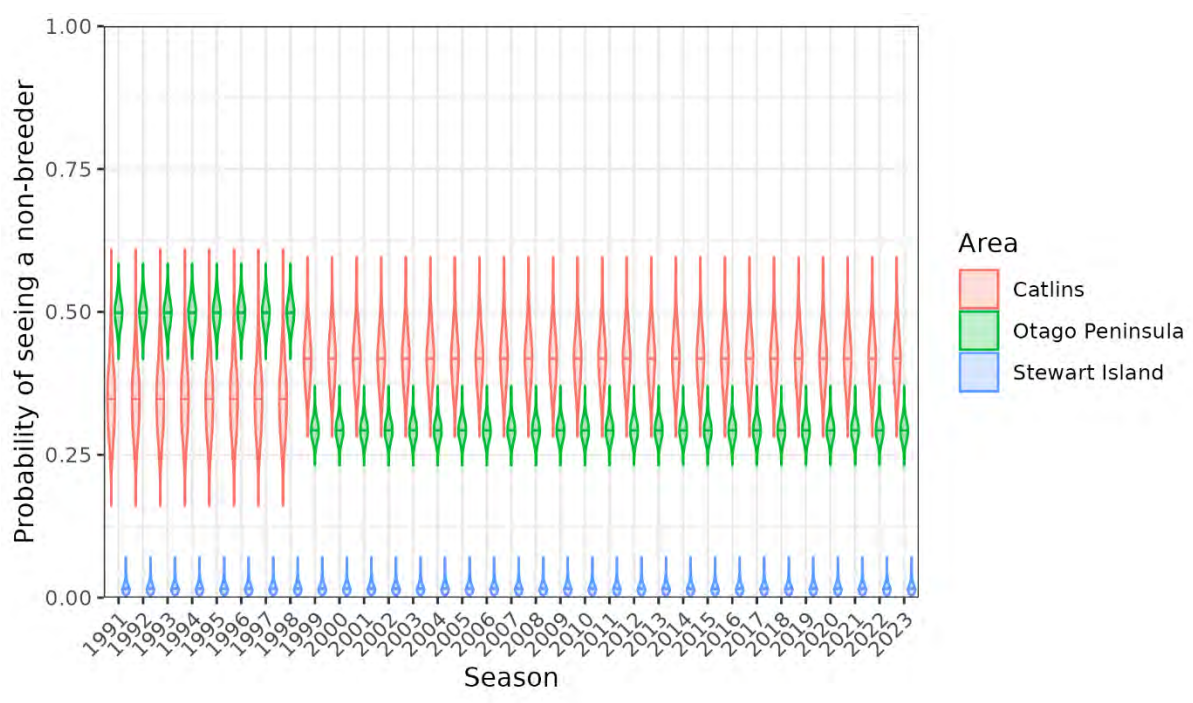


Figure B.48: Posterior distributions of the probability of a non-breeder being seen by season and regional sub-population, for the <u>female southern model</u> run (Otago Peninsula, Catlins, and Stewart Island).

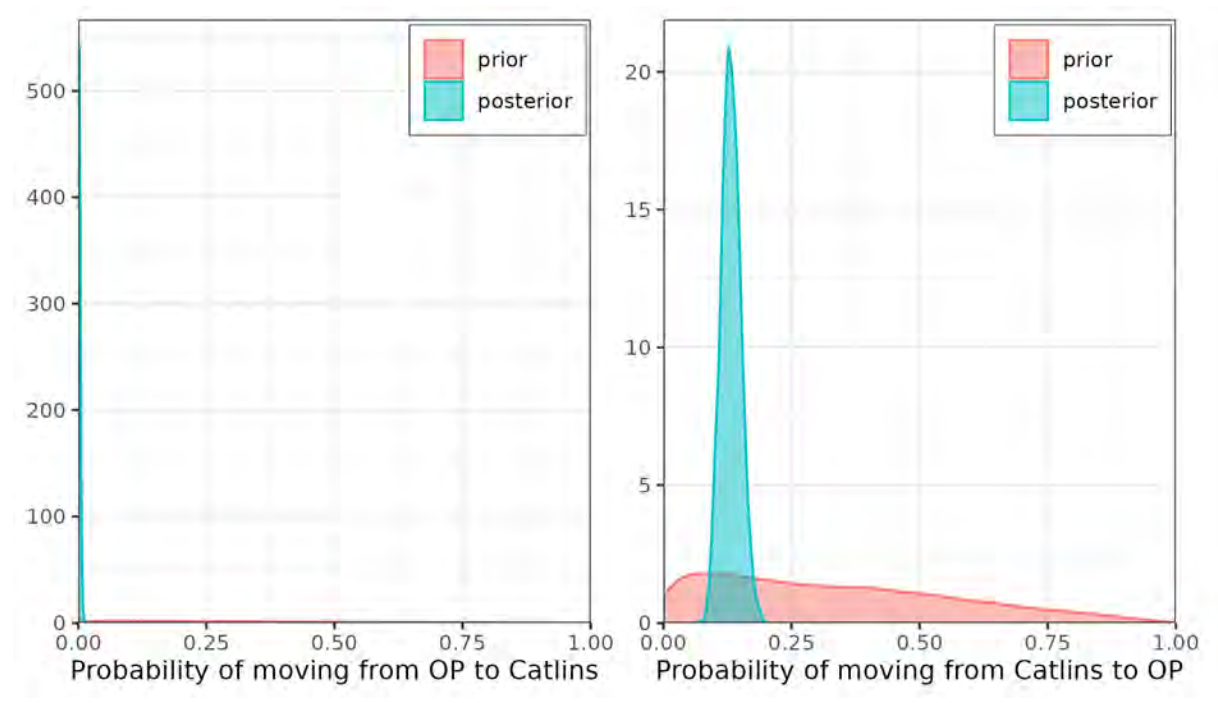


Figure B.49: Prior and posterior distributions (pink and blue polygons, respectively) of the annual probabilites of immature birds moving between regions of the <u>female southern model</u> run (Otago Peninsula, Catlins, and Stewart Island). Note that it was assumed that there was no movement of juveniles between Stewart Island and the other model regions.

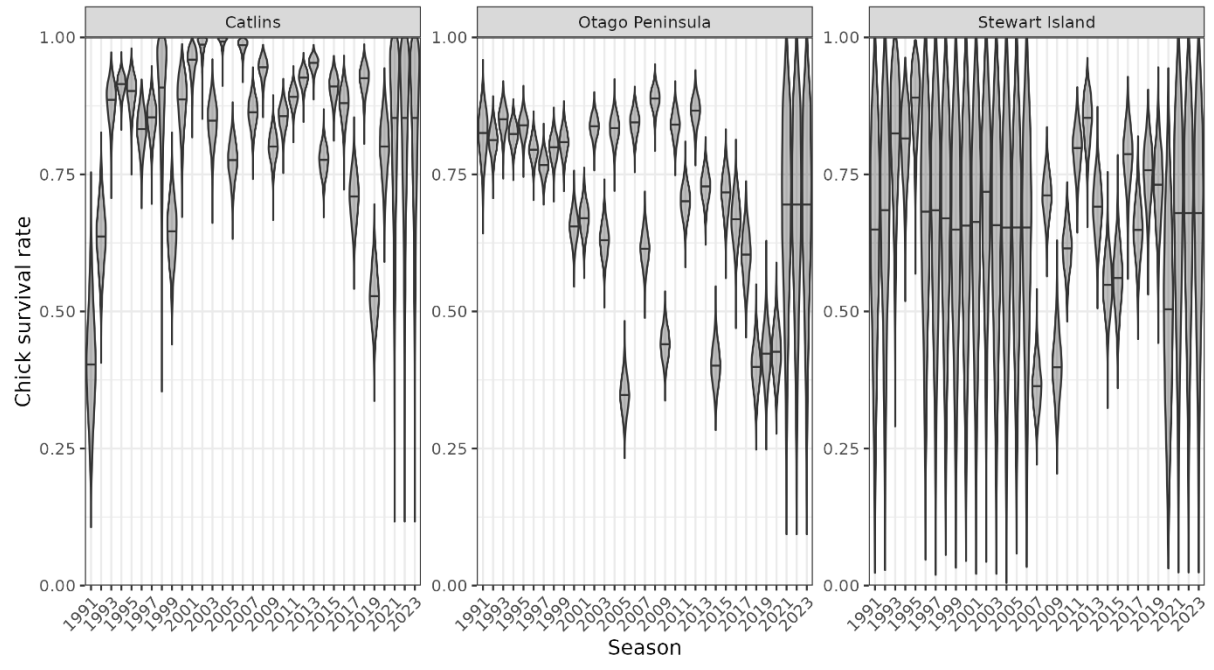


Figure B.50: Posterior distributions of the probability of chick survival (from hatching to fledgling) by season and regional sub-population, for the <u>female southern model</u> run (Otago Peninsula, Catlins, and Stewart Island).

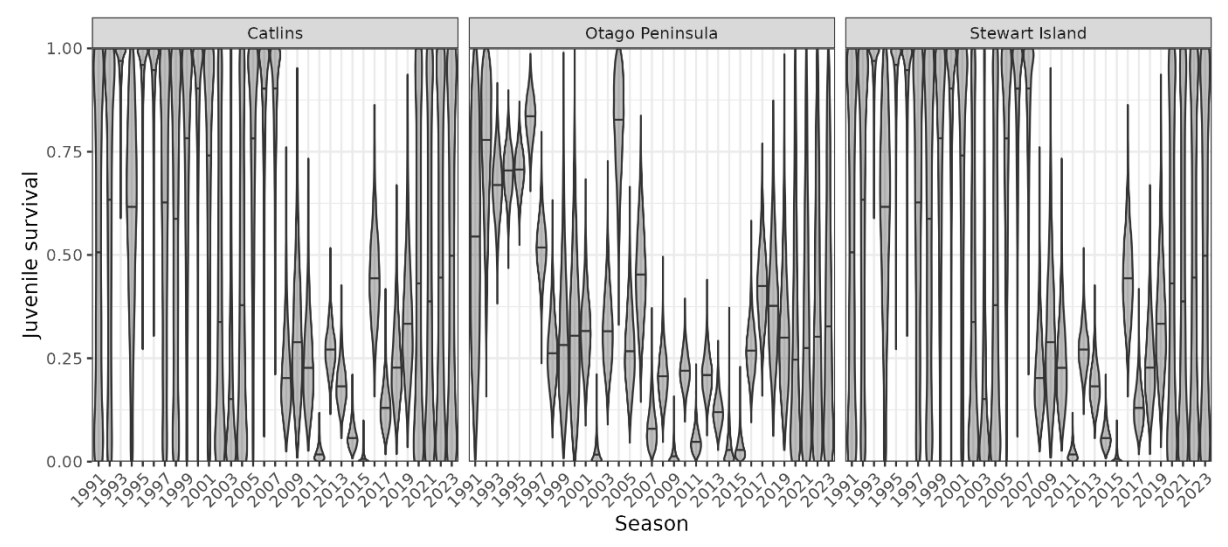


Figure B.51: Posterior distributions of the probability of juvenile survival (from fledgling to the following year) by season and regional sub-population, for the <u>female southern model</u> run (Otago Peninsula, Catlins, and Stewart Island). Note that these were assumed to be the same across both regions. Note that these were assumed to be the same for Catlins and Stewart Island.

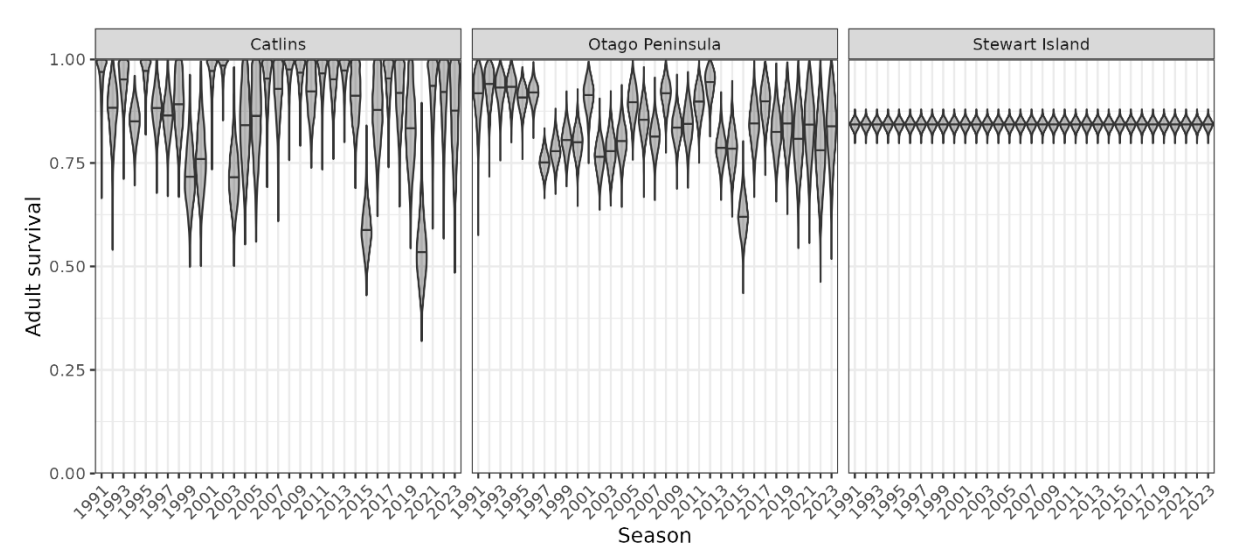


Figure B.52: Posterior distributions of the probability of adult survival by season and regional subpopulation, for the <u>female southern model</u> run (Otago Peninsula, Catlins, and Stewart Island).

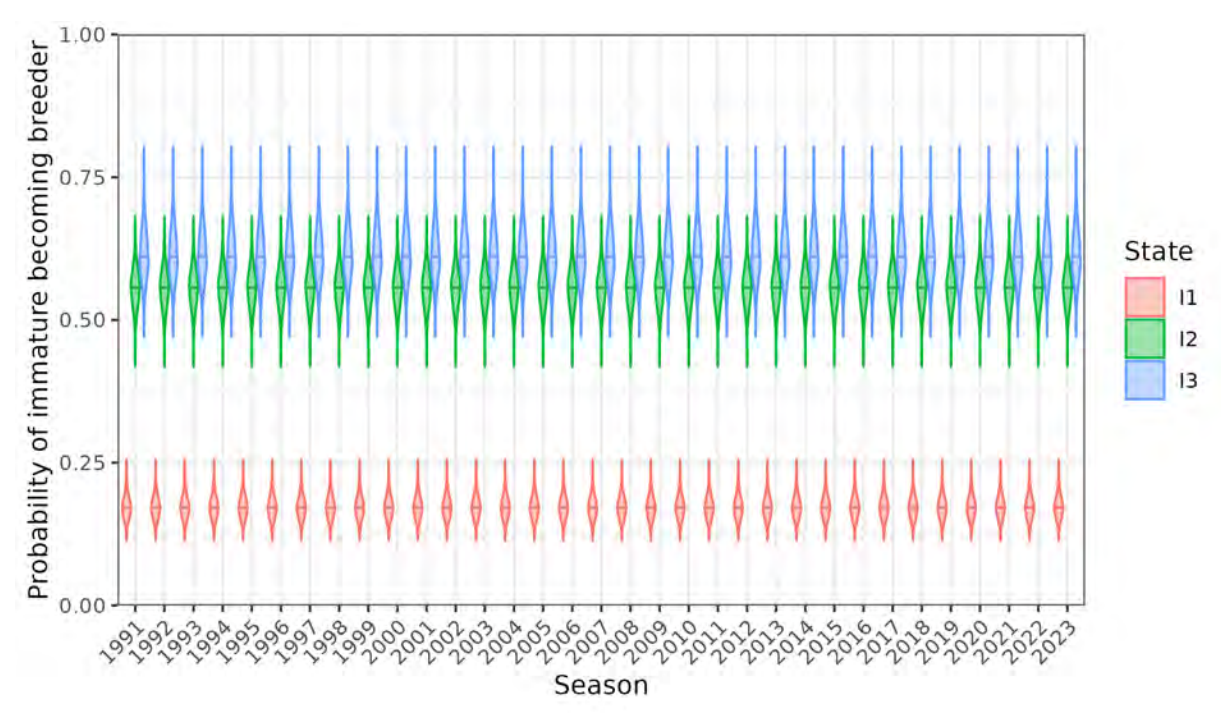


Figure B.53: Posterior distributions of the annual probabilities of immature birds at ages 1 (I1), 2 (I2), and 3 (I3) becoming breeders at the following ages, for the <u>female southern model</u> run (Otago Peninsula, Catlins, and Stewart Island).

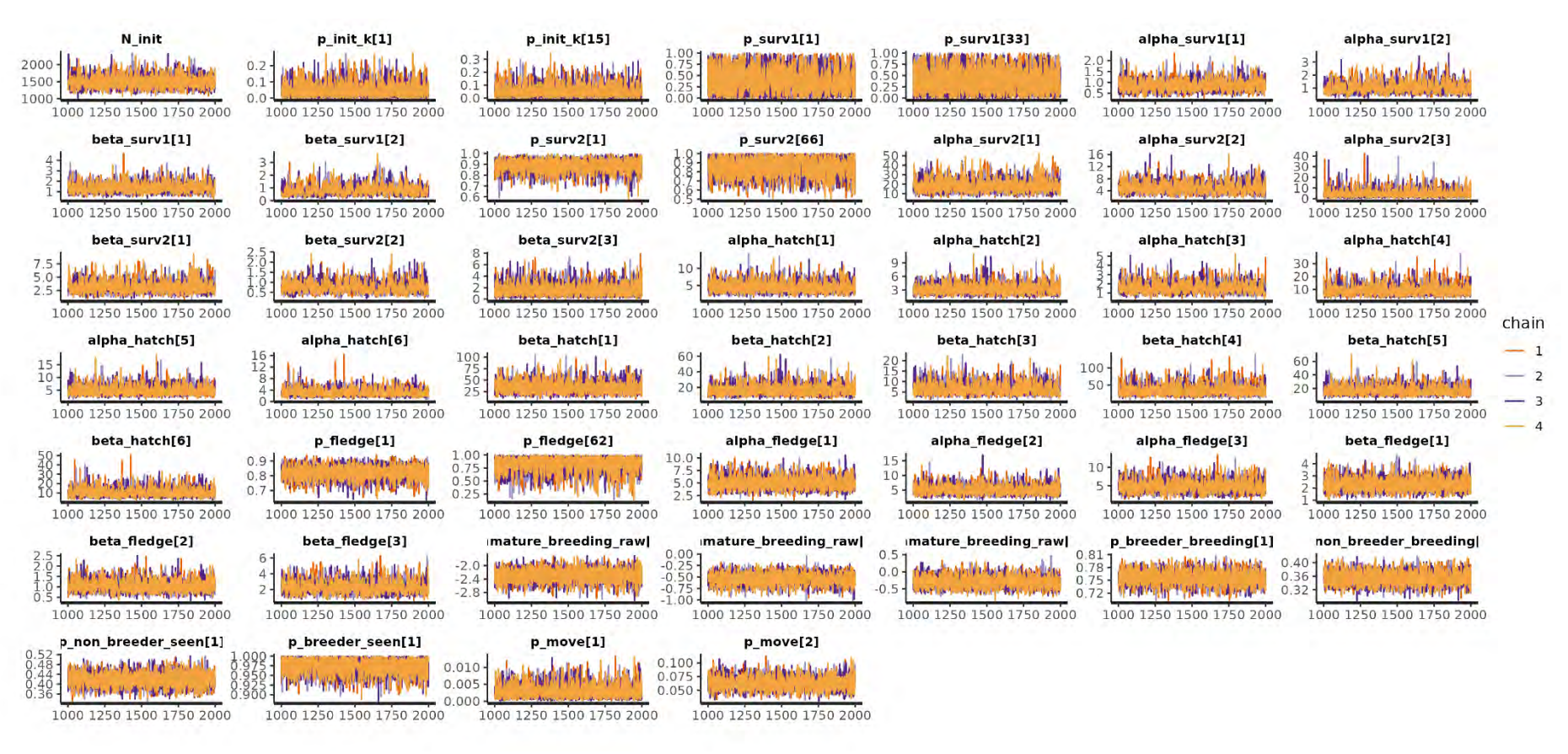


Figure B.54: MCMC trace plots for a subset of estimated parameters from the male southern model run (Otago Peninsula, Catlins, and Stewart Island).

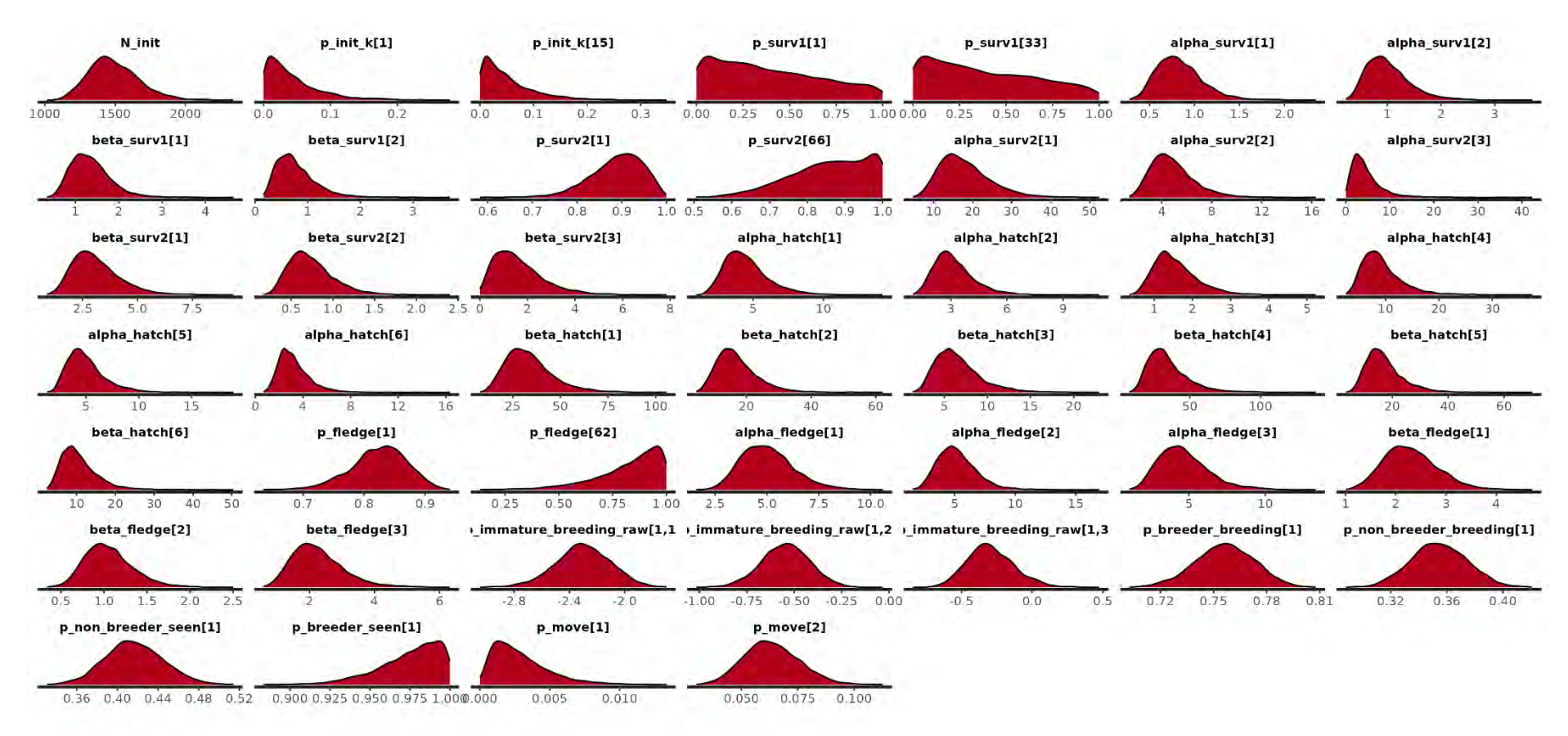


Figure B.55: Posterior distribution for a subset of parameters from the male southern model run (Otago Peninsula, Catlins, and Stewart Island).

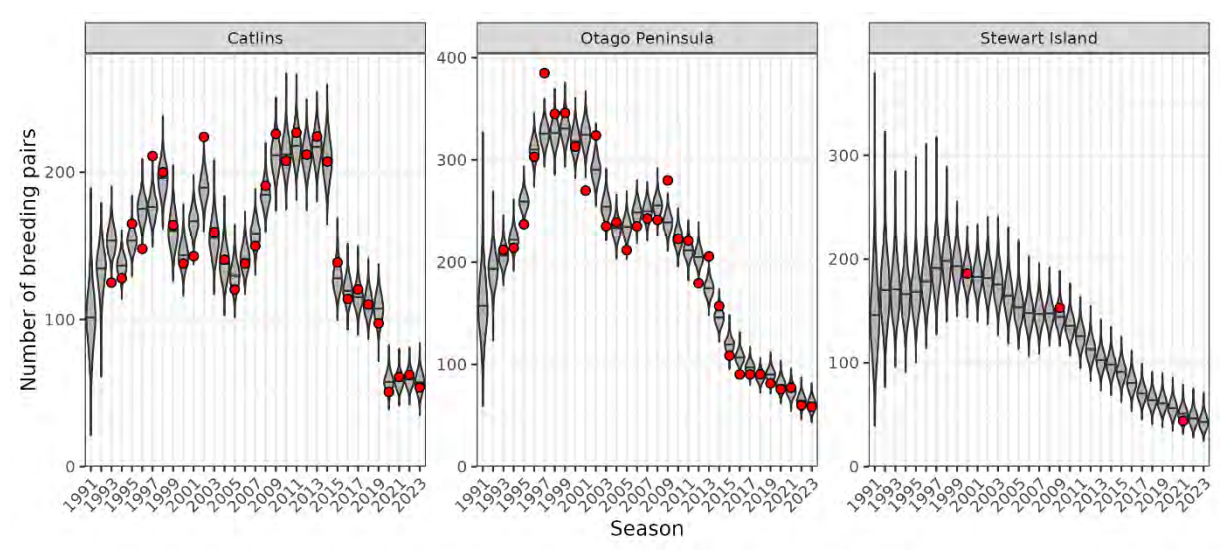


Figure B.56: Posterior distribution of the number of breeding pairs by season from the <u>male southern model</u> run (Otago Peninsula, Catlins, and Stewart Island, compared with the 'observed' estimate of breeding pairs for each regional sub-population (red points).

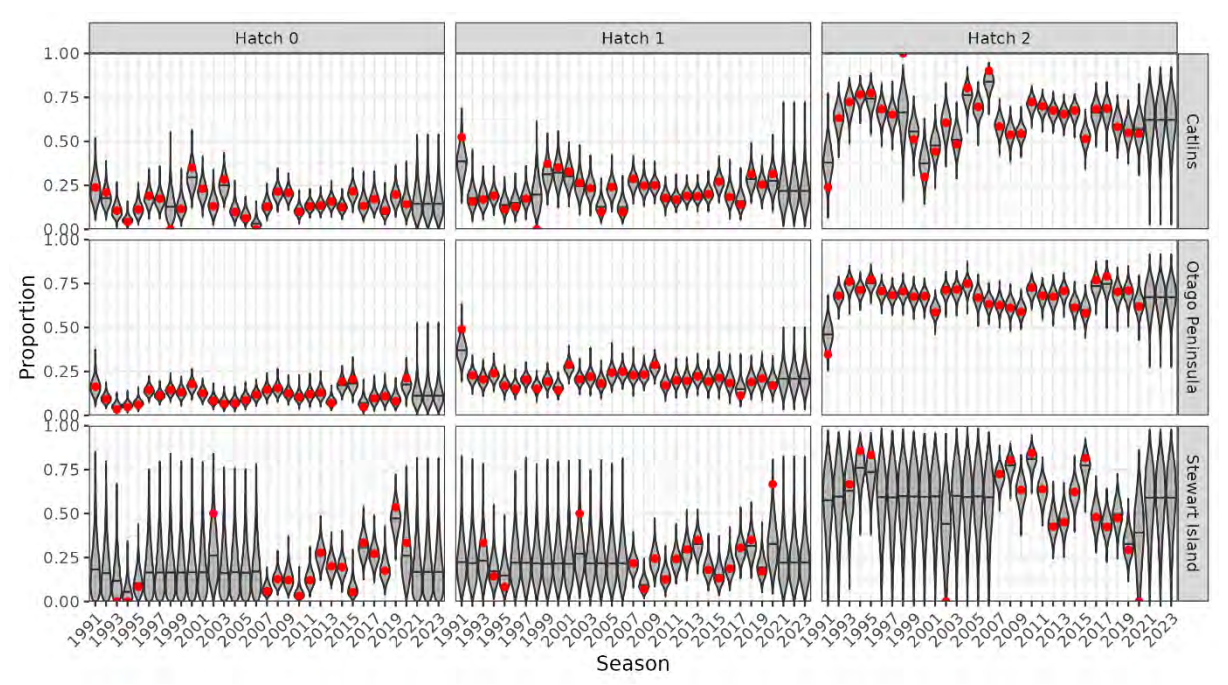


Figure B.57: Posterior distribution of the proportion of nests producing zero, one, two hatchlings by season from the <u>male southern model</u> run (Otago Peninsula, Catlins, and Stewart Island), compared with the 'observed' proportions for each regional sub-population (red points).

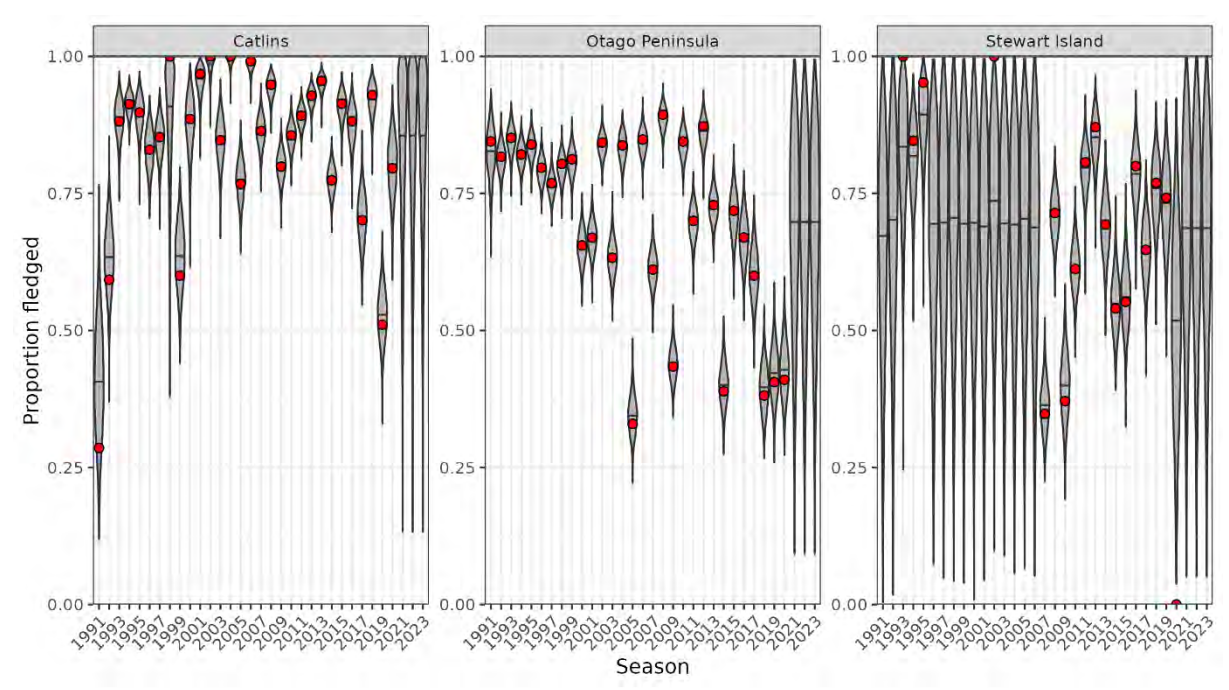


Figure B.58: Posterior distribution of the proportion of hatchlings that fledged by season from the <u>male southern model</u> run (Otago Peninsula, Catlins, and Stewart Island) (violin plots, horizontal lines represent the median values), compared with the 'observed' proportions for each regional sub-population (red points).

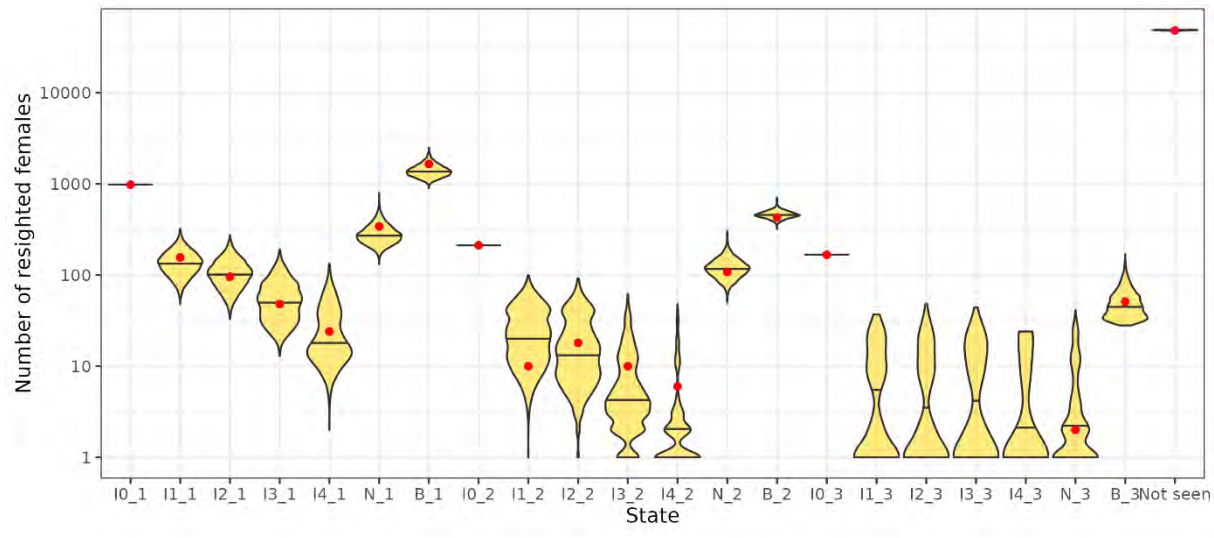


Figure B.59: Posterior distribution of the observed number of resighted birds by model state from the <u>male southern model</u> run (Otago Peninsula, Catlins, and Stewart Island) (violin plots, horizontal lines represent the median values), compared with the 'observed' numbers for each regional sub-population (red circles). Model states with suffix '-1', '-2', and '-3' apply to Otago Peninsula, Catlins, and Stewart Island, respectively.

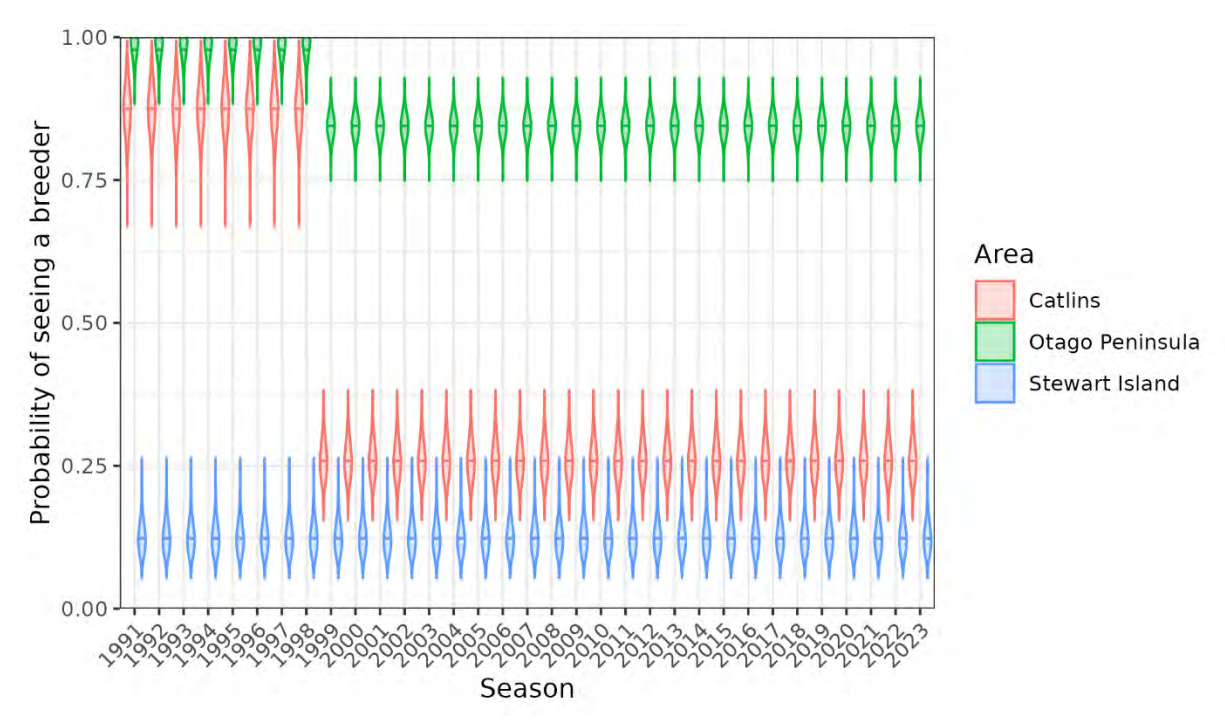


Figure B.60: Posterior distributions of the probability of a breeder being seen by season and regional sub-population, for the <u>male southern model</u> run (Otago Peninsula, Catlins, and Stewart Island).

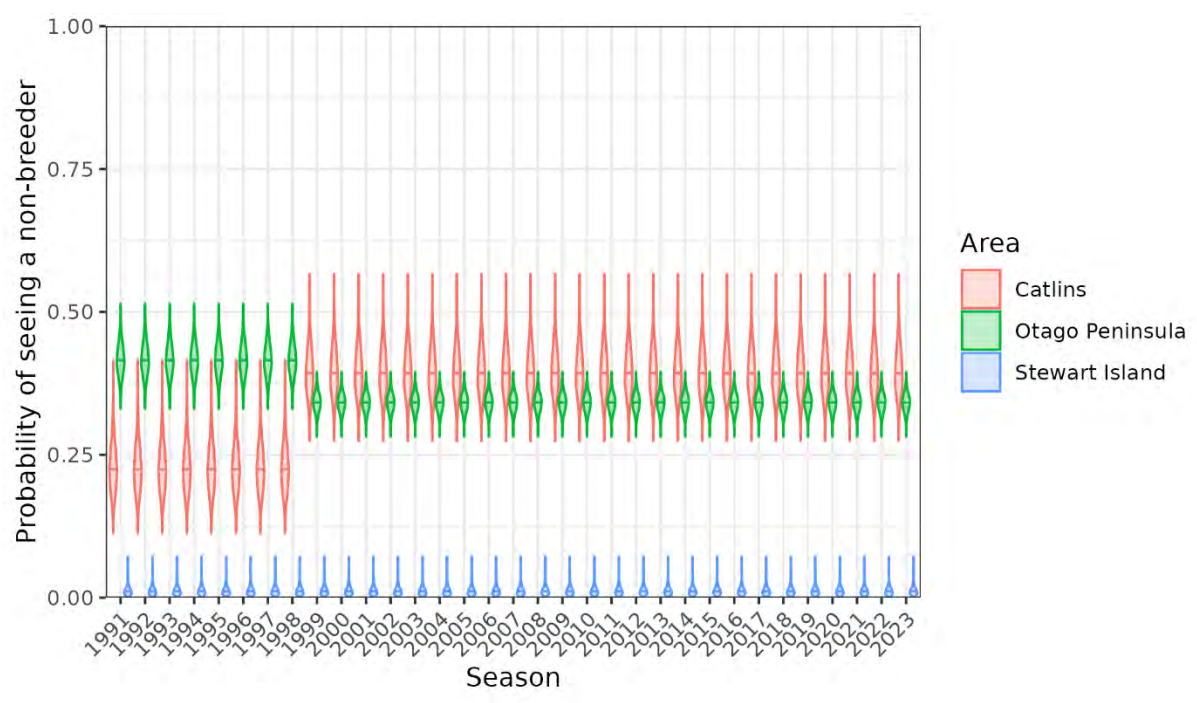


Figure B.61: Posterior distributions of the probability of a non-breeder being seen by season and regional sub-population, for the <u>male southern model</u> run (Otago Peninsula, Catlins, and Stewart Island).

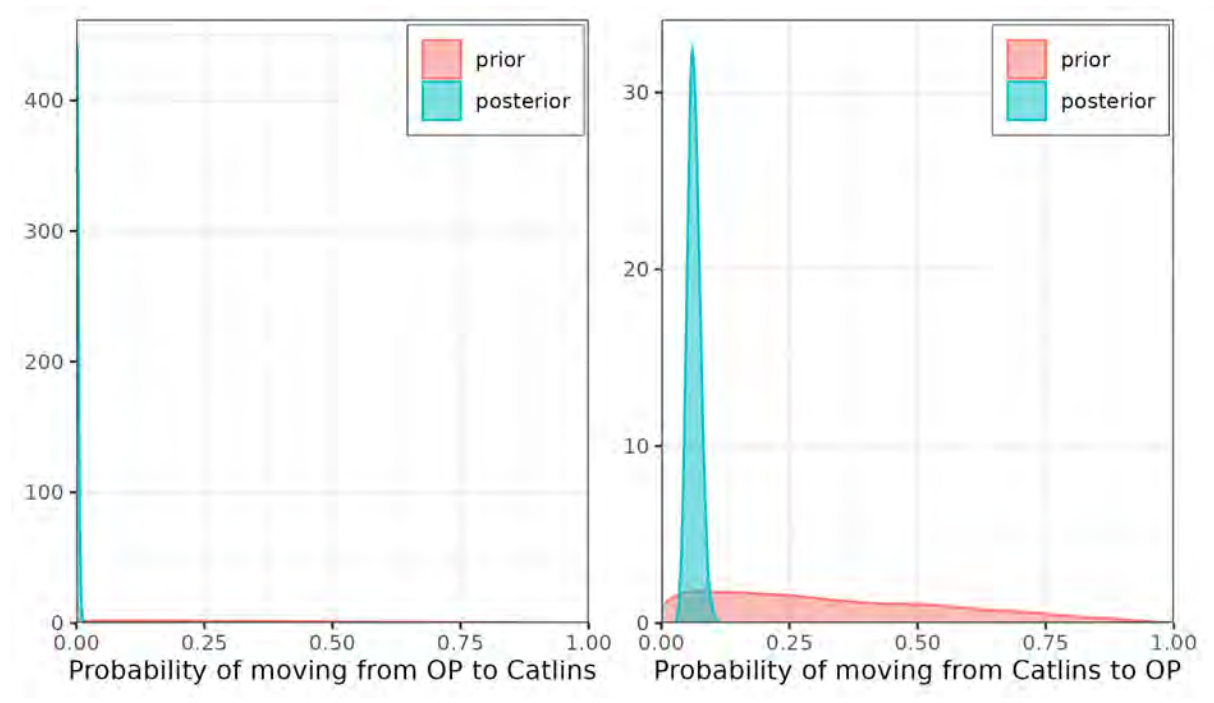


Figure B.62: Prior and posterior distributions (pink and blue polygons, respectively) of the annual probabilites of immature birds moving between regions of the <u>male southern model</u> run (Otago Peninsula, Catlins, and Stewart Island). Note that it was assumed that there was no movement of juveniles between Stewart Island and the other model regions.

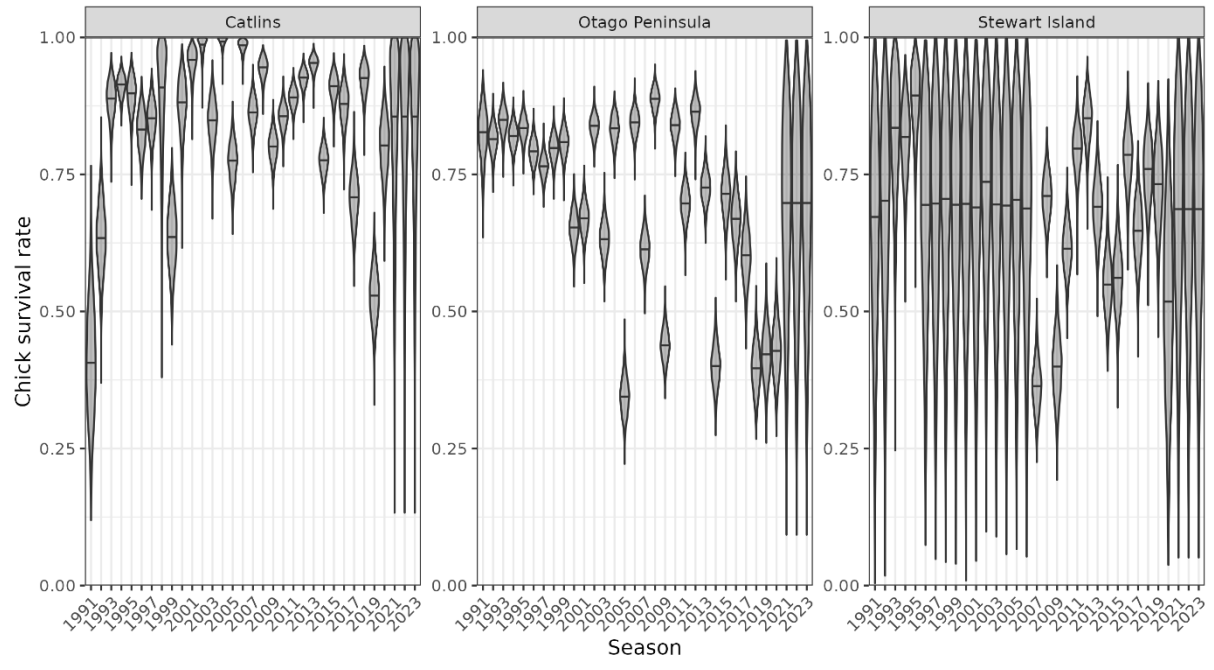


Figure B.63: Posterior distributions of the probability of chick survival (from hatching to fledgling) by season and regional sub-population, for the <u>male southern model</u> run (Otago Peninsula, Catlins, and Stewart Island).

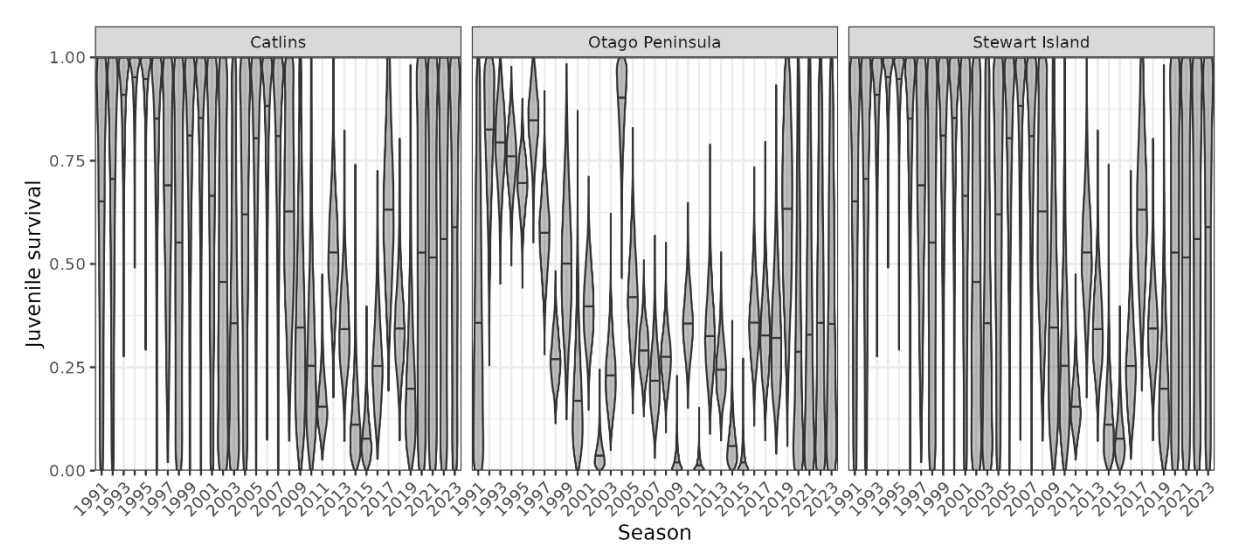


Figure B.64: Posterior distributions of the probability of juvenile survival (from fledgling to the following year) by season and regional sub-population, for the <u>male southern model</u> run (Otago Peninsula, Catlins, and Stewart Island). Note that these were assumed to be the same across both regions. Note that these were assumed to be the same for Catlins and Stewart Island.

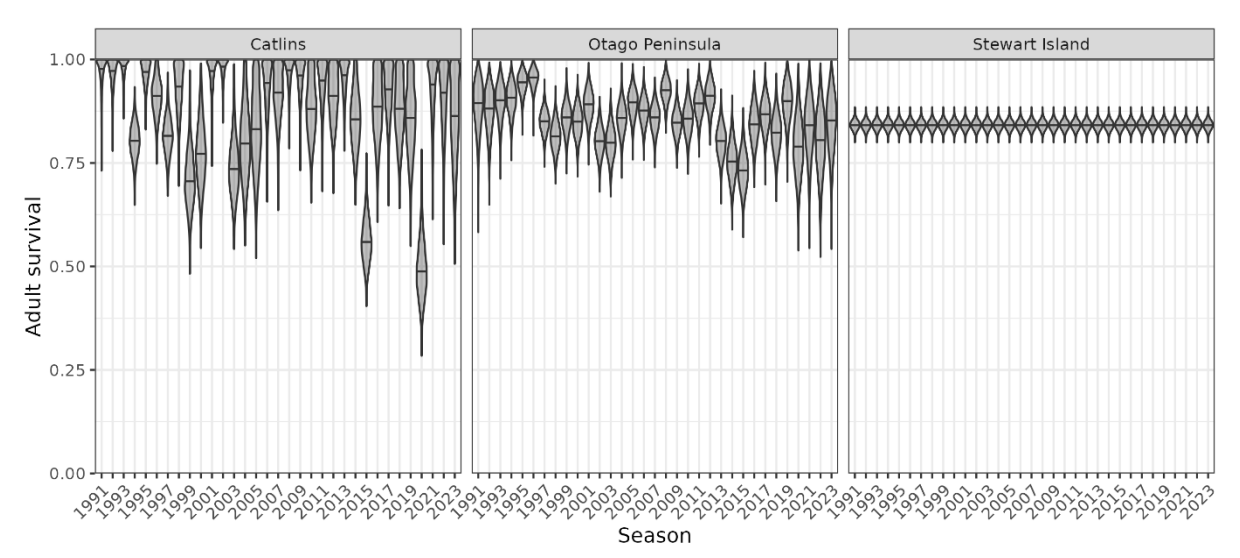


Figure B.65: Posterior distributions of the probability of adult survival by season and regional sub-population, for the <u>male southern model</u> run (Otago Peninsula, Catlins, and Stewart Island).

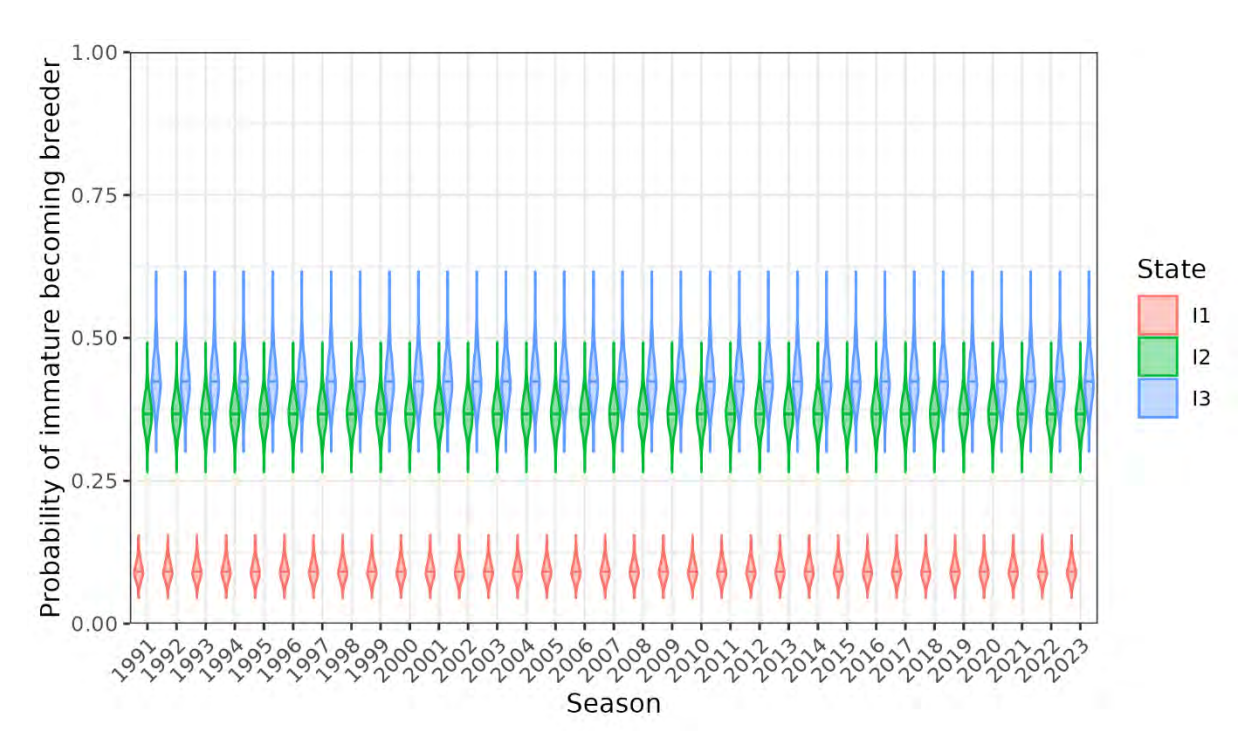


Figure B.66: Posterior distributions of the annual probabilities of immature birds at ages 1 (I1), 2 (I2), and 3 (I3) becoming breeders at the following ages, for the <u>male southern model</u> run (Otago Peninsula, Catlins, and Stewart Island).

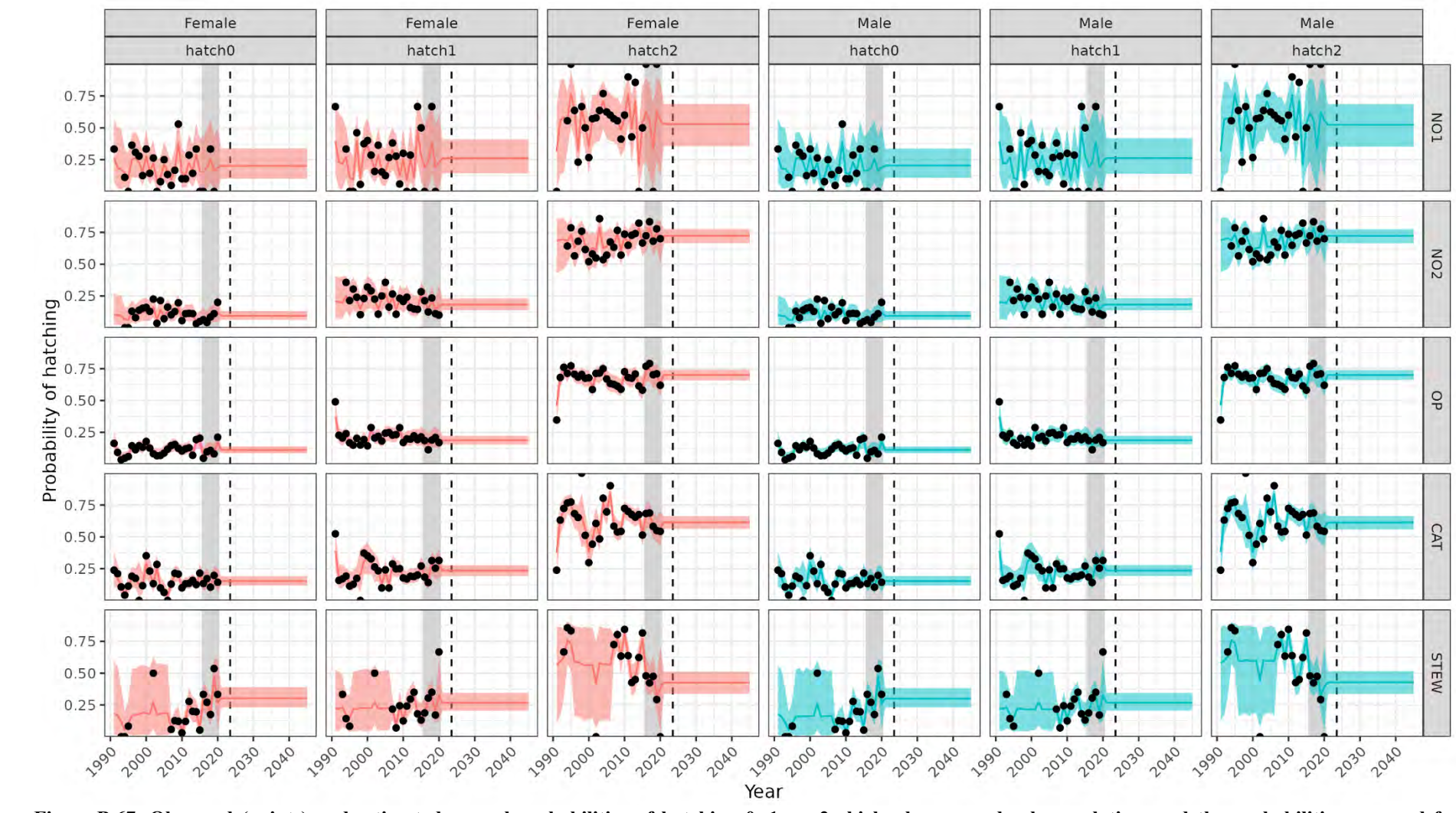


Figure B.67: Observed (points) and estimated annual probabilities of hatching 0, 1, or 2 chicks, by sex and sub-population, and the probabilities assumed for population projections, which was based on the mean and standard deviation of model estimates from 2016–2020, highlighted using dashed lines (solid lines represent median values and shaded areas represent the 95% credible intervals). The future survival rates shown here are without the alleviation of future rates. Note that the rates are effectively the same for females and males, because the nest data on fledgling rates could not be resolved by sex.

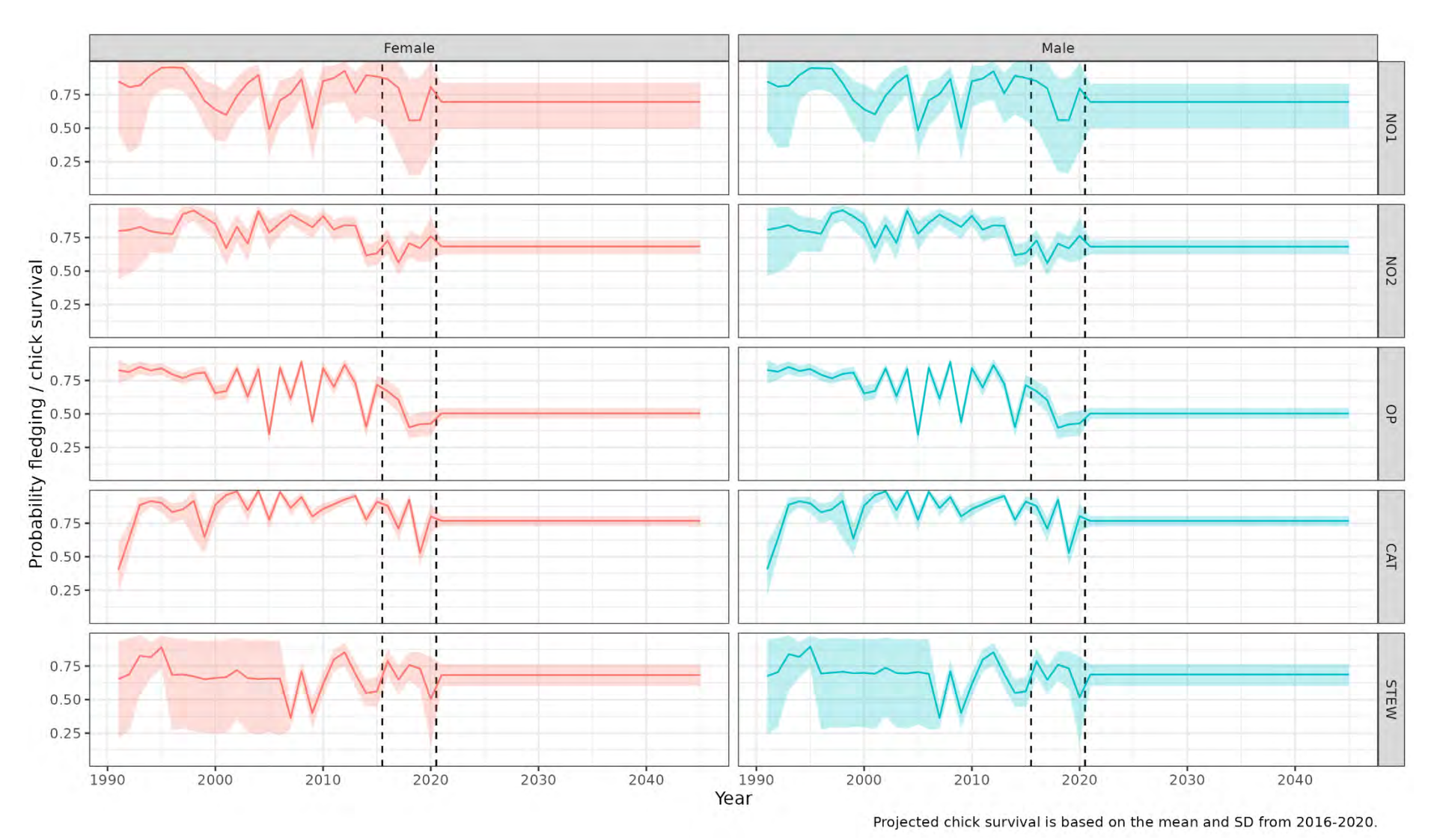


Figure B.68: Annual chick survival probabilities estimated by sex and sub-population, and the respective probabilities assumed for population projections, which was based on the mean and standard deviation of model estimates from 2016–2020, highlighted using dashed lines (solid lines represent median values and shaded areas represent the 95% credible intervals). The future survival rates shown here are without the alleviation of future rates. Note that the rates are effectively the same for males and females, because the nest data on fledgling rates could not be resolved by sex.

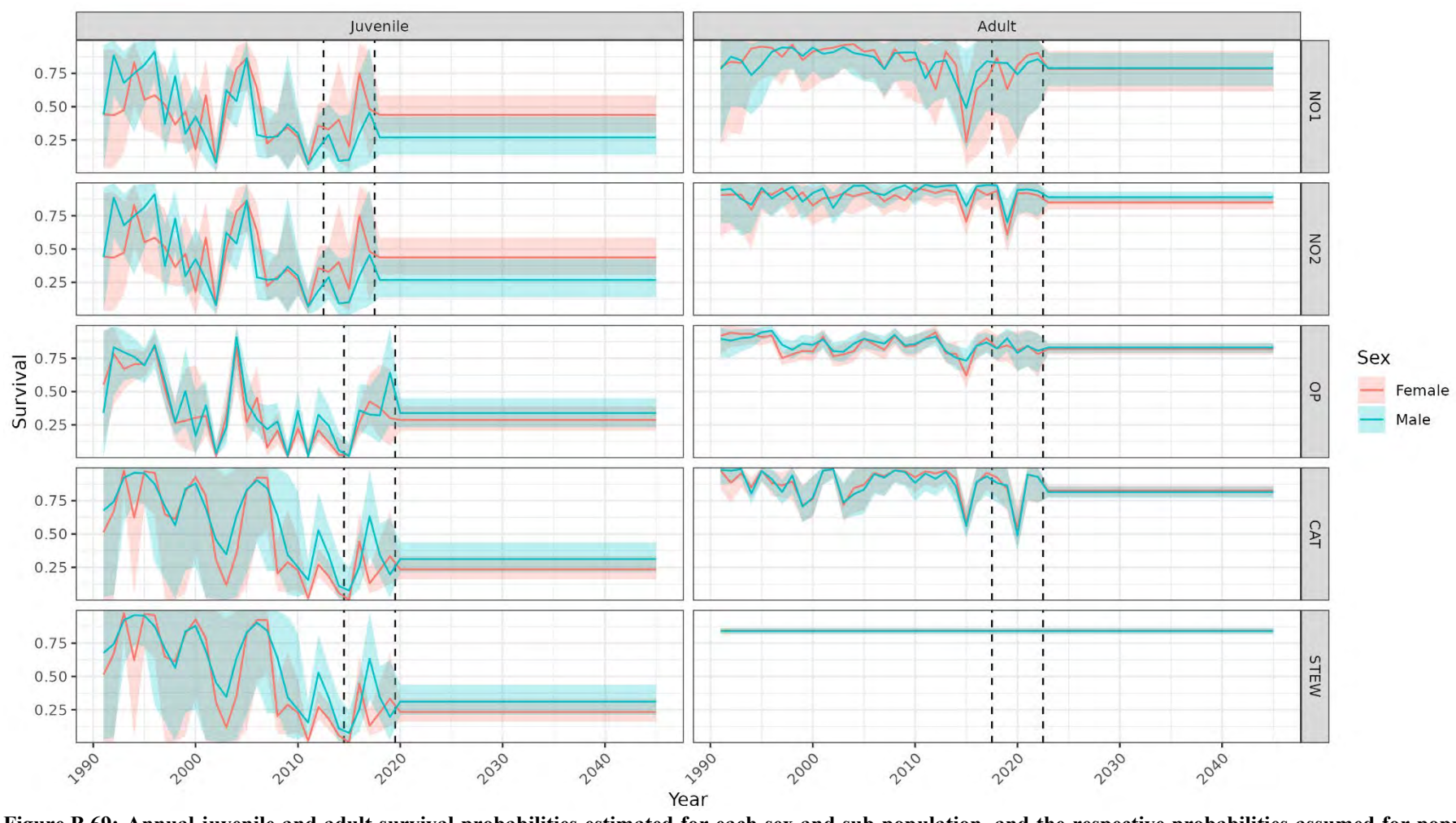


Figure B.69: Annual <u>juvenile and adult</u> survival probabilities estimated for each sex and sub-population, and the respective probabilities assumed for population projections. Projected juvenile survival was based on the mean and standard deviation of model estimates from 2013–2017 (North Otago 1 and 2) or 2015–2019 (Otago Peninsula, Catlins, and Stewart Island) and projected adult survival was based on the mean and standard deviation of estimates from 2018–2022 (all sub-populations), highlighted using dashed lines (solid lines represent median values and shaded areas represent the 95% credible intervals). The future survival rates shown here are without the alleviation of future rates.

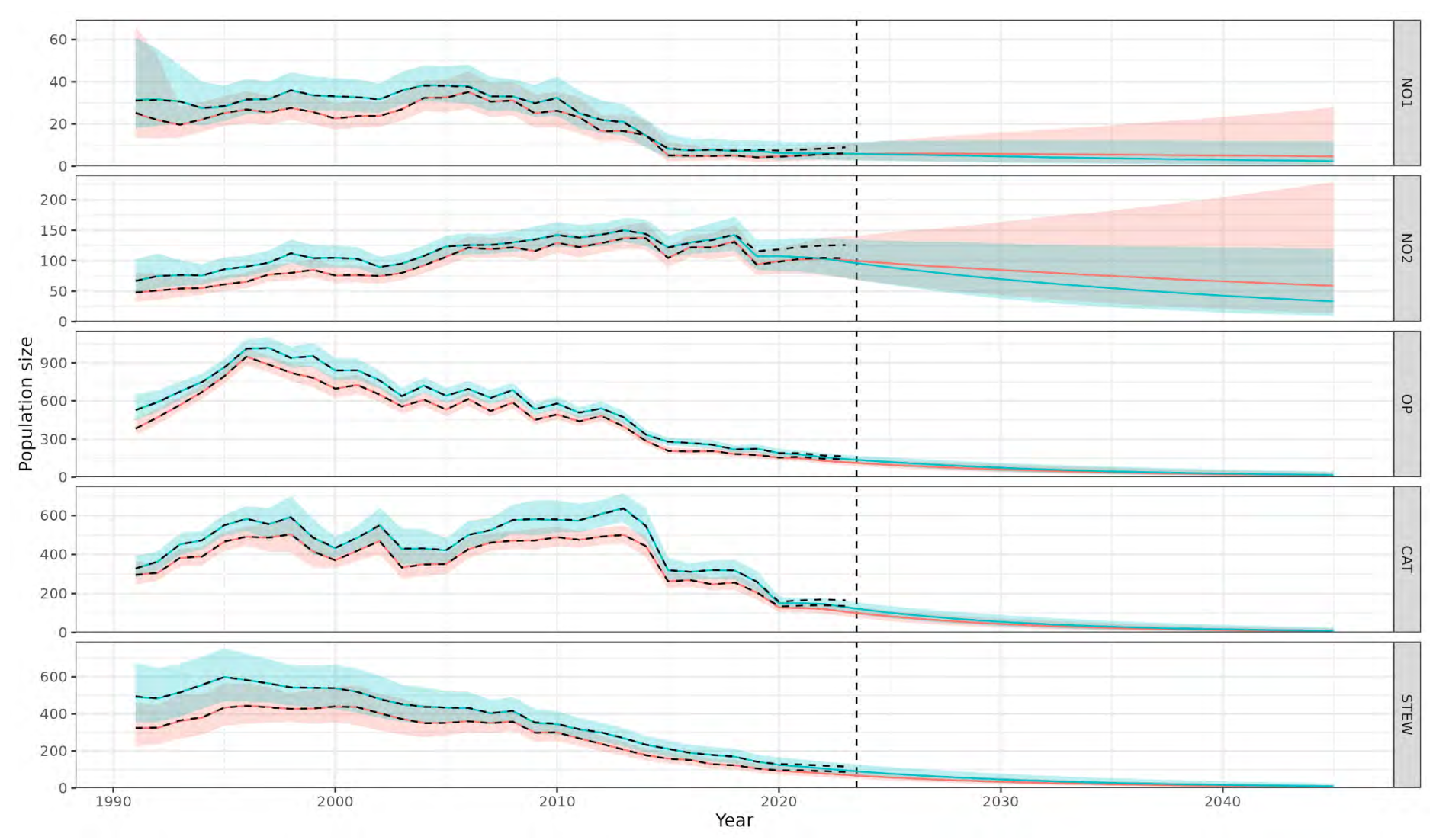


Figure B.70: Estimated and projected total population size (number of individuals) by sex and sub-population (solid lines represent median values and shaded areas represent the 95% credible intervals, dashed lines represent the median from the model as a cross check). The projected population size estimates (to the right of the dashed lines) shown here are without the alleviation of future mortality rates.

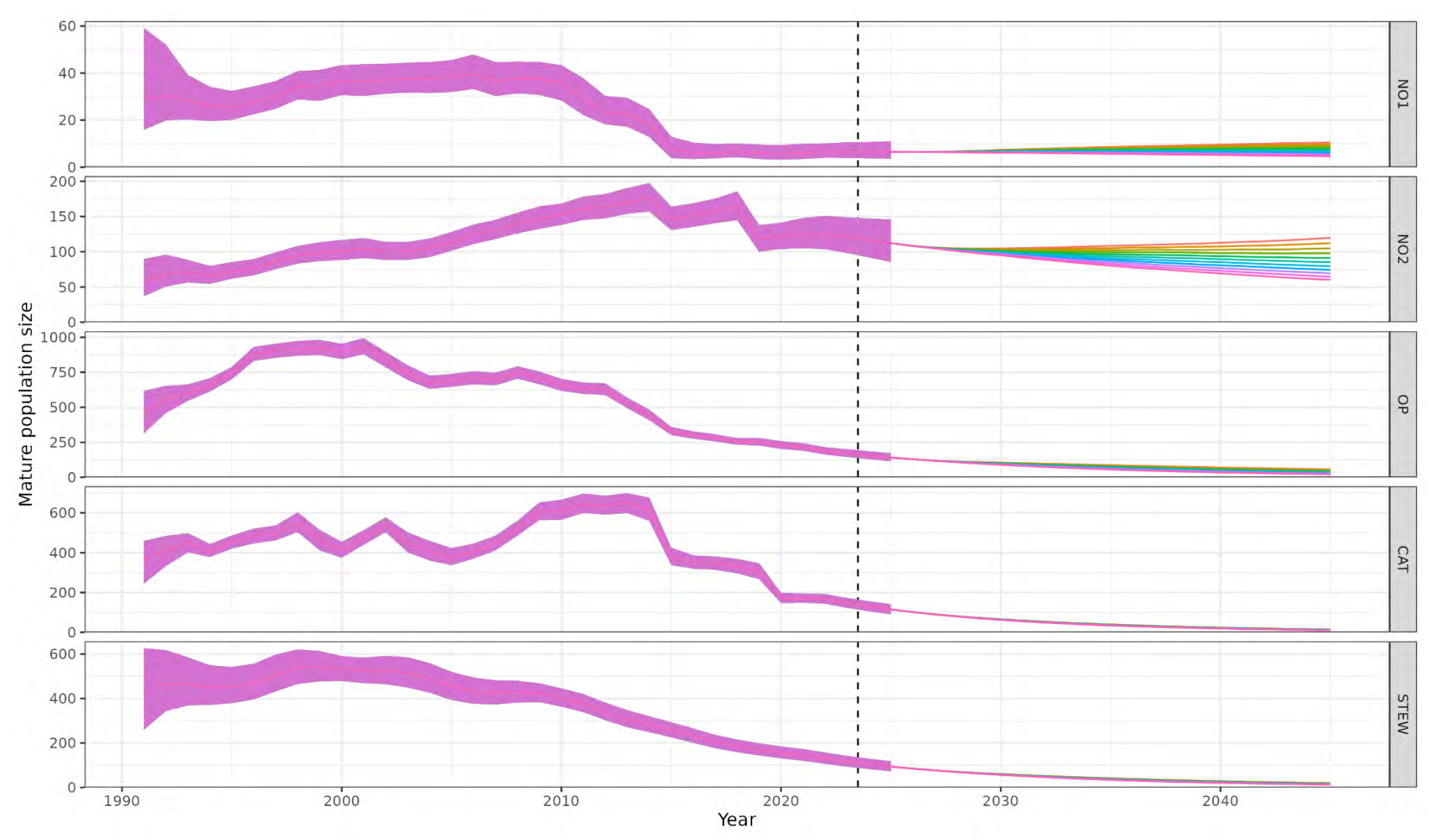


Figure B.71: Predicted mature population size by sub-population assuming alternative future levels of chick mortality rate, ranging from 0% alleviation of recent rates (the bottom projection line) up to 100% alleviation (the top projection line) in 10% increments. The shaded period up to 2025 represents the 95% credible interval of the combined predictions of the male and female models.

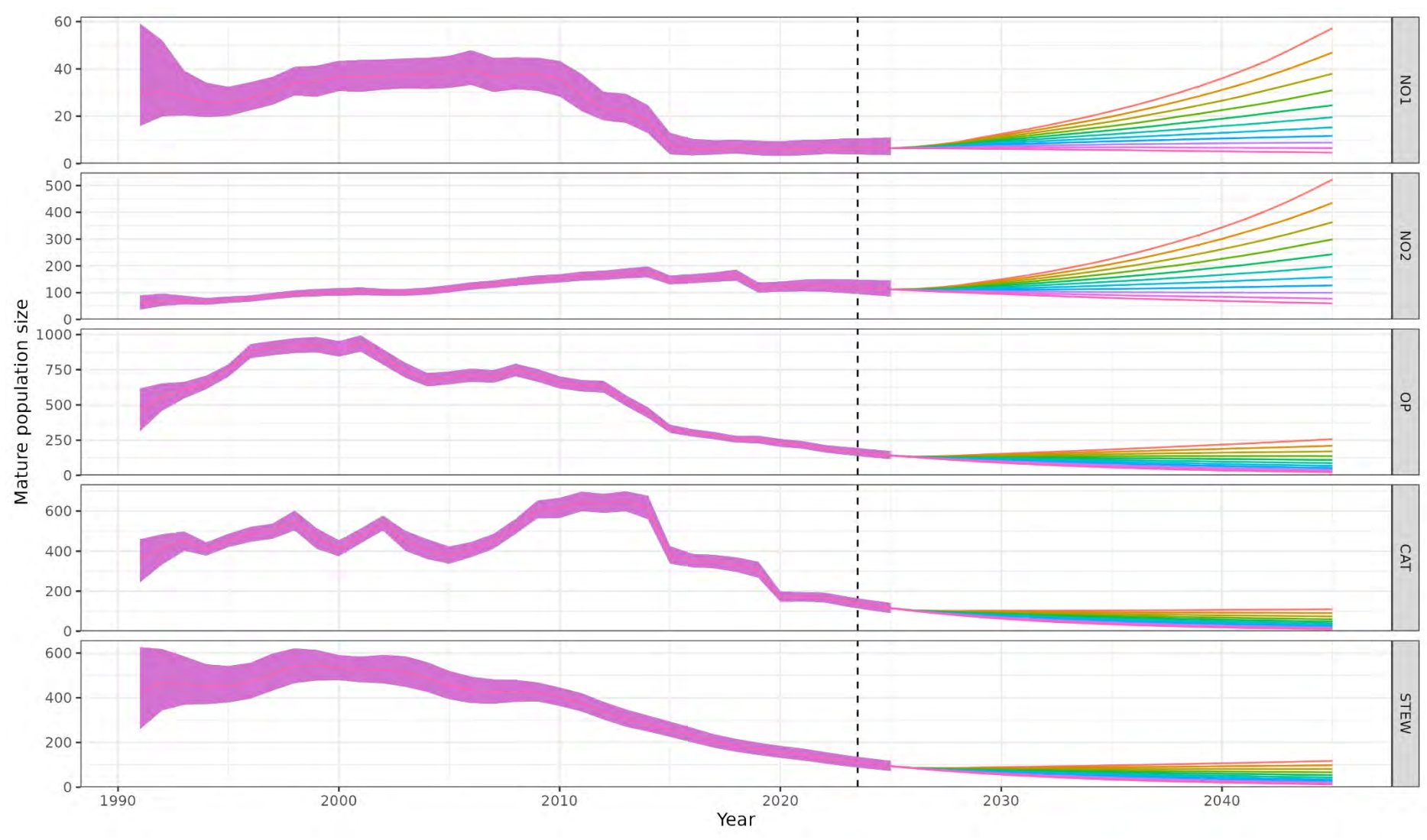


Figure B.72: Predicted mature population size by sub-population assuming alternative future levels of <u>juvenile mortality</u> rate, ranging from 0% alleviation of recent rates (the bottom projection line) up to 100% alleviation (the top projection line) in 10% increments. The shaded period up to 2025 represents the 95% credible interval of the combined predictions of the male and female models.

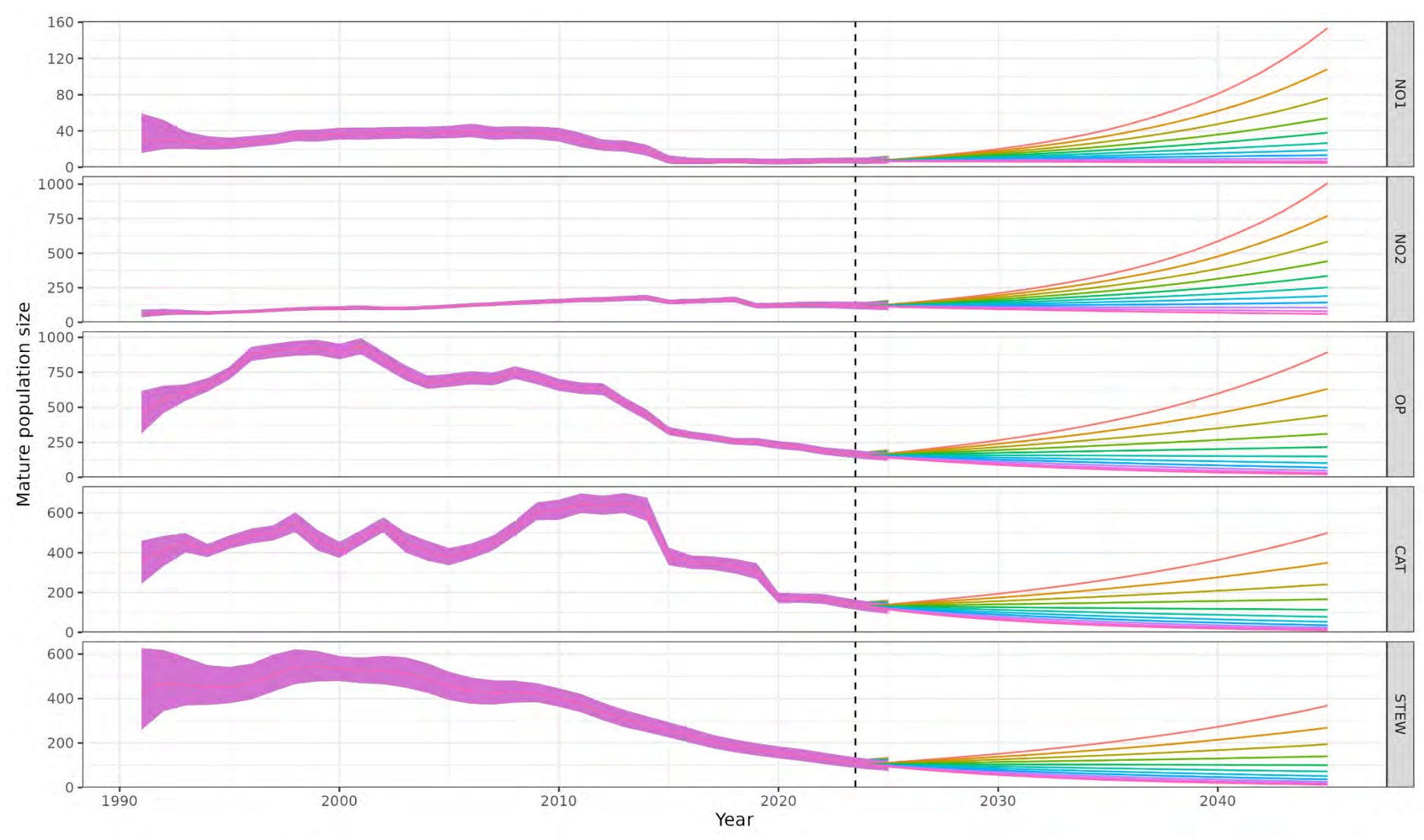


Figure B.73: Predicted mature population size by sub-population assuming alternative future levels of <u>adult mortality</u> rate, ranging from 0% alleviation of recent rates (the bottom projection line) up to 100% alleviation (the top projection line) in 10% increments. The shaded period up to 2025 represents the 95% credible interval of the combined predictions of the male and female models.

Appendix C. VALIDATION OF STAN POPULATION MODEL USING SEABIRD

An early version of the bespoke *Stan* demographic population model was also done using *Seabird* (Francis & Sagar 2012), to check that the bespoke model was performing as expected with respect to the estimation of model parameters.

The interim models had the same model states as the models used in the final analysis (Table 2) and the same transitions, although only used observations of females from the Otago Peninsula regional sub-population and, so, did not include movement of immature birds. Other differences from the final models described in Section 3 include:

- not estimating annual hatching and fledging rates or chick survival and, instead, specifying the
 annual number of recruits (in terms of fledglings rather than hatchlings) as the number of
 breeders times 1.2 (approximating to the average number of fledged birds per nest across all
 years at Otago Peninsula);
- using an odds multiplier (e.g., Francis & Sagar 2012) to specify the maturation rate of birds at ages 1, 2, and 3 (i.e., the probability that they would breed first at ages 2, 3, and 4, respectively), instead of estimating these rates as independent parameters;
- using year blocks for survival (instead of estimating separate values of each year), and maturation/breeding rate parameters (instead of assuming these were constant with respect to year); and
- starting models in 1987 instead of 1991, and using mark-recapture data for birds banded since 1987.

MCMC outputs from the *Stan* model were compared with maximum posterior density (MPD) point estimates from the *SeaBird* model (Figure C.1 and Figure C.2). This was shown to a meeting of the Aquatic Environment Working Group (21 March 2023), which concluded that the agreement was good between the outputs of the *Stan* and *SeaBird* models, and that the *Stan* was behaving as expected. As such, all modelling thereafter was done using the *Stan* model and no further *SeaBird* models were developed.

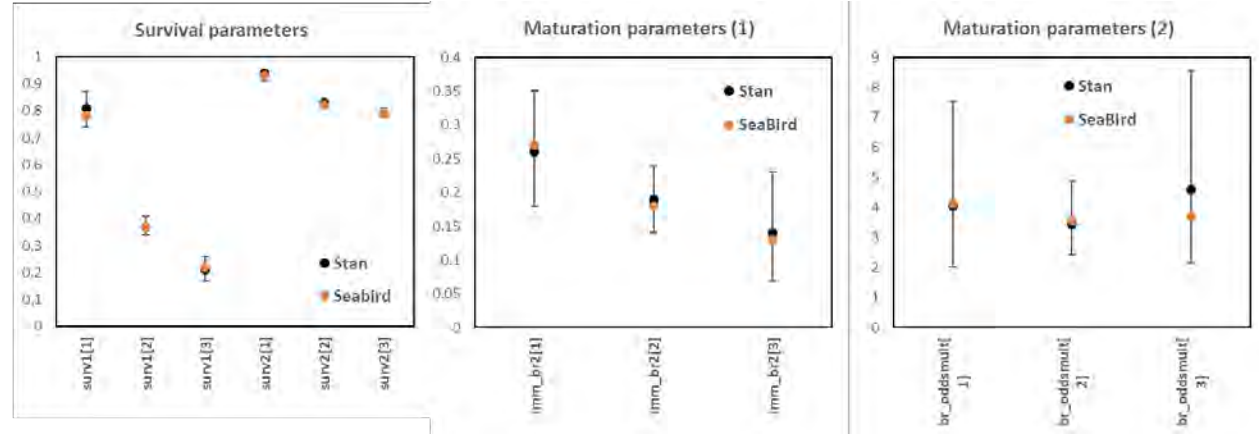


Figure C.1: Comparison of survival and maturation parameter estimates from the *Stan* (black points and whiskers represent median and 95% credible interval) and *Seabird* model (orange points represent point estimate values). Parameter label prefixes 'surv1', 'surv2' are the annual survivorship of juveniles and adults and 'br_oddsmult' is the odds multiplier for the increase in maturation rate at ages 2 and 3; the parameter label suffixes '[1]', '[2]', and '[3]' denoted year blocks for each parameter for 1987–1995, 1996–2011 and since 2012, respectively.

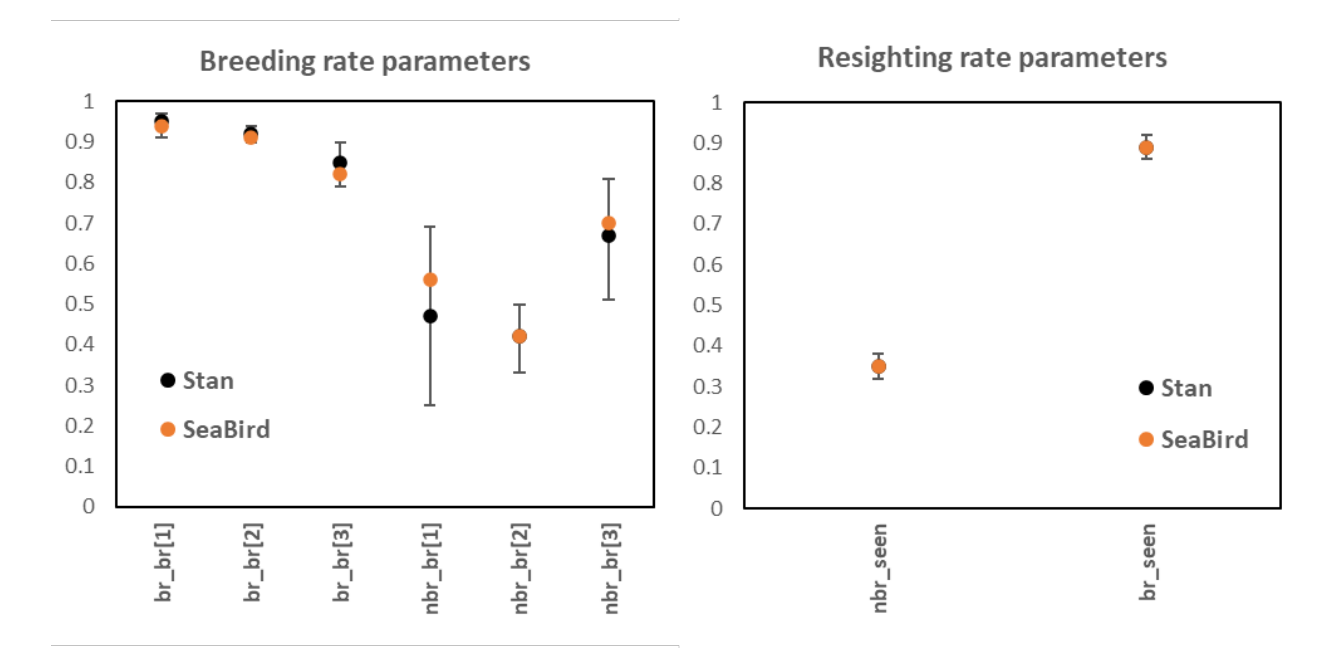


Figure C.2: Comparison of annual breeding rate and resighting probability parameter estimates from the *Stan* (black points and whiskers represent median and 95% credible interval) and *Seabird* model (orange points represent point estimate values). Parameter label prefixes 'br_br' and 'nbr_br' are the annual breeding rate of birds that bred or did not breed in the previous year; 'nbr_seen' and 'br_seen' are the annual probabilities of non-breeders and breeders being seen; the parameter label suffixes '[1]', '[2]', and '[3]' denoted year blocks for each parameter for 1987–1995, 1996–2011 and since 2012, respectively.

Appendix D. SUPPLEMENTARY TABLES & FIGURES FROM THE SEFRA ASSESSMENT

SEFRA model inputs

Table D.1: Summary table of commercial fishery captures of yellow-eyed penguin that were reported by fisheries observers. Target species are: school shark (SCH; *Galeorhinus galeus*), rig (SPO; *Mustelus lenticulatus*), blue moki (MOK; *Latridopsis ciliaris*), and elephant fish (ELE; *Callorhinchus milii*).

Fishing method	Target species	Fishing year	Month	Age	Sex	Model region
Set-net	SCH	2006-07	December	Adult	Unknown	Stewart Island
Set-net	SCH	2006-07	January	Adult	Male	Stewart Island
Set-net	SPO	2007-08	December	Adult	Female	Catlins
Set-net	SCH	2008-09	February	Adult	Male	North Otago 1
Set-net	SCH	2008-09	February	Juvenile	Female	North Otago 1
Set-net	MOK	2008-09	January	Adult	Female	North Otago 2
Set-net	SPO	2008-09	February	Adult	Female	North Otago 1
Set-net	SCH	2008-09	January	Adult	Female	Stewart Island
Set-net	SPO	2009-10	November	Adult	Female	Otago Peninsula
Set-net	SCH	2015–16	March	Adult	Male	North Otago 1
Set-net	SCH	2015-16	March	Adult	Male	North Otago 1
Set-net	SCH	2015–16	June	Adult	Male	Catlins
Set-net	SCH	2017–18	January	Adult	Male	Stewart Island
Set-net	SCH	2017–18	March	Adult	Female	Otago Peninsula
Set-net	ELE	2017–18	May	Unknown	Unknown	North Otago 1
Set-net	SCH	2018-19	May	Adult	Female	Stewart Island
Set-net	SPO	2019–20	November	Adult	Female	Otago Peninsula
Set-net	SPO	2021-22	October	Unknown	Unknown	Stewart Island
Set-net	SPO	2021-22	October	Juvenile	Male	Otago Peninsula
Set-net	SCH	2021-22	March	Juvenile	Female	North Otago 1
Set-net	SPO	2022-23	October	Adult	Male	Otago Peninsula
Set-net	SPO	2022-23	November	Adult	Male	Otago Peninsula
Set-net	SPO	2022-23	March	Adult	Female	North Otago 2
Set-net	ELE	2022-23	March	Juvenile	Male	North Otago 2

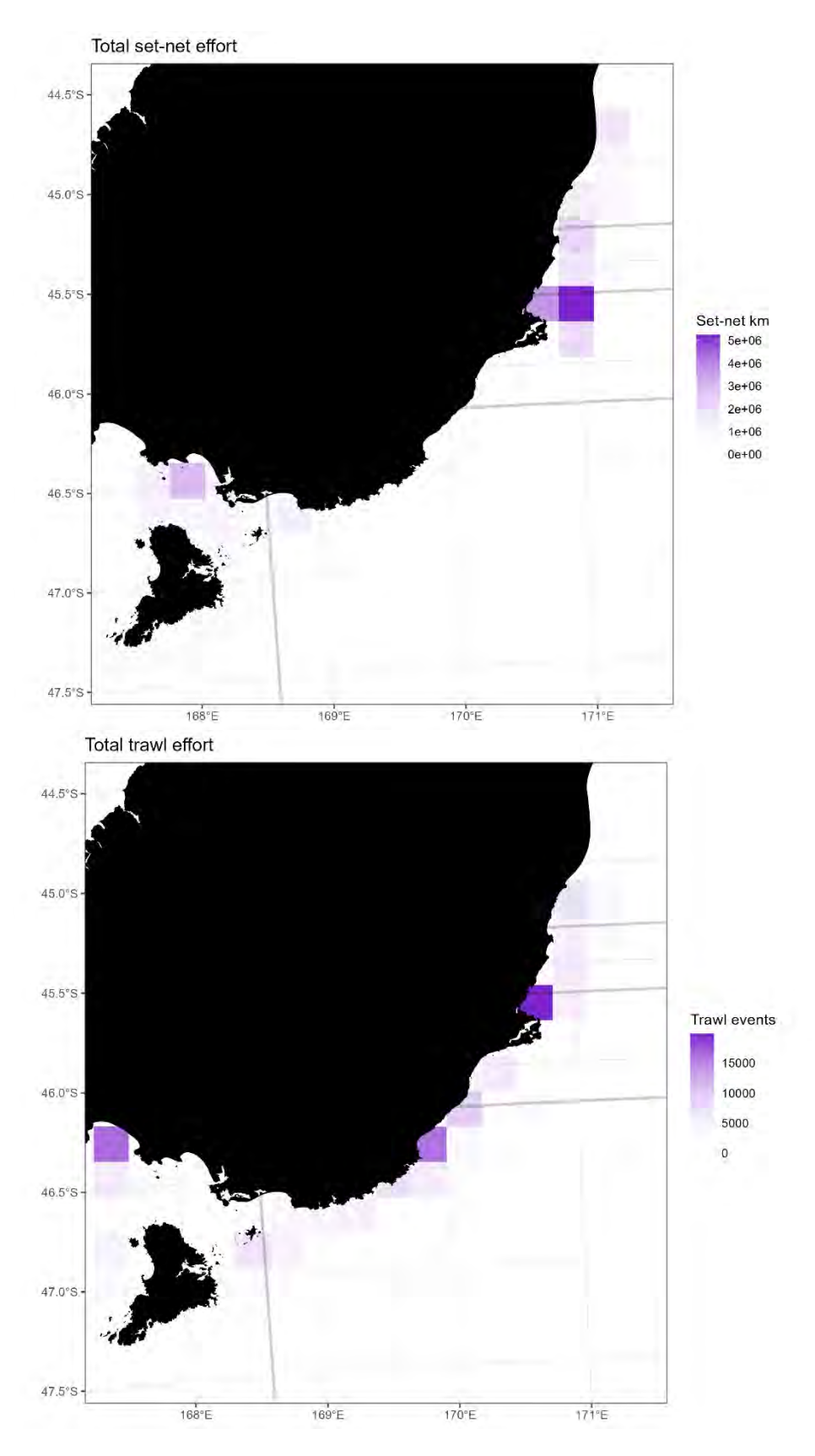


Figure D.1: Total fishing effort from 1992–93 to 2022–23 for commercial set-net (top plot) and trawls (bottom plot). Grid cells used by only 1-2 vessels were redacted to comply with Data Confidentiality rules. These cells comprised 0.0016% of the total set-net length and 0.0005% of the total trawls, respectively, inside the plot domain.

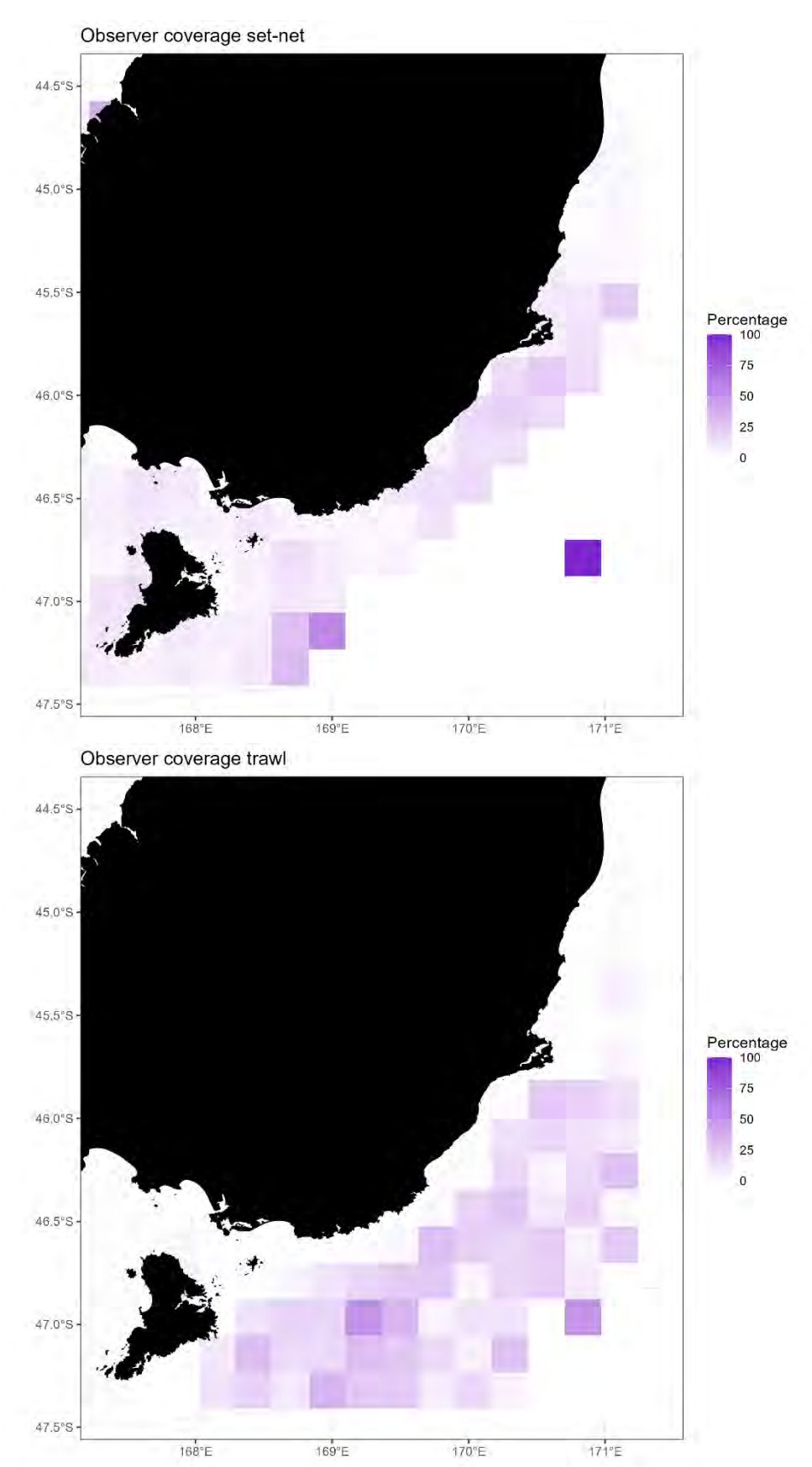


Figure D.2: Percentage coverage of fishing effort from 1992–93 to 2022–23 by fisheries observers for commercial set-net (top plot, in terms of km of set net) and trawls (bottom plot, in terms of events).

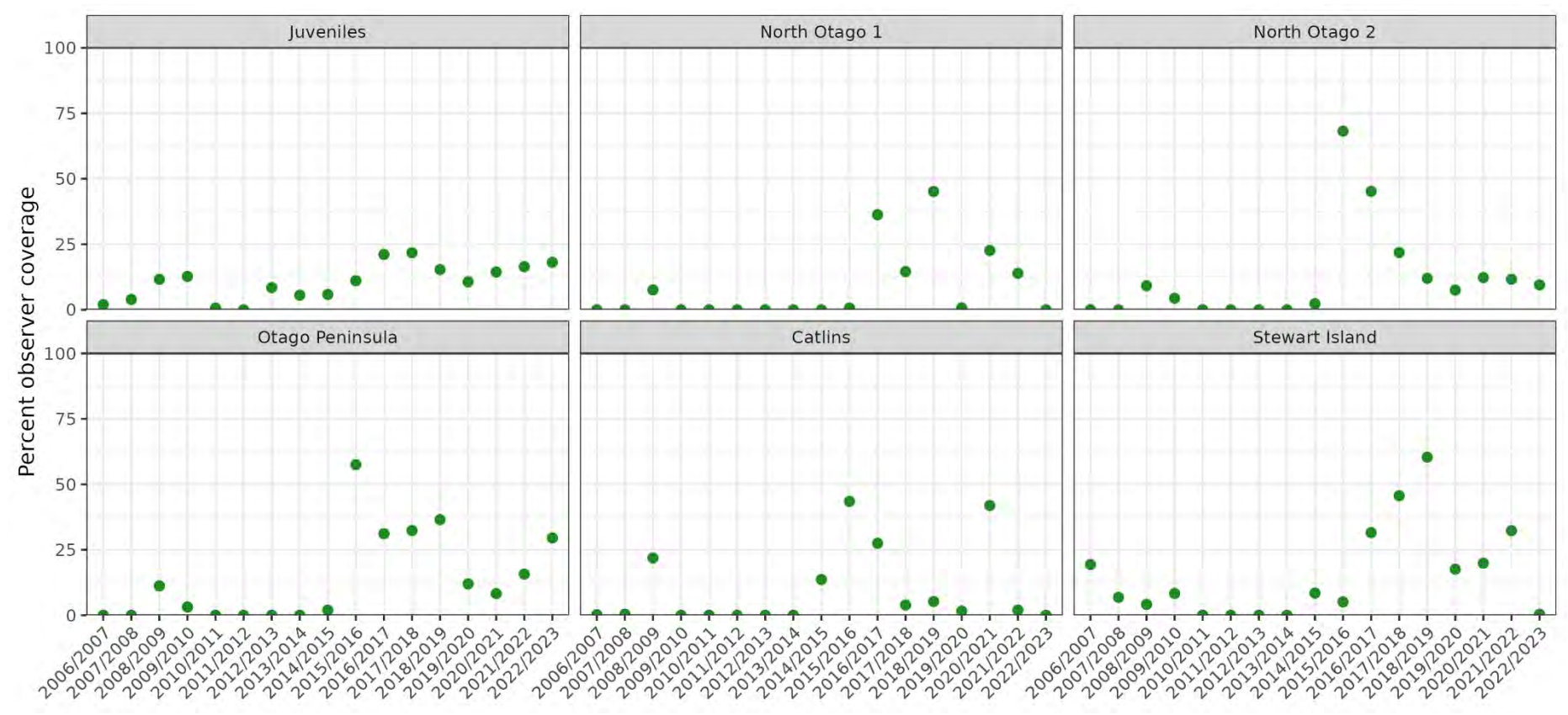


Figure D.3: Percentage coverage of commercial set-net fishing events by fisheries observers, by fishing year and age class/assessment region.

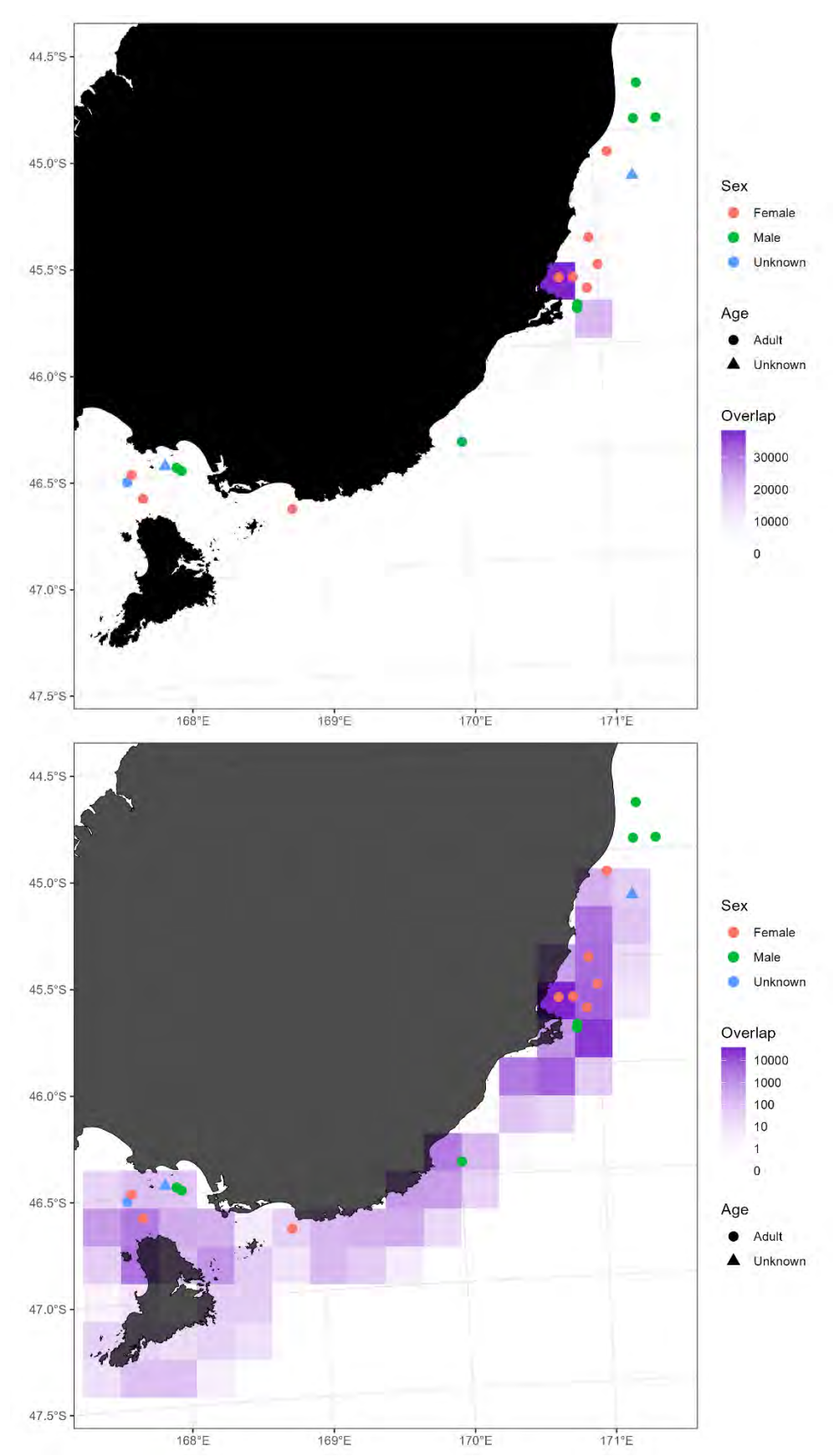
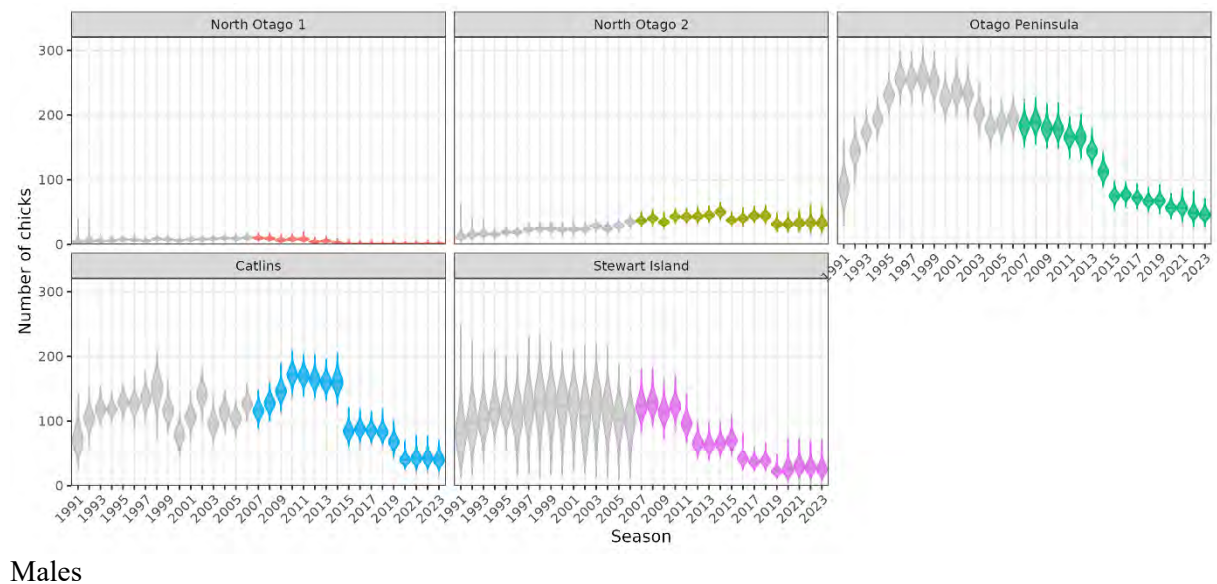


Figure D.4: The locations of adult yellow-eyed penguin captures reported by fisheries observers including males, females and individuals of unknown sex (points), and the spatial overlap of fishing events with the predicted spatial abundance of adult yellow-eyed penguins (gridded to a 20 km resolution) using a colour scale in natural space (top plot) and in log space (bottom plot).

Females



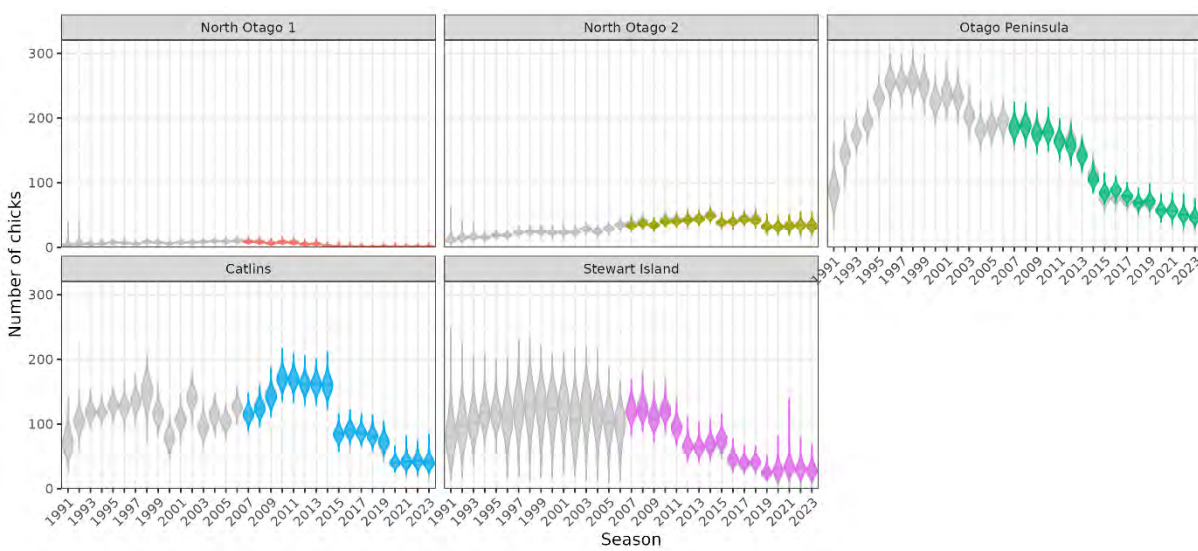
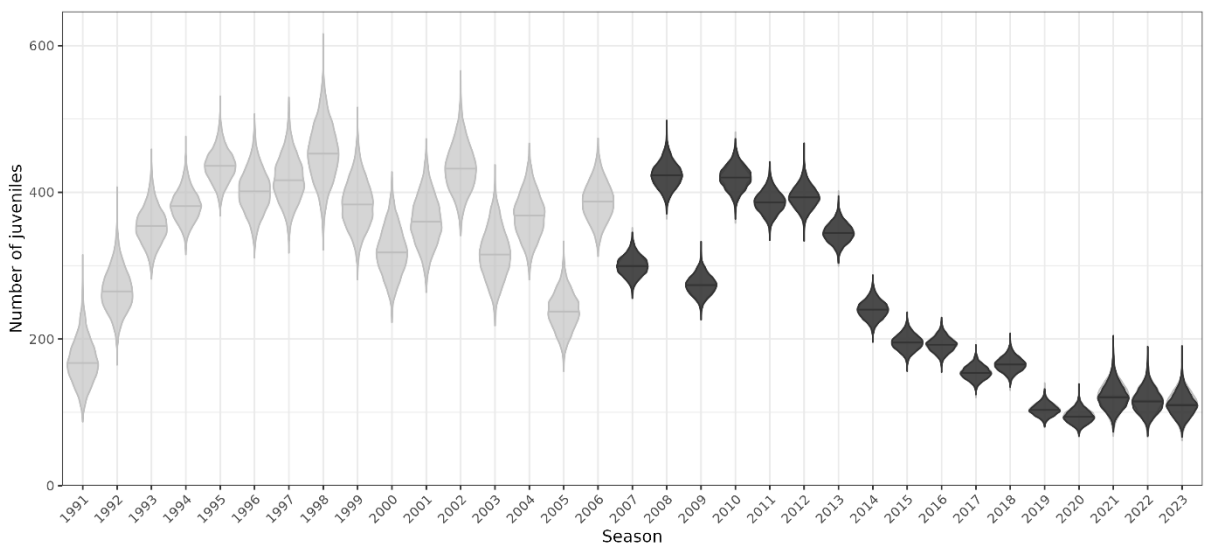


Figure D.5: Posterior distributions of the number of female (top) and male (bottom) chicks by season and region from the demographic population models (grey violins), and posterior distributions from the SEFRA model (coloured violins).





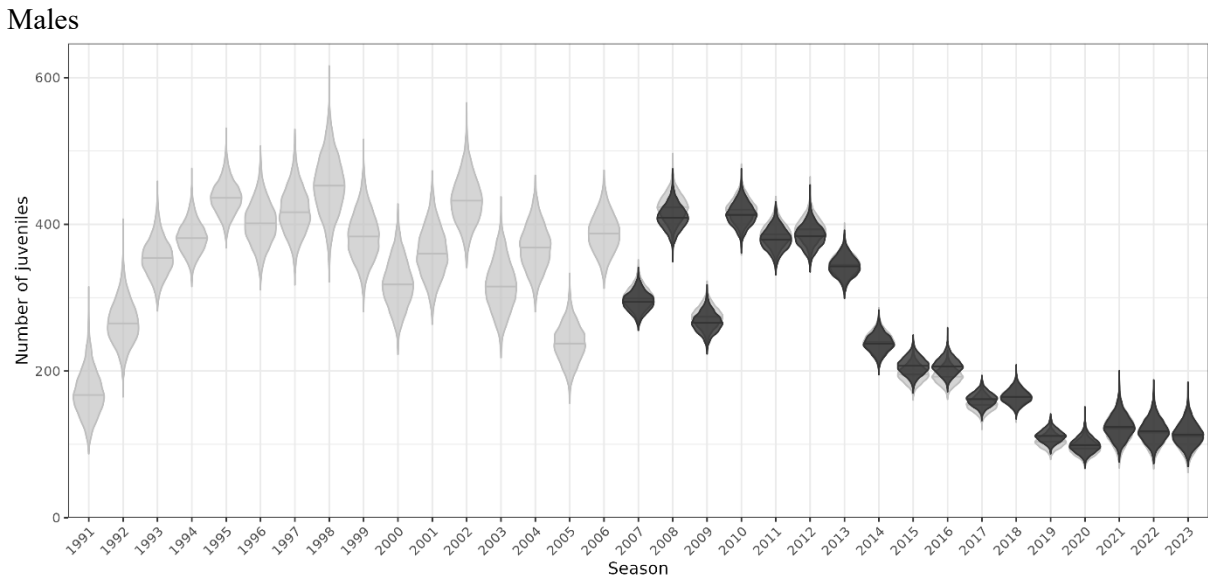
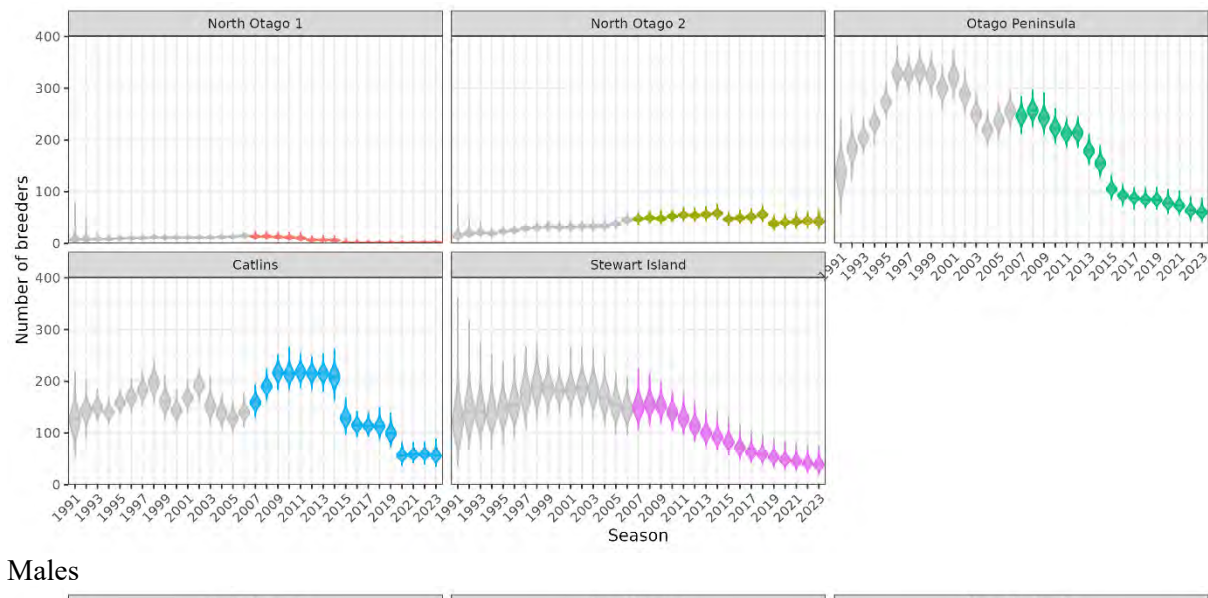


Figure D.6: Posterior distributions of the number of female (top) and male (bottom) juveniles by season from the demographic population models (light-grey violins), and posterior distributions from the SEFRA model (dark-grey violins).

Females



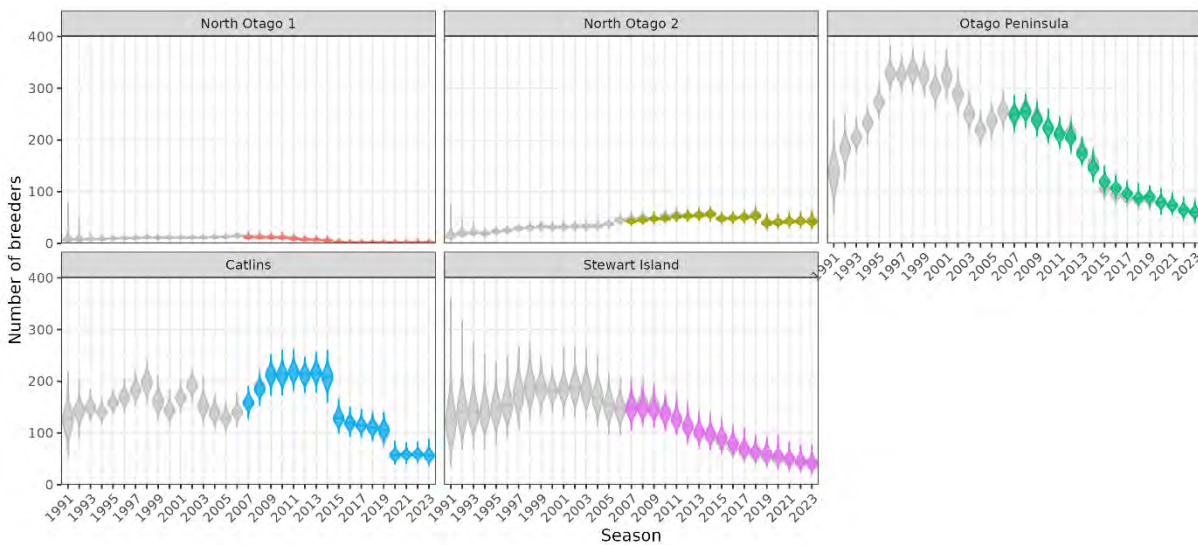
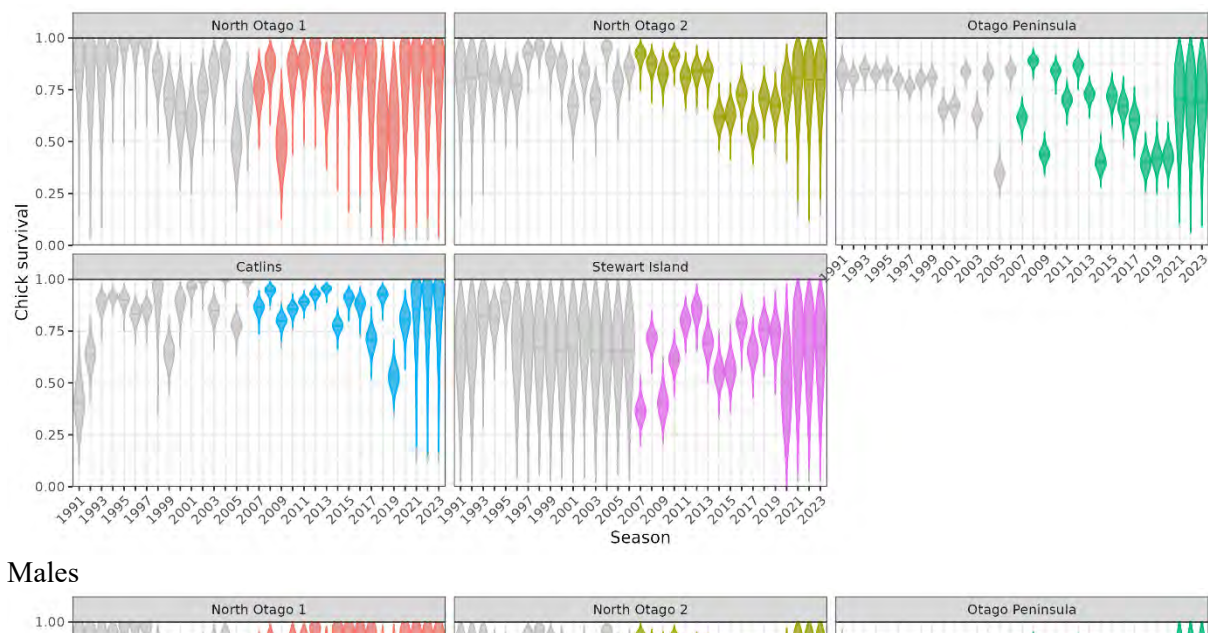


Figure D.7: Posterior distributions of the number of female (top) and male (bottom) non-breeders by season and region from the demographic population models (grey violins), and posterior distributions from the SEFRA model (coloured violins).





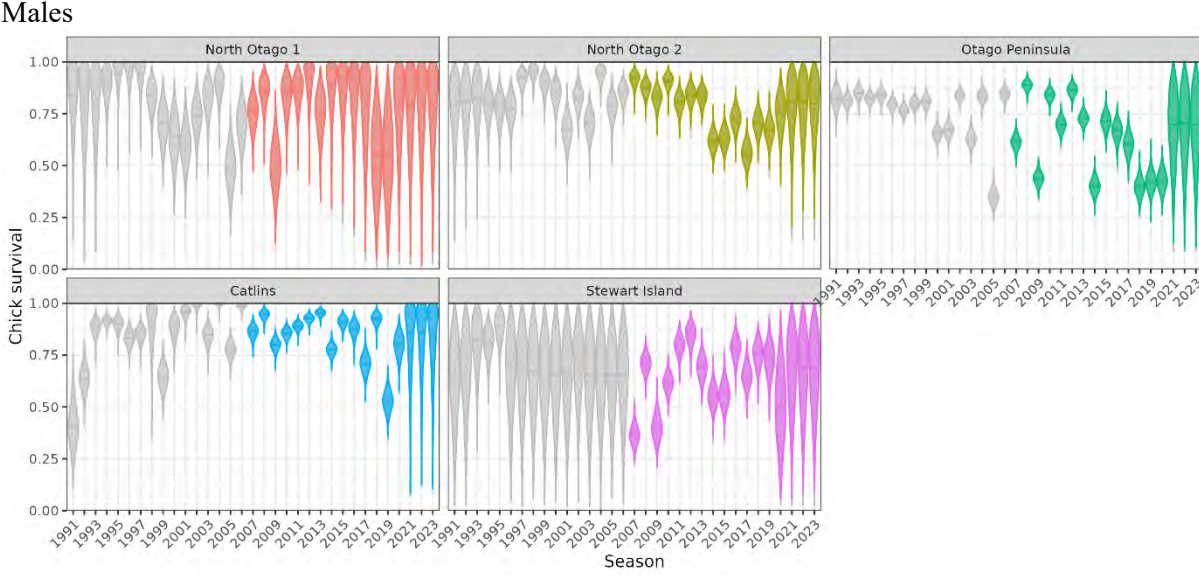
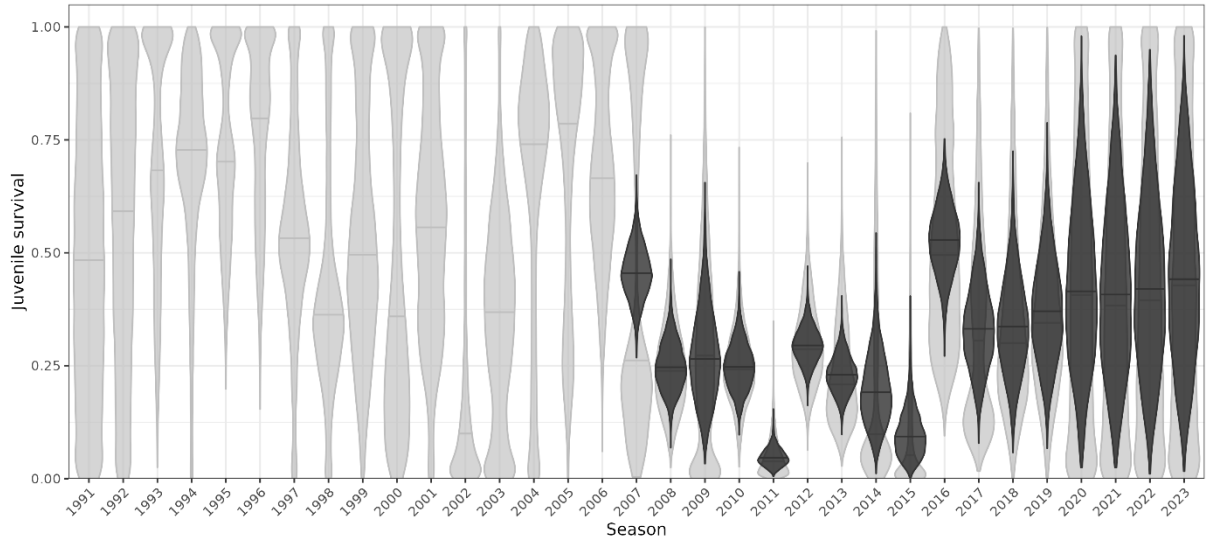


Figure D.8: Posterior distributions of chick survival by season and region from the female demographic population models (grey violins), and posterior distributions from the SEFRA model (coloured violins).





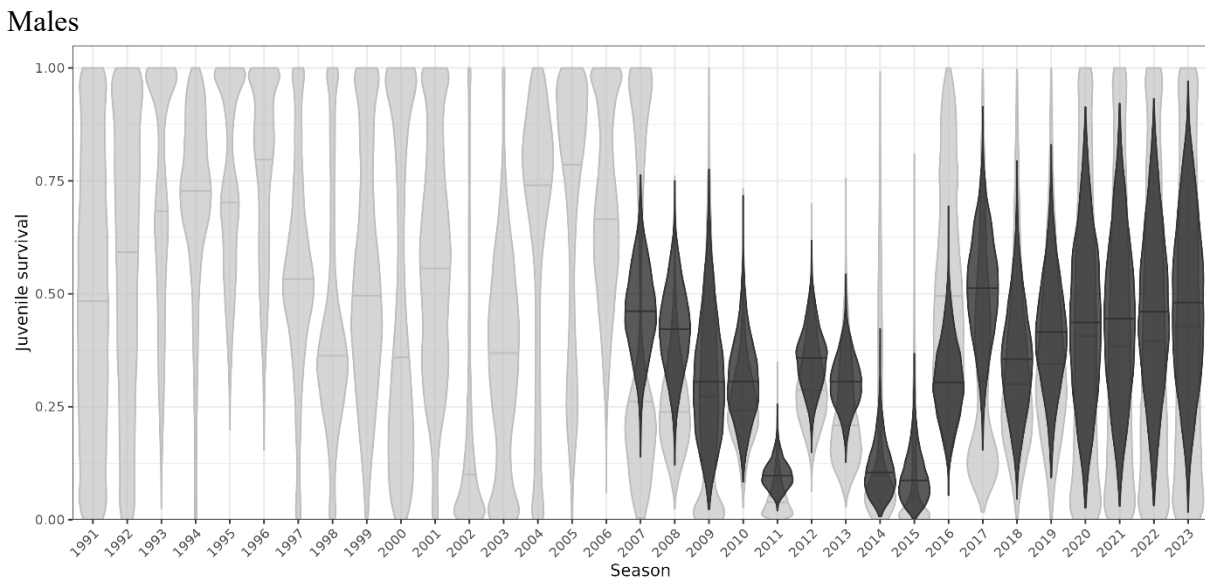


Figure D.9: Posterior distributions of juvenile survival by season from the female (top) and male (bottom) demographic population models (light-grey violins), and posterior distributions from the SEFRA model (dark-grey violins).



0.50

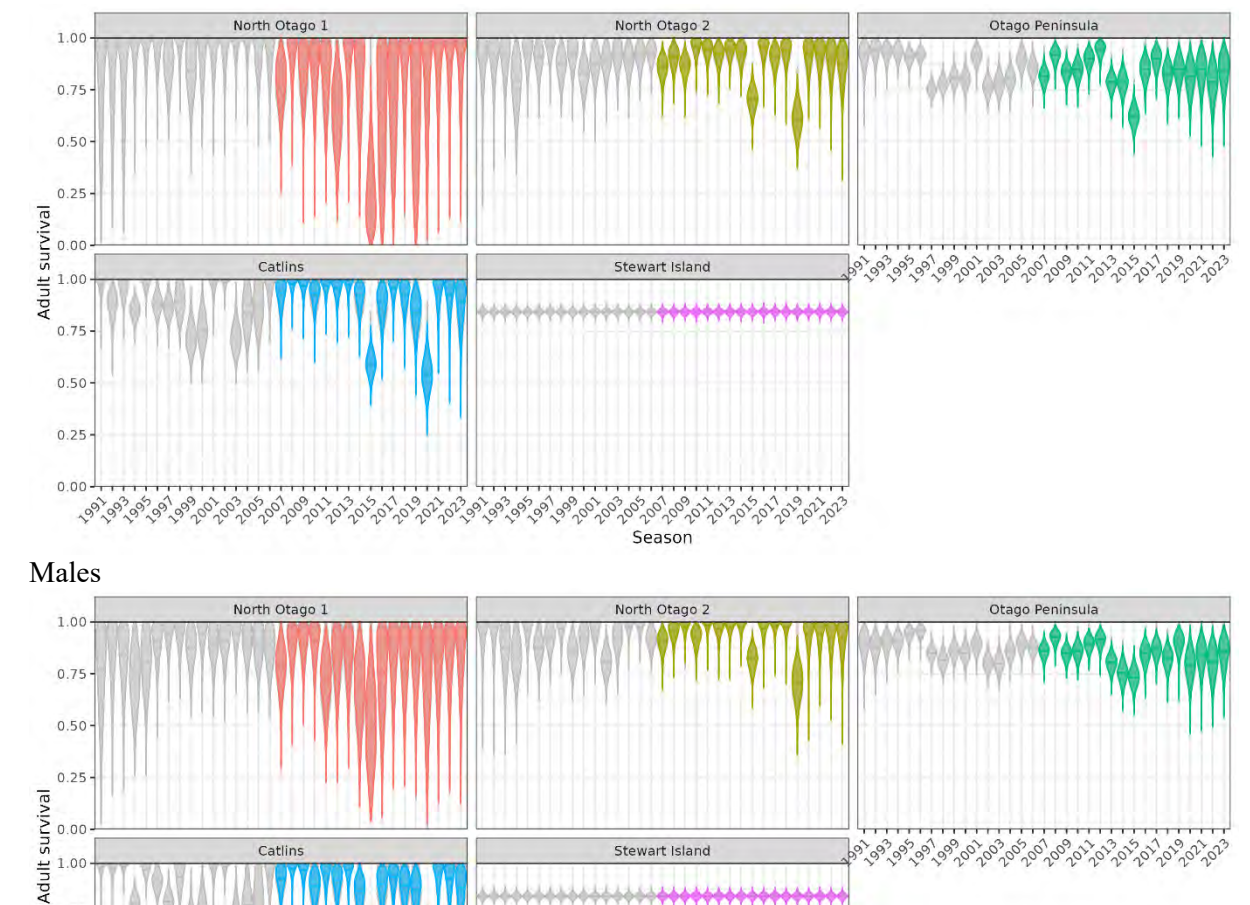


Figure D.10: Posterior distributions of the annual survival of females (top) and males (bottom) adults by season and region from the demographic population models (grey violins), and posterior distributions from the SEFRA model (coloured violins).

SEFRA model outputs

Table D.2: Summary of parameter estimates from the <u>reference</u> run of the SEFRA model for <u>females</u>.

Label	Parameter	Mean	2.5%	Median	97.5%	Effective N	Rhat
q_zg[1,1]	$q_{z,g}$	0.081	0.010	0.068	0.227	3 895	0.999
q_zg[1,2]	$q_{z,g}$	0.003	0.000	0.000	0.026	3 792	1.001
q_zg[2,1]	$q_{z,g}$	0.109	0.049	0.105	0.189	3 847	1.000
q_zg[2,2]	$q_{z,g}$	0.001	0.000	0.000	0.006	3 751	1.000
p observable m[1]	$p_g^{ m obs}$	0.750	0.501	0.760	0.929	4 241	1.001
p observable m[2]	$p_g^{ m obs}$	0.778	0.565	0.788	0.931	3 985	1.000
rmax	r^{\max}	0.140	0.134	0.140	0.145	4 138	1.000
p_necropsy_chick_k[1]	$ ho_{z,k}$	0.555	0.398	0.556	0.708	3 789	0.999
p_necropsy_chick_k[2]	$ ho_{z,k}$	0.169	0.067	0.161	0.310	3 720	1.000
p_necropsy_chick_k[3]	$ ho_{z,k}$	0.111	0.031	0.105	0.233	3 615	1.000
p_necropsy_chick_k[4]	$ ho_{z,k}$	0.082	0.019	0.074	0.188	3 375	1.001
p_necropsy_chick_k[5]	$ ho_{z,k}$	0.083	0.018	0.077	0.189	3 533	1.000
p_necropsy_juv_k[1]	$ ho_{z,k}$	0.501	0.285	0.500	0.713	3 967	1.000
p_necropsy_juv_k[2]	$ ho_{z,k}$	0.100	0.014	0.088	0.263	3 677	1.000
p_necropsy_juv_k[3]	$ ho_{z,k}$	0.199	0.058	0.189	0.399	3 994	1.000
p_necropsy_juv_k[4]	$ ho_{z,k}$	0.101	0.014	0.088	0.260	3 928	1.001
p_necropsy_juv_k[5]	$ ho_{z,k}$	0.099	0.012	0.087	0.263	3 909	1.000
p_necropsy_adult_k[1]	$ ho_{z,k}$	0.269	0.123	0.264	0.448	3 680	0.999
p_necropsy_adult_k[2]	$ ho_{z,k}$	0.076	0.010	0.066	0.204	3 689	1.000
p_necropsy_adult_k[3]	$ ho_{z,k}$	0.384	0.206	0.382	0.566	3 588	1.000
p_necropsy_adult_k[4]	$ ho_{z,k}$	0.078	0.010	0.068	0.205	3 610	0.999
p_necropsy_adult_k[5]	$ ho_{z,k}$	0.193	0.067	0.184	0.374	3 808	1.000

Table D.3: Summary of parameter estimates from the <u>reference</u> run of the SEFRA model for <u>males</u>.

Label	Parameter	Mean	2.5%	Median	97.5%	Effective N	Rhat
q_zg[1,1]	$q_{z,g}$	0.081	0.010	0.069	0.218	3 699	0.999
q_zg[1,2]	$q_{z,g}$	0.003	0.000	0.000	0.026	4 056	1.000
q_zg[2,1]	$q_{z,g}$	0.074	0.032	0.072	0.135	3 926	1.000
q_zg[2,2]	$q_{z,g}$	0.001	0.000	0.000	0.005	3 888	1.000
p_observable_m[1]	$p_g^{ m obs}$	0.750	0.495	0.760	0.931	3 988	1.000
p_observable_m[2]	$p_g^{ m obs}$	0.776	0.553	0.788	0.931	3 824	1.000
rmax	r^{\max}	0.140	0.134	0.140	0.145	3 848	1.000
p_necropsy_chick_k[1]	$ ho_{z,k}$	0.400	0.236	0.396	0.575	3 831	1.000
p_necropsy_chick_k[2]	$ ho_{z,k}$	0.335	0.185	0.332	0.509	3 974	1.001
p_necropsy_chick_k[3]	$ ho_{z,k}$	0.100	0.022	0.092	0.224	3 926	1.000
p_necropsy_chick_k[4]	$ ho_{z,k}$	0.066	0.009	0.057	0.176	3 563	1.000
p_necropsy_chick_k[5]	$ ho_{z,k}$	0.099	0.022	0.090	0.224	3 986	1.001
p_necropsy_juv_k[1]	$ ho_{z,k}$	0.384	0.149	0.379	0.644	3 704	1.000
p_necropsy_juv_k[2]	$ ho_{z,k}$	0.153	0.021	0.136	0.381	3 991	1.000
p_necropsy_juv_k[3]	$ ho_{z,k}$	0.232	0.056	0.216	0.493	3 778	1.000
p_necropsy_juv_k[4]	$ ho_{z,k}$	0.154	0.022	0.135	0.380	3 195	1.001
p_necropsy_juv_k[5]	$ ho_{z,k}$	0.078	0.002	0.057	0.268	3 976	0.999
<pre>p_necropsy_adult_k[1]</pre>	$ ho_{z,k}$	0.307	0.144	0.300	0.514	3 233	1.000
p_necropsy_adult_k[2]	$ ho_{z,k}$	0.129	0.028	0.119	0.293	3 307	0.999
p_necropsy_adult_k[3]	$ ho_{z,k}$	0.347	0.170	0.343	0.546	3 650	1.000
p_necropsy_adult_k[4]	$ ho_{z,k}$	0.174	0.053	0.165	0.352	3 960	1.000
p_necropsy_adult_k[5]	$ ho_{z,k}$	0.043	0.001	0.030	0.150	3 959	1.002

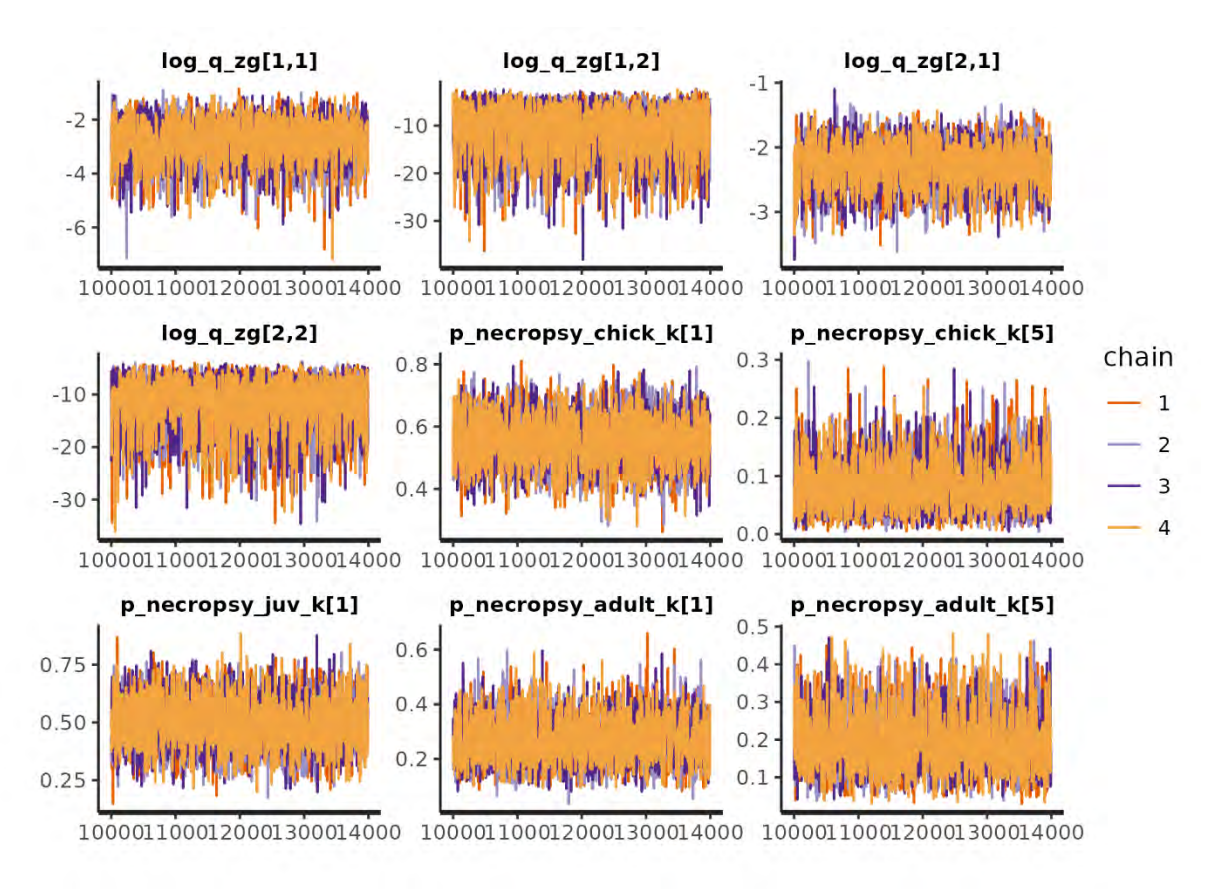


Figure D.11: Trace plots for selected estimated parameters of the female <u>reference</u> SEFRA model run: catchability of juveniles in commercial set nets ($log_q_zg[1,I]$), catchability of adults in commercial trawls ($log_q_zg[2,I]$), catchability of adults in commercial trawls ($log_q_zg[2,I]$), catchability of adults in commercial trawls ($log_q_zg[2,I]$), proportion of chicks dying from malnutrition ($p_necropsy_chick_k[I]$), proportion of chicks dying from malnutrition ($p_necropsy_iuv_k[I]$), proportion of adults dying from malnutrition ($p_necropsy_adult_k[I]$) proportion of adults dying from other causes of death ($p_necropsy_adult_k[I]$).

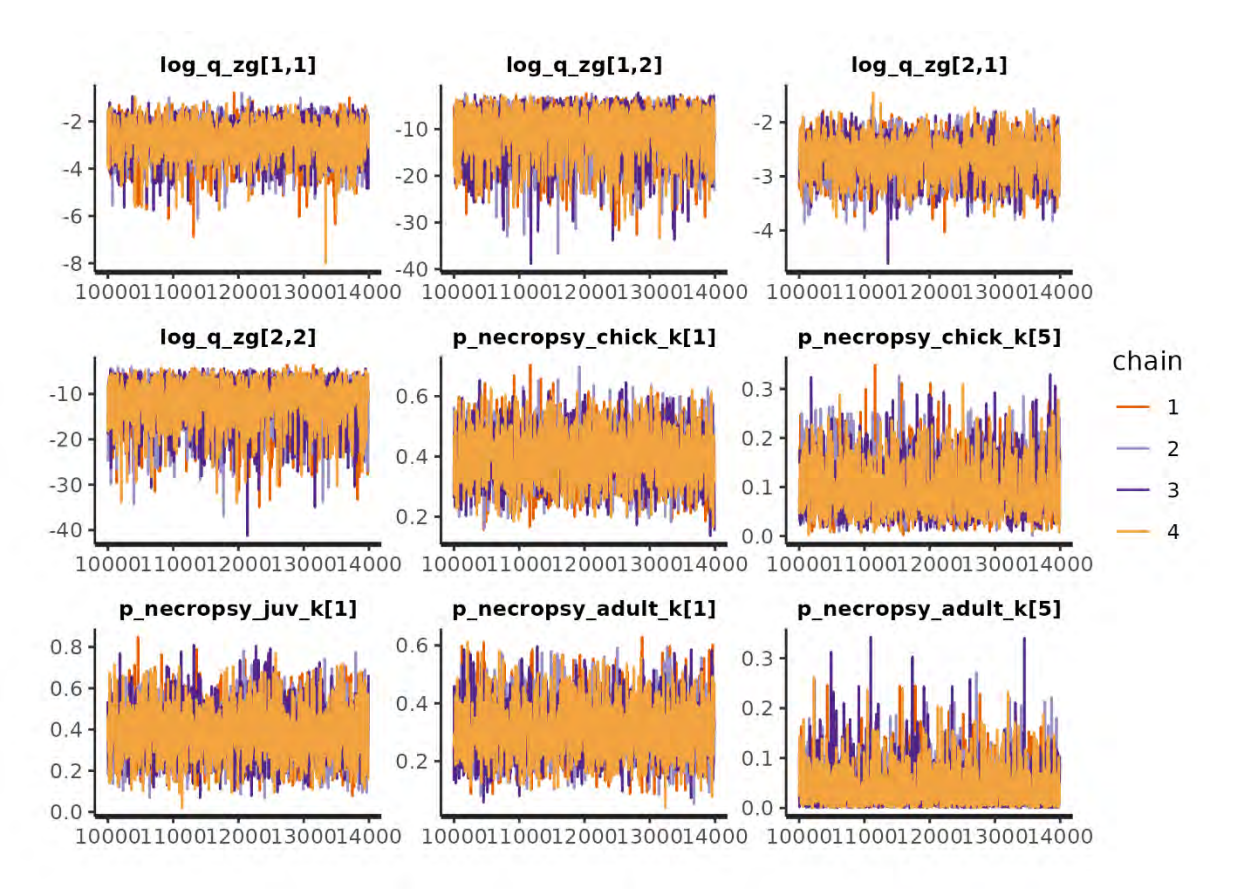


Figure D.12: Trace plots for selected estimated parameters of the male <u>reference</u> SEFRA model run: catchability of juveniles in commercial set nets ($log_q_zg[1,I]$), catchability of adults in commercial set nets ($log_q_zg[2,I]$), catchability of adults in commercial trawls ($log_q_zg[2,I]$), catchability of adults in commercial trawls ($log_q_zg[2,2]$), proportion of chicks dying from malnutrition ($p_necropsy_chick_k[I]$), proportion of juveniles dying from malnutrition ($p_necropsy_dult_k[I]$), proportion of adults dying from malnutrition ($p_necropsy_adult_k[I]$) proportion of adults dying from other causes of death ($p_necropsy_adult_k[I]$).

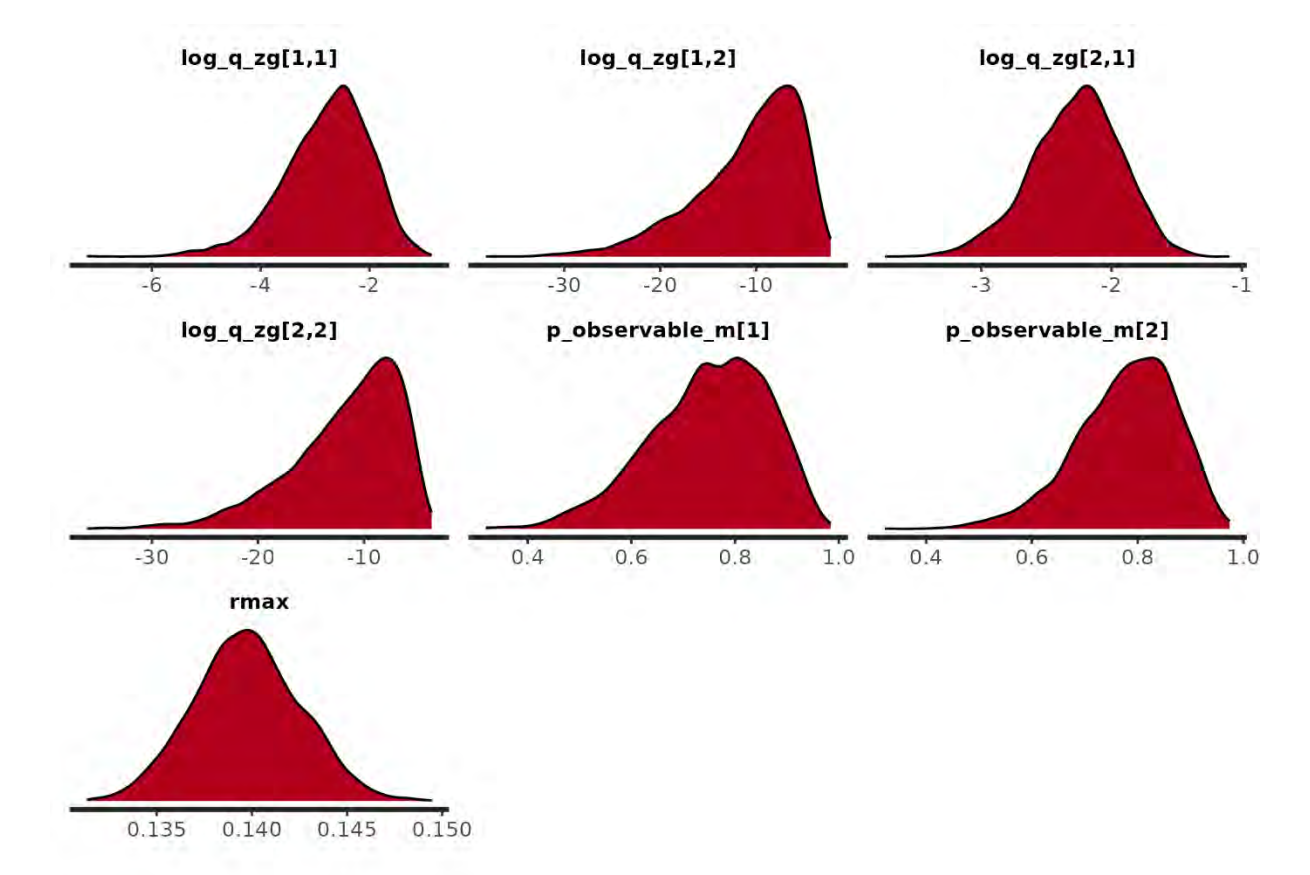


Figure D.13: Posterior distribution for selected parameters of the female <u>reference</u> SEFRA model run: catchability of juveniles in commercial set nets $(log_q_zg[1,1])$, adults in commercial set nets $(log_q_zg[1,2])$, adults in commercial trawls $(log_q_zg[2,1])$, and adults in commercial trawls $(log_q_zg[2,2])$; the observability of mortalities in commercial set-nets $(p_observable_m[1])$, and trawls $(p_observable_m[2])$; and intrinsic population growth rate (r^{max}) .

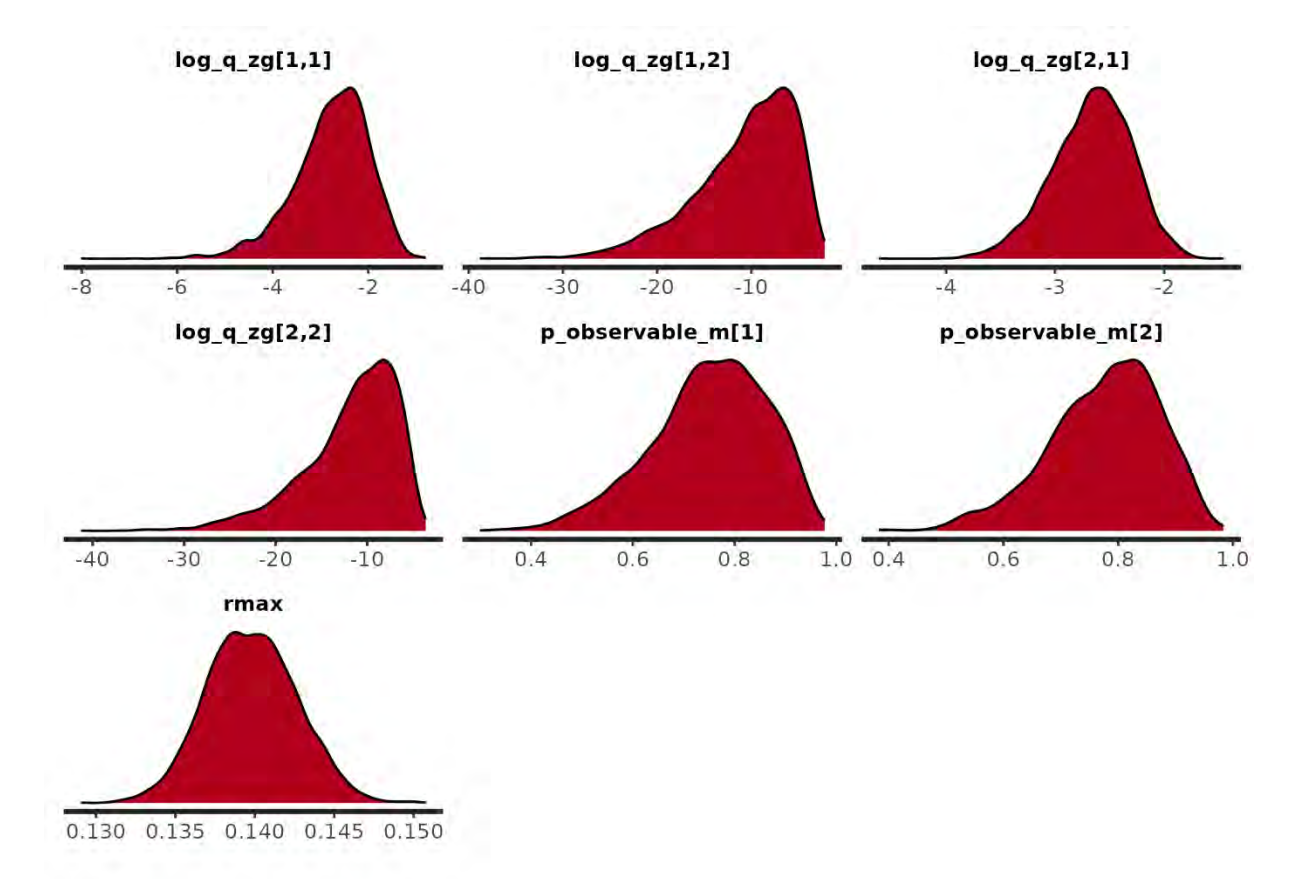
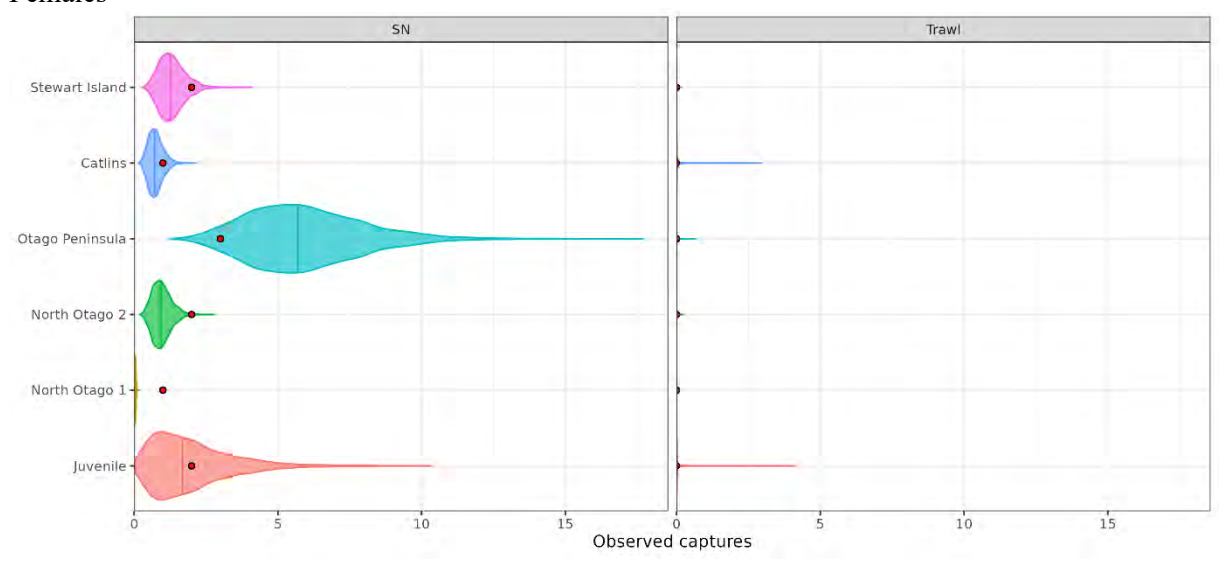


Figure D.14: Posterior distribution for selected parameters of the male <u>reference</u> SEFRA model run: catchability of juveniles in commercial set nets $(log_q_zg[1,1])$, adults in commercial set nets $(log_q_zg[1,2])$, adults in commercial trawls $(log_q_zg[2,1])$, and adults in commercial trawls $(log_q_zg[2,2])$; the observability of mortalities in commercial set-nets $(p_observable_m[1])$, and trawls $(p_observable_m[2])$; and intrinsic population growth rate (r^{max}) .

Females



Males

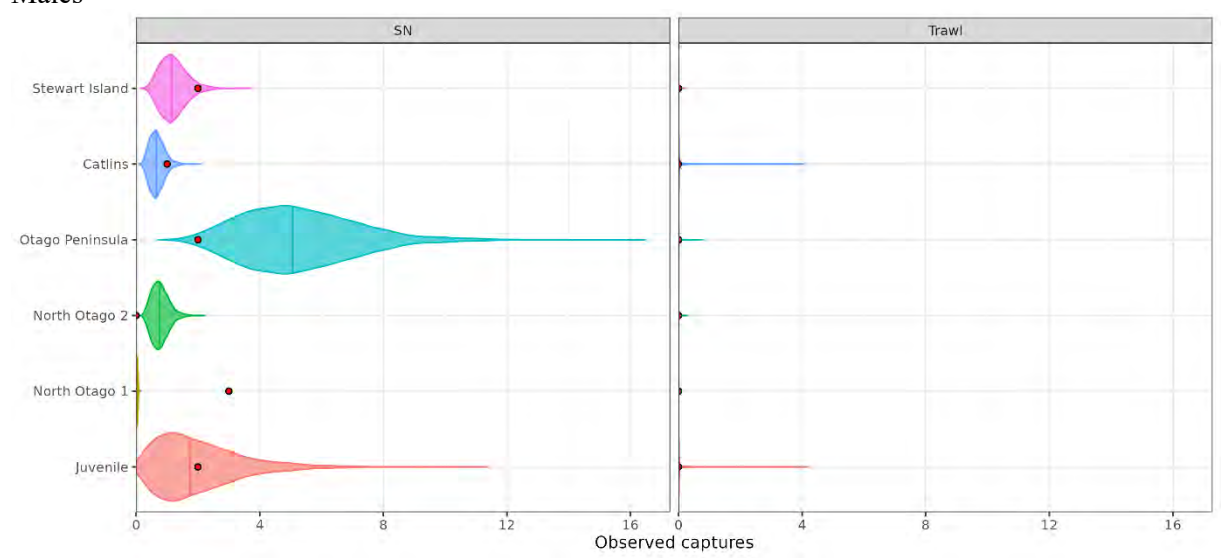


Figure D.15: Model posteriors from the <u>reference</u> run of total observed captures (violin plots) and observed female captures (red circles) by fishery and age class or region (for adults only) across the fishing years 2006–07 to 2022–23.

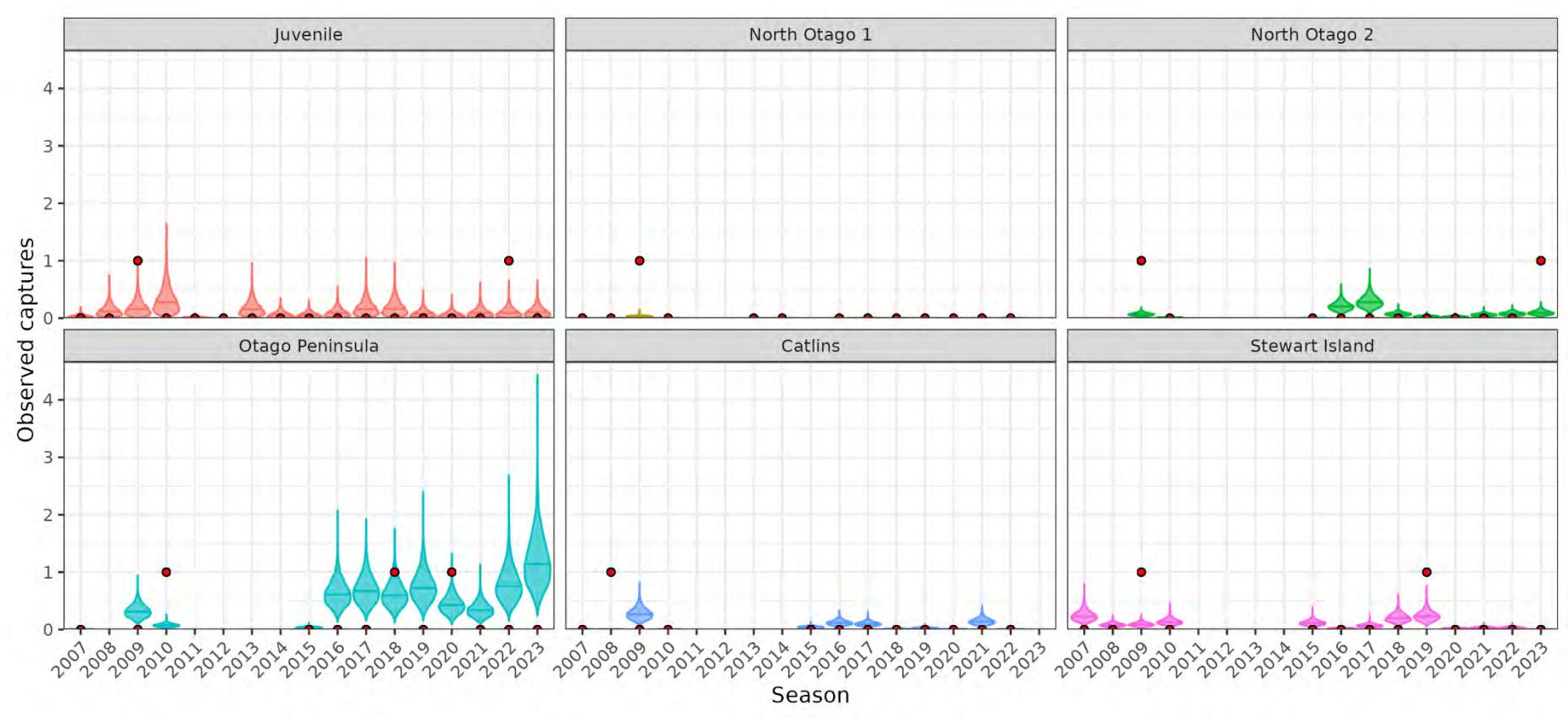


Figure D.16: Model posteriors from the <u>reference</u> run of observed female captures (violin plots) and observed female captures (red circles) for the commercial setnet fishery by fishing year and age class and region (for adult females only).

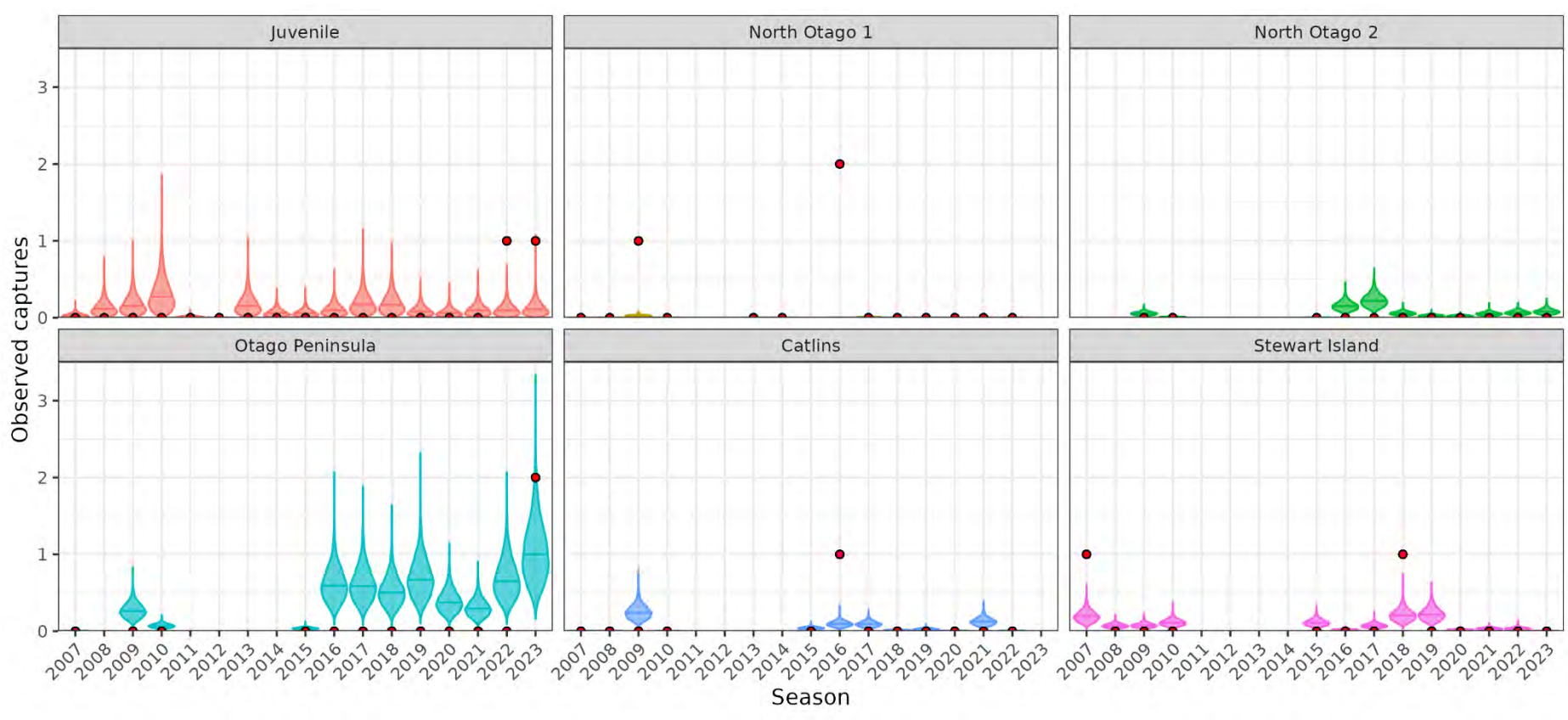
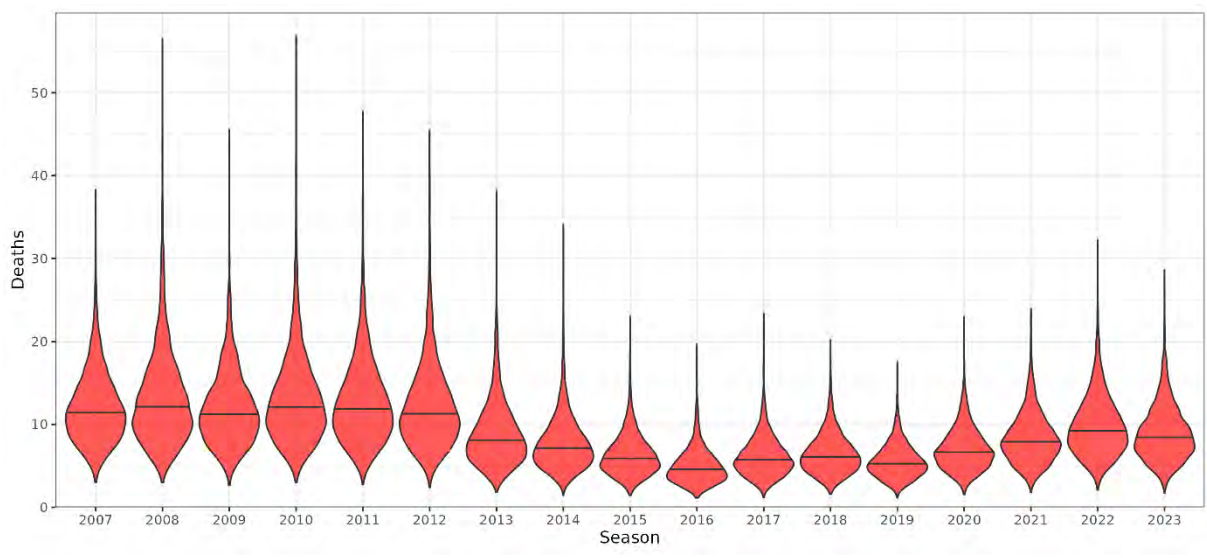


Figure D.17: Model posteriors from the <u>reference</u> run of observed female captures (violin plots) and observed female captures (red circles) for the commercial setnet fishery by fishing year and age class and region (for adult males only).





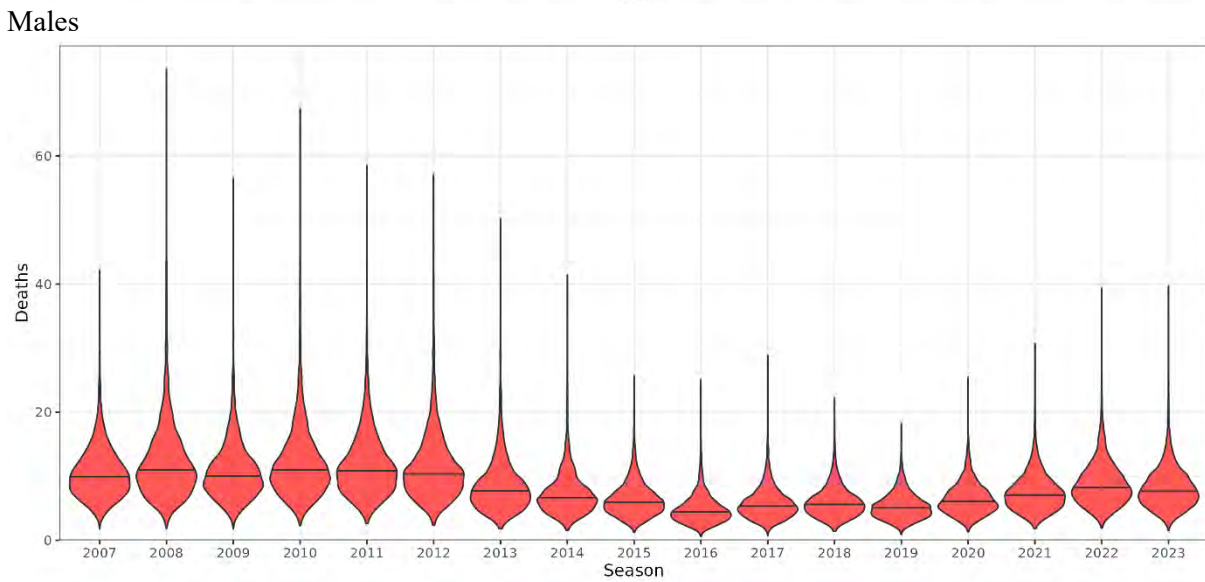


Figure D.18: Model posteriors from the <u>reference</u> run of female (top) and male (bottom) deaths for commercial set-net and trawls by fishing year.

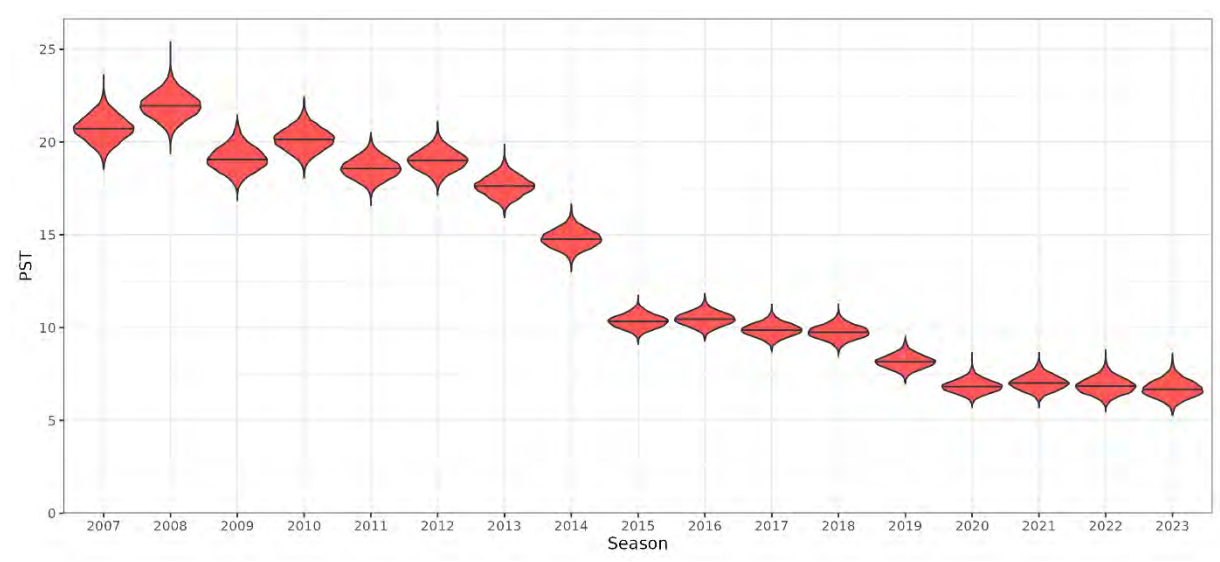


Figure D.19: Model posteriors from the <u>reference</u> run of the female population sustainability threshold for the nothern population of yellow-eyed pengiuns (assuming $\phi = 0.2$).

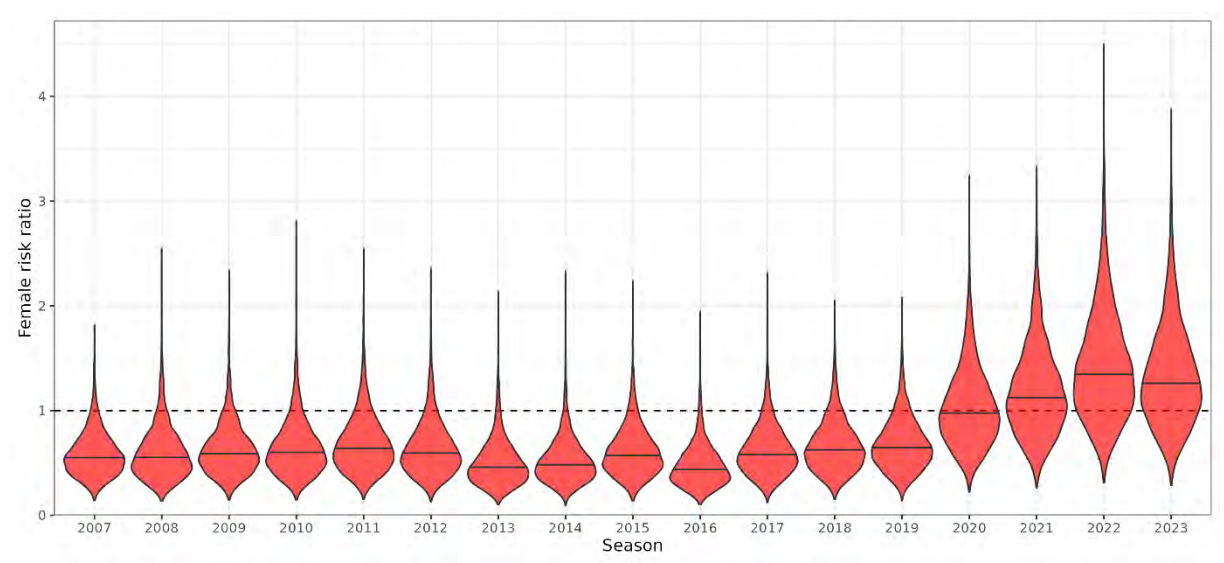


Figure D.20: Model posteriors from the <u>reference</u> run of female risk ratio for commercial set-net and trawls by fishing year (assuming $\phi = 0.2$). The dashed line represents a risk ratio equal to 1, above which the management goal would not be achieved at equilibrium.

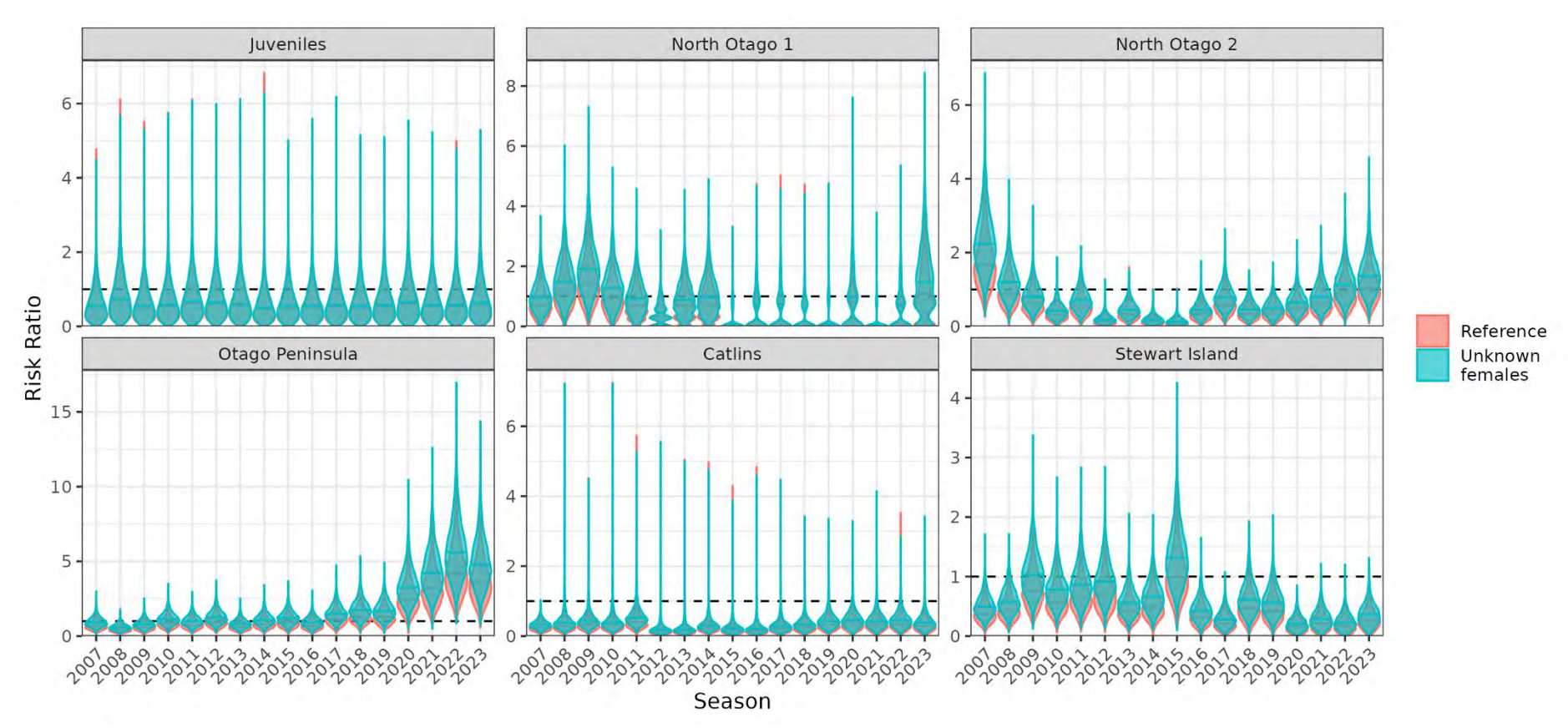


Figure D.21: Sensitivity of the model posteriors from the <u>unk fem</u> run (blue densities) and <u>reference run</u> (red densities) of risk ratio for commercial set-nets by fishing year, age group and regional sub-population (adults only), when assuming $\phi = 0.2$. The dashed line represents a risk ratio equal to 1, above which the management goal would not be achieved at equilibrium.

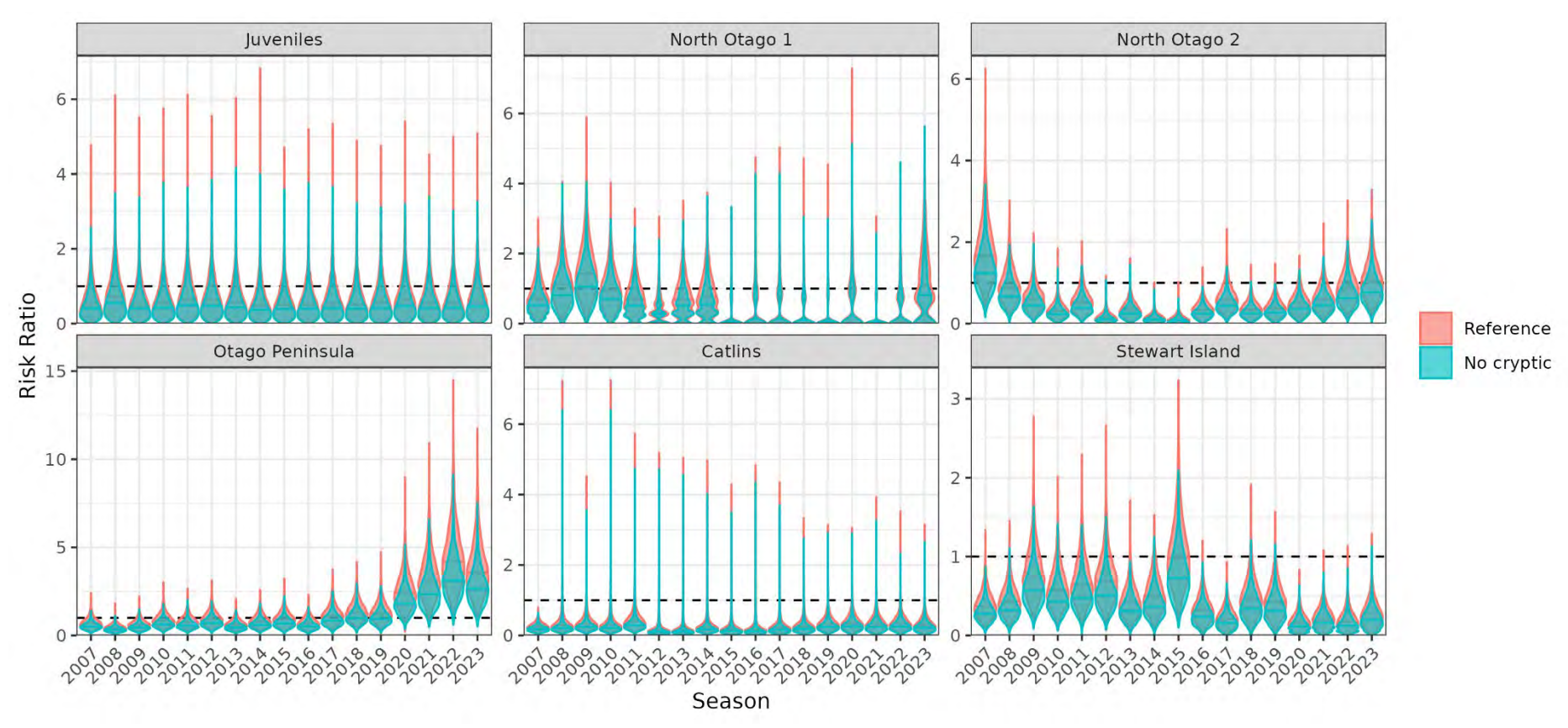


Figure D.22: Sensitivity of the model posteriors from the <u>no cryptic</u> run (blue densities) and <u>reference run</u> (red densities) of risk ratio for commercial set-nets by fishing year, age group and regional sub-population (adults only), when assuming $\phi = 0.2$. The dashed line represents a risk ratio equal to 1, above which the management goal would not be achieved at equilibrium.

Appendix E. AT-SEA DENSITY OF YELLOW-EYED PENGUINS

Adults

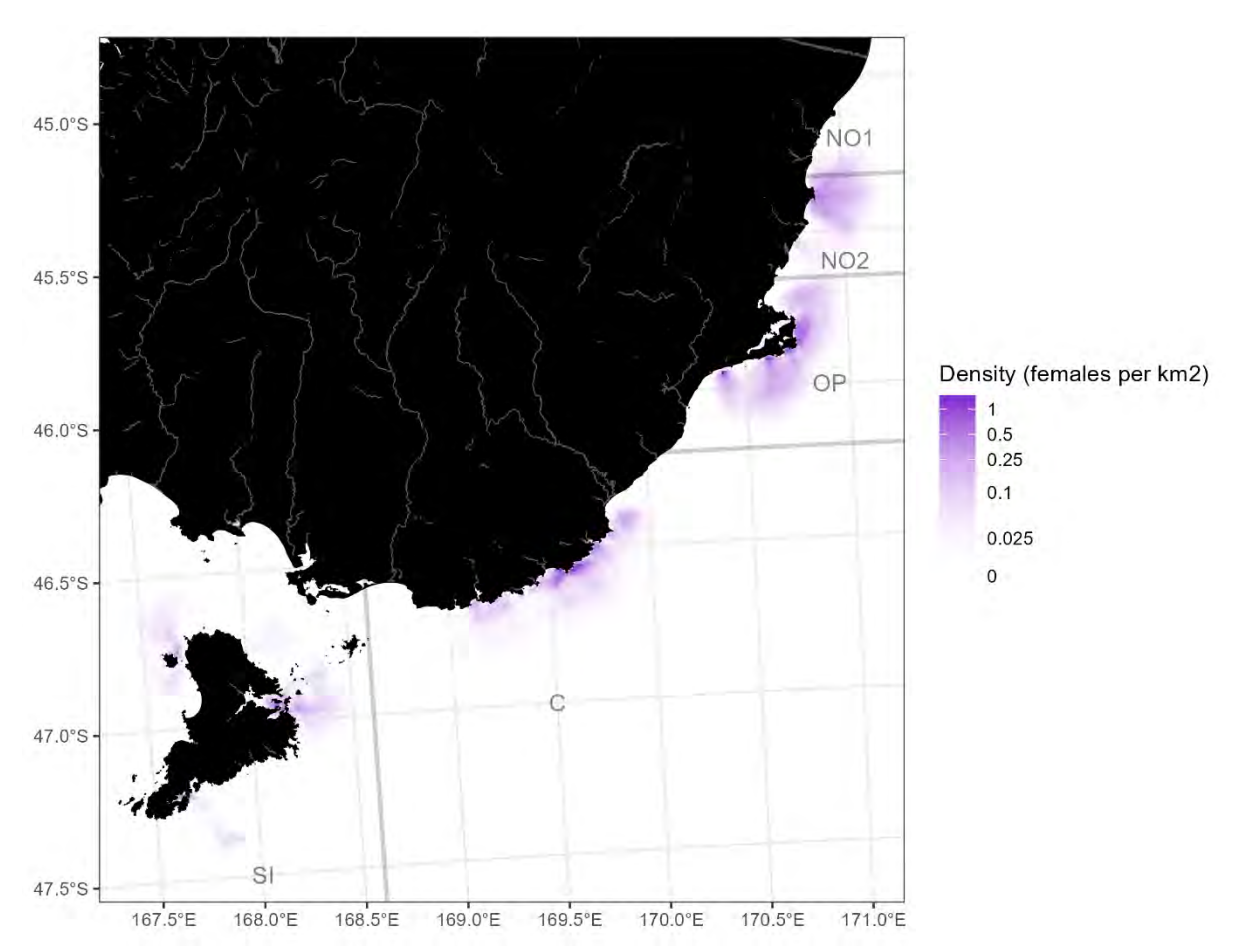


Figure E.1: Predicted at-sea density of <u>adult yellow-eyed penguin in all months</u>. Note the use of non-linear colour scale, which will emphasise areas of low density. Regional sub-population labels are "NO1" = North Otago 1, "NO2" = North Otago 2, "OP" = Otago Peninsula, "C" = Catlins, and "SI" = Stewart Island/Rakiura.

Juveniles

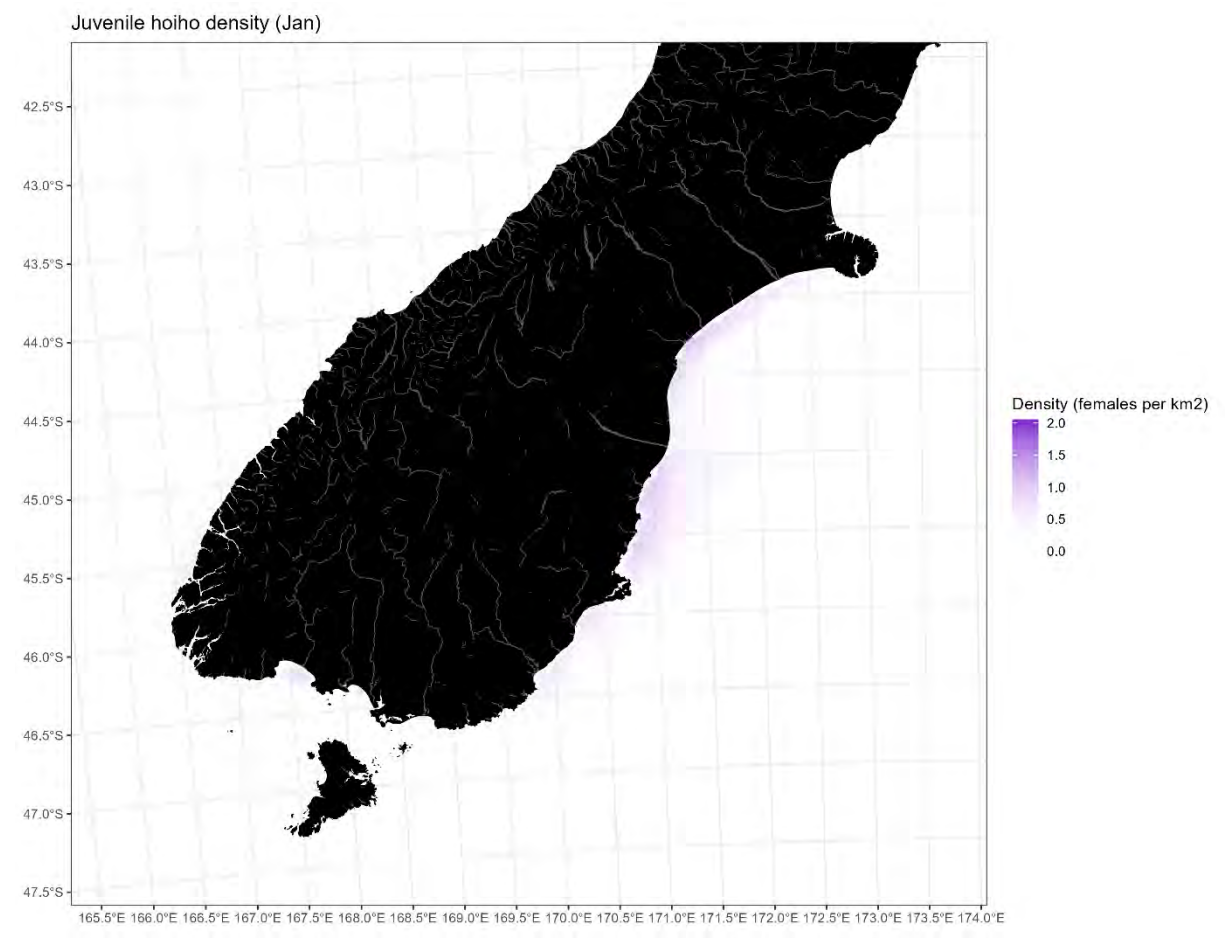


Figure E.2: Predicted at-sea density of <u>juvenile yellow-eyed penguin in January</u>.

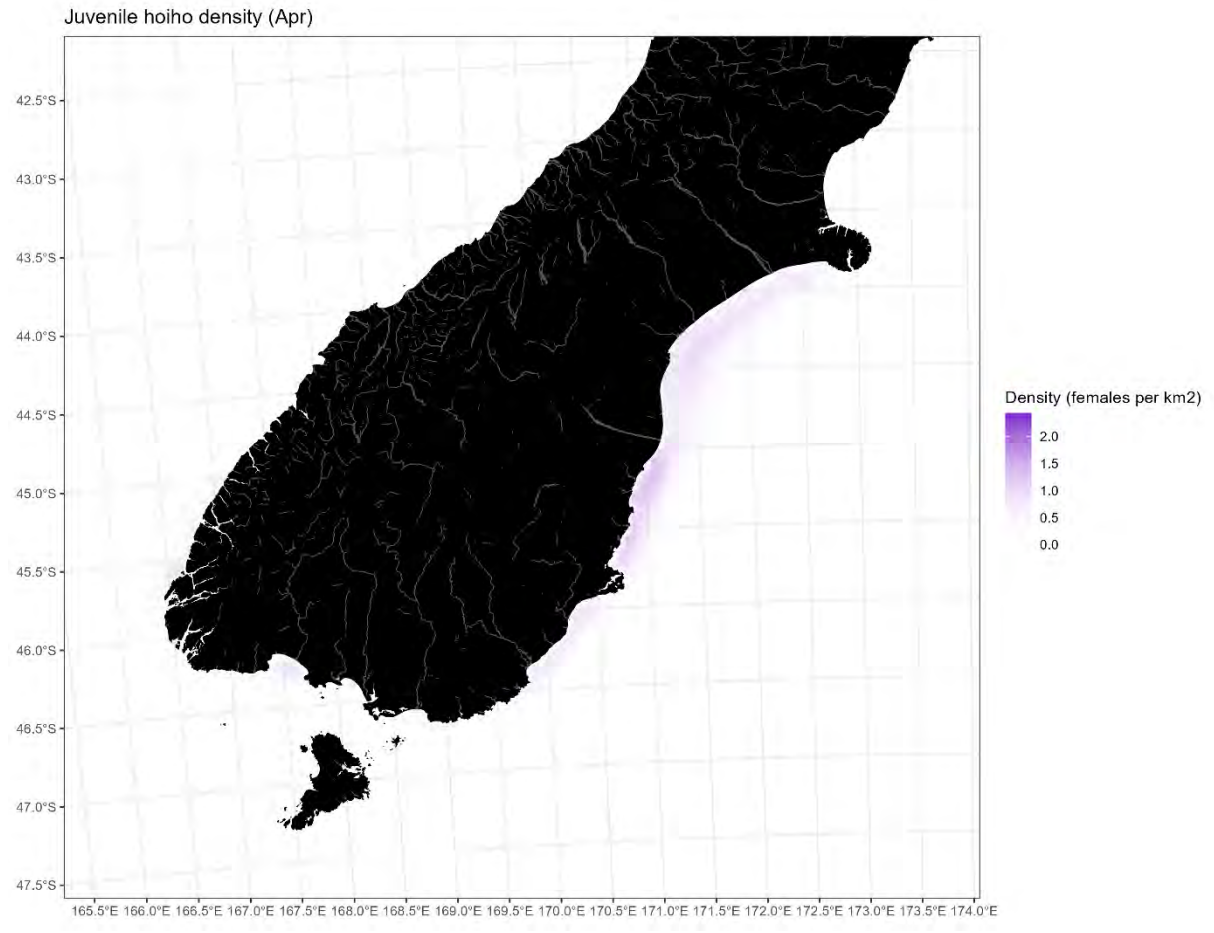


Figure E.3: Predicted at-sea density of <u>juvenile yellow-eyed penguin in April</u>.

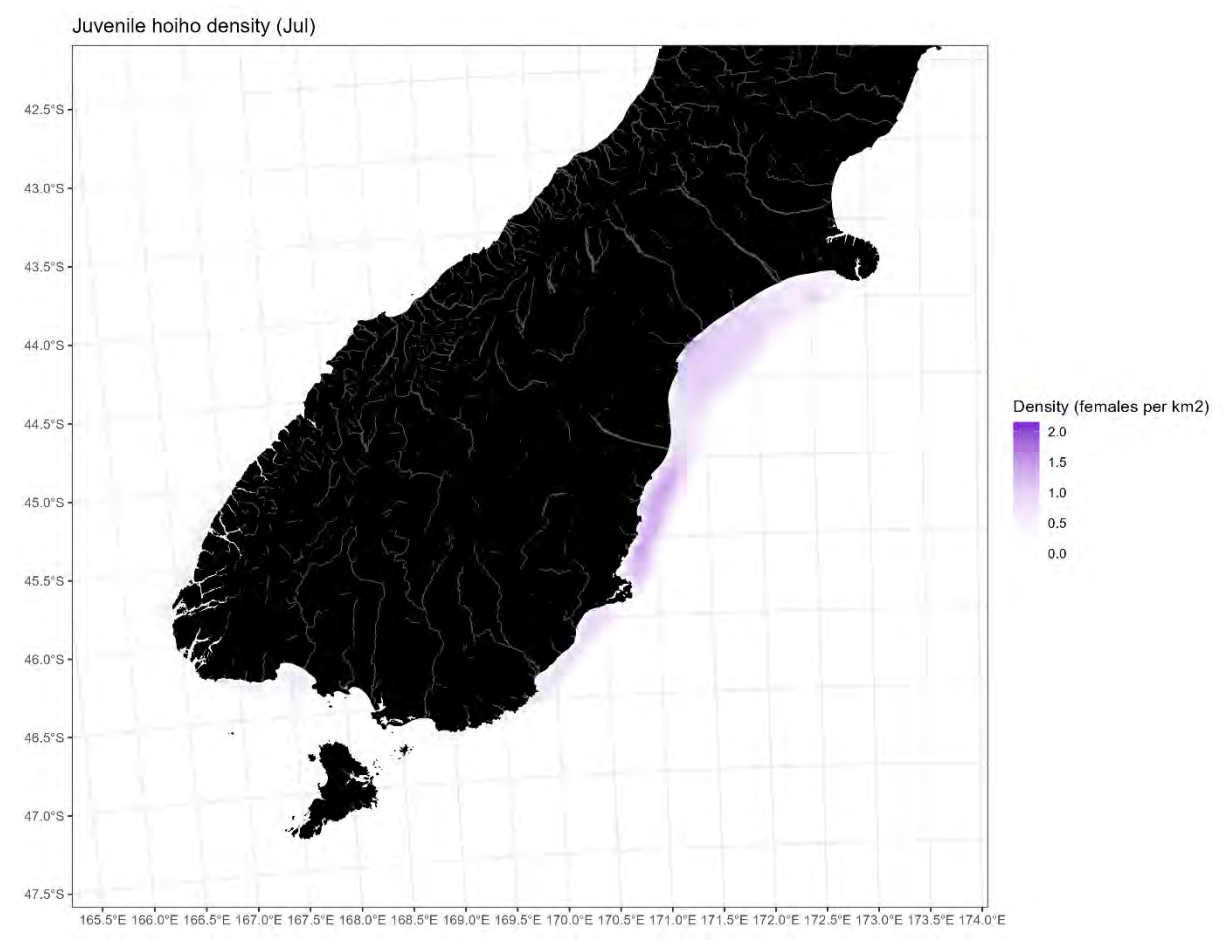


Figure E.4: Predicted at-sea density of <u>juvenile yellow-eyed penguin in July</u>.

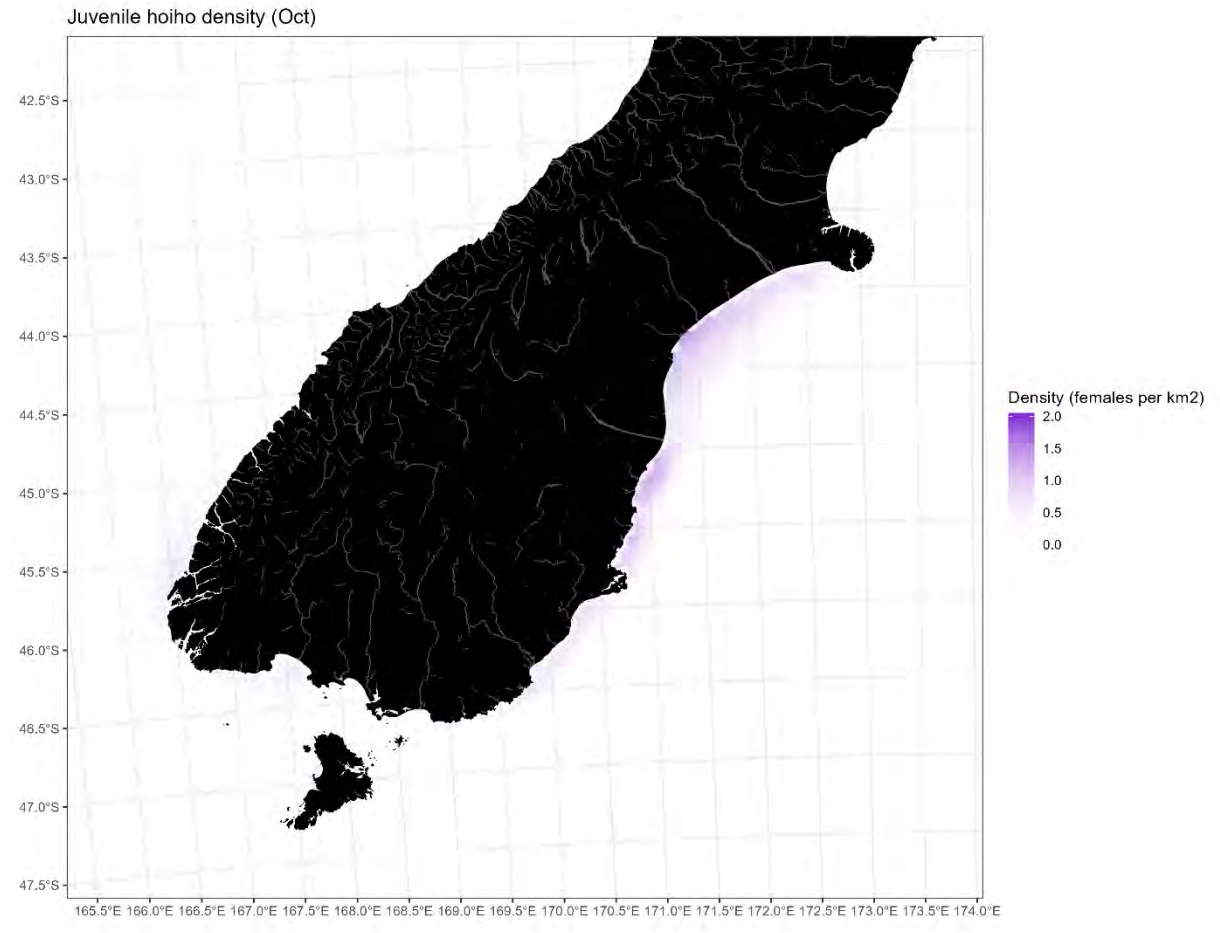


Figure E.5: Predicted at-sea density of <u>juvenile yellow-eyed penguin in October</u>.

Appendix F. THREAT MAPS

Table F.1: Summary of threat layers included in this assessment.

Threat	Measure	Source
Marine threats		
Direct interactions with commercial fishing	Geolocated fishing events of commercial set-net and trawl	Protected Species Captures (PSCv9) database, provided by Fisheries New Zealand January 2025.
Direct interactions with recreational netting	Relative intensity of recreational netting (summer and winter)	Reused from Roberts et al. (2019).
Interactions with aquaculture	Locations of operational aquaculture structures (fishcage based and other)	Shapefile provided by Fisheries New Zealand (unpublished data).
Oil pollution	Marine oil spill risk	Reused from Roberts et al. (2019), although produced by Navigatus Consulting (2015).
Effects of long-term changes in sea temperature	Slope in sea surface temperature from 1990– 2022	ERA5 climate data re-analysis (Hersbach et al. 2023).
Predation by sharks	Predicted probability of presence of broadnose sevengill shark	Reused from Roberts et al. (2019).
Terrestrial threats		
Direct interaction with humans/dogs	Human population density (residents per square kilometre)	New Zealand human population density by mesh block (Davis 2014).
Predation by cats	Predicted probability of presence of unowned cats (i.e., stay, but not feral)	Reused from Roberts et al. (2019), although ultimately produced by Aguilar et al. (2015) (Model B prediction).
Predation by stoats	Probability of presence of stoats	Department of Conservation (2014)
Predation by New Zealand sea lions	Index of relative sighting rate of New Zealand sea lions	Produced by this project. Derived from 'research-grade' land-based public sightings of New Zealand sea lions, related to New Zealand human population density by census mesh block (see Section 5.1.1).
Fire effects	Potential evapotranspiration deficit (1972–2014)	Porteous et al. (1994).
Road traffic accident	Centre lines of New Zealand roads	Land Information New Zealand (2011)

Marine threat maps

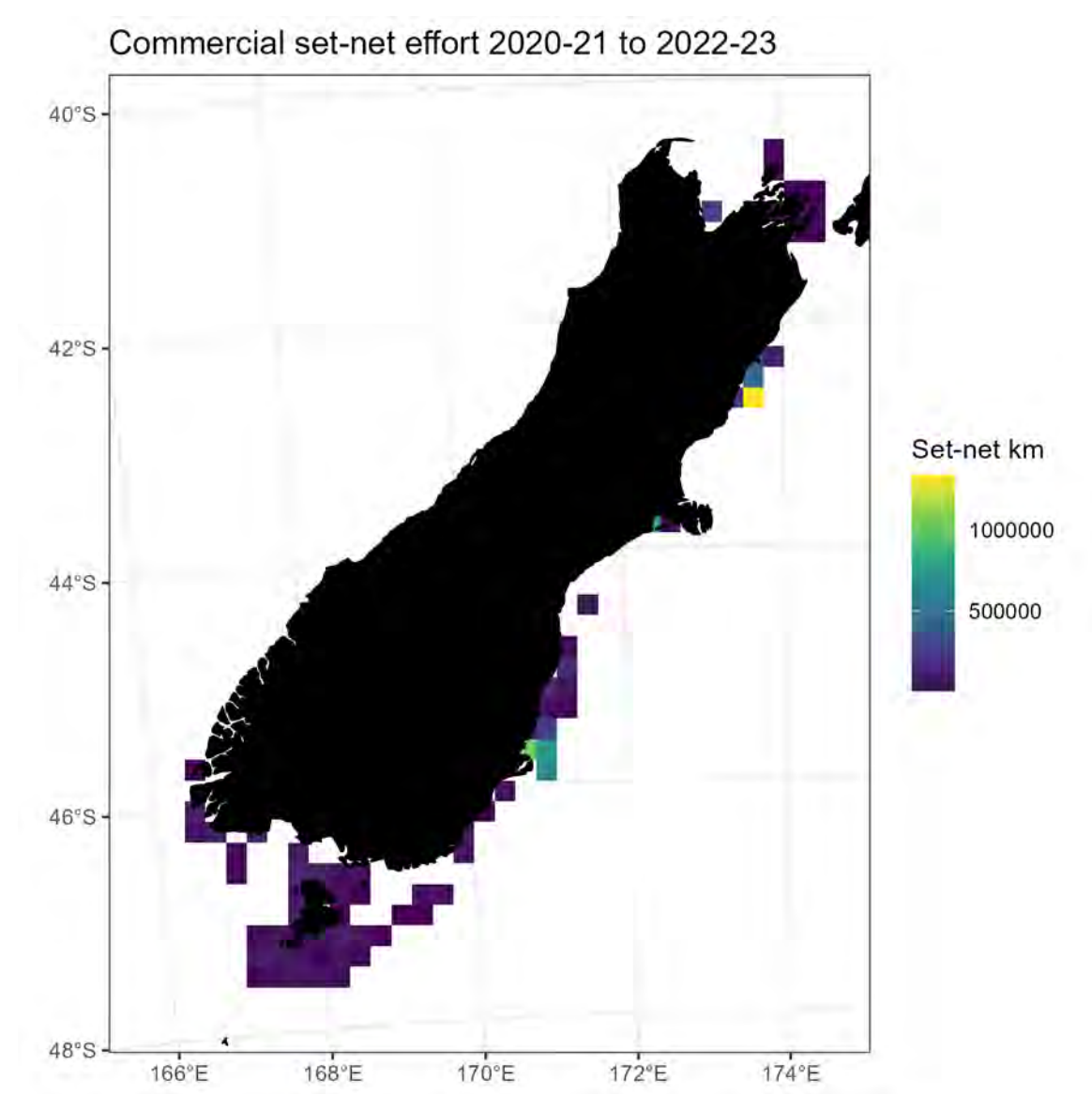


Figure F.1: Spatial density of commercial set net effort (km per 20 km grid cell) across fishing years 2020–21 to 2022–23. Grid cells used by only 1-2 vessels were redacted to comply with Data Confidentiality rules. These cells comprised 22.66% of the total set-net length inside the plot domain.

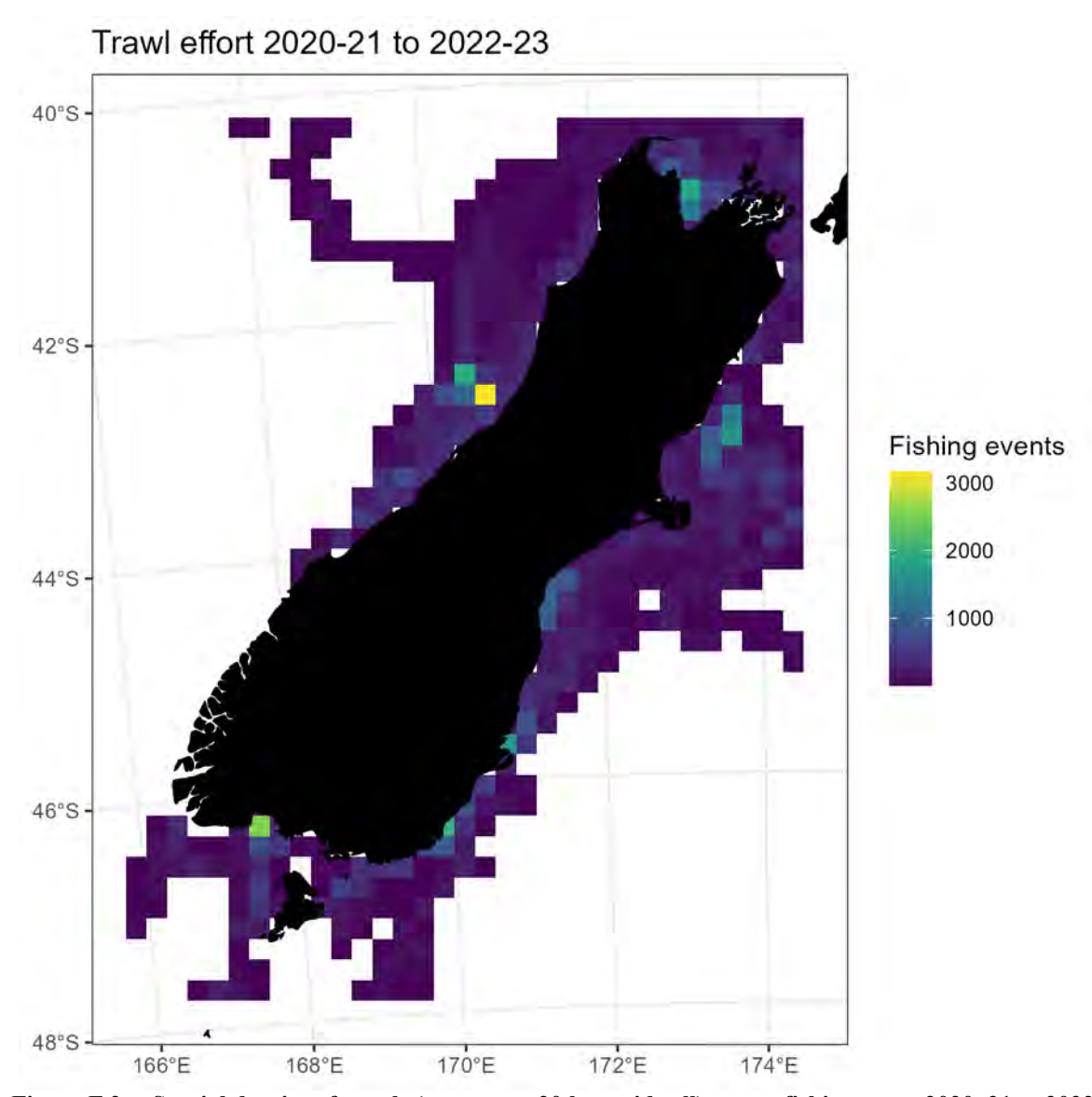


Figure F.2: Spatial density of trawls (events per 20 km grid cell) across fishing years 2020–21 to 2022–23. Grid cells used by only 1-2 vessels were redacted to comply with Data Confidentiality rules. These cells comprised 1.50% of the total trawls inside the plot domain.

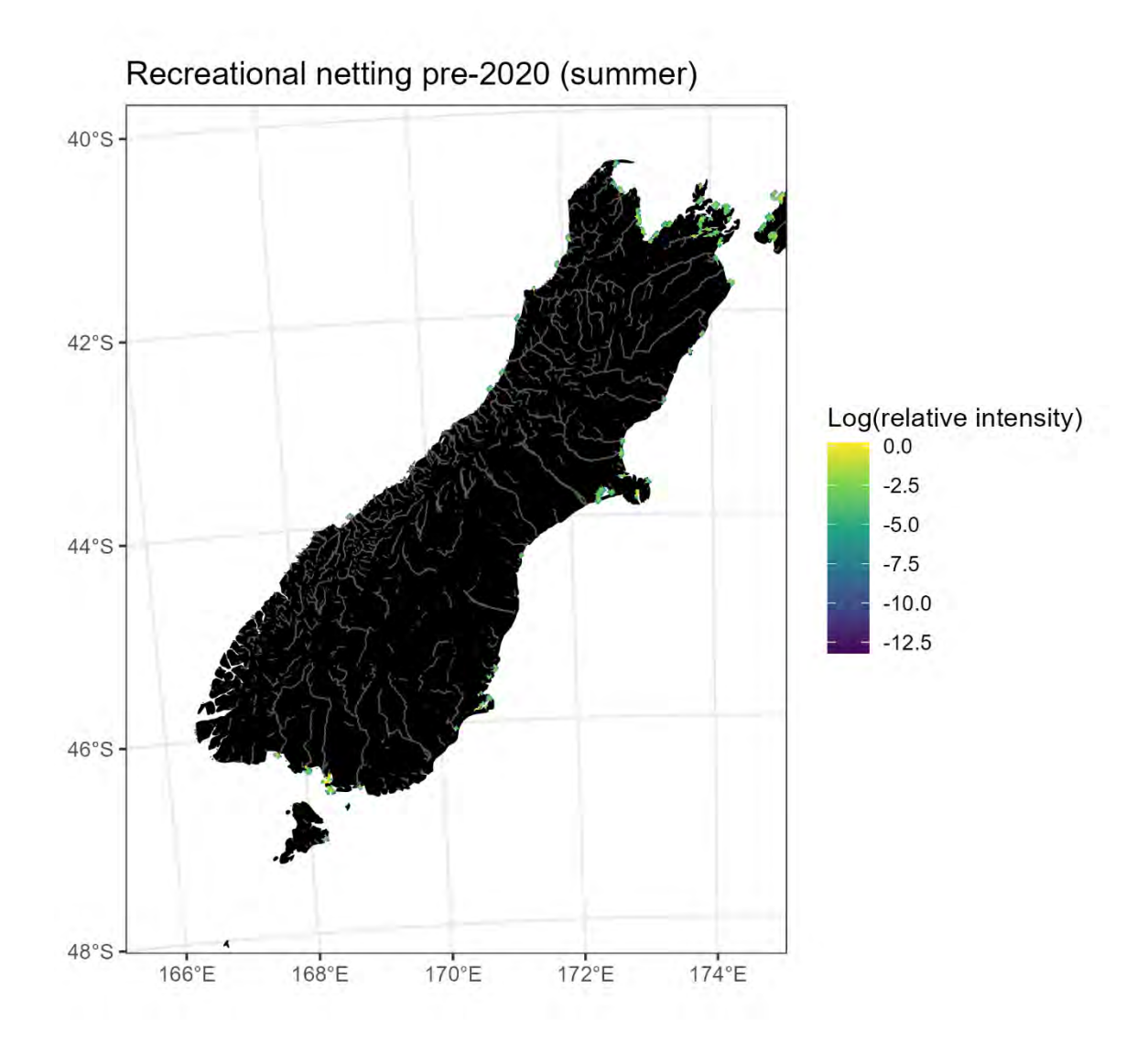


Figure F.3: Spatial intensity of recreational netting (log of relative intensity) in summer, as used by Roberts et al. (2019).

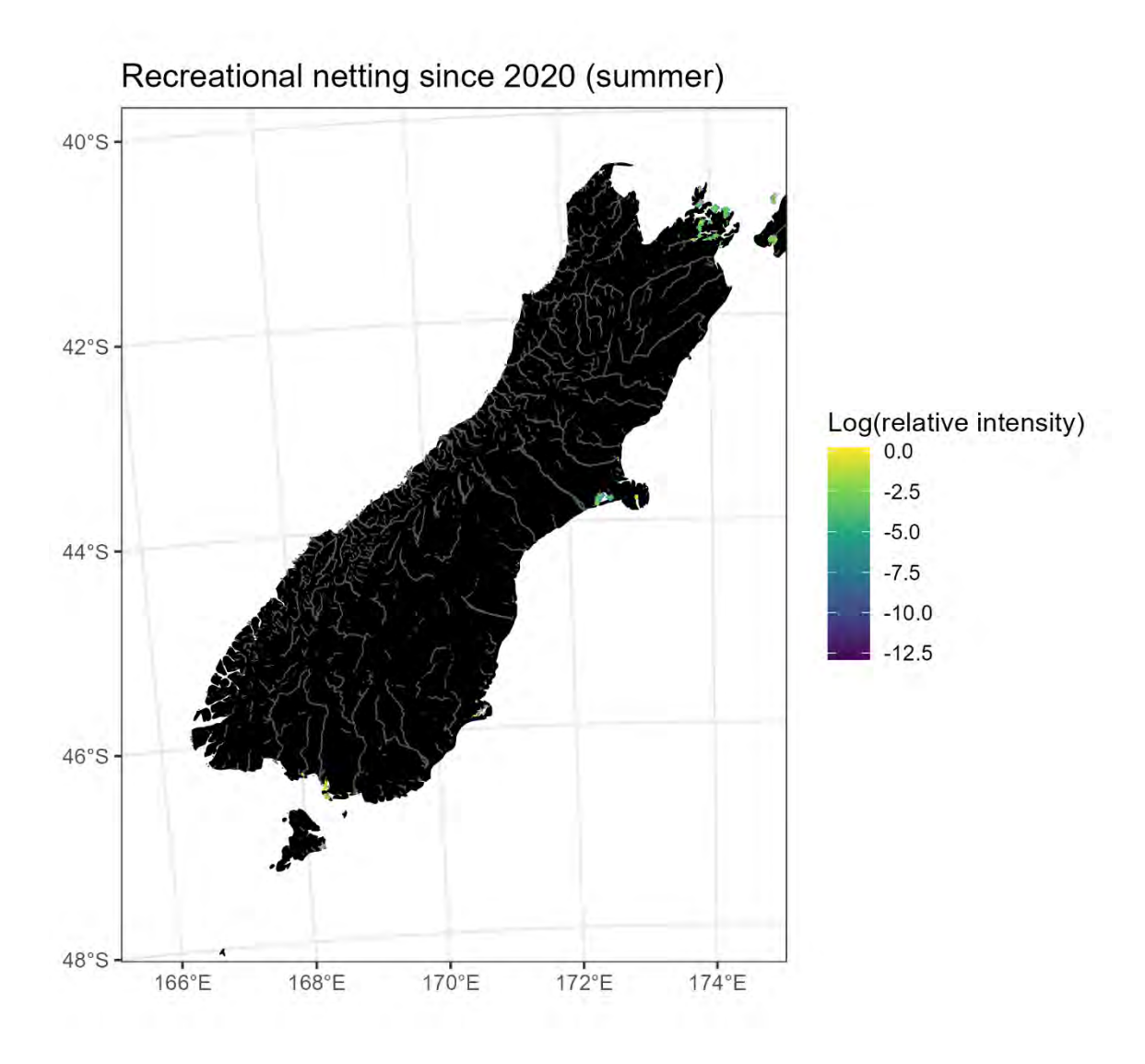


Figure F.4: Spatial intensity of recreational netting (log of relative intensity) in summer, excluding locations inside current amateur fishing prohibition areas.

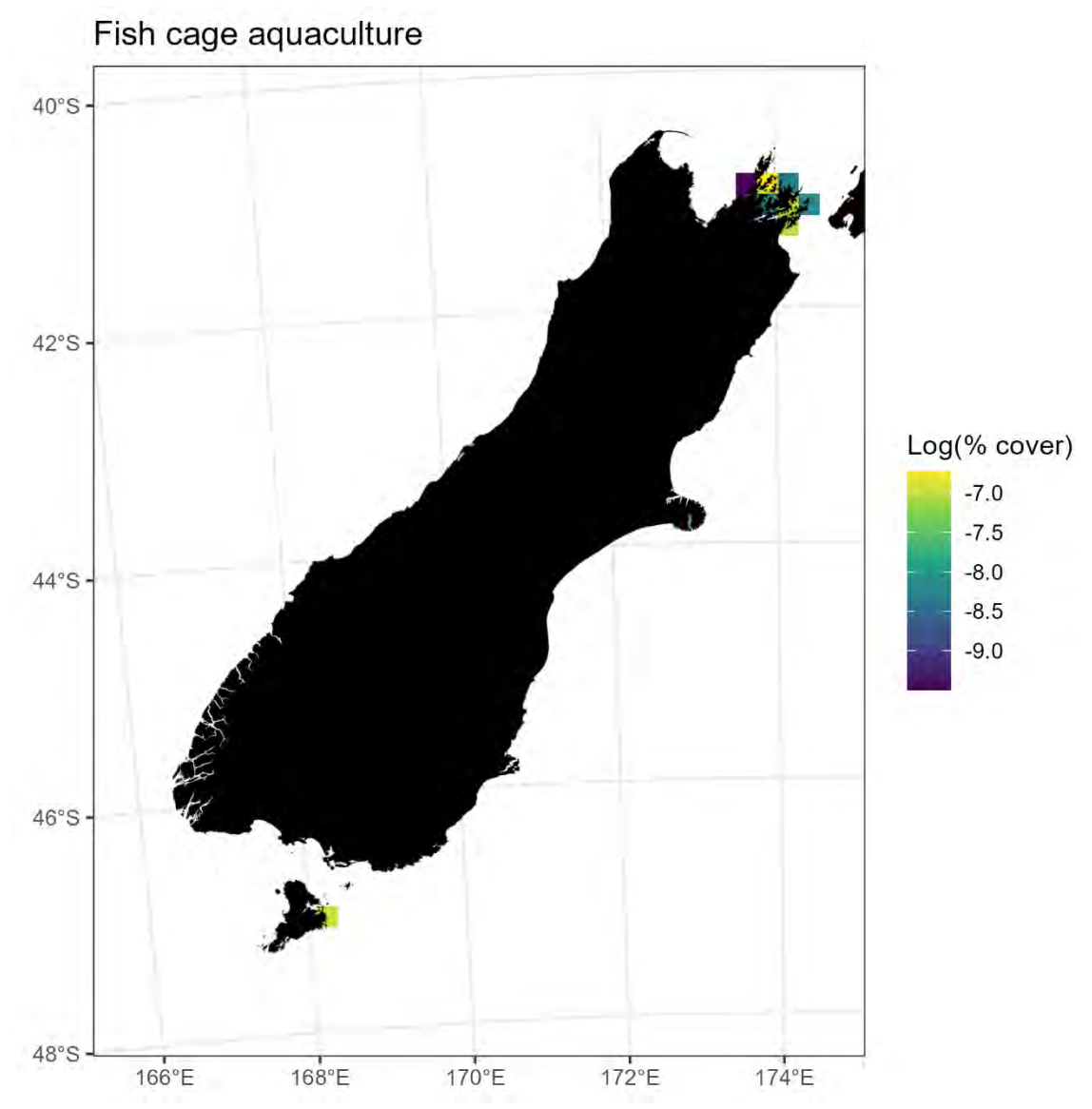


Figure F.5: Spatial plot of fish cage-based aquaculture (log of percentage cover). Plot shown at 20 km spatial resolution, so that locations can be seen more easily.

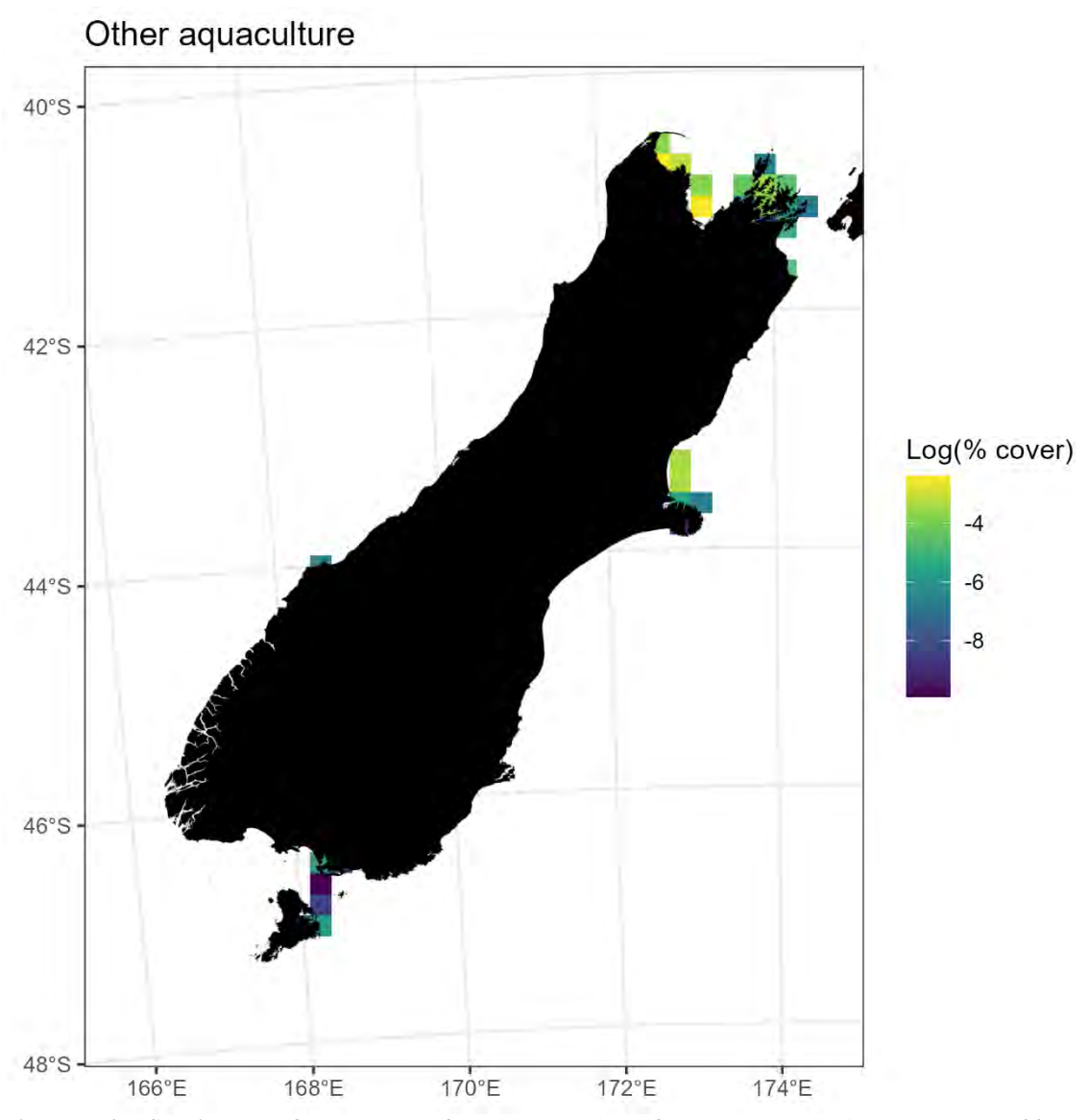


Figure F.6: Spatial plot of other types of aquaculture (log of percentage cover). Plot shown at 20 km spatial resolution, so that locations can be seen more easily.

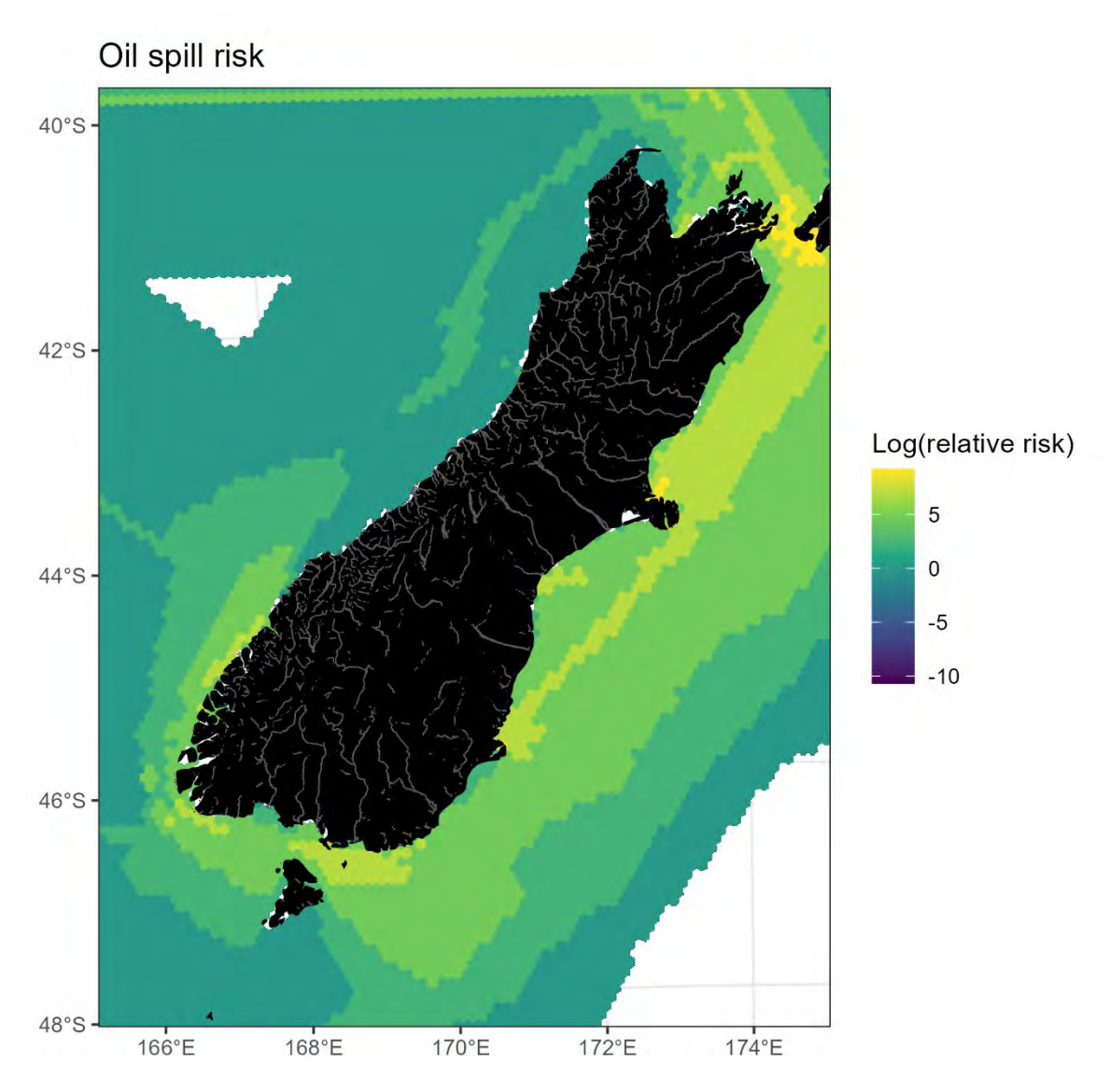


Figure F.7: Spatial oil spill risk (log of relative risk).

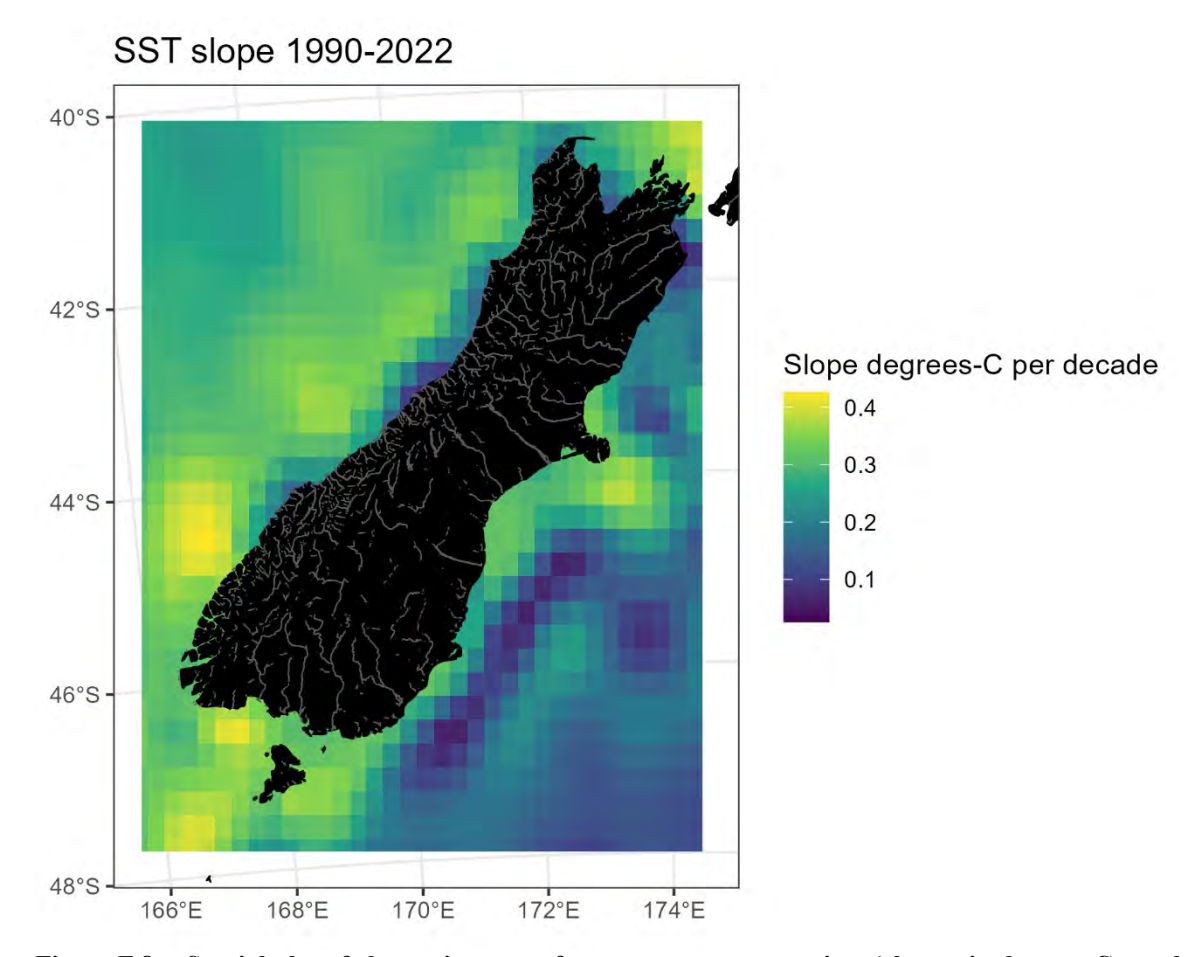


Figure F.8: Spatial plot of change in sea surface temperature over time (change in degrees-C per decade from 1990 to 2022).

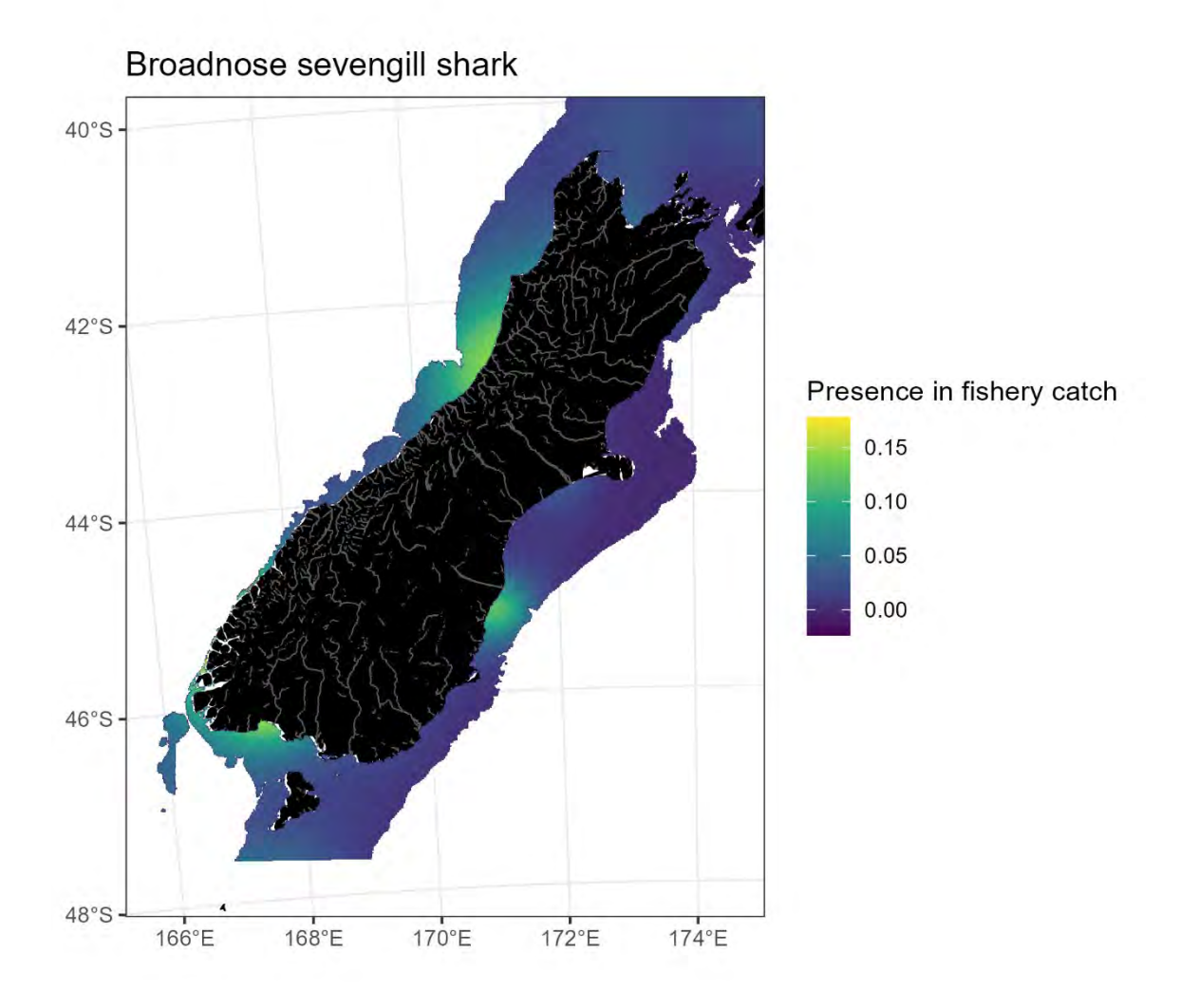


Figure F.9: Predicted spatial distribution of broadnose sevengill shark (probability of presence in fishery catch).

Terrestrial threat maps

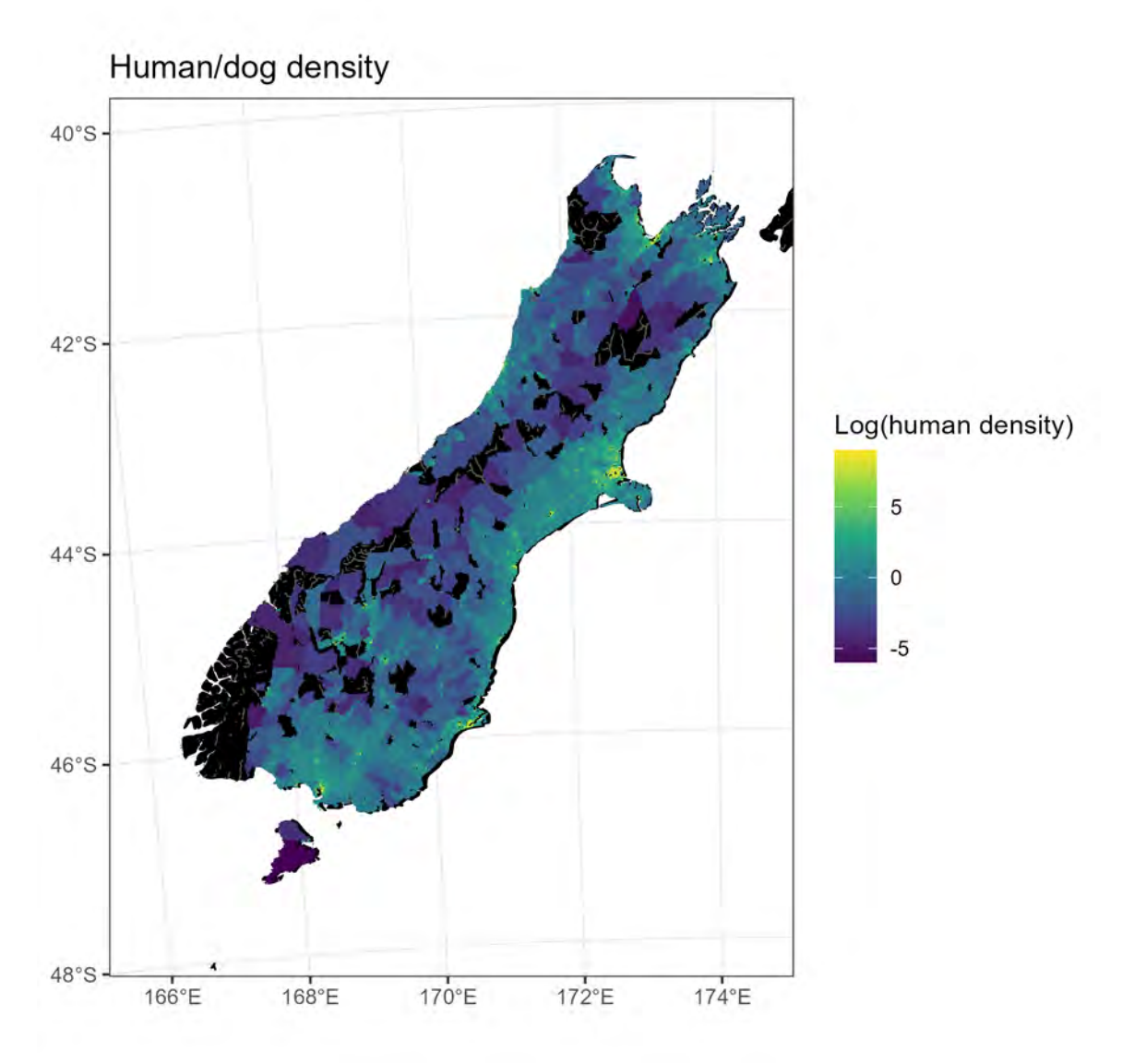


Figure F.10: Human and assumed dog density (logarithm of human density).

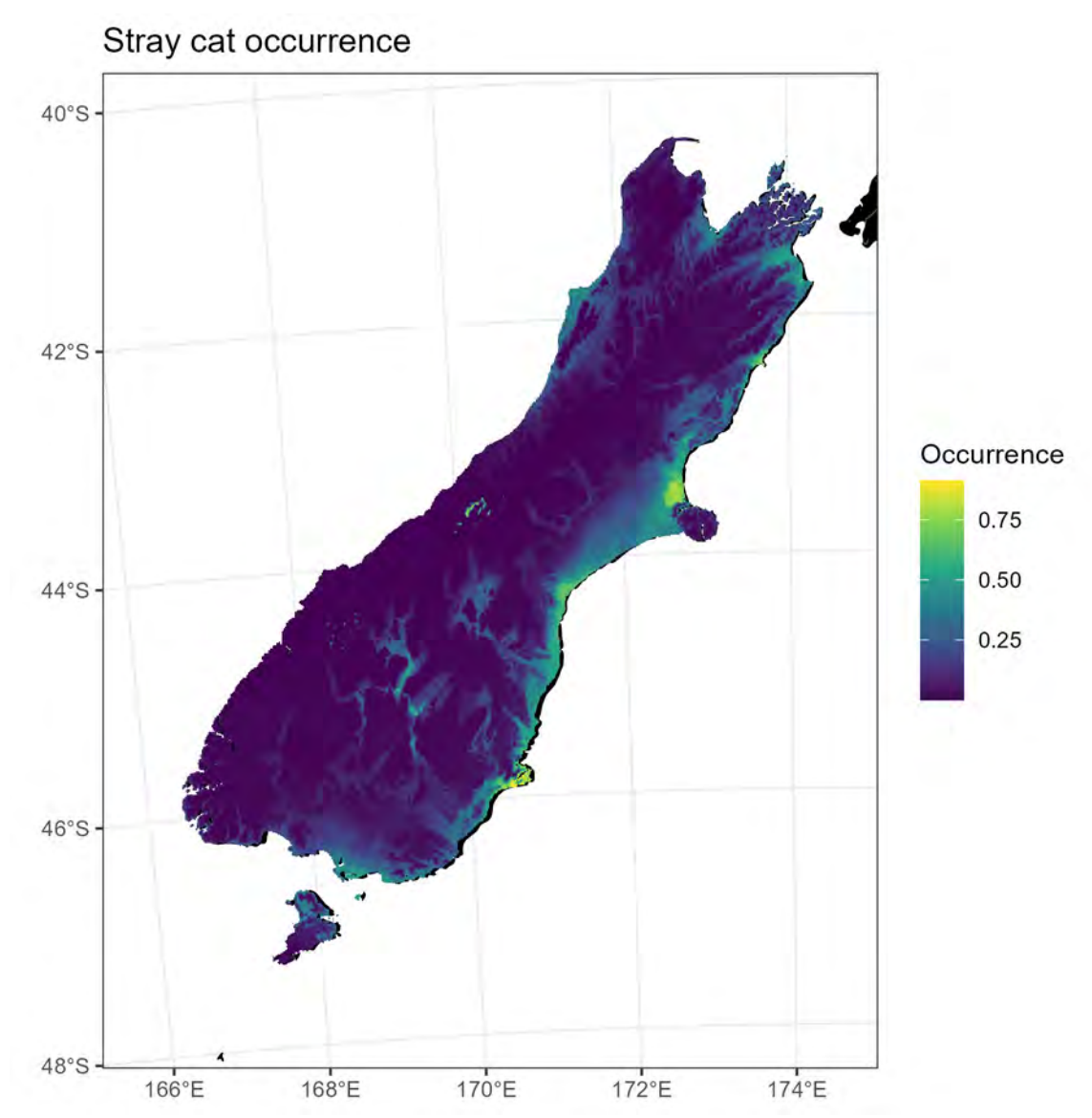


Figure F.11: Predicted occurrence of stray cats.

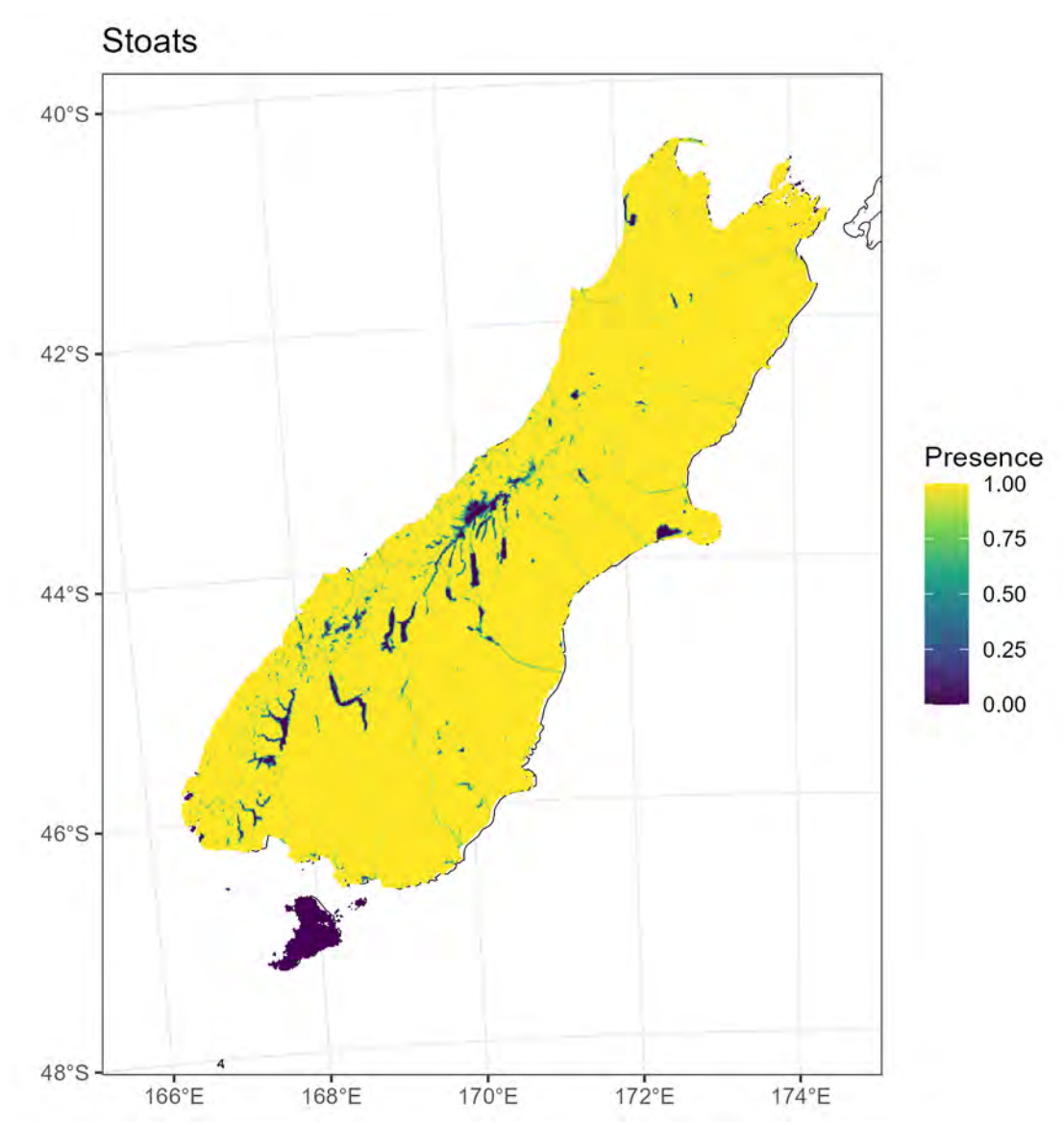


Figure F.12: Occurrence of stoats.

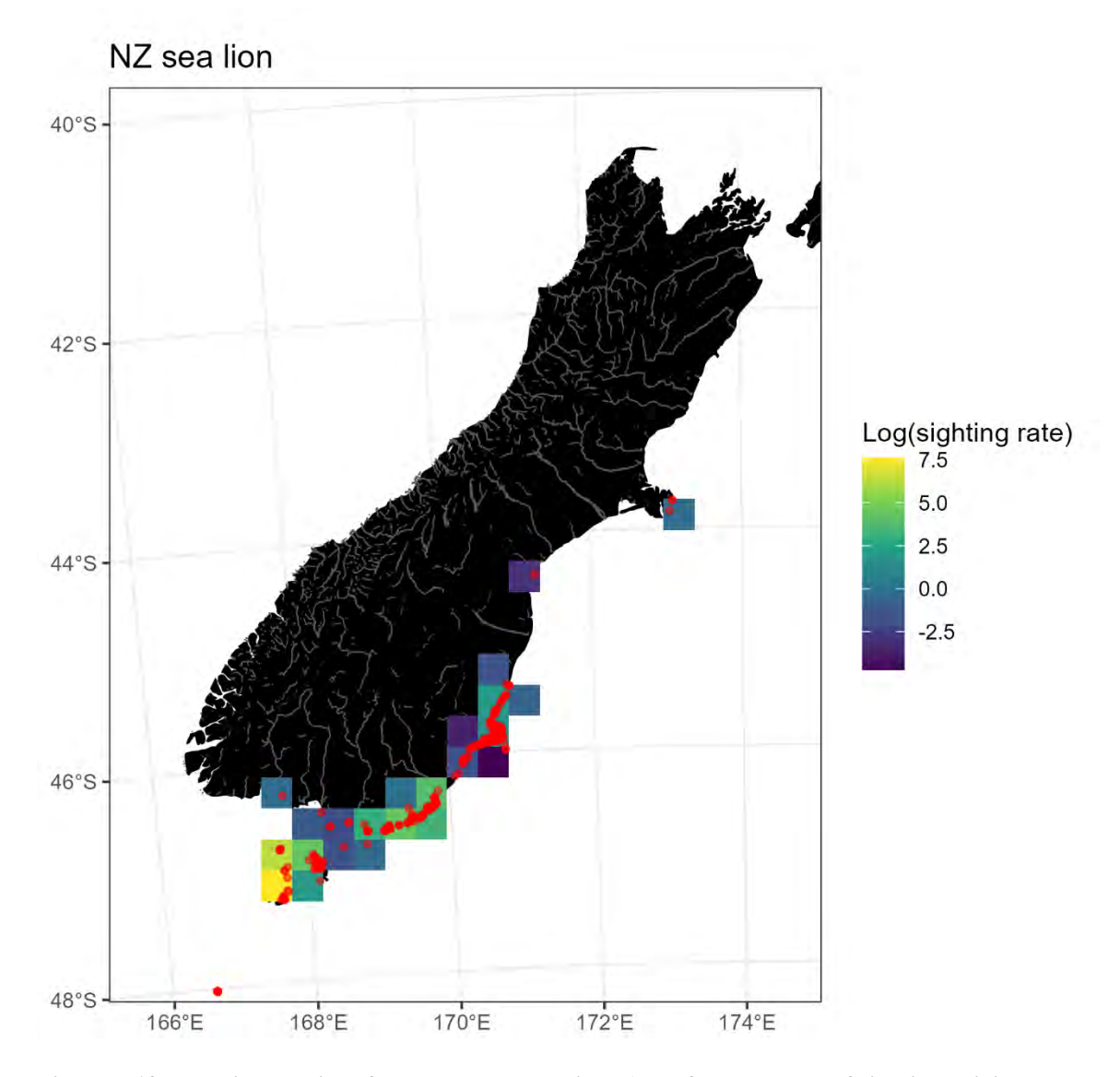


Figure F.13: Relative density of New Zealand sea lions (log of the number of sightings divided by human density). The red points show the locations of public sightings of New Zealand sea lions (iNaturalist Community 2023).

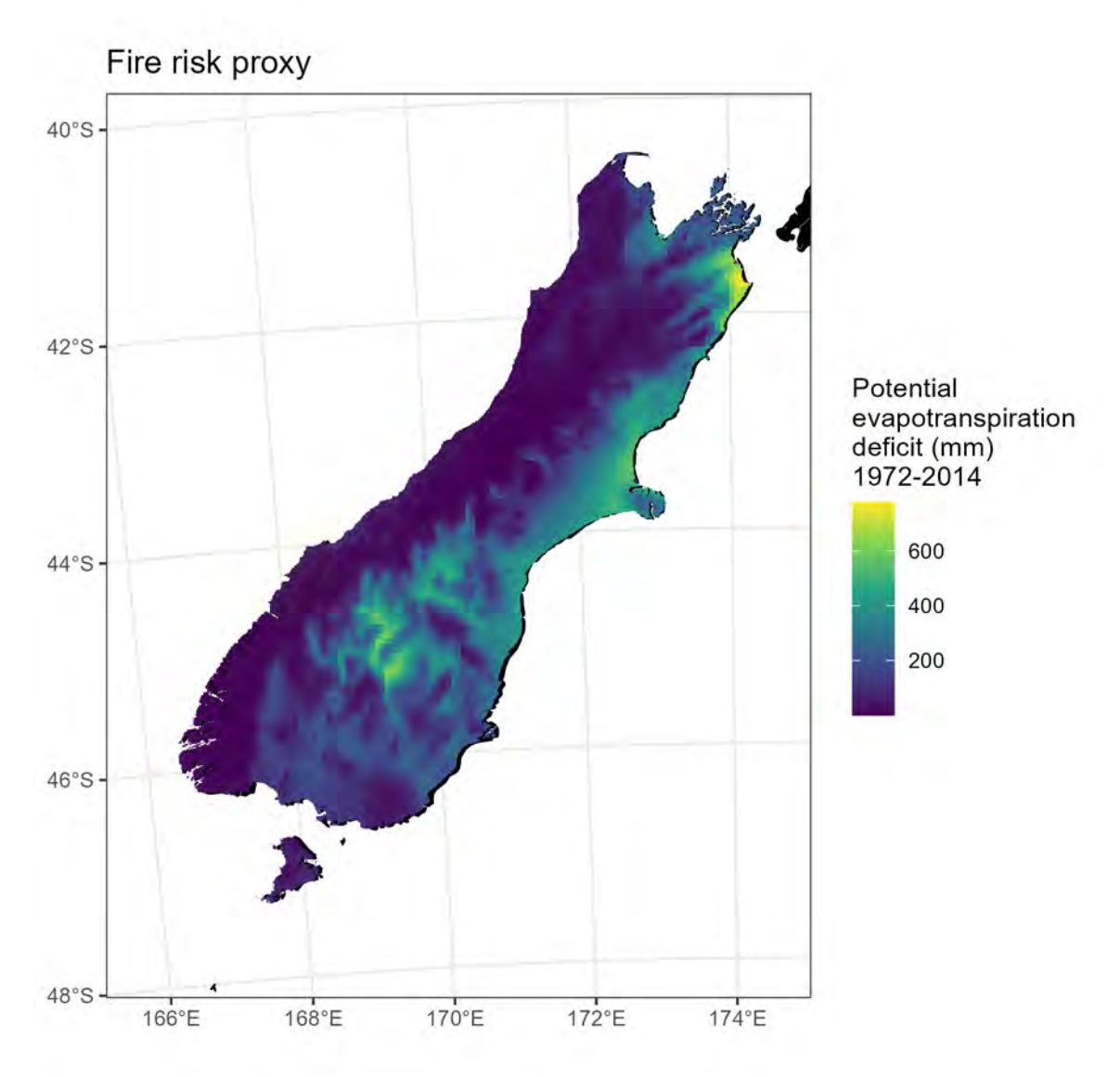


Figure F.14: Spatial fire risk (potential evapotranspiration deficit from 1972–2014 (mm)).

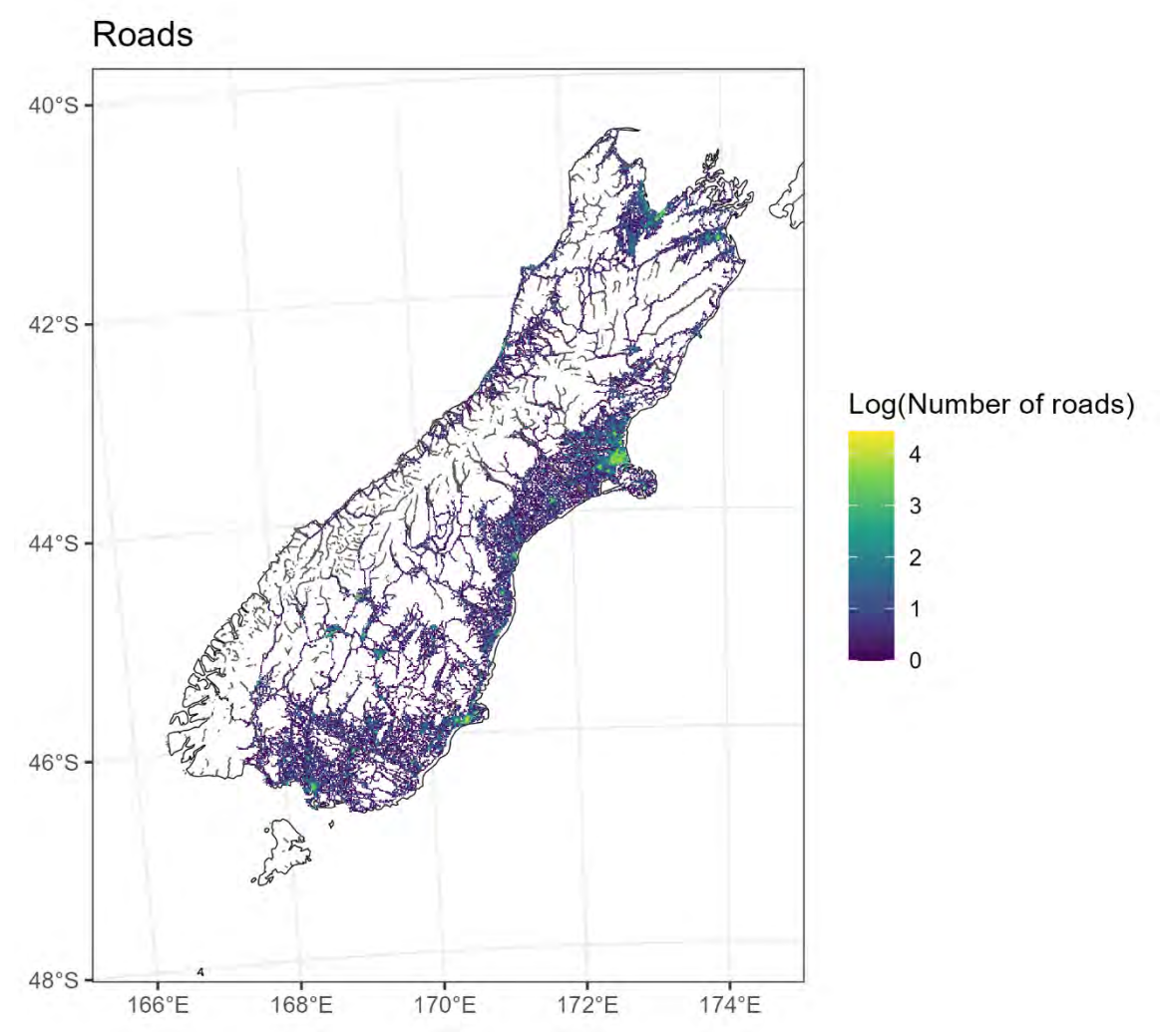


Figure F.15: Spatial density of roads (log of the number of roads per 1 km grid cell).

Appendix G. SUPPLEMENTARY TABLES & FIGURES FOR SEA TEMPERATURE ANALYSIS

Chick survival to fledgling

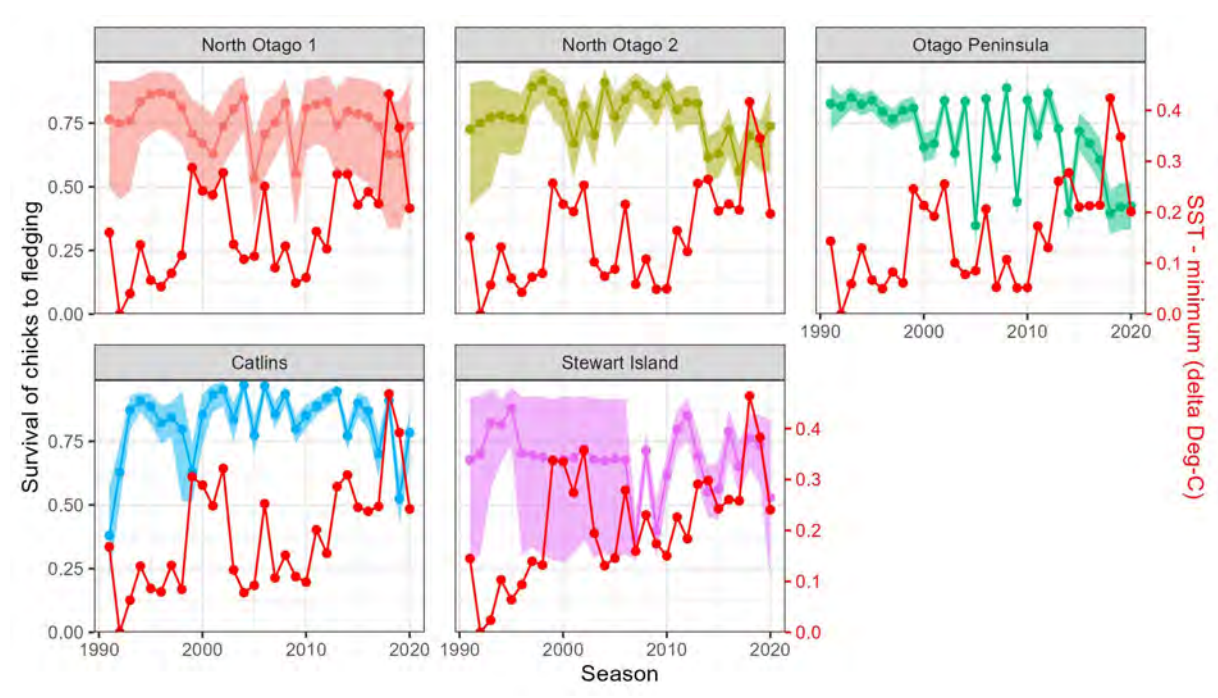


Figure G.1: Time series of female chick survival to fledging (points and lines with 95% credible interval) and sea surface temperature (red lines), by regional sub-population.

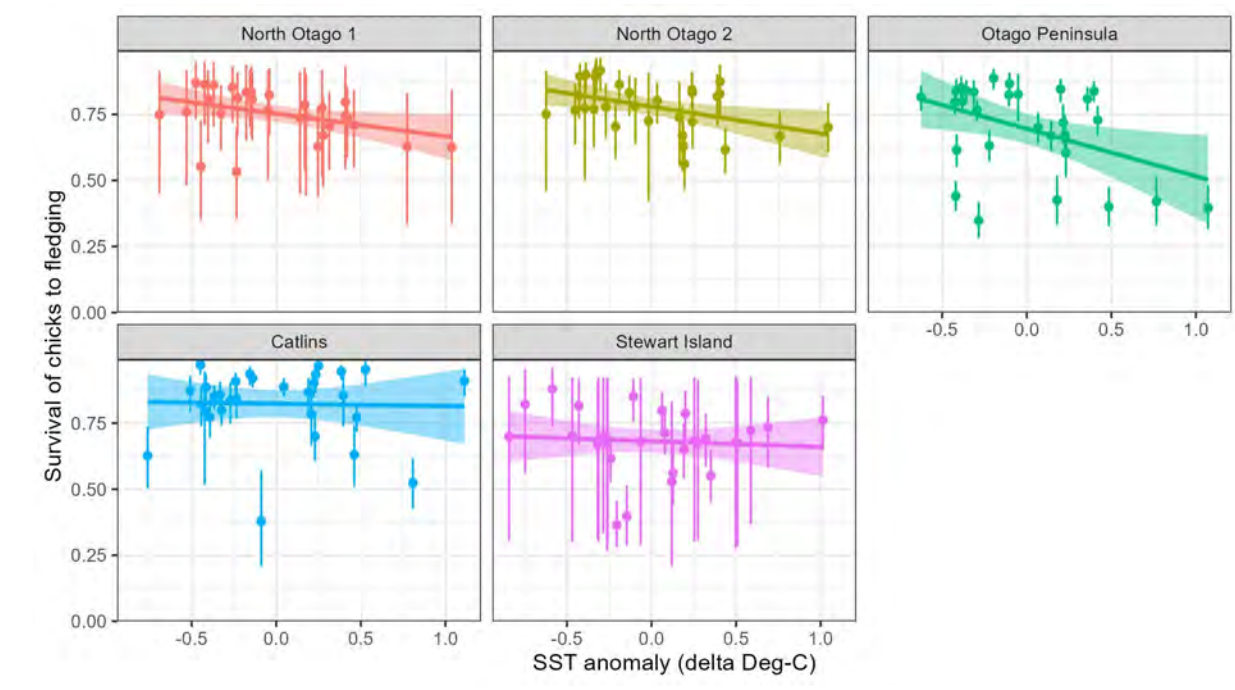


Figure G.2: Plot of female chick survival to fledging (with 95% credible interval) in response to sea surface temperature, by year and regional sub-population. The straight line and shaded area in each plot represent the mean and 95% confidence interval of linear models fitted to this relationship.

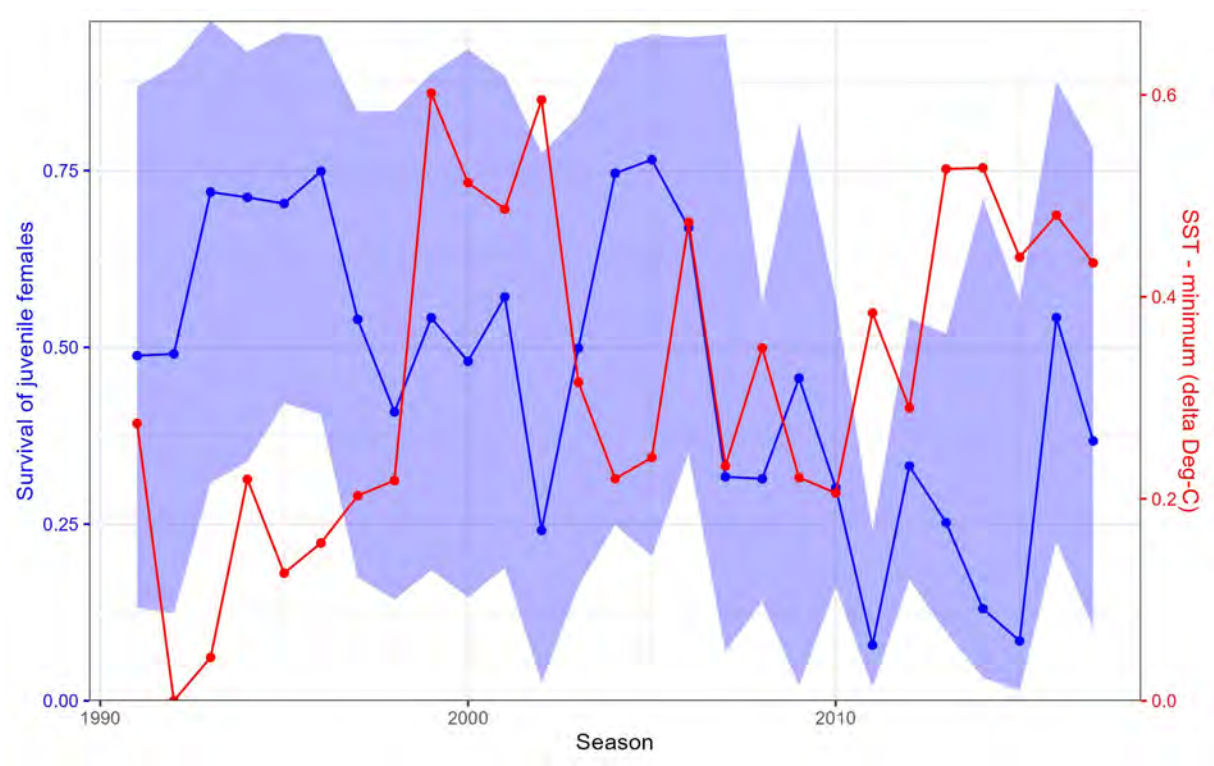


Figure G.3: Time series of juvenile female survival (points and lines with 95% credible interval) and sea surface temperature (red lines).

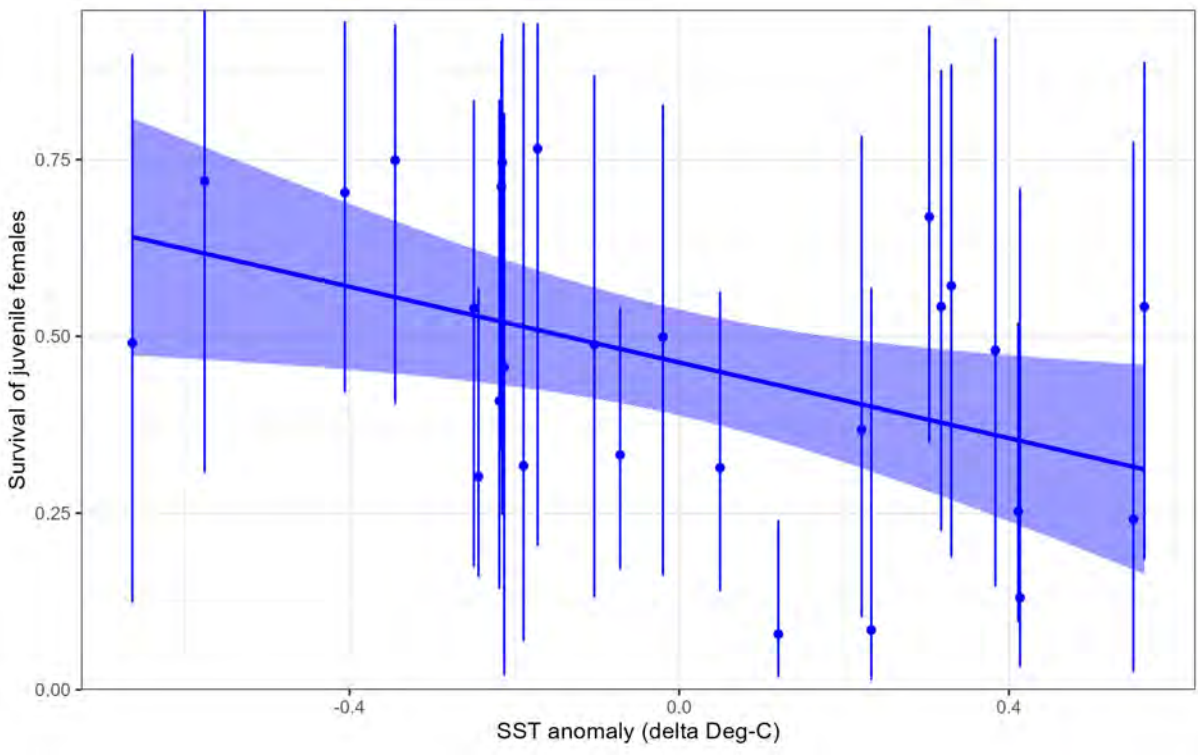


Figure G.4: Plot of juvenile female survival (with 95% credible interval) in response to sea surface temperature, by year. The straight line and shaded area represent the mean and 95% confidence interval of a linear model fitted to this relationship.

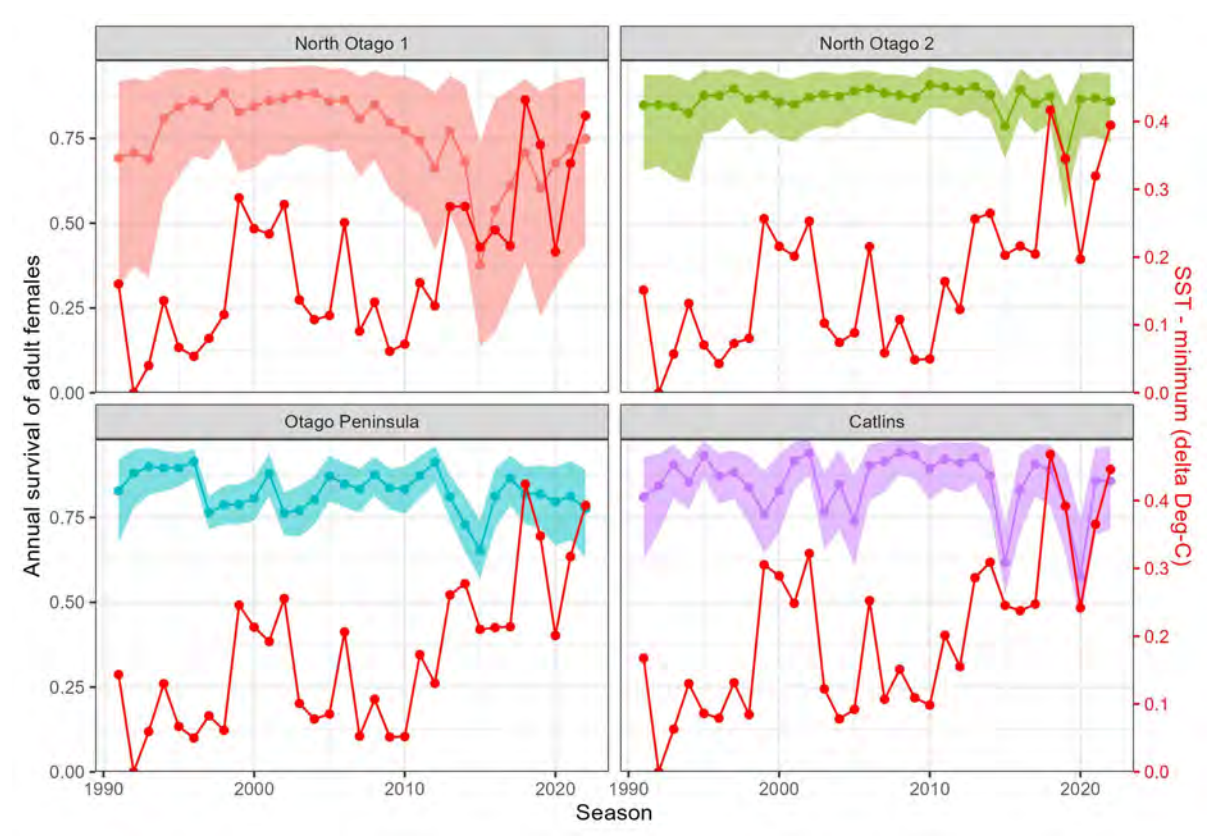


Figure G.5: Time series of adult female survival (points and lines with 95% credible interval) and sea surface temperature (red lines), by regional sub-population.

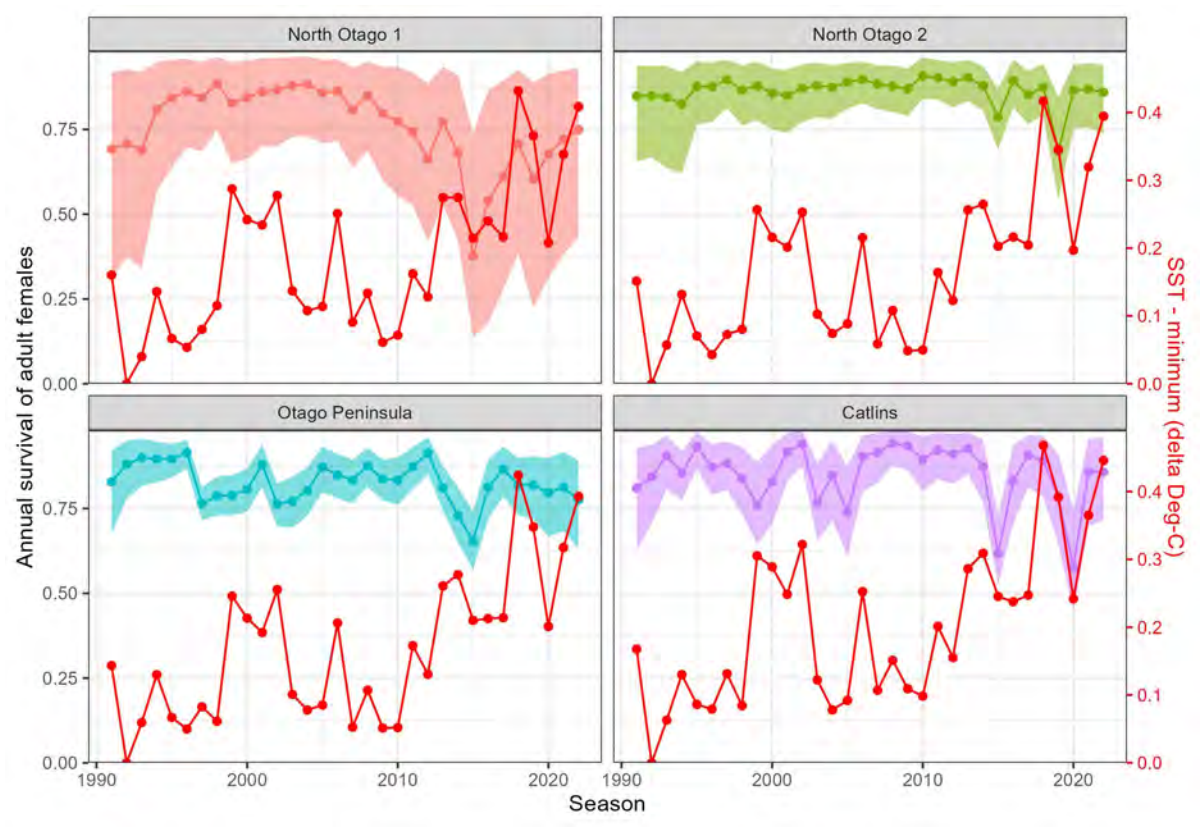


Figure G.6: Plot of adult female survival (with 95% credible interval) in response to sea surface temperature, by year and regional sub-population. The straight line and shaded area in each plot represent the mean and 95% confidence interval of linear models fitted to this relationship.